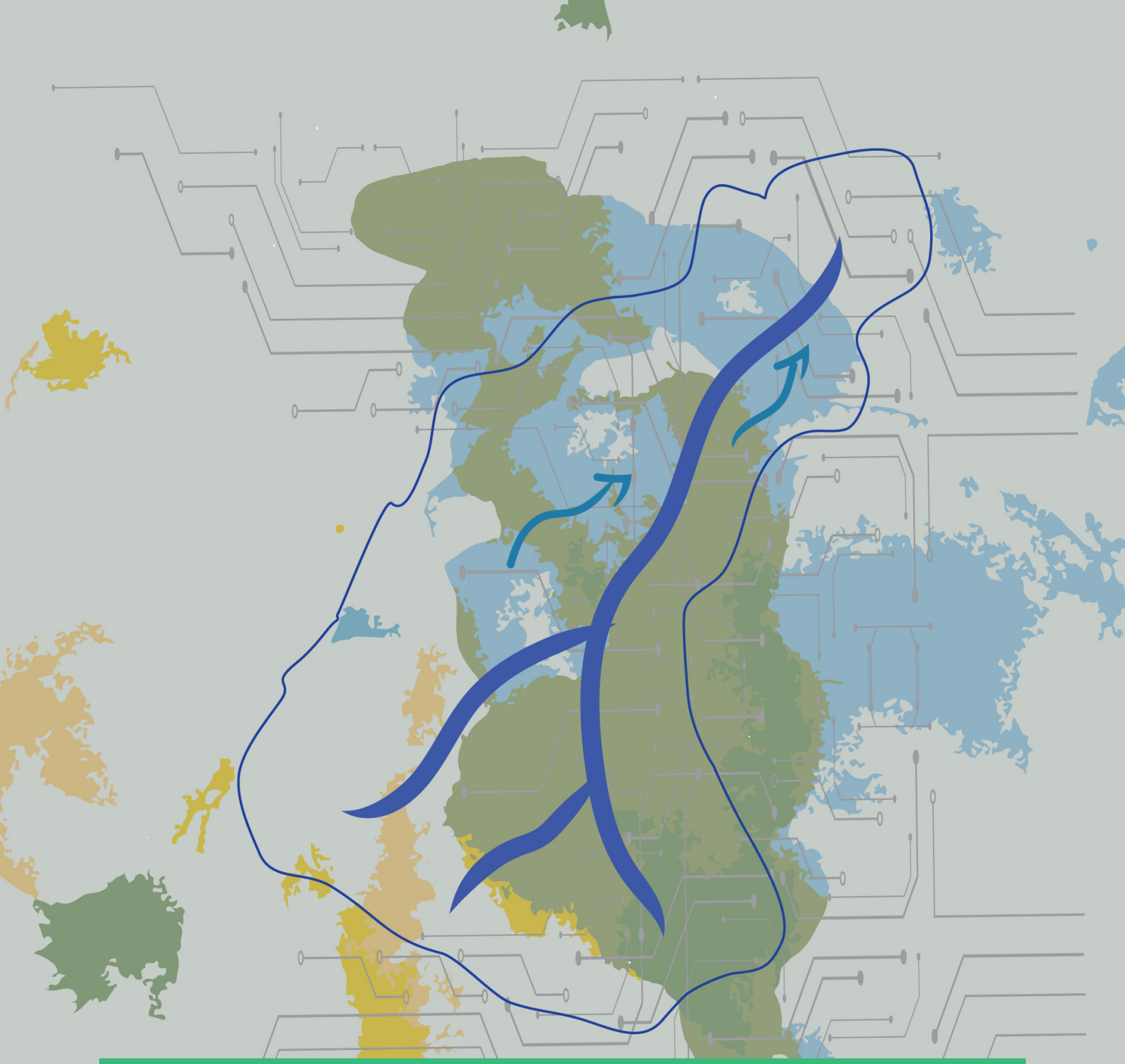

Earth Observations-Informed Modelling for the Design of Nature-Based Climate Adaptation Strategies

Muhammad Haris Ali

EARTH OBSERVATIONS-INFORMED MODELLING FOR THE DESIGN OF NATURE-BASED CLIMATE ADAPTATION STRATEGIES

Muhammad Haris Ali

EARTH OBSERVATIONS-INFORMED MODELLING FOR THE DESIGN OF NATURE-BASED CLIMATE ADAPTATION STRATEGIES

DISSERTATION

for the purpose of obtaining the degree of doctor
at Delft University of Technology
by the authority of the Rector Magnificus Prof.dr.ir. H. Bijl,
chair of the Board for Doctorates
and
in fulfilment of the requirement of the Vice Rector of IHE Delft
Institute for Water Education, Prof.dr. G.P.W. Jewitt,
to be defended in public on
Wednesday, 4 February 2026 at 12:30 hours

by

Muhammad Haris ALI

This dissertation has been approved by the promotors.

Composition of the doctoral committee:

Rector Magnificus TU Delft	chairperson
Vice Rector IHE Delft	vice-chairperson
Em.prof.dr. D.P. Solomatine	TU Delft / IHE Delft, promotor
Prof.dr. I.I. Popescu	TU Delft / IHE Delft, promotor
Prof.dr. M. Hrachowitz	TU Delft, promotor

Independent members:

Prof.dr. T.A. Bogaard	TU Delft
Prof.dr. L. Beevers	University of Edinburgh, UK
Prof.dr. G.P.W. Jewitt	TU Delft / IHE Delft
Dr. H. Madsen	DHI, Denmark
Prof.dr. M.E McClain	TU Delft / IHE Delft, reserve member

Dr. A. Jonoski, Associate Professor of Hydroinformatics, IHE Delft Institute for Water Education, has significantly contributed towards the supervision of this dissertation

This research was conducted under the auspices of the Graduate School for Socio-Economic and Natural Sciences of the Environment (SENSE)

Published by IHE Delft Institute for Water Education
www.un-ihe.org
ISBN 978-90-73445-77-2

To the hours that stretched and the hands that held me.

To every late night and every struggling nudge forward.

To effort, to grace, and to those who never let me fail - My family.

ACKNOWLEDGEMENTS

First and foremost, my deepest gratitude goes to Prof. Ioana Popescu, my daily supervisor, mentor, and role model. Her continuous support, insightful feedback and encouragement have been instrumental throughout my PhD journey. Thank you for always finding time to guide me, no matter how busy your schedule was. I am sincerely grateful to Dr. Andreja Jonoski for his guidance and constructive input, which were invaluable to the development of my research. I am profoundly thankful to both of you for entrusting me with the opportunity to pursue this PhD. I am deeply thankful to my promoters: Prof. Dimitri Solomatine and Prof. Markus Hrachowitz, for their valuable support and expert advice, which helped me a lot in refining my research ideas. I would also like to extend special thanks to Dr. Schalk Jan van Andel and Dr. Claudia Bertini for their valuable feedback and thoughtful suggestions.

I thank my IHE friends and PhD fellows for the cherished moments, thoughtful chit-chat, and for listening to spontaneous ideas, no matter how lame they were at the time. Your camaraderie made my PhD journey more memorable. Further, to my dear Pakistani community and friends, I extend a heartfelt thanks. You were a great source of joy and comfort, helping to ease my mind from constant PhD thoughts.

Special thanks to my wife for her unconditional love, patience, for tolerating my long working hours, and for supporting me throughout the PhD journey. Thank you for pretending to understand what hydrological modeling is and nodding along even when you had no clue what I was talking about. To my adorable daughter for being a daily reminder of joy and not bothering me (too much) on busy days. Your laughter and hugs were the best source of motivation. The PhD was a long journey but having you two by my side made it the best kind of adventure.

I owe special thanks to my parents and my sister, whose love and prayers kept me motivated and going. Above all, I thank Allah for the opportunity to pursue this study and the perseverance to complete it. Alhamdulillah.

SUMMARY

Climate change poses prodigious challenges to water resource management. In addressing these challenges, traditional grey measures lack adaptability and long-term sustainability. In contrast, Nature Based Solutions (NBSs) offer flexible, sustainable and eco-friendly alternatives. The design and effectiveness of NBS-based adaptation strategies could be potentially assessed through integrated hydrological models, which simulate both surface and subsurface complex hydrological processes. However, the accuracy of models to efficiently simulate the hydrological processes significantly depends on the quality and availability of input data. Earth Observation (EO) datasets offer a wide range of hydrological data with comprehensive spatial and temporal coverage, yet their quality remains uncertain and requires evaluation across different scales and regions.

To gain insights, the most frequently utilized EO datasets in distributed hydrological modelling were systematically reviewed and categorised across different catchment scales, including the micro-, meso- and macro-scales. The knowledge gaps identified through this detailed review of the articles demonstrate that dataset suitability for hydrological simulations varies substantially depending on location, scale, and evaluation criteria. Recognizing the inadequacies of single metric evaluation, the research further explores the sensitivity of the choice of metrics to the identification of the most suitable dataset for hydrological simulations. By applying a multi-metric, multiple-combination approach, it evaluates gridded precipitation products such as ERA5-Land, IMERG-Final, MSWEP, and EOBS in reproducing hydrological processes, revealing that the choice of performance metrics significantly influences the selection of suitable datasets.

Further, the research analyses the separate and combined effects of climate and LULC change on the hydrology of the Aa of Weerijs catchment in the near future. Future meteorological data under climate change scenarios were obtained from the Royal Netherlands Meteorological Institute (KNMI). An Artificial Neural Network - Cellular Automata (ANN-CA) based prediction model was used to simulate the future LULC map. The model results showed that the combined effects of climate change with LULC changes did not significantly differ from the individual impact of climate change at the catchment scale. However, at the local scale, the changes in LULC can significantly influence the variations in hydrological components such as groundwater table, soil moisture, and actual evapotranspiration, depending on the specific change in LULC class and season. The research underscores the importance of considering both climate and land use dynamics for a comprehensive understanding of hydrological changes in the face of future challenges.

Finally, the research evaluates the effectiveness of various NBSs and presents a methodology for designing NBS-based adaptive strategies for drought mitigation with a

focus on surface as well as subsurface hydrological components using an integrated distributed hydrological model. The NBSs assessed include ditch blocking, tree planting, wetland restoration, infiltration ponds, heathland restoration and brook bed barriers. Based on the model results, individual measures were spatially mapped to develop two adaptation strategies, each differing in spatial extent. The Key Performance Indicators (KPIs) were designed in consultation with key stakeholders and facilitated the clear communication of outcomes. Results indicated that the spatial extent of NBSs substantially influences their effectiveness. Overall, the NBS-based adaptation strategies showcased the potential to enhance the groundwater recharge and reduce the number of ban days for groundwater extraction, with almost eliminating the ban days in the downstream part of the catchment.

In summary, this research integrates comprehensive EO dataset evaluation, combined climate and LULC scenario analyses, and the formulation and assessment of NBS-based adaptive strategies for water resource management in the context of a changing climate.

SAMENVATTING

Klimaatverandering stelt het waterbeheer voor enorme uitdagingen. Traditionele infrastructurele (grijze) maatregelen bieden onvoldoende aanpassingsvermogen en duurzaamheid. Op de natuur gebaseerde (groene) oplossingen (Nature Based Solutions (NBS)) bieden daarentegen flexibele, duurzame en milieuvriendelijke alternatieven. Hydrologische modellen die grond- en oppervlaktewater geïntegreerd simuleren, kunnen mogelijk worden gebruikt voor het ontwerpen van aanpassingsstrategieën op basis van NBS en voor het beoordelen van de effectiviteit van zulke strategieën. De nauwkeurigheid van modellen om hydrologische processen te simuleren hangt echter sterk af van de kwaliteit en beschikbaarheid van invoergegevens. Aardobservatie (Earth Observation (EO)) datasets bieden een breed scala aan hydrologische gegevens met een uitgebreide ruimtelijke en temporele dekking, maar de kwaliteit ervan blijft onzeker en moet op verschillende schalen en in verschillende regio's worden geëvalueerd.

Om inzicht te krijgen, zijn de voor gedistribueerde hydrologische modellering meest gebruikte EO datasets systematisch gereviewed en gecategoriseerd voor micro-, meso- en macro-stroomgebieden. De kennisleemtes die middels deze gedetailleerde literatuurreview zijn geïdentificeerd, laten zien dat de geschiktheid van datasets voor hydrologische simulatie aanzienlijk varieert per locatie, schaal en evaluatiecriteria. Het onderzoek erkent de tekortkomingen van evaluatie op basis van een enkel criterium en onderzoekt hoe gevoelig de identificatie van de meest geschikte dataset voor hydrologische simulaties is voor de keuze van evaluatiecriteria. Door een benadering van meerdere-criteria in verschillende combinaties toe te passen, evalueert het onderzoek ruimtelijke neerslagproducten zoals ERA5-Land, IMERG-Final, MSWEP en EOBS op geschiktheid voor het reproduceren van hydrologische processen. Hieruit blijkt dat de keuze van evaluatiecriteria de selectie van geschikte datasets aanzienlijk beïnvloedt.

Daarnaast analyseert het onderzoek de afzonderlijke en gecombineerde effecten van klimaat- en LULC-veranderingen (landgebruik) op de hydrologie van het stroomgebied van de Aa of Weerijs in de nabije toekomst. Meteorologische gegevens onder klimaatscenario's werden verkregen van het Koninklijk Nederlands Meteorologisch Instituut (KNMI). Een voorspellingsmodel gebaseerd op kunstmatige intelligentie (Artificial Neural Network - Cellular Automata (ANN-CA)) werd gebruikt om de toekomstige LULC-kaart te simuleren. De modelresultaten toonden aan dat op de schaal van het stroomgebied de gecombineerde effecten van klimaat- en landgebruikveranderingen niet significant verschilden van de individuele effecten van klimaatverandering. Op lokale schaal kunnen de veranderingen in LULC echter wel de variaties in hydrologische componenten zoals grondwaterspiegel, bodemvocht en actuele evapotranspiratie aanzienlijk beïnvloeden, afhankelijk van het seizoen en de specifieke

verandering in LULC-klasse. Het onderzoek benadrukt hoe belangrijk het is voor een volledig begrip van hydrologische veranderingen met het oog op toekomstige uitdagingen om rekening te houden met dynamiek van zowel klimaat als landgebruik.

Tot slot evalueert het onderzoek de effectiviteit van verschillende NBS voor het verkleinen van droogte risico's en presenteert het een methodologie voor het ontwerpen van adaptieve strategieën op basis van NBS, met een focus op zowel oppervlakte- als grondwater met behulp van een geïntegreerd gedistribueerd hydrologisch model. De beoordeelde NBS omvatten het afdammen van sloten, het planten van bomen, moerasherstel, infiltratievijvers, heideherstel en beekbedbarrières. Op basis van de modelresultaten werden de afzonderlijke maatregelen in kaart gebracht om twee aanpassingsstrategieën te ontwikkelen die elk in ruimtelijke omvang verschillen. In overleg met belanghebbenden werden kritieke prestatie-indicatoren opgesteld (Key Performance Indicators (KPI's) hetgeen communicatie van de resultaten makkelijker maakte. De resultaten gaven aan dat de ruimtelijke omvang van NBS de effectiviteit aanzienlijk beïnvloedt. In het algemeen laten de NBS aanpassingsstrategieën zien de potentie te hebben om de grondwateraanvulling te verbeteren en het aantal dagen met een verbod op grondwateronttrekking te verminderen, waarbij in het benedenstroomse deel van het stroomgebied dagen met een onttrekkingsverbod vrijwel achterwege blijven.

Kort samengevat integreert dit onderzoek uitgebreide evaluatie van EO datasets, analyse van gecombineerde klimaat- en LULC scenario's en de formulering en evaluatie van klimaatadaptatie-strategieën met NBS voor het waterbeheer.

CONTENTS

1

INTRODUCTION

1.1 BACKGROUND

The indications of escalating climate change are prominent and can no longer be ignored in any region or sector of the world (Forster et al., 2024). The IPCC Sixth Assessment Report (AR6, 2023) stated with a high degree of confidence that the rate of rise in global surface temperature since 1970 has surpassed that of any other 50-year period in the past 2000 years. Due to these changes, the hydrological cycle is accelerating leading to more frequent and stronger weather extremes including floods and droughts both at regional and global scales (Wang et al., 2021; Chiang et al., 2021). In a warming climate, frequent periods with less than average precipitation are anticipated. During such periods, the decrease in runoffs may be comparatively more than the corresponding decrease in precipitation (Massari et al., 2022) driven by higher evaporation rate and drier soil resulting from higher temperatures. In general, water management systems around the world are designed based on the assumption that the statistical properties of the flow remain constant over time, also known as stationarity (Villarini and Wasko, 2021). However, due to human influence and climate change, the assumption about the stationarity has become questionable (Milly et al., 2008). As a result, water management creates a prodigious impediment for the decision makers. Often, grey measures such as dams and reservoirs are built to alleviate flood and drought hazards due to their rapid and visible effects but these measures need large investment, frequent maintenance and are categorized as inflexible approaches (Brink et al., 2016; Wu et al., 2023; Schneider et al., 2017). In addition to adverse effects on the downstream ecosystem, such measures are generally designed for certain life periods, are not environmentally friendly and lack the capability to adapt to changing climate.

Many countries are nowadays focused on envisaging adaptation and mitigation strategies based on green infrastructure and ecosystem-based adaptive measures to reduce their exposure to hydro-meteorological hazards (Shah et al., 2023; Davies et al., 2021). This kind of measures offer greener and eco-friendly alternatives to traditional engineering solutions for hydro-meteorological risk reduction (Ruangpan et al., 2020) in cost effective ways (Ruangpan et al., 2024). The International Union for Conservation of Nature (IUCN) defines Nature Base Solution (NBS) as “actions to protect, sustainably manage, and restore natural and modified ecosystems that address societal challenges effectively and adaptively, simultaneously providing human well-being and biodiversity benefits” (IUCN, n.d.). In addition to risk reduction and confronting climate change, NBSs also provide co-benefits such as carbon storage, urban heat mitigation, ecosystem services and biodiversity enhancement (Keesstra et al., 2018).

However, in order to assess the usefulness of nature based adaptive measures on local and basin scale and their long-term efficacy to mitigate or reduce climate change induced risks, detailed hydrological and/or hydrodynamic models are required to be developed. These numerical models are comprehensive tools that incorporate the laws of physics and

real state response variable equations to simulate floods and droughts, as well as to test NBSs. One of the hindrances in their use is the extensive data requirements (Kumar et al., 2021). Moreover, the accuracy of models to efficiently simulate hydrological processes generally depends on the quality of input data.

The in-situ data is often considered as the most suitable to feed the models. However, these ground observations lack the ability to provide proper spatial coverage (Glenn et al., 2007; Fernandes et al., 2012; Lai et al., 2019) and are often not readily and freely available. Moreover, in a transboundary catchment case, the challenges regarding the in-situ data's availability are compounded due to a lack of data sharing, inconsistencies arising due to differences in recording time and methodologies applied for data collection (UNECE, 2024). Alternatively, EO based datasets offers a wide range of hydrological variables with time series spanning over multiple years (Jiang and Wang, 2019). As of 2023, there are more than seven thousand satellites orbiting the Earth. Out of them, approximately 64 % are active and about 17 % are launched for EO purposes (UCSSD, n.d.). Advancing from panchromatic and red green blue (RGB) imagery, the sensor technology has expanded to capture data such as multi hyperspectral visible to near-infrared bands, thermal bands, microwave emissions. From hydrological perspective, this data provided a new and independent source of information covering the range of water cycle component (McCabe et al., 2017). Many research activities took advantage of this spatially available long sequence of temporal observations to compile long-term global datasets (Beck et al., 2017). Such datasets provide an independent mean of analyzing and studying hydrological system dynamics and response (Brocca et al., 2014) as well as for conducting trend analysis and anomaly detection in water cycle components.

1.2 PROBLEM STATEMENT

In the last three decades, a wide range of EO based datasets providing insight into a vast variety of hydrological variables are developed (Xu et al., 2014; Jiang and Wang, 2019). Seamless and prompt accessibility of these datasets makes them attractive to hydrological modelers and water managers as substitute or complementary data sources for setting up detailed models and testing solutions for better water management. EO has driven significant advancements in hydrological science. Many assume that hydrological variables such as precipitation, evapotranspiration, soil moisture, etc. are directly retrieved from EO. However, in reality, complex retrieval models with various parameterizations and simplifications are applied to convert earth emitted and reflected radiations to desired variables which increases the potential for errors (McCabe et al., 2017). Further, due to budget constraints and the limited life span of satellites, the development of long time series of EO datasets required merging of data from different sensors. This can cause artificial fluctuations due to inconsistencies in satellites constellations (van Oostende et al., 2022) resulting in spatial and temporal variation in

the quality of datasets across regions of the globe. The accuracy of hydrological models is dependent not only on their structure but also highly on the quality of input data (Wang et al., 2023; Rasheed et al., 2024). Water cycle varies significantly across multiple spatiotemporal scales (Dash and Kumar, 2025; Chen and Wang, 2018) and the ability of global datasets to accurately capture this variability also differs across regions, leading to spatial variation in data quality. Consequently, selecting appropriate datasets for model setup is critical to ensure model accuracy for simulating hydrological processes. Despite the growing abundance of EO datasets, their performance and applicability in hydrological models across different geographical scales and regions remain unclear (Gebrechorkos et al., 2024; Beck et al., 2017). Therefore, there is a need to identify the potential of EO datasets for use in hydrological models particularly for different catchment scales ranging from micro-scale (<10 km^2) to macro-scale (>1000 km^2). Further, due to associated uncertainty, the quality of these datasets needs demonstration (Craglia et al., 2017). For instance, precipitation is one of the main drivers of the terrestrial hydrological cycle and an important input to hydrological models. However, it is challenging to estimate precipitation using satellite data or models (Gebrechorkos et al., 2024; Beck et al., 2017). The uncertainties in the precipitation products can cause up to 50 % error in variables simulated by hydrological models (Bárdossy et al., 2022), resulting in poor representation of hydrological responses. The suitability of EO products is evaluated mainly using two approaches (i) comparing the variable directly with observed data from ground stations (Yang et al., 2024; Sun et al., 2018; Ayehu et al., 2018) and (ii) using EO products to force hydrological models and comparing the reproduced variables (e.g. streamflow) with observed data (Gebrechorkos et al., 2024; Ji et al., 2024; Lakew et al., 2020). In both approaches, researchers rely on error metrics to evaluate the goodness of fit between estimated and in-situ time series (Gebrechorkos et al., 2024; Dembele et al., 2020; Alexopoulos et al., 2023), which is standard practice for hydrologists (Jackson et al., 2019). The Nash-Sutcliffe efficiency (NSE) (Nash and Sutcliffe, 1970) and the Kling-Gupta efficiency (KGE) (Gupta et al., 2009) are frequently used metrics for the quantitative comparison between simulated timeseries and observed ones (Cinkus et al., 2023; Clark et al., 2021). However, each metric has its limitations: NSE over-emphasises peak values due to use of squared sum of errors (SSE) which leads to an inflated importance of the absolute errors during high flows at the expense of low flows (Knoben et al., 2019; Onyutha, 2024), whereas the KGE complements the deficiencies of the NSE to some extent but still underestimates the variability of timeseries data (Liu, 2020). Both NSE and KGE can be strongly swayed by a few outliers (Clark et al., 2021; Beven and Westerberg, 2011). In addition to these, many other error metrics are used by researchers; however, no single metric can comprehensively capture all aspects of a specific variable (see e.g. Jackson et al. (2019), Onyutha (2024)). Different metrics may lead to opposing and unclear conclusions about the identification of the most suitable EO product for a given application. Therefore, there is a need to evaluate the

influence of choice of performance metrics on the identification of the most suitable data product and to formulate a method that can comprehensively identify the suitable product for the hydrological application.

Beyond data challenges, hydrological systems are further complicated by climate change and land use/land cover (LULC) changes. Droughts are among the most devastating natural hazards and have extensive impacts on water resources affecting agriculture, ecosystems, and socio-economic systems. In the summer of 2018, large parts of Europe, particularly north-western and central regions, experienced extreme hot and dry conditions (Philip et al., 2020; Bakke et al., 2020). Such droughts, similar to those of 2018–2019, are expected to occur more frequently in the future (Philip et al., 2020). The Netherlands was one of the countries most affected by these extreme weather events, particularly in its eastern and southern regions (van den Eertwegh et al., 2019). The country, which is traditionally focused on managing surplus water, the severe impacts of the 2018–2019 droughts marked a turning point where water managers began searching for solutions to prepare for more frequent drought conditions. To counter these new challenges, a thorough understanding of climate change's impact on hydrological systems both at regional and catchment scales is essential (IWMI, 2019; Adib et al., 2020). However, the positive or negative changes in the climate signals are quite uncertain as different Global Climate Models (GCM)/Regional Climate Models (RCM) produce varying projections for each study site depending on local climate and land use characteristics (Blöschl et al., 2019; Song et al., 2021). Additionally, alongside climate change, land use/land cover (LULC) change is also one of the important drivers of hydrological variations (Rigby et al., 2022; Kundu et al., 2017; Trang et al., 2017). Research examining the impact of human-induced changes in landscape patterns and climate change has gathered significant attention. However, primarily the research is focused on either the effects of climate change or changes in land use, rather than considering both factors combined (Nazeer et al., 2022; Gurara et al., 2021; Kay et al., 2021). In addition to that, when these factors are examined together, the emphasis of the study is often centered on evaluating variations in surface hydrological variables alone (Ma et al., 2023; Lyu et al., 2023; Zhang et al., 2023; Iqbal et al., 2022; Sinha et al., 2020) or only on groundwater dynamics (Hanifehlou et al., 2022; Ghimire et al., 2021). Therefore, before envisaging the adaptive strategies, the individual and combined effects of the climate and LULC change on the catchment's surface and sub-surface hydrological variables need to be analyzed. Additionally, it seeks to address a knowledge gap that how crucial is it to consider future LULC changes alongside changes in meteorological variables under climate change when assessing the future hydrological state of a catchment.

The formulation of adaptive strategies for droughts is primarily focused on retaining the water in the catchment either by increasing storage or by slowing surface or sub surface

flow. Some of these actions are considered important for flood management as well but are imperative for droughts (POM, 2014). NBSs are the potential alternative to the grey infrastructure for climate adaptation (Yimer et al., 2024; Debele et al., 2019; Ruangpan et al., 2020) with their multiple co-benefits such as better water quality, improved soil health, biodiversity enhancement, natural area for recreation and better land use management and planning (Nesshöver et al., 2017; Penning et al., 2023). However, in research, much attention has been given to testing the potential of NBSs for flood management while their potential for drought management is barely touched. For instance, recent literature review by Yimer et al. (2024) found that only 6 % of European case studies and 14 % of global case studies were focused on NBSs for drought adaptation. Apart from this, the research on the potential of NBSs in urban areas is more developed compared to their implementation in rural areas at the catchment scale for drought management (Yimer et al., 2024; Johnson et al., 2022). Moreover, the lack of proper modelling approaches to test the impact of NBSs is another hindrance in understanding their potential for drought adaptation particularly in evaluating their impact on both surface and subsurface water resources.

In summary, while EO datasets have transformed hydrological science, their reliability and applicability in hydrological modeling remain uncertain due to retrieval errors, data inconsistencies, and spatial-temporal variations in quality. Furthermore, the choice of error metrics influences the identification of suitable EO products, necessitating a more comprehensive evaluation framework. Additionally, the interplay of climate change and LULC change in hydrological systems is often analyzed in isolation, despite their combined impact on surface and subsurface hydrology. Lastly, while NBSs offer potential alternatives to grey measures, their potential remains underexplored for drought mitigations, particularly at the catchment scale.

Addressing these knowledge gaps will provide crucial insights into improving EO-based hydrological modeling, assessing climate and land-use impacts, and enhancing adaptive strategies for drought management.

1.3 RESEARCH OBJECTIVES AND QUESTIONS

The main objective of the present research is to evaluate the potential of EO data products for hydrological modelling and to assess the effectiveness of NBSs for drought adaptation through modelling.

The specific objectives are:

I. To analyse the potential of EO data products for distributed hydrological modelling

II. To evaluate the influence of choice of performance metrics on the identification of the most suitable data product for hydrological simulations and to develop a comprehensive method to identify suitable products

III. To analyse the individual and combined impacts of future projected changes in LULC and meteorological variables on surface and subsurface hydrology

IV. To evaluate the potential of NBSs for mitigating drought impacts

The research objectives will be achieved by answering the following research questions:

I. What is the potential of different types of EO datasets for use in distributed hydrological modelling across different catchment scales?

II. What are the literature gaps regarding the use of EO dataset across different spatial scales for future research?

III. How can the most suitable EO datasets be comprehensively identified for hydrological simulations?

IV. What is the influence of the selection of evaluation metrics on the identification of the most suitable dataset for hydrological simulations?

V. What is the significane of considering future LULC changes alongside changes in meteorological variables under climate change when assessing the future hydrological condition of a catchment?

VI. What is the potential of the NBSs for mitigating drought impact considering both surface and subsurface water resources?

VII. How individual NBS measures can be spatially mapped to formulate adaptation strategies to achieve maximum water conservation in subsurface?

1.4 THESIS OUTLINE

Chapter 1 provides the theoretical background and describes the problem statement, along with the research objectives and questions that this research has addressed.

Chapter 2 presents the systematic literature review conducted to seek the potential of EO datasets for distributed hydrological and their performance across different geographical scales of catchments, including the micro-scale (<10 km^2), meso-scale (10 km^2–1000 km^2), and macro-scale (>1000 km^2). The review covers EO datasets relevant to hydrological modeling including rainfall, evapotranspiration, soil moisture, temperature, digital elevation model, land use, soil distribution, leaf area index and snow-covered area.

The chapter also identifies the knowledge gaps associated with the application of each dataset type at different spatial scales and insights which can assist in steering the possible future research directions in the field.

Chapter 3 provides the description of the study area and a comprehensive overview of the hydrological model used in this research.

Chapter 4 analyse the influence of evaluation metrics on the selection most suitable EO dataset for reproducing hydrological variables. It also presents the methodology developed for the comprehensive identification of suitable datasets for hydrological applications. The methodology is demonstrated using four different gridded EO precipitation data products for the study area.

Chapter 5 provides insights into the impact of climate change on the surface and sub-surface hydrological variables within the study area. Along with climate change, the chapter analyses the impacts of future LULC change on the hydrological processes. Further, this chapter also investigates the significance of considering future land use changes along with meteorological changes under climate change to comprehensively analyse the future hydrological state of the catchment.

Chapter 6 presents a model-based methodology for designing and evaluating the potential of NBSs based adaptative strategies for mitigating drought impact on both surface and sub-surface hydrological variables. The NBS measures assessed include ditch blocking, tree planting, wetland restoration, infiltration ponds, heathland restoration and brook bed barriers. It covers the approach to model for each individual measure, evaluates their performance under climate change scenarios and formulation of combined adaptative strategies by combining these individual measures to maximum benefit, particularly in terms of groundwater resources.

Chapter 7 complies the synthesis and outlook in the light of research questions. This chapter also includes the limitations of the study and constraints along with outlook on the topic as general with identifying future directions.

2

EARTH OBSERVATION DATASETS FOR DISTRIBUTED HYDROLOGICAL MODELLING: A REVIEW

This chapter presents a systematic literature review on the use of Earth Observation (EO) datasets in distributed hydrological modelling. The study aims to investigate the most commonly used datasets in hydrological models and their performance across different geographical scales of catchments, including the micro-scale (<10 km^2), meso-scale (10 km^2–1000 km^2), and macro-scale (>1000 km^2). The analysis included a search for the relation between the use of these datasets to different regions and the geographical scale at which they are most widely used. Additionally, co-authorship analysis was performed on the articles to identify the collaboration patterns among researchers. The study further categorized the analysis based on the type of datasets, including rainfall, digital elevation model, land use, soil distribution, leaf area index, snow-covered area, evapotranspiration, soil moisture and temperature. The research concluded by identifying knowledge gaps in the use of each data type at different scales and highlighted the varying performance of datasets across different locations. The findings underscore the importance of selecting the right datasets, which has a significant impact on the accuracy of hydrological models. This chapter provides valuable insights into the potential of EO datasets in hydrological modelling, and the identified knowledge gaps can inform future research directions.

This chapter is based on the journal publication: Ali, M. H., Popescu, I., Jonoski, A., & Solomatine, D. P., 2023. Remote Sensed and/or Global Datasets for Distributed Hydrological Modelling: A Review. Remote Sensing, 15(6), 1642. https://doi.org/10.3390/rs15061642.

2.1 INTRODUCTION

One of the important issues that the world is facing in the current era is climate change (MacAlister and Subramanyam, 2018), which will have adverse effects on the hydrological cycle of catchments (Jehanzaib et al., 2020). These effects will not be the same across the world (Konapala et al., 2020), hence their quantification and early prediction effects are important for preparedness. In order to obtain those quantifications, hydrological models are useful tools. The simulations of these models are used by water managers to study the current state of hydrological processes in areas of focus. The development of distributed hydrological models has the potential to provide large-scale predictions (Clark et al., 2017; Ocio et al., 2019), but these models need to be informed and assessed with distributed observational data for the better representation of spatio-temporal processes (Baroni et al., 2019). However, one of the main challenges faced by the modellers is the lack of data (Khan et al., 2022).

Commonly, the in-situ data are considered to be the most accurate. However, these ground observations are local and lack the ability to provide proper spatial coverage (Glenn et al., 2007; Fernandes et al., 2012; Lai et al., 2019). Further, the required huge amount of input data is often not readily and freely available. Luckily, the advancement in remote sensing technologies during the last decade has enabled mankind to gather huge datasets using satellite observations (Xu et al., 2014; Jiang and Wang, 2019). These observations are providing insights about the vast variety of the parameters that are required for building up a hydrological model (Karimi and Bastiaanssen, 2015). The immense diversity of these datasets covers digital elevation maps, land-use maps, soil distribution maps, rainfall, evapotranspiration, soil moisture, leaf area index and others. Moreover, for several of the sources of these datasets, the inventories span back half a century or even more. These freely available datasets are attractive to modellers, as these can fulfill data requirements.

In addition to the model structure, the performance accuracy of a hydrological model is dependent upon the quality of input data. This makes the selection of the right data important. However, the performance of Earth observation (EO) datasets cannot be treated as uniform throughout the globe as it varies across different climatic zones (Dembele et al., 2020). Moreover, no remote sensed datasets can be regarded as actual observations due to uncertainties being common in them (Rajib et al., 2018). The quality of such data products needs demonstration (Craglia et al., 2017) and verification with ground observation before use in models (Khairul et al., 2018; Huang et al., 2019). With the increasing computing power, adding new data into the inventories of these datasets is happening very rapidly. Because of the abundance in variety and non-uniform performance, the selection of datasets is difficult. Therefore, there is a need to investigate the research that has been conducted in this specific field over the past few years. Jiang and Wang (2019) performed the overview of the role of satellite-based remote sensing

data products in hydrological modelling. However, their study is limited to the exploration of the performance of datasets for flow simulations only. The other model outputs, apart from discharge were not considered. Further, the remotely sensed datasets such as digital elevation models, land-use maps, soil distribution maps and leaf area indices, which are equally important in representing hydrological processes, were not covered by the authors. Likewise, Sheffield et al. (2018) reviewed the current satellite missions and datasets that are being used by national agencies in the regions of Latin American and the Caribbean for water resource management. However, the study is region-specific and the focus is on water resource management instead of distributed hydrological modelling. In both previously mentioned studies, the authors did not mention the years when the publications covered by their review were issued, nor did they describe their methodology for selecting the articles. Additionally, neither study investigated the performance of remote sensed datasets at different geographical scales.

In this paper, we performed a systematic literature review. The aim of study was to investigate the research articles which were published on this topic in six years (2016 to 2021) and which used one or more types of remotely sensed and/or global datasets to establish the distributed hydrological model. More specifically, we aimed to answer the following questions: Which datasets are most widely used by the researchers? At what catchment scale are the remotely sensed datasets mostly used? Have researchers evaluated the performance of these datasets for hydrological simulations? What are the knowledge gaps in this respective field?

To answer the questions, we started the systematic literature review by sourcing 205 articles from Scopus and 208 articles from Web of Science. After that, the final analysis was carried out on 120 articles. Then, we looked into different types of datasets that were used in hydrological models for different catchment sizes. The terms ‘micro-scale’, ‘meso-scale’, and ‘macro-scale’ were used to categorize the sizes of catchments (i.e., less than 10 km^2 (Tomasella et al., 2008); 10 km^2 to 1000 km^2 (Wu et al., 2021); and greater than 1000 km^2 (Cornelissen et al., 2016), respectively). We performed this to detect the knowledge gaps at each scale concisely. Lastly, we concluded our analysis results and identified the scale-wise knowledge gaps that can act as the way forward for future work in the field.

After this introduction, the chapter presents the methodology used for paper selection, which is followed by the results and discussion in Section 2.3. The chapter ends with the Conclusion in Section 2.4.

2.2 METHODOLOGY

The review methodology is based on preferred reporting items for systematic reviews and meta-analyses (PRISMA) criteria (Page et al., 2021), consisting of three main steps. The

first step includes the identification of relevant articles and for that we used the keywords, such as “hydrological modelling”, “remote sensing”, “global data”, etc. All keywords are shown in Figure 2.1. The process of identification was started by consulting two websites. The first was Scopus and the second was the Web of Science. Studies published between 2016 and 2021 were selected for inclusion in this review to capture the latest advancements and trends in the use of remote sensed and/or global datasets for distributed hydrological modelling and to make the search manageable and feasible. Initially, 413 articles were sourced from the two websites that were mentioned earlier. The second step included the screening of the articles. From the initially sourced 413 articles, some occurred twice because of their presence in both databases, and some were not classified as articles, such as conference papers, conference reviews and book chapters. This reduced the list of articles. Five more articles were excluded as they were not retrievable from the source. After this screening process, we ended up with 246 articles. In the third step, the abstracts of the article were read in order to eliminate the articles with research focuses outside the scope of this review, i.e., detailed distributed hydrological modelling, which included 126 articles. These 126 articles were excluded and the detailed analysis was finally conducted on 120 research articles. The schematic representation of the whole methodological process of selecting the papers for review can be seen in Figure 2.1.

In the detailed analysis, firstly, the bibliographic analysis was performed to find the link between the regions and/or scale with the use of remote sensed and/or global datasets. Secondly, the shortlisted articles were categorized based on the type of datasets used by the authors for the hydrological modelling. Thirdly, for each dataset type, we further categorized the articles on the basis of catchment scale. Finally, we ascertained the progress of scientific community, both in terms of dataset type and scale.

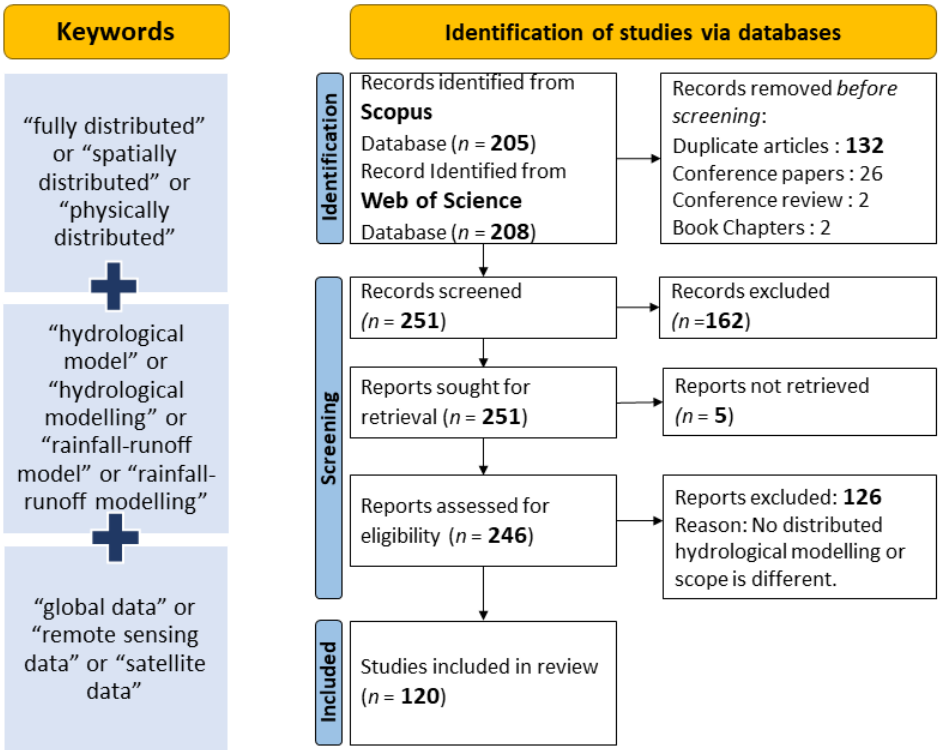

Figure 2.1. Schematization for identification of research articles for systematic literature review

2.3 Results and discussion

In the beginning, we classified the articles country-, region- and scale-wise. The purpose was to analyze the locations around the world where the remote sensed and/or global datasets were being used most. As shown in Figure 2.2, out of 120 full-text articles reviewed, most studies have been found to be conducted in China, followed by the USA. Conversely, continent-wise, most studies have been conducted in Asia, followed by Europe. If we look at the number of studies conducted at different catchment sizes, then the majority are being performed at the macro-scale.

The main aim of this classification was to find a relationship between the performance of remote sensing datasets and geographic locations, as well as the sizes of catchments. However, after reviewing the literature, we were unable to establish any clear links. For example, we did not find any evidence to suggest that the performance of remote sensing data is consistently better in one region or country over another, such as Asia versus Europe or China versus the rest of the world. However, if we consider the catchment size and number of studies, a direct relationship can then be framed: these studies are more focused on the macro-scale, followed by the meso-scale and micro-scale. Thus, the trend

of using remote sensed and/or global datasets in large catchments is more as compared to the use in small ones.

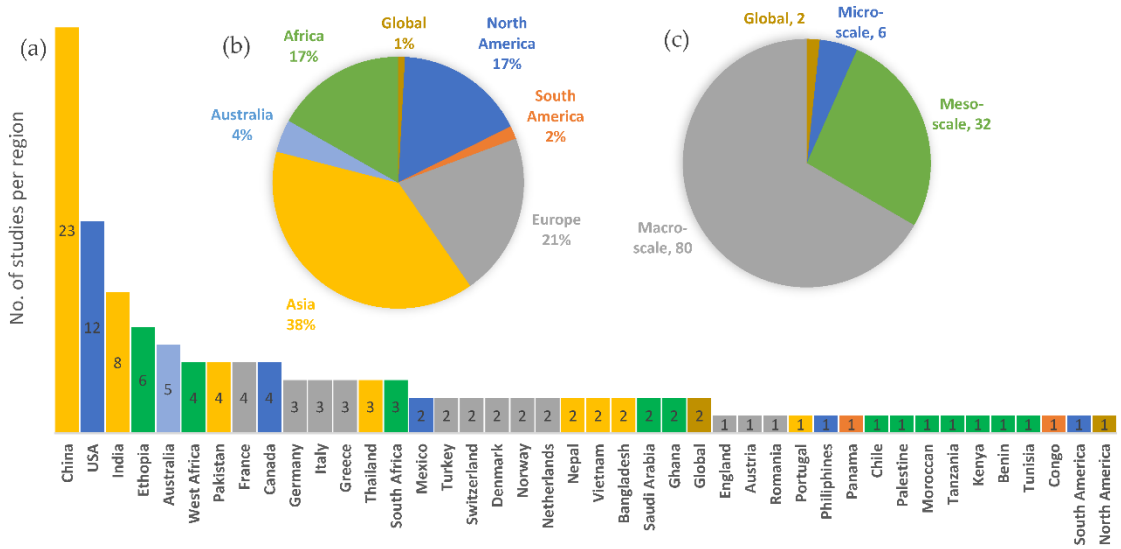

Figure 2.2. (a) Number of case study areas per country, (b) percentage contribution per continent, (c) number of studies per catchment scale

The main aim of this classification was to find a relationship between the performance of remote sensing datasets and geographic locations, as well as the sizes of catchments. However, after reviewing the literature, we were unable to establish any clear links. For example, we did not find any evidence to suggest that the performance of remote sensing data is consistently better in one region or country over another, such as Asia versus Europe or China versus the rest of the world. However, if we consider the catchment size and number of studies, a direct relationship can then be framed: these studies are more focused on the macro-scale, followed by the meso-scale and micro-scale. Thus, the trend of using remote sensed and/or global datasets in large catchments is more as compared to the use in small ones.

Further, we performed the co-authorship analysis on the articles in order to identify the collaboration patterns among the researchers. For this, VOSviewer software had been used and the method was selected as a full counting method. The threshold of a minimum of two articles by a researcher was chosen as there was no author who had authored three or more articles among the shortlisted articles. Out of 594 authors, only 46 met the threshold. Based on the strength of co-authorship link, 20 clusters were drawn, which are graphically presented in Figure 2.3.

It can be seen in Figure 2.3 that there are only three clusters where the number of authors is more than three. The largest clusters are cluster 1 (shown in red) and cluster 2 (shown

in green), which have seven authors each. Cluster 3 (shown is blue) is the third largest cluster, with five authors.

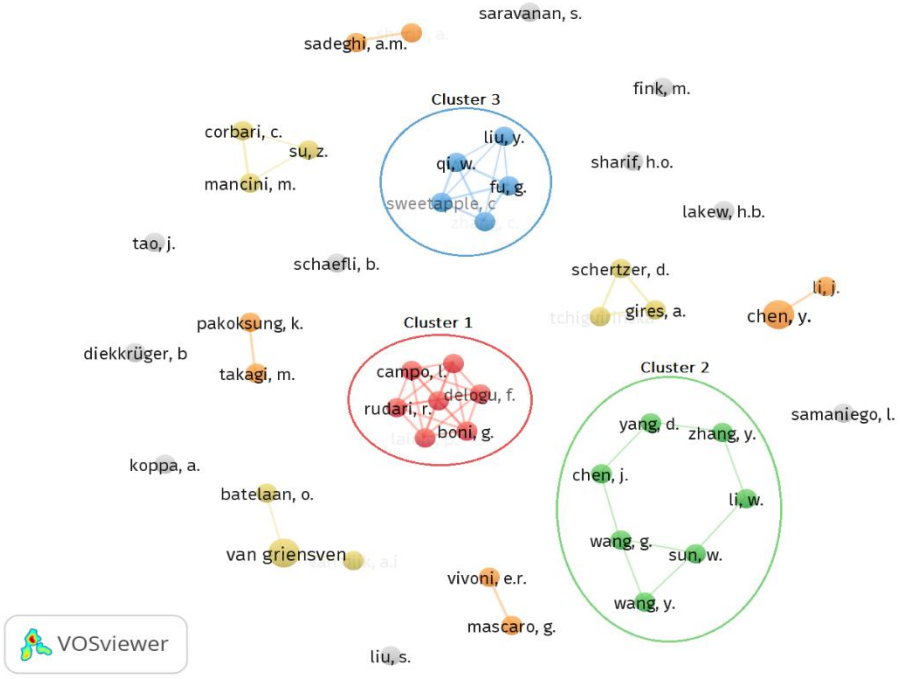

Figure 2.3. Clusters of authors collaboration patterns (the size of node is proportional to number of articles by the author)

The research work of the authors of cluster 1 is focused on assimilation of soil moisture in hydrological models. For cluster 2, the research work is more versatile, covering the subjects of stream flow simulation with limited observed data, the evaluation of satellite-based precipitation products, the merging of satellite-based precipitation products with in-situ data, the calibration of hydrological models with limited data and the evaluation of snow melt contribution in catchment hydrological processes. Likewise, the research work of the authors of cluster 3 is focused on flood simulation uncertainty and the uncertainty quantification of satellite-based precipitation for stream flow simulation. However, Figure 2.3 also represents that there are many authors which have no strong collaborations with others (represented in grey colour).

In order to better analyse the contributions of the authors regarding the use of remotely sensed datasets at different scales for the purpose of hydrological modelling, the following discussions have been categorized based on the type of datasets.

2.3.1 Rainfall Datasets

One of the main components of the water cycle is the rainfall. Given its importance, several efforts have been prompted regarding its estimation and the capture of spatio-

temporal variability on earth (Cui et al., 2019). For planning and decision-making in a variety of disciplines, including hydrology, meteorology, climate, and agriculture, its correct observation is crucial (Amjad et al., 2020). In hydrological models, precipitation data constitute central input that regulate the spatio-temporal variability of other hydrological fluxes (Thiemig et al., 2013).

In recent years, many remote sensed satellite-based rainfall datasets with high spatio-temporal coverage have been produced at a globe scale. These are available in near real time at zero cost (Khairul et al., 2018). Further, such estimates of precipitation from space are spatially uniform and encompass areas that are difficult to access (Beck et al., 2019). However, satellite-based datasets are vulnerable to both systematic and random errors due to various factors. For instance, these datasets are indirectly derived from radiance, which can lead to issues with sampling frequency and the algorithms used for estimation. Additionally, the accuracy of these estimation methods may vary depending on factors such as latitude, altitude, and the type of rainfall being measured (Ehret et al., 2012; Chen et al., 2016a). Considering these factors, such data products need to be evaluated with observed data.

Among the reviewed articles, there are six studies out of one hundred twenty in which the size of study area is in the range of micro-scale catchment. Only in one study, the authors analyzed the influence of rainfall variability on discharge simulation using physically based distributed hydrological model for small semi urban French catchment. For this study, Paz et al. (2019) used rainfall data from two radars. Unfortunately, at the micro-scale no author used the remote sensed satellite-based rainfall for hydrological modelling. Likewise, there are thirty-two studies in the reviewed articles where the study areas are in the range of meso-scale catchments. Surprisingly, no author used the remote sensed rainfall dataset for setting up a hydrological model even at this scale.

On the macro-scale, the in-situ rainfall data have been mostly used, a fact which revealed that the data observed in-situ are the first preference of the researchers. Many authors mentioned using remote sensed rainfall data products as well. It is notable that if only different types of remote sensed datasets are compared, then rainfall is among the most used remote sensed dataset. In some of the studies, the authors used both satellite rainfall data products and in-situ gauge data in combination. Few authors used the gauge data for the evaluation of satellite-based rainfall products. For instance, for the area of Biliu basin China, Qi et al. (2016) compared six rainfall products statistically with gauge station data and also with respect to hydrological simulation. These products are Tropical Rainfall Measuring Mission (TRMM) versions 3B42 and 3B42RT, Global Land Data Assimilation System (GLDAS), Asian Precipitation-Highly Resolved Observational Data Integration Towards Evaluation of water resources (APHRODITE), Precipitation Estimation from Remotely Sensed Information using Artificial Neural Networks (PERSIANN) and Global Satellite Mapping of Precipitation (GSMaP) products. They

developed two hydrological models for the analysis. The first one was fully distributed, while the second one was a semi-distributed hydrological model. The results showed that the APHRODITE rainfall dataset outperformed the five other datasets in statistical comparison with gauge data and also in stream flow simulation by both hydrological models. Likewise, Pakoksung and Takagi (2016) evaluated the performance of five rainfall data products (Global Precipitation Measurement (GPM), GSMaP, TRMM 3B42V7, Climate Prediction Center Morphing technique (CMORPH), and PERSIANN) as an input to rainfall–runoff–inundation (RRI) hydrological model for simulating run-off in the Nan River basin, Thailand. CMORPH and GPM was reported as the best performers based on the statistical comparison with gauge rainfall data while GPM has performed best with respect to stream flow simulation by the model.

As satellite-based rainfall datasets may have some systematic and random errors because of indirect estimation by remote sensing techniques, some researchers tried to correct them based on the use of in-situ data. For example, Khairul et al. (2018) evaluated four rainfall products statistically with gauge data. These datasets used were TRMM multi-satellite precipitation analysis (TMPA), Climate Hazards Group InfraRed Precipitation with Station data (CHIRPS), Multi-Source Weighted-Ensemble Precipitation (MSWEP) and GSMaP. They found that all products were weak in apprehending the magnitude and spatial distribution but good in capturing events. They used the merged product of these datasets for hydrological modelling of the Meghna catchment in Bangladesh. However, they did not compare the performance of the merged product with individual datasets in terms of their capability to simulate a hydrological model. Müller-Schmied et al. (2021) evaluated the performance of global hydrological model WaterGAP v2.2d based on total water storage anomalies, streamflow and water use using observed data. To simulate the model, they developed the homogenized series of precipitation data using the Water and Global Change (WATCH) forcing data (1901–1978) and WATCH Forcing Data ERA-Interim (WFDEI) (1979–2016). They further adjusted the data to the monthly precipitation sum based on Global Precipitation Climatology Centre (GPCC) data. The authors discussed the effects that modifications in the model algorithm and calibration routine had on the results, but did not make any explicit comments on the performance of the model based on the selection of forcing data.

A total of 17 different rainfall products in combination with 6 different temperature datasets are compared by Dembele et al. (2020) as inputs to the meso-scale hydrologic model (mHM) to simulate the hydrological process in the Volta River basin, Africa. The model simulations have been evaluated based on four parameters. These parameters are (1) in-situ stream flow data, (2) Global Land Evaporation Amsterdam Model (GLEAM) evaporation data, (3) European Space Agency (ESA) Climate Change Initiative (CCI) soil moisture data and (4) Gravity Recovery and Climate Experiment (GRACE) terrestrial water storage (TWS) data. Among the 17 utilized datasets, no single rainfall dataset

ranked first consistently with respect to evaluation parameters. Tropical Applications of Meteorology using SATellite data (TAMSAT), African Rainfall Climatology (ARC), Modern-Era Retrospective analysis for Research and Applications (MERRA-2) and MSWEP are best-performing datasets for streamflow, TWS, soil moisture and actual evaporation simulations, respectively. Lakew et al. (2020) evaluated the performance of five rainfall data products based on their capability to simulate daily flow in three catchments (Gilgel Abbay, Kessie station and Abbay basin) of Ethiopia using the Coupled Routing and Excess STorage (CREST) distributed hydrological model. The used datasets were CMORPH, TRMM TMPA 3B42v7, Re-Analysis (ERA) Interim, GPCC and MSWEP. The results indicated that the MSWEP rainfall data product performed better in flow simulation than the rest of them.

Similarly, Singh and Saravanan (2020) evaluated four rainfall products for the Wunna Riveris catchment in India and found that the Global Precipitation Climatology Project (GPCP) rainfall data, TRMM and APHRODITE to be more suitable products for the simulation of hydrological processes in India. Mao et al. (2019) evaluated three rainfall products, namely GLDAS, TRMM, China Meteorological Forcing Dataset (CMFD) and MERRA-2. They assessed that, for runoff simulation, MERRA-2 performed better for the Nujiang River basin, China.

Researchers have used a variety of rainfall datasets in their work. Their frequent use advocates their potential worth for hydrological modelling. However, if the aim is to determine one single dataset that is performing well in all catchments, then it is difficult to clearly identify a single product performing better from all perspectives. Datasets vary from catchment on the basis of size and region and depend a lot on evaluation criteria. For instance, either the evaluation criteria are a direct comparison of a dataset with in-situ observation, or the criterion is the capacity of a dataset to simulate the hydrological variables. These variables can be runoff, soil moisture, terrestrial water storage, actual evapotranspiration or others. Therefore, it is suggested to test and compare the hydrological simulation capability of different rainfall datasets for the aimed study area rather than relying only on a single dataset.

2.3.2 Digital Elevations Models

Topography influences the generation of overland flow in the physical hydrological models and is defined by the digital elevation models (DEMs). The river network, slope and drainage area are some of the key characteristics of catchments. These morphological attributes can be estimated by DEMs for representation in distributed hydrological models (Pakoksung and Takagi, 2021). Thus, the accuracy of these parameters is directly associated with the precision of DEMs. There are many procedures for the generation of DEMs, including photogrammetry, light detection and ranging systems, satellite optical imagery, SAR interferometry and field surveys. However, remote sensed technologies

have the advantage of being relatively less expensive, both in cost and time, at covering larger areas (Pakoksung and Takagi, 2021; Mohammadi et al., 2020).

In the reviewed articles, for the micro-scale catchments the authors have only used the national-level datasets for their research. For instance, Ichiba et al. (2018) developed the multi-hydro physically based distributed hydrological model of an urban catchment in France in order to understand the effect of model scale on its hydrological performance. They used the local DEM data from the National Institute of Geographic and Forest Information to carry out the analysis. Likewise, Her and Heatwole (2016) developed the 2D fully distributed hydrological model based on the time–area method to provide an alternative way to simulate hydrological processes. The modelling was performed on the Owl Run catchment using the national elevation data from the United States Geological Survey (USGS).

Similar trends have been observed at the meso-scale, with a greater focus on local or national sources of datasets. Some authors have mentioned using DEM data from the Shuttle Radar Topography Mission (SRTM) and Advanced Spaceborne Thermal Emission and Reflection Radiometer Global Digital Elevation Model (ASTER GDEM) for model development. However, they did not analyse the effect of selecting global DEM datasets on their findings. For macro-scale catchments, the trend of using DEMs is the opposite, with more researchers using global DEMs than local topographic datasets. Out of 79 articles, 52 studies used global DEMs, while only 12 utilized local or national-level topographic datasets. Among the global DEMs, SRTM was the most commonly used product, appearing in 28 articles, followed by the use of ASTER GDEM in 9 articles.

Out of the reviewed articles, only one study, that of Pakoksung and Takagi (2021), has compared the runoff and inundation area simulation performance of five satellite products for a 2011 flood event in the Nan River basin, Thailand, through distributed hydrological modelling. The datasets used were SRTM, ASTER GDEM, Global Multi-resolution Terrain Elevation Data 2010 **(**GMTED 2010), Global 30 Arc-Second Elevation **(**GTOPO-30) and Hydrological data and maps based on Shuttle Elevation Derivatives at multiple Scales (HydroSHEDS). For the simulation of run-off, GMTED 2010 performed comparatively better, while SRTM gave the highest accuracy for inundation area simulation. Although GMTED 2010 has a coarser resolution (1000 m by 1000 m), it performed better in run-off simulation as compared to other finer-resolution data products, whereas SRTM performed better for inundation area imitation. Some researchers have utilized multiple data products to cater to their utility needs. For instance, Ayala et al. (2020) used local 55 m contour lines, SRTM, and TanDEM-X datasets to extract DEMs for the years 1955, 2000, and 2013, respectively. They used the derived DEM for glacier change and runoff studies in the Maipo River basin, Chile. Similarly, Siqueira et al. (2018) used SRTM DEMs and HydroSHEDS data for flow accumulation. However, in these studies, the authors did not perform any performance evaluation.

The analysis showed that the use of global DEM datasets in the hydrological models is a common practice among the researchers. It is the only dataset where the use of remote sensed-derived global products has exceeded the use of local or national datasets. DEM is one of the essential inputs to the models and the accuracy of many terrain features, such as extents, slopes, elevations, is dependent on the accuracy of DEM. Despite its importance, only one study among the reviewed article is focused on the hydrological evaluation of different global DEMs (Pakoksung and Takagi, 2021). However, this study was limited to a macro-scale catchment and there is a lack of such evaluations for micro- and meso-scale catchments. The selection of a suitable source of DEM is an important step in the hydrological modelling procedure and the dearth of literature in this respect is concerning.

2.3.3 Land-Use Land-Change Datasets

Land cover plays a vital role in hydrology as it defines the properties of land surface in the models. In the physically based models, land cover represents the distribution of vegetation over the area which is used to calculate the spatial and temporal distribution of actual evapotranspiration (AET). In the overland component of models, the resistance to flow is represented by Manning values, which are often linked with the land-use type. Studies showed that the major portion of earth's surface is altered due to human's activities (Bhatta, 2010) and these changes are also represented in models through land-use land-change (LULC) maps. In recent years, there has been a proliferation of global-scale LULC datasets produced using remote sensing techniques. Despite the fact that these LULC datasets give a typical reflection of the Earth's surface, they still differ in certain ways, such as in the methodology used to collect data and to construct land-use maps, the number and type of sensors used for detections, their spatial resolution, and their classification definition (Yang et al., 2017). Nevertheless, many countries have developed their local- or national-level LULC datasets using classification techniques based on fine-resolution aerial or satellite images. Even though these products may be regarded as the best datasets to be input into hydrological models, their availability and quality cannot always be guaranteed (Chirachawala et al., 2020).

Among the reviewed articles, researchers have primarily used local- or national-level data products for all three catchment scales. At the meso-scale, the most frequent used regional or global data product is the Coordination of Information on the Environment (CORINE) land-cover map which has a spatial resolution of 100 m (Cenci et al., 2016; Heße et al., 2017; Höllering et al., 2018). For studies conducted in the USA, the National Land Cover Database (NLCD), produced by USGS and with a spatial resolution of 30 m, is the most commonly used dataset (Rajib et al., 2016; Gleason and Nolin, 2016; Evenson et al., 2018).

At the macro-scale, the most commonly used LULC dataset among the reviewed articles is the Global Land-Cover Characteristics (GLCC) by USGS (in 8 articles), followed by Globcover by ESA (in 7 articles), CORINE land-cover by Copernicus (in 5 articles) and moderate-resolution imaging spectroradiometer (MODIS) Terra+Aqua land-cover products (in 5 articles).

The literature shows that new LULC datasets can be prepared for specific areas by using techniques such as supervised, unsupervised and semi-supervised classification algorithms. For instance, Wang and Chen (2019) used the Landsat-8 satellite imagery to develop the land-cover maps for the Shahe Creek in Guangzhou, China, using support vector machine (SVM) algorithms, which are a type of supervised classification technique. They identified the key hydrological processes for flood forecasting by setting up the distributed hydrological model using the land-use map developed. Similarly, Gampe et al. (2016) derived the LULC map for the Gaza Strip from SPOT-5 satellite images, which are made to be used in a water balance simulation model (WaSiM) to assess future drought risk. However, they did not mention the technique used for the development of land-use maps.

Similarly, at the macro-scale, Maza et al. (2020) used (Linear Imaging Self-Scanning-IV) LISS-IV satellite images for the development of two LULC maps for the Kangsabati reservoir catchment India. The first had 8 vegetation classes, while the second had 16 vegetation classes. The study showed that the variable infiltration capacity (VIC) hydrological model, having a fine land-use dataset with 16 vegetation classes, had performed better in low as well as in high flows. Sahoo et al. (2021), Singh and Saravanan (2020) and Munzimi et al. (2019) used Landsat satellite images data to derive the LULC maps. Sharif et al. (2017) and Alataway and El Alfy (2019) used the satellite imagery data from the Landsat satellite as well as from the SPOT-5 satellite images for the development of the LULC map. Likewise, Arthur et al. (2020) used images data from Landsat satellite and MODIS satellite to derive the LULC map. These authors mentioned the development of land-cover maps using the satellite images, but they did not analyse the accuracy of using the specific algorithm to compile them or how this affects hydrological simulations.

Although global land-cover datasets are widely used, they may lack specific land-cover classifications that are required for certain studies, such as glacier coverage, crop type, etc. In light of this, some researchers have modified global land-cover maps by incorporating additional data sources to achieve the necessary specificity for their particular study. For instance, Mao et al. (2019) modified the GLCC data with glacier coverage data from the International Center for Integrated Mountain Development (ICIMOD) for Nujiang River basin, China. Similarly, Soulis et al. (2020) updated the CORINE land cover with data from the Integrated Administration and Control System, Greece, (IACS) for the agricultural part to be used in the distributed hydrological

modelling of Greece. However, no author evaluated the effect of LULC data source on the hydrological simulations. Only Busari et al. (2021) studied the effect of incorporating the multiple LULC maps into hydrological modelling. They developed two physically based distributed hydrological models using mHM modelling software for the Karasu Basin in Turkey. The first model was based on a single dataset of LULC from Globcover, while the second model was based on multiple LULC datasets sourced from CORINE for years 1990 and 2000 and from the MODIS land-cover product for years from 2001 to 2008. The research concluded that the model with multiple LULC datasets (dynamic) had better performance in flow prediction at outlet than the model having static information of the land use.

One of the crucial inputs in hydrological modelling is LULC data, and their usefulness needs to be carefully assessed. The common goal of the development of global LULC datasets is to develop a harmonized coverage for the whole globe that can be used for studies related to environmental assessment and climate change. The key characteristic of each initiative is that it is ensured that the same technique and classification rule is applied for the whole area. These exclusive properties make these products perfect inputs for hydrological modelling across different areas of the world. However, their taxonomy and class definition differ, resulting in a different legend (Chirachawala et al., 2020). The typical way of mapping LULC is through the use of field surveys. However, mapping at the catchment scale is time consuming and expensive, and in many cases is not practical (Wang and Chen, 2019). The applicability of global datasets to simulate hydrological models must be analysed in order to understand their performance in comparison to that of fine-resolution LULC datasets. Further, it is required to determine up to what standard these global datasets may be utilized as an alternative or as the only source in the data-scarce regions. Moreover, the literature review also depicts that there is a lack of such investigations.

2.3.4 Soil Distribution and Properties Datasets

Soil is one the dominant factors in regulating the hydrology of the catchment as it controls the streamflow generation, defines the flow path and influences the water balance. This makes the soil information an important input for physically based hydrological models (Worqlul et al., 2018). The limited availability of distributed soil information is common around the globe. This may be because the traditional soil survey methods are time consuming and expensive (Moore et al., 1993). Moreover, the soil information is not often readily available in formats suitable for inclusion in models (Lilly et al., 1998). During recent years, many global-scale soil distribution and properties datasets have been produced by many agencies with the aim to provide harmonized soil information coverage throughout the earth's surface. At the same time, many countries have their own soil information and properties databases.

Among the reviewed articles, researchers have primarily used soil information data from local or national databases for all three catchment scales. For instance, Ichiba et al. (2018) used the local soil data from the Bureau de Recherches Géologiques et Minières database for setting up the multi-hydro physically based distributed hydrological model of an urban micro-scale catchment in France. Similarly, Her and Heatwole (2016) used the national soil data from soil survey geographic database (SSURGO) for the hydrological modelling on Owl Run catchment, USA. It is important to mention that none of the reviewed articles used any global soil information dataset for micro-scale catchments.

At the meso-scale, few researchers mentioned using the global soil information datasets such as Digital Soil Map of the World (DSMW) by Food and Agriculture Organization (FAO) (Macalalad et al., 2021), Harmonized World Soil Database (HWSD) (Appel et al., 2019) and SoilGrids—global gridded soil information—by ISRIC (International Soil Reference and Information Centre) with a 1000 m resolution (Chen et al., 2016b). In one study, Wang and Chen (2019) noted that DSMW by FAO is not a recent dataset. Thus, the authors updated it based on the land-cover data and used it for hydrological model setup to identify the key hydrological process in the highly developed Shahe Creek catchment, China. However, in these studies, none of the authors evaluated the effect of soil-related datasets used at the meso-scale on hydrology.

At the macro-scale, the number of studies that have used the global soil datasets as compared to one using local soil inventories for distributed hydrological modelling are more. The most frequently used global products for soil distribution information are DSMW by FAO (13 articles), followed by its updated version HWSD (11 articles), SoilGrids by ISRIC (9 articles) and European Soil Database (ESDB) by European Soil Data Centre (ESDAC) (3 articles). In addition, some studies reported using two global products to extract the desired soil information for developing distributed hydrological models. For instance, SoilGrids by ISRIC plus The Global Lithological Map (GLiM) v1.0 data has been used by Dembele et al. (2020) and Dembélé et al. (2020) to develop hydrological models for the Volta River basin, Africa. SoilGrids by ISRIC, in addition to Global Hydrologic Soil Groups (HYSOGs250m) data for hydrologic soil groups identification, have been used by Al-Areeq et al. (2021) to develop two hydrological models for the Makkah region in Saudi Arabia using Gridded Surface Subsurface Hydrologic Analysis (GSSHA) fully distributed modelling tool and Hydrologic Engineering Center-Hydrologic Modelling System (HEC-HMS), a semi-distributed hydrological modelling tool. Busari et al. (2021) used ESDB in combination with HWSD, while Dahri et al. (2021) HWSD in combination with High-Resolution Soil Maps of Global Hydraulic Properties (HiHydroSoil) by Future Water. Ha et al. (2018) developed a new soil map by combining SoilGrids by ISRIC and DSMW by using unsupervised classification for the Red River Day basin, Vietnam. However, none of these studies performed a performance evaluation of the merged products.

Global soil datasets are frequently regarded as an alternate source of soil property information for large-scale hydrological modelling and for areas with limited local data (Huang et al., 2022). We analysed that, in the reviewed articles, few researchers used global soil products in combination with local data to achieve the required spatial resolution or to cover the intended study area. For example, Siqueira et al. (2018) mentioned using the Brazilian soil database in combination with DSMW to obtain soil properties at a 400 m spatial resolution and used in region-scale hydrological modelling of South America using Modelo hidrológico de Grandes Bacias (MGB), a large-scale hydrological model. Sharif et al. (2017) used local data plus DSMW for hydrological modelling of the Hafr-Al-Batin region in Saudi Arabia. Huang et al. (2019) used local data plus soil information by ISRIC to develop a hydrological model of Norway. Yet, again, none of these studies performed a performance evaluation of the merged products.

Global soil information datasets give the traditional reflection of earth's soil characteristics but they also vary in many aspects such as their mode of compilation, spatial resolution, number of incorporated soil profiles, number of depth layers. Most of these datasets are developed from soil surveys in one of two ways. The first way is the linkage method in which the soil profiles and soil mapping units are linked to form polygon-shaped soil type maps. The second method is digital soil mapping, in which machine learning techniques are used to map the spatial distributed soil properties. However, global soil datasets represent the average state of the last decades (Huang et al., 2022; Dai et al., 2019). We analysed that, on one hand, many researchers have used the global soil information datasets for setting up the hydrological models but that, on the other hand, in the reviewed articles, no scholars evaluated the hydrological performance of these soil datasets. In light of this, there is a necessity to investigate the influence of these global datasets on hydrological simulations in order to determine the extent to which these datasets can be trusted as the only sources in data-scarce regions.

2.3.5 Leaf Area Index Datasets

Vegetation plays an important role in the hydrological process as it determines the separation of rainfall into runoff and ET, tasks which it performs largely through 2 processes. One is transpiration through the canopy and the other is loss by interception (Vertessy et al., 2001). Transpiration mostly varies according to leaf area index (LAI). Changes in LAI not only influence the ET but also the soil moisture. Consequently, other processes in the catchment will be affected such as baseflow, recharge, saturation and infiltration (Western et al., 1999). Therefore, the improper dynamic representation of LAI in the hydrological model may result in a poor performance of the model (Tesemma et al., 2015).

At the meso-scale, some researchers in the reviewed articles used the LAI values from the field surveys found in the literature. For instance, Sonnenborg et al. (2017) use the

values of LAI from the literature related to phenology to set up a MIKE-SHE-SWET model for the Skjern River and Lejre catchment Denmark with the aim to test the impact of forest type and coverage on water resources. Gleason and Nolin (2016) study effect of forest fire on snow ablation and snow-cover duration using the SnowModel for Oregon Cascades catchment in the USA. They modified the values of LAI in the model to postfire conditions based on field values and were able to capture the snow water equivalent (SWE) values. Gampe et al. (2016) used the value of LAI from literature to set up the WaSiM hydrological model for the Gaza Strip, Palestine, to assess future drought risk. For the in-situ measurement of LAI, the number of techniques are available such as destructive sampling, allometry, optical observations (Jonckheere et al., 2004) but the problem is that these techniques are geographically limited as well as cost and time expensive.

In the past few years, many global LAI datasets have been produced with moderate resolution. The estimation of LAI from remote sensing data is mostly derived from one of these methods: passive optical sensors, the active light detection and ranging instruments, and microwave sensors using empirical transfer and model inversion methods (Fang et al., 2019). In the reviewed articles, for meso-scale catchments, the authors had used the remote sensed LAI for setting up the distributed hydrological model. However, they did not explicitly comment on the hydrological performance quality of these datasets. For example, Cornelissen et al. (2016) developed a distributed hydrological model of Erkensruhr catchment in Germany to study the parametrization of the hydrological model by transferring calibrated parameters from a well-equipped head water catchment. They used the monthly mean value of LAI, derived from the MODIS/Terra-8-day LAI (MOD15A) dataset at a spatial resolution of 1 km, as an input for the model. Abiodun et al. (2018) set up the SWAT hydrological model for the Sixth Creek catchment in Australia to compare the MODIS Actual ET with the simulated ET from the SWAT model and used the LAI value from the default SWAT database.

The commonly used remote sensed LAI products at a macro-scale level were the Global Inventory Modelling and Mapping Studies (GIMMS) LAI (mentioned in 3 articles), MODIS/Terra+Aqua (MCD15A) LAI (mentioned in 3 articles), and MOD15A LAI (mentioned in 5 articles). While the researchers incorporated global LAI datasets as inputs into their hydrological model, their study's primary focus was not on LAI, and they did not assess the impact of using these specific data products on the model's performance. Out of the reviewed articles, only that of Rajib et al. (2018) utilized the MCD15A LAI product to evaluate the SWAT hydrological model of Pipestem Creek catchment located in North Dakota, USA. Their findings revealed that calibrating the model with spatial ET enhanced the model's performance in simulating both ET and LAI. In contrast, only one study conducted by Jiang et al. (2020) incorporated dynamic vegetation properties by utilizing the advanced very high-resolution radiometer (AVHRR) LAI record from 1981 to 1994 in the VIC hydrological model for the Columbia River basin located in the USA.

They updated the model with the Global Land Surface Satellite (GLASS) / MODIS LAI for the duration from 2004 to 2013. The results showed improvement in evapotranspiration and run-off simulation.

The LAI is an important biophysical variable in process-based modelling. For the assessment of this index, remote sensing has emerged as the major source, both at the local and global levels (Kappas and Propastin, 2012). These global LAI products have been used as input data in the reviewed articles for the development of hydrological models and their inclusion in the modelling setup has the potential to improve the model performance, as reported by Jiang et al. (2020). Although researchers have used different LAI datasets from various sources as inputs in their hydrological models, they have not specifically examined how different LAI datasets affect model performance. Such analysis would be essential in understanding variability in model results due to different LAI inputs, which can be particularly important in areas where ground-based LAI measurements are not readily available. It would also help to identify the most suitable LAI product for a given study area and hydrological model, potentially improving the accuracy of model predictions. Therefore, future research could focus on conducting a comparative analysis of different LAI datasets and evaluating their impact on hydrological model simulations.

2.3.6 Snow-Covered Area Datasets

Glaciers and seasonal snow packs are the sources of water for one sixth of the global population (Barnett et al., 2005). Snowmelt makes a noteworthy contribution to hydrology as it influences the vegetation growth and the consumption of water resources. In cold and mountainous catchments, snowmelt is a major contributor of water supply, especially in the middle and lower portions of these areas (Li et al., 2019). Snow cover is also an indicator of climate change, as increase and decrease in this is temperature dependent (Brown and Mote, 2009). Therefore, the accurate assessment of snow-related parameters is of considerable importance in hydrology.

One of the traditional methods to measure snow parameters is through ground-based monitoring of snow characteristics, along with other variables, at a meteorological station. However, the availability of in-situ readings is still very limited because of several reasons including remote and far off areas, cost expensive and laborious (Appel et al., 2019).

In recent years, remote sensing technology has been considerably advanced and can be used as a substitute for traditional methods to obtain snow-cover information at catchment level. It can also provide near real-time monitoring of snow cover over large areas (Dong, 2018). For instance, at the meso-scale, Gleason and Nolin (2016) used MODIS snow-cover product (MOD10A1) for the calculation of snow-cover frequency to study effect of pre- and post-forest fire on snow ablation and snow-cover duration. Similarly,

Teweldebrhan et al. (2018) used MODIS Aqua (MYD10A1) and MODIS Terra (MOD10A1) snow-cover products for parameter uncertainty analysis in addition to the assessment of stream flow data.

Another approach for the estimation of snow cover is through the hydrological model, which is based on meteorological and geomorphological data. In the reviewed articles, studies have been found in which the researchers have used hydrological models for snow simulation and used the remote sensed snow-related datasets for the evaluation of model simulated snow parameters. For example, at the meso-scale, Mimeau et al. (2019) used MODIS satellite images to derive a snow-cover map with spatial resolution of 250 m for the Pheriche sub-catchment of the Dudh Koshi basin in Nepal and used this snow-cover map to evaluate the simulated snow-cover area using the glacio-hydrological model (DHSVM-GDM), in addition to assessing outflows and glacier mass balances. Appel et al. (2019) derived binary information, conveying whether the snow is dry or wet from, Sentinel-1 satellite images and used these data to validate the simulated snow information with the Processes of Radiation, Mass and Energy Transfer (PROMET) model for the Forêt Montmorency catchment, Canada. Multitemporal snow extent maps derived from Landsat satellite images, in addition to MODIS SCA products (MOD10A1 and MYD10A1), were used by Hanzer et al. (2016) to validate AMUNDSEN model simulations.

Likewise, at the macro-scale, Luo et al. (2017) used a MODIS (MOD10A2) data product to compare with MIKE-SHE-modelled snow cover and found the model to be performing adequately. Ren and Liu (2019) developed a distributed hydrological model for the Upper Yangtze River basin, China, using MODIS land surface temperature, daily snow-cover data products (MOD10A1 and MYD10A1) and in-situ data to calculate snow depths, while special sensor microwave/imager (SSM/I) snow-cover data were used to validate the model's results. The Global Randolph Glacier Inventory (RGI), the Global Land Ice Measurements from Space (GLIMS) geospatial glacier database and the Glacier Monitoring of Switzerland (GLAMOS) database were utilized by Imhoff et al. (2020) for glacier coverage and initial storage assessment in order to be input into the hydrological model. Liao and Zhuang (2017) used cloud-free MODIS images for snow-cover data. Li et al. (2019) validated the snow distribution model results with integrated product of MODIS Terra/Aqua and local data (Interactive Multi-sensor Snow and Ice Mapping System) for catchment in the Tibetan Plateau region. Ayala et al. (2020) used the MODIS SCA product in addition to Snow Water Equivalent (SWE) data from the Chilean version of the Catchment Attributes and Meteorology for Large-Sample Studies (CAMELS-CL) database for calibration and validation of the Topographic Kinematic Approximation and Integration (TOPKAPI)-ETH hydrological model for the Mapio River basin in Chile. Overall, the performance of the model in flow simulation was improved, but the

individual effect of including the SCA product in the calibration process was not reported and/or analysed.

From the reviewed articles it can be observed that, although different snow-related remote sensed datasets have been used by researchers, no one has compared these datasets with in-situ measurements. Moreover, no study can be found in which the remote sensed and/or global SCA or SWE products from different sources have been compared with each other or with the modelled results. Further, no author explored the potential of these products for assimilation into distributed hydrological models. Remote sensing techniques have the potential to estimate the snow properties well at different scales. However, there are several limitations as well. For example, remote sensing snow data gathering started in the past decades so the length of available data is limited and the observations may be influenced by cloud cover, leading to large errors. Further, the misclassification of surface features due to spectral misperception is possible (Dong, 2018). Therefore, the evaluation of the global snow datasets is required to determine their suitability for use in hydrological applications.

2.3.7 Evapotranspiration Datasets

Evapotranspiration (ET) and precipitation are among the main components of the water balance in most of the hydrological systems (Nachabe et al., 2005). ET often exceeds precipitation, particularly in arid and semi-arid regions, and creates a sink for groundwater (Raz-Yaseef et al., 2012). Thus, the reliable assessment of ET is important for effective water management.

ET is traditionally measured through ground-based methods such as Bowen ratio-energy balance, eddy covariance, large aperture scintillometers and lysimeters (Liu et al., 2013), but these are often not well spatially distributed (Glenn et al., 2007). Further, different measurement methods have different associated uncertainties and errors related to instrument installation (Zhang et al., 2008; Allen et al., 2011). The availability of remote sensed data has eased the spatial estimation of ET (Abiodun et al., 2018). The variables that are derived from remote sensing data, such as land surface temperature, reflectance and vegetation indices, can be used to develop algorithms for ET estimation. Moreover, the cost of finer-resolution ET products covering the wide range is significantly lower than that of observing through ground-based monitoring stations (Bugan et al., 2020).

There are many hydrological and remote sensing-based surface energy balance models currently in use for simulating ET datasets. In the reviewed articles, the researchers have used the actual evapotranspiration (AET) datasets for four different purposes, namely the (1) calibration, (2) validation, (3) assimilation and (4) evaluation of the ET products, by comparing them with modelled results. Surprisingly, there is no study related to micro-scale catchments in which an ET dataset has been used. At the meso-scale, Gampe et al. (2016) used satellite the Landsat TM Images dataset to calculate actual evapotranspiration

in order to validate simulated AET by WaSiM hydrological model for the Gaza Strip, Palestine, for drought studies. Interestingly, there was only one AET product (MODIS MOD16A) that had been evaluated by undergoing a comparison with model results in two studies. In the first study, Abiodun et al. (2018) performed the hydrological modelling using SWAT for Sixth Creek Catchment, Australia, and evaluated the MODIS AET data product MOD16A with model simulated AET. The authors reported good agreement between MODIS AET and SWAT ET on the catchment scale but the poor agreement at the fine scale. Similarly, in the second study, Bugan et al. (2020) evaluated MOD16A with simulated AET by using the Jena Adaptable Modelling System (JAMS) J2000 for the Sandspruit catchment, South Africa. In this study the authors reported a good correlation at the catchment level and poor results at the hydrological response unit (HRU) level.

At the macro-scale, researchers have primarily used AET datasets for the calibration and validation of hydrological model simulations. For instance, Dembélé et al. (2020) evaluated the potential of 12 satellite or reanalysis evaporation datasets in improving model performance of mHM modelling tool through calibration for the Volta River basin, West Africa. These datasets are MOD16A2, Operational Simplified Surface Energy Balance (SSEBop), Atmosphere-Land Exchange Inverse (ALEXI), CSIRO MODIS Reflectance Scaling EvapoTranspiration (CMRSET), Surface Energy Balance System (SEBS), Global Land Evaporation Amsterdam Model (GLEAM) v3.2a, GLEAM v3.3a, GLEAM v3.2b, GLEAM v3.3b, ERA-5, MERRA-2 and Japanese 55-year ReAnalysis (JRA-55). Further, they used ESA CCI Soil Moisture (SM) v4.2 dataset along with terrestrial storage data from GRACE and in-situ streamflow data for evaluation of hydrological model simulations. All calibration strategies outperform streamflow only calibration. MERRA-2, GLEAM v3.3a and SSEBop gave the best performance as calibration datasets.

Nesru et al. (2020), used MODIS (level 1-B) satellite data along with meteorological data for calculation of AET by SEBS for the upper Omo–Gibe basin, Ethiopia. The authors used this calculated AET along with stream flows for calibration of the hydrological model. Further, they also used AET from SEBS in addition to stream flows for validation of model results and reported that the inclusion of AET in calibration had improved the model performance compared to the case where the model was calibrated only with stream flows. Becker et al. (2019) reported the use of AET derived by MODIS (level 1-B) satellite data by Surface Energy Balance Algorithm (SEBAL) and modified it based on land use. The modified data was used for calibration of the SWAT hydrological model for the Lower Chenab Canal System, Pakistan. The mean Kling–Gupta Efficiency (KGE) of the HRUs in simulating AET improved from 0.27 to 0.40 by using the modified SEBAL AET for calibration in comparison to the model which was calibrated with unmodified SEBAL AET. The authors recommended a detailed analysis of spatial

variability of SEBAL AET for using it for model calibration. Similarly, Pan et al. (2018) used SEBAL to calculate the AET based on MODIS satellite images data and used it for calibration of Distributed Hydrology Soil Vegetation Model (DHSVM) of the Jinhua River Basin, China. The authors achieved the reduction in equifinality by considering multiple variables in the calibration of the model. Koppa et al. (2019) used GLEAM AET data for calibration of hydrological model for the Omo–Gibe River basin, Ethiopia. It improved the ET simulation sense of the model. Jin and Jin (2020) also used the GLEAM AET for calibration of the SWAT model for the Bayinhe River basin in northwest China. The authors reported the improved simulation of stream flows and water balance.

Rajib et al. (2018) included the MODIS ET data in the calibration of each sub-catchment in the SWAT model by a spatially explicit approach and were not only able to achieve improvements in simulated ET and flows but also obtained more realistic results of vegetation growth. Similarly, the MODIS AET product has been used by Jiang et al. (2020) for spatially distributed model calibration of the VIC hydrological model of the Columbia River basin, North America. They reported that 75 % of the sub-basins showed the improved or comparable KGE values for streamflow simulations as compared to the base-model. Kunnath-Poovakka et al. (2016) used Advanced Microwave Scanning Radiometer-Earth Observing System (AMSR-E) version 5.0 (25 km) soil moisture data along with Evapotranspiration data from CMRSET for the calibration of the gridded Australian Water Resource Assessment—Landscape (AWRA-L) hydrological model in order to evaluate its efficiency in streamflow prediction. The authors analysed fifteen different objective functions to carry out the calibration and reported that most of the objective functions performed satisfactory in the catchments with medium to high average flows. This is the only found study among the reviewed articles in which the authors also compared the CMRSET AET with the ground station AET for the dry Loddon River catchment, Australia, and CMRSET underestimated on most of the days. Herman et al. (2018) explored two different techniques of model calibration using local data of streamflow and spatially distributed AET dataset from SSEBop model (1 km) and ALEXI model (4 km). They concluded that better simulation results can be achieved by selection of the right calibration technique. So not only the inclusion of AET in calibration can bring positive impact but also the selection of right calibration technique is equally significant. Ha et al. (2018) ensembled linearly four different ET models, i.e., SEBS (5 km), CMRSET (5 km), SSEBop (1 km), and MOD16A (1 km). The ensembled ET data in addition to LAI data were used for calibration of the SWAT model developed for the Red River Day Basin, Vietnam. Overall, in these studies, the authors reported the improved model simulated results by incorporating AET in calibration. Moreover, the issue of equifinality can also be addressed by considering multivariate calibration.

Like multi-objective calibration, it is a better practice to evaluate the model performance based on multiple variables instead of relying on a single output. Considering this, few

researchers used the remote sensed-based AET data products for evaluating the model simulated AET in addition to other observed or remote sensed variables. For example, Lazin et al. (2020), in addition to discharge and Terrestrial Water Storage Change, used the GLEAM AET data for validation of hydrological model simulations for Upper Blue Nile catchment, Ethiopia. Imhoff et al. (2020) used AET data from the Land Surface Analysis Satellite Application Facility (LSA SAF), for validation of the hydrological model of three sub-basins in Rhine basin along with discharge and snow water equivalent data. AET, calculated through ETwatch software, has been used by Zhang et al. (2020c) for the evaluation of DHSVM model results to compare the performance of two different interpolation techniques of precipitation data. Likewise, Zhang et al. (2018) and Hedrick et al. (2020) used the MODIS ET dataset for validation of hydrological model performance. Although the researchers had used different AET datasets for evaluation of their model's performance, they did not comment on the liability or accuracy of these used remote sensed-based AET products.

From the reviewed articles, only one study is about the use of AET product for assimilation into hydrological model. In this study, Hartanto et al. (2017) calculated AET from MODIS / Terra satellite data using ITA-MyWater algorithm and used the calculated AET for assimilation into the distributed hydrological model for the region of Rijnland, the Netherlands. The results showed an increase in precision of simulated discharge.

The use of remote sensed-based AET datasets by the researchers show their potential to bring improvement in the simulation of the hydrological processes. However, for the small catchments with highly varied land use, keeping the spatial heterogeneity of remotely sensed datasets intact, remain one of the main challenges (Becker et al., 2019). The performance of datasets also varies across different climatic zones (Dembele et al., 2020). Moreover, none of remote sensed dataset can be regarded as actual observations as uncertainties are common in them (Rajib et al., 2018). Among the reviewed articles, only the MODIS AET product has been evaluated against the simulated AET from hydrological models (Abiodun et al., 2018; Bugan et al., 2020) and reported a poor performance at a fine scale. Further, only in one study (Kunnath-Poovakka et al., 2016), the comparison of AET products with the ground-based observations has been performed and even in that, remote sensed AET product is reported to be under estimating. Therefore, the accuracy of these datasets relative to one another and ground observations should be extensively explored to improve our understanding of the ET estimation from different algorithms and sources.

2.3.8 Soil Moisture Datasets

In hydrology, soil moisture regulates the nonlinear separation of rainfall into infiltration and runoff. The knowledge of soil moisture in the catchment before any meteorological event, is an imperative factor to be known, as for the same rainfall magnitude, different

soil moisture states may lead to different hydrographs (Cenci et al., 2016). Similarly, in many of the hydrological models, the soil moisture steers the partition of water and energy fluxes. Thus, the better representation of soil moisture in the models has a potential to enhance the simulation accuracy of other key variables as well (Hostache et al., 2020).

Like other meteorological variables, soil moisture is commonly measured by in-situ observations but these ground base observations give local readings. Further, considering the spatio-temporal variability of soil moisture, these methods have limitations and lack proper coverage (Jiang and Wang, 2019; Seneviratne et al., 2010). On the other hand, the satellite based remote sensing technique can provide large scale observations and the problem of poor spatial representation can be resolved (Cenci et al., 2016; Kumar et al., 2018). The microwave remote sensing, both active and passive, are among the widely and commonly applied methods for estimations of soil moisture (Wanders et al., 2012). However, these estimations cannot be blindly trusted as passive microwave products performed more reliable over bare to sparsely vegetated areas (Brocca et al., 2011) while active microwave products gave better estimates over moderately vegetated areas (Liu et al., 2012).

For the micro-scale catchment, no article found where the remote sensed soil moisture data has been used for hydrological applications. At the meso-scale, remote sensed soil moisture satellite products have been used by few researchers with the purpose of performing calibration, model evaluation and assimilation. For example, Rajib et al. (2016) used the gridded soil moisture dataset AMSR-E Aqua daily level-3, version 2, having a resolution of 25 km in addition to streamflow data at the outlet for calibration of a SWAT model for two catchments in the USA: Upper Wabash (macro-scale) and Cedar Creek (meso-scale). In addition to AMSR-E soil moisture, the authors also used in-situ soil moisture data for calibration in the case of Cedar Creek. No major change in stream flow simulation has been observed due to the application of soil moisture in calibration. Conversely, improved soil moisture simulation by model was reported in the case of Cedar Creek, where KGE improved from 0.13 to 0.35 when the calibration was performed with in-situ soil moisture data. In contrast, KGE remained almost the same upon performing the calibration using AMSR-E Aqua daily soil moisture. However, any direct comparison of in-situ soil moisture with AMSR-E Aqua daily soil moisture was not reported. Khan et al. (2018) used the surface soil moisture data product ESA CCI SM for evaluating the performance of a model built on an equivalent cross-section-based semi-distributed hydrologic modelling approach for the McLaughlin catchment, Australia, to simulate the soil moisture. The authors did not comment on the quality of soil moisture product used.

Cenci et al. (2016) tested the effect of soil moisture assimilation on discharge prediction by using a Continuum distributed hydrological model of the Orba, Casentino, and Magra catchments in Italy. Three soil moisture products from H-SAF were tested. These

products were SM-OBS-1, available at 25 km resolution, SM-OBS-2, available at 1 km resolution data product and SM-DAS-2, available at 25 km root zone soil moisture data product. The enhancement of discharge prediction has been assessed by using all three products. However, SM-OBS-1, despite having coarse resolution, outperformed others as assimilation data. The authors also concluded that the results of assimilation are also strongly dependent on catchment characteristics. Similarly, Laiolo et al. (2016) used four soil moisture data products for testing the effect of soil moisture data assimilation into a Continuum hydrological model for the study area, i.e., Orba, Italy. Three of the used datasets (SM-OBS-1, SM-OBS-2, SM-DAS-2) were from H-SAF while the fourth, Soil Moisture Content (SMC) Level 2, was obtained from the Soil Moisture and Ocean Salinity (SMOS) mission of the ESA. The authors reported that the assimilation of SM-OBS-1 and SM-DAS-2 data provided the greatest benefit in discharge prediction.

Likewise, in the reviewed article related to macro-scale catchments, it can be seen that the remote sensed soil moisture datasets have mostly been used for calibration, evaluation and assimilation in hydrological models. For instance, Dembélé et al. (2020) evaluated the potential of 12 satellite or reanalysis evaporation datasets to improve performance through model calibration and used ESA CCI SM (v4.2) soil moisture data product, along with terrestrial storage data from GRACE and in-situ streamflow data, for the evaluation of hydrological model simulations. Similarly, Dembele et al. (2020) tested the suitability of 17 rainfall and 6 temperature data products for hydrological modelling and evaluated model response using GLEAM v3.2a AET, ESA CCI SM v4.2 soil moisture and GRACE terrestrial water storage. Strohmeier et al. (2020) used ET from GLEAM v 3.0 and soil moisture data from ESA CCI SM v02.2 in calibration of SWAT and PCRaster Global Water Balance (PCR-GLOBWB) model for surface a flow and drought management study in the Oum Er Rbia basin, Morocco. The models showed the good simulation of surface flow, even without the consideration of in-situ data in calibration. Leroux et al. (2016) assimilated SMOS L3 soil moisture product into the DHSVM distributed hydrological model and revealed that the soil moisture assimilation can have positive impacts on hydrological variable estimations. Abhishek and Kinouchi (2021) used GRACE data, PCR-GLOBWB simulations, and in-situ groundwater data for the assessment of Terrestrial water storage, soil moisture storage (SMS) and groundwater storage for the Godavari, Krishna and Mahanadi river basins in India. Soil moisture was simulated by PCR-GLOBWB using the TRMM 3B43 rainfall data, which were corrected based on gauge data. The authors noted that, by using these global datasets, it is possible to quantify the different components of water storage for any catchment worldwide. However, the study did not comment on the performance evaluation of the datasets used in the research.

Among the reviewed articles, only Van Der Velde et al. (2021) validated the SMAP passive-only soil moisture products, using the in-situ soil moisture data and model

simulations devised by the Dutch National Hydrological Model (LHM) for the region of Twente, the Netherlands. The authors concluded that the single-channel algorithm at vertical polarization (SCA-V) is a better algorithm compared to the single-channel algorithm at horizontal polarization (SCA-V) and the dual-channel algorithm (DCA). Moreover, the SMAP's soil moisture values in the afternoons are closer to in-situ observed values as compared to morning values.

Overall, the use of soil moisture remote sensed products as calibration datasets or for assimilation has been assessed by researchers in the reviewed articles, but any uniformity in the results with respect to improvement in hydrological simulation is hard to ascertain. These are dependent on a number of factors such as the type of datasets used, the catchment characteristics, assessment criteria, modelling structure, techniques and algorithms used for calibration and/or assimilation, and so on. Moreover, it is difficult to pick a single better-performing dataset for any of the cases. Among the reviewed articles, only one study (Van Der Velde et al., 2021) conducted the validation of SMAP passive-only soil moisture products against the in-situ observation. Overall, the validation of such data products before their use in applications such as model calibration, validation or data assimilation need further exploration to increase confidence in their applicability.

2.3.9 Temperature Datasets

Air temperature plays a crucial role in climate research, serving as a valuable proxy for energy exchange between the land surface and the atmosphere (Hansen et al., 2010). Commonly, air temperature is measured at a height of around 2 m above the land surface. It is considered a critical parameter in glacio-hydrological studies, as it controls the rate of snow and ice melting (Kumar et al., 2016). Similarly, the land surface temperature (LST) is the temperature of the Earth's top layer, known as the canopy skin, and provides an indication of its perceived hotness or coldness (Bense et al., 2016). Air temperature is closely related to LST. The difference in temperature between the air and the surface is an important parameter for calculating the convective heat loss from the earth surface to the air. The heat loss is used for the calculation of the surface energy balance (Seiler and Moene, 2011). Additionally, the temperature difference between the earth surface and the air is particularly relevant for estimating evapotranspiration (Stoll and Brazel, 1992).

Similar to the other datasets needed for hydrological modelling, obtaining measurements of air temperature using in-situ meteorological stations can be expensive as it involves significant instrumentation and maintenance costs. This costliness often results in sparse spatial continuity of data, especially in remote environments (Singh et al., 2019). Due to the synoptic spatial coverage, satellite LST has become a good alternative for assessing air temperature. There are five commonly used methods for estimating air temperature from LST. These methods include statistical approaches, the empirical solar zenith angle approach, the energy balance approach, the temperature–vegetation index approach, and

the neural network approach (Shah et al., 2013). Although satellite LST data can help researchers to overcome many of the limitations and difficulties associated with in-situ measurements, thermal infrared remote sensing data requires correction for atmospheric and surface emissivity, which can introduce significant uncertainties. In addition, due to the spatial heterogeneity of the land surface, the satellite instrument footprint may encompass various canopy types and soils, which can exhibit large variations in emissivity and LST over both space and time. Consequently, satellite measurements tend to represent a complex weighted mean temperature within each pixel, which can make retrieving and interpreting LST data a challenging task (Guillevic et al., 2012).

The articles reviewed showed that no studies have utilized remote sensed LST or air temperature datasets at the micro-scale. Furthermore, at the meso-scale, there was one study that used LST datasets for assimilation in hydrological models. In this study, Laiolo et al. (2016) incorporated four soil moisture data products and one LST product to evaluate the impact of data assimilation on the Continuum hydrological model in the Orba, Italy. The LST product used was the Satellite Application Facility on Land Surface Analysis (SAFLSA) from the European Organisation for the Exploitation of Meteorological Satellites (EUMETSAT). The effect of assimilation was analyzed by considering the model's discharge simulation performance at the outlet. The authors reported that the assimilation of soil moisture datasets was more effective compared to that of LST dataset. Although the assimilation of LST resulted in an improvement in the Nash–Sutcliffe efficiency (NSE) from 0.63 to 0.64, the improvement was not as significant as that achieved through soil moisture assimilation. In addition, the authors emphasized that careful pre-processing of the LST data is required for several reasons. These include the importance of precise geometric registration between model and satellite pixels, the possibility of shadowing due to mountainous terrain, and variations in the satellite viewing angle across different pixels resulting from the sensor scanning geometry. However, due to the lack of ground data, the authors were unable to evaluate the accuracy of the remote sensed LST using local observed data.

At the macro-scale, air temperature has been used as forcing datasets in hydrological models. For instance, Dembele et al. (2020) used 6 different temperature reanalysis datasets in combination with 17 different rainfall products as forcing data for the mHM modelling tool to simulate hydrological processes in the Volta River basin in Africa. The temperature datasets used are JRA-55, EWEMBI, WFDEI, MERRA-2, PGF and ERA5. They evaluated a total of 102 combinations of rainfall–temperature data based on four parameters: (1) in-situ stream flow data, (2) GLEAM evaporation data, (3) ESA CCI soil moisture data, and (4) GRACE TWS data. They ranked different temperature datasets in combination with rainfall datasets using multiple criteria. For instance, during the evaluation period, the MERRA-2 temperature dataset was ranked first based on the mean KGE of stream flow simulations, while the WFDEI dataset was ranked first based on the

mean NSE of stream flow simulations. The authors reached the conclusion that there was no single temperature dataset that consistently outperformed others in reproducing the spatio-temporal variability of all hydrological processes.

In another study, Sen-Gupta and Tarboton (2016) developed a downscaling approach and utilized MERRA temperature data to test their approach. To evaluate their method, they compared MERRA temperature data with temperature data from 173 snowpack telemetry (SNOTEL) sites operated by the U.S. Department of Agriculture in Utah, Nevada, Idaho, and California. The results showed that the NSE of the downscaled daily mean temperature increased from 0.83 to 0.84, while the NSE for daily maximum temperature increased from 0.23 to 0.86. Notably, the NSE value of 0.83 for mean temperature on direct comparison with SNOTEL's site data suggests a good performance for the MERRA data, whereas the NSE values for maximum temperature were not as high.

Two studies were found where the authors performed biased correction of the temperature datasets before using them for modelling purposes. Beck et al. (2020) explored the parameter regionalization approach by using streamflow data from 4,229 catchments, and they tested the approach by implementing it on a global scale using a distributed version of the HBV hydrological model. The authors used temperature data from both the ERA-Interim and JRA-55 datasets, which were bias-corrected and averaged before being incorporated into the model. However, the effects of bias correction on the model performance were not reported by the authors. Dahri et al. (2021) utilized temperature data from the ERA5 reanalysis dataset, which had been recommended by a previous study for Indus catchment. Prior to using the data as forcing data for the VIC hydrological model, the authors conducted a bias correction. The authors also noted that existing global- and regional-scale gridded datasets are inadequate for capturing accurate meteorological variables in complex and orographically influenced high-mountain terrains.

In some of the reviewed studies, authors used temperature datasets as inputs for their models. However, they did not comment on the performance of these datasets and only used them for their intended purposes. For instance, Singh and Saravanan (2020) used temperature data from Climate Prediction Centre (CPC) of the National Oceanic and Atmospheric Administration (NOAA) for the Wunna Riveris catchment in India. Rajib et al. (2018) used temperature data from Daily Surface Weather Data for North America (Daymet) for a catchment in North Dakota, USA. Busari et al. (2021) used temperature data from the European gridded dataset of daily observations version 20 (E-OBS 20.0e) and also from MODIS for the Karasu catchment in Turkey. Lazin et al. (2020) used temperature data from ERA-Interim for the Upper Blue Nile catchment. Ha et al. (2018) and Mao et al. (2019) used air temperature datasets from GLDAS for Vietnam and the Nujiang river catchment in China, respectively. However, the lack of comment on the performance of the temperature datasets used in these studies makes it difficult to assess

the accuracy and reliability of these datasets. It is important to evaluate the performance of the input temperature datasets to ensure the validity of the hydrological model simulations.

In the reviewed articles related to macro-scale uses, LST datasets have been found only in three studies. In two of them, LST was used as an input to energy and water balance based hydrological model, while in one study it was used for model calibration. The hydrological Flash flood Event-based Spatially distributed rainfall–runoff Transformation Energy–Water Balance model (FEST-EWB) had been used by Corbari et al. (2020) to explore the feasibility of combining remotely sensed LST data with the model for better simulation of ET and soil moisture. The model was built for the Capitanata Irrigation Consortium, Italy. The satellite images from Landsat-7 Enhanced Thematic Mapper Plus (ETM+) and Landsat-8 Thermal InfraRed Sensor (TIRS) were used for the calculation of LST. The remote sensed LST was evaluated with ground station LST values. The values of correlation coefficient were 0.88 and 0.92 for ETM+ and TIRS, respectively. This was the only study found in the reviewed articles in which remote sensed LST was evaluated with ground observation prior to application for model calibration. Ren and Liu (2019) utilized temperature data from ground stations and the MODIS LST in the cold regions hydrological model (CRHM) to estimate snow depths in the Upper Yangtze catchment, China. The authors also employed MODIS data to determine the precipitation separation (critical) temperature. However, the authors did not perform an evaluation of the quality of the LST dataset used in the study. Corbari et al. (2019) utilized the MODIS LST product in addition to lake altimetry, water extent, and ground discharges to calibrate the FEST-EWB hydrological model of Yangtze River catchment, China. The incorporation of LST into the calibration process significantly enhanced the model's performance in simulating representative equilibrium temperature (RET), leading to a reduction in RMSE from 9.4 °C to 3.1 °C.

Overall, the reviewed literature shows limited use of air temperature and LST datasets compared to other datasets (e.g., precipitation, DEM). Except for glacio-hydrological models, air temperature is typically included in the calculation of potential/reference ET, which is often used as input for hydrological models. Additionally, the performance of temperature datasets is not uniform and depends on various factors such as geographical location, evaluation criteria, and modelling structure, as pointed out by Dembele et al. (2020). Although many different temperature datasets have been used by researchers, only the air temperature dataset from MERRA has been evaluated in comparison to local observation, which was performed by Sen-Gupta and Tarboton (2016). Most studies that have used air temperature datasets did not explicitly comment on their performance evaluation. LST datasets have been used in only four studies, and only Corbari et al. (2020) evaluated the developed LST from Landsat-7 and Landsat-8 data with reference to ground observations. The accuracy of the data is crucial for hydrologic applications as it can

significantly affect the reliability of any conclusions drawn from the analysis. Therefore, further exploration is necessary to assess the accuracy of air temperature and LST datasets for hydrological simulations.

2.4 CONCLUSIONS

This chapter presents a systematic literature review. This was performed on the one-hundred twenty shortlisted articles with the aim to gauge progress in and identify knowledge gaps regarding the use of remote sensed and/or global datasets for distributed hydrological models. The analysis was categorized on the types of datasets and the catchment scale on which these had been used. The identified catchment scale-wise knowledge gaps are presented in Table 2.1. These identified future research prospects can help hydrologists and modellers to steer their efforts towards potentially needed research areas.

Table 2.1. Identified scale-wise knowledge gaps.

Dataset Type	Knowledge Gaps	Catchment Scale
Rainfall	Evaluation of rainfall datasets for hydrological simulation at micro-scale and meso-scale.	Micro- and meso-scale
	Comparison of rainfall data products accuracy relative to one another and ground observations at meso- and micro-scale.	Micro- and meso-scale
	Comparison of different rainfall products' computational algorithms and their effects on product capability for hydrological simulation.	Micro-, meso- and macro-scale
DEM	Evaluation of global DEMs for hydrological simulations at micro-scale and meso-scale catchment.	Micro- and meso-scale
	Quantification of hydrological model uncertainties from different DEM sources.	Micro-, meso- and macro-scale
	Effect of DEM sources on surface-subsurface interactions in distributed physical hydrological models.	Micro-, meso- and macro-scale
	Effect of upscaling or downscaling of global DEMs on distributed hydrological model simulations.	Micro-, meso- and macro-scale
LULC	Response of model simulated water balance to different LULC data sources.	Micro-, meso- and macro-scale
	Effect of LULC sources on surface water–groundwater interactions in distributed hydrological models.	Micro-, meso- and macro-scale

	Use of dynamics LULC maps in hydrological in comparison to static input of LULC data.	Micro- and meso-scale
	Effect of different classification algorithms use for developing LULC maps on hydrological simulations.	Micro- and meso-scale
	How the number of land-use classes effect the hydrological simulation.	Micro- meso- and macro-scale
	Scale wise identification of optimal number of land-use classes for reasonable performance of hydrological models.	Micro-, meso- and macro-scale
	Evaluation of different global LULC datasets for hydrological simulations.	Micro-, meso- and macro-scale
	Test the model performance by including long-term land use-induced changes in hydrology.	Micro-, meso- and macro-scale
Soil distribution and properties	Evaluate the impact of different levels of soil information on model performance.	Micro-, meso- and macro-scale
	To evaluate which datasets, support better hydrological performance.	Micro-, meso- and macro-scale
	Exploring the effect of temporal variation in soil properties on the hydrological simulations.	Micro-, meso- and macro-scale
Leaf area index	The role of LAI dynamics in model calibration.	Micro-, meso- and macro-scale
	Effect of LAI source on hydrological model simulation.	Micro-, meso- and macro-scale
	Evaluation of Global LAI datasets for hydrological simulations.	Micro-, meso- and macro-scale
	Updating the vegetation state of hydrological model by assimilation of near real-time LAI data.	Micro-, meso- and macro-scale
Snow-covered area	Potential use of considering SCA in data assimilation.	Micro-, meso- and macro-scale
	Direct comparison of remote sensed SCA datasets with in-situ data.	Micro-, meso- and macro-scale
	Comparison of different SCA datasets with modelled SCA results.	Micro-, meso- and macro-scale

	Comparison of SCA datasets used for calibration or for assimilation.	Micro-, meso- and macro-scale
Evapo-transpiration	The accuracy of AET datasets relative to one another and ground observations.	Micro-, meso- and macro-scale
	The effect of spatial heterogeneity in AET data product on catchment hydrological simulations.	Micro-, meso- and macro-scale
	Comparison of hydrological performance of AET as calibration data or as assimilation data?	Micro-, meso- and macro-scale
	Effect of AET assimilation or calibration on the issue of equifinality in hydrological models.	Micro-, meso- and macro-scale
Soil moisture	Performance evaluation of soil moisture datasets for calibration and as data assimilation for micro-scale catchments.	Micro-scale
	Role of soil moisture data in calibration to resolve the problem of equifinality.	Micro-, meso- and macro-scale
	Evaluation of soil moisture product by comparing with model simulated soil moisture or with ground-based observations.	Micro-, meso- and macro-scale
	Soil moisture as calibration dataset vs. as assimilation dataset for better hydrological model performance.	Micro-, meso- and macro-scale
Temperature	Performance evaluation of LST datasets for calibration and as data assimilation.	Micro-scale
	Performance evaluation of air temperature datasets for hydrological simulations.	Micro- and meso-scale
	Comparison of temperature data products accuracy relative to one another and ground observations.	Micro- and meso-scale
	Effect of bias correction on hydrological prediction accuracy of model.	Micro-, meso- and macro-scale
	Role of LST data in calibration to resolve the problem of equifinality.	Micro-, meso- and macro-scale
	Evaluation of LST products by comparing with ground-based observations.	Micro-, meso- and macro-scale

	LST as calibration dataset vs. as assimilation dataset for better hydrological model performance.	Micro-, meso- and macro-scale

The identified knowledge gaps are based on a detailed review of the considered articles. The authors acknowledge that some articles were skipped due to the keyword selection or due to a poorly written abstract which caused the elimination of the article from the review.

Overall, we concluded that the use of remote sensed datasets is more focused on the macro- or large-scale catchments. Rainfall datasets are among the most used remote sensed datasets, while DEMs are the only global datasets which exceeded the local datasets in use for hydrological modelling. LST is the least used dataset. The performance of different remote sensed datasets is dependent upon many factors such as size of catchment, region of catchment, performance evaluation criteria and so on. It is difficult to determine a single consistently better performing dataset. The selection of datasets has a major influence on a model's simulations. Therefore, the evaluation of a selected dataset for a specific study area is an important step.

It is advisable to carry out investigations focused on exploring the effectiveness of different remote sensed datasets for the setting up, calibration, evaluation and data assimilation of distributed hydrological models at various scales, keeping in view the knowledge gaps highlighted in Table 2.1. Furthermore, it has been noticed that there is a lack of available literature as well as current research on the evaluating of remote sensed and/or global datasets in the case of distributed hydrological modelling, especially at the micro- and meso-scale catchment levels. This knowledge gap highlights the need for future research to explore and evaluate the effectiveness of different remote sensed datasets in hydrological modelling at various scales, with a particular focus on micro- and meso-scale catchments. This information could lead to the identification of more appropriate datasets for hydrological modelling, ultimately improving the accuracy of model simulations and contributing to better water resource management.

3

STUDY AREA AND MODELLING SETUP

This chapter describes the study area and provides a comprehensive overview of the hydrology model used in this research. The aim was to setup the modelling system that can represent the surface as well as sub-surface hydrological processes and interaction between them. The developed hydrological model for the study area is used to carry out the analyses presented in the subsequent chapters.

This chapter is based on the journal publications:

Ali, M. H., Bertini, C., Popescu, I., & Jonoski, A., 2025. Comparative analysis of hydrological impacts from climate and land use/land cover changes in a lowland mesoscale catchment. International Journal of River Basin Management, 1–19. https://doi.org/10.1080/15715124.2025.2454692

Jonoski, A., Ali, M. H., Bertini, C., Popescu, I., van Andel, S.J., & Lansu, A., 2025. Model-based design of drought-related climate adaptation strategies using nature-based solutions: case study of the Aa of Weerijs catchment in the Netherlands. Nature-Based Solutions, 100264. https://doi.org/10.1016/j.nbsj.2025.100264

3.1 DESCRIPTION OF THE STUDY AREA

The chosen study area for this research is the Aa of Weerijs, a transboundary mesoscale catchment shared between the Netherlands and Belgium. It covers an area of 346 km² out of which approximately 147 km² is located in the Netherlands. The main stream originates from Brecht, a region in Belgium and flows northwards towards the city of Breda, the Netherlands where it enters the city canals and eventually joins River Mark (Figure 3.1).

It is a lowland catchment, mostly flat with a gentle slope of approximately 0.5 % (de Klein and Koelmans, 2011). In the last five decades of the 20th century, the area underwent many alterations to adapt to the changing demands of urbanization, agriculture and for the purpose of flood protection. The streams and channels were normalized and the drainage network was intensified to reclaim the land (Witter and Raats, 2001). Almost

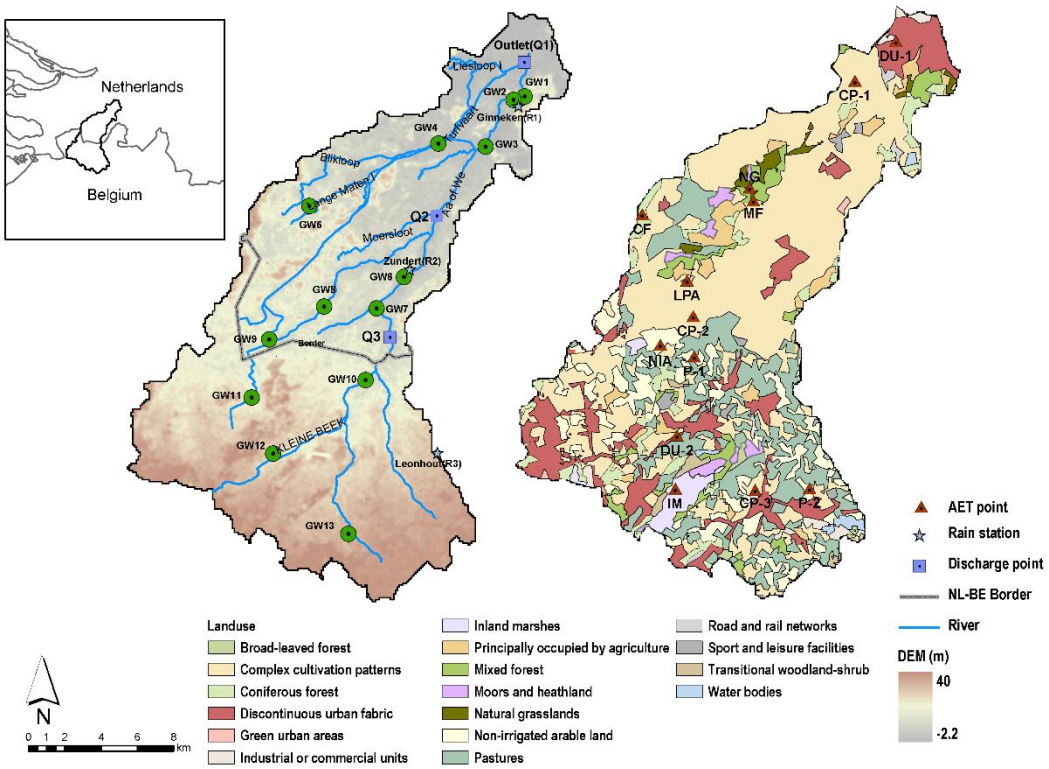

Figure 3.1. Location of the study area, river network, and elevations (CLMS n.d.-a) and LULC (CLMS n.d.-b). The map also shows the discharge, groundwater, and AET locations where the model performance has been evaluated. The abbreviations used for AET locations represent the LULC, according to the following convention: CP: Complex cultivation pattern; DU: Discontinuous urban fabric; NIA: Non-irrigated arable land; LPA: Land principally occupied by agriculture; CF: Conifer forest; NG: Natural grassland; IM: Inland marshes; MF: Mixed forest; P: Pastures

no remnants of the original swamps remain. The number of weirs has also been constructed to maintain the target water levels in the channels.

Based on the in-situ gauged data from 2010 to 2020, the average annual gross rainfall in the area is approximately 850 mm y^{-1}, resulting in approximately 249 mm y^{-1} flow at the catchment's outlet. The modest value of the runoff ratio (30 %) suggests a high level of water consumption within the catchment. The main land use in the area is agriculture and pastures. According to the Corine Land Cover (CLC) 2018 (CLMS, n.d.-a), the agriculture area comprises around 72.8 % of the total area which includes a tree nurseries sector of high commercial export value. Built-up areas cover 13.6 %, while forest and natural grassland areas collectively cover 9.3 % which are mainly located along the Bijloop and Turfvaart channels towards the western side of the catchment.

In the catchment, sandy soils are the main soil type and are characterized by sand-covered ridges with streams typically deeply incised within them. In recent years, the catchment is facing challenges regarding water shortages during the summer season. This is attributed to the degradation of subsurface soil, affecting water retention and canal networking. Various factors exacerbate this situation, including climate change, growing demand for water in the tree-nursery export sector, and hot dry summers. These pressures are intensifying, compounded by the simultaneous high demand for protected and dedicated nature and recreation areas expressed by the residents of Breda, Zundert, and Roosendaal (Beers et al., 2018). The recent summer drought in 2018 and then again in 2022 compelled the water managers to begin searching for solutions to prepare for more frequent drought conditions, whereas prior to these events the focus was primarily on managing the surplus water.

3.2 MODEL SETUP AND DATA

3.2.1 MIKE SHE hydrological model

To achieve the objectives of the study, a fully distributed physically based hydrological model has been set up using the MIKE SHE (Systeme Hydrologique Europeen) modelling tool developed by the Danish Hydraulic Institute (DHI), Denmark. It contains physics-based modules on overland flow (2D Saint-Venant equation, (Popescu, 2013)), unsaturated zone (1D Richards' equation, (Richards, 1931)), groundwater (3D Boussinesq equation, Boussinesq (1904)), and fully dynamic channel flow, incorporating complex interactions and feedback between these modules. It uses a finite difference approach to solve the partial differential equations describing these processes (Thompson et al., 2004). It has the capacity to simulate all significant processes of the hydrological cycle (Refsgaard et al., 2010) and the capability to simulate integrated surface-subsurface hydrology more efficiently, especially in flat areas characterized by dense river networks

and shallow groundwater, by employing physically based methods, in contrast to conceptual models like Soil and Water Assessment Tool (SWAT) that rely on empirical equations for simulating interactions (Ma et al., 2016). The study area (Aa of Weerijs) is a lowland area with flat topography due to which it experiences strong surface sub-surface exchange of flows. Further, the river network also has weirs with target water levels to maintain. Moreover, the research also aims to test different NBSs based adaptative strategies spatial represented in different locations of the catchment. To meet these requirements, MIKE SHE was selected because of its ability to capture the complex interactions between surface water and groundwater. Under the MIKE package of DHI, MIKE SHE is fully integrated with MIKE 11 which allows the representation of river network along with structures. Further, as it is a fully distributed physically based model, it allows spatial representation and evaluation of NBS measures at different. It has been recently used for NBS analysis (Fennell et al., 2023; Holden et al., 2022) although the focus in these studies was on streamflow only whereas we aim to analyse both surface and groundwater together.

3.2.2 Model setup

The main meteorological forcing data for the model are precipitation and Potential Evapotranspiration (PET). Daily rainfall data at two stations situated in the Netherlands (Ginneken and Zundert, marked in Figure 3.1) was sourced from the Royal Netherlands Meteorological Institute (KNMI, n.d.). The data for the third station (Leonhout, marked in Figure 3.1) located in Belgium was obtained from the Flemish Environment Agency (VMM, n.d.). These stations are all located towards the Eastern side of the catchment, as no rain gauges are available on the West side of the catchment. In general, a uniform spatial distribution of rain gauges ensures a better representation of rainfall and its variability over wide areas. In this research, however, the catchment itself is small (346 km^2) and relatively flat, which reduces the potential for significant spatial variability in meteorological data. Moreover, the average rainfall on these stations is in close range (Ginneken: 2.3 mm d^{-1}, Zunder: 2.3 mm d^{-1} and Leonhout: 2.2 mm d^{-1} for the period 2010-2019), which shows that the spatial variability of rainfall in the catchment is limited and these stations can describe the rainfall distribution over the catchment reasonably well. There are many interpolation techniques available for upscaling rainfall data from point observations for representing over the model domain. However, each technique has its advantages and limitations (Hofstra et al., 2008). Considering the relatively flat topography of the catchment, the rainfall was presented over the model domain using Thiessen polygons as it is reported as simple method (Liu et al., 2015).

The daily PET data was obtained from the closest weather station (Gilze Rijen) located in the Netherlands towards the North-East side of the catchment and provided as spatially uniform over the entire grid in the model. We acknowledge that PET varies depending

upon topography, soil and vegetation cover characteristics but the due to small size of the catchment and relatively flat terrain, PET is expected not to vary considerably with topography. The variations of land (vegetation) cover is taken into account when calculating actual evapotranspiration using varying vegetation parameters (root depth, leaf area index etc.). An alternative option to the use of uniformly distributed PET over the catchment was to obtain PET data from Earth observation gridded products, but these datasets have many associated uncertainties and cannot be regarded as actual observations (Rajib et al., 2018; Ali et al., 2023). Therefore, to avoid any additional uncertainties and ambiguities, PET data from the weather station was provided as spatially uniform over the entire grid in the model.

The topography in the model was represented using elevation data from EU-DEM version 1.1 (resolution: 25 m, (CLMS, n.d.-b)), while the LULC was represented using CLC 2018 (resolution: 100 m, (CLMS, n.d.-a)). The data on vegetation characteristics, including Leaf Area Index (LAI) and root depth was acquired from the National Hydrologic Instrumentation (NHI) sub-report on crop characteristics (NHI, 2008). The values of Manning's roughness coefficient corresponding to CLC classes were used from Papaioannou et al. (2018).

The grid resolution of MIKE SHE model was set as 500 m. The selected grid resolution reflects a compromise between computational efficiency and the need for spatial detail in representing the modelled parameters and processes. Finer resolutions can capture smaller-scale spatial variability but they would significantly increase computational time without proportionate improvement in model's accuracy (Vázquez et al., 2002). The chosen resolution is sufficient for simulating the river and surrounding catchment dynamics effectively while allowing for reasonable simulation times, as supported by similar studies in the literature (Loliyana and Patel, 2020). Further compared to lumped or semi-distributed hydrological models where often each sub catchment is represented as a single unit, 500 m grid cell provides much greater spatial detail. The main tributary of the river network, the Aa of Weerijs, has an average bed width of approximately 10 meters. The routing within the river is modelled using MIKE 11, with its geometry defined through detailed cross-sectional data. The exchange between MIKE 11 and MIKE SHE occurs at each grid cell, based on the dynamic relationship between river water levels and groundwater levels at those cells after each computational time step. Therefore, the selected grid cell size did not affect the representation of river and flow routing process.

The data of the river cross-sections was obtained from the water authority of the Dutch part of the catchment, the Water Board Brabantse Delta (WBD). A discharge of 0.03 m^3s^{-1} was set as upstream boundary condition to ensure numerical stability by preventing drying conditions. All streamflow is subsequently generated through interactions between MIKE 11 river component and the MIKE SHE grid cells. A rating curve was provided as a downstream boundary condition. The Manning's roughness coefficient value was

provided as 0.03 (Chow, 1959). The model incorporated the primary 29 weirs, out of which 7 were automated. The crest levels and target upstream water levels for the automated weirs were also provided by WBD. The model integrated these specified gate operation values for weirs to account for flow regulation.

For the unsaturated zone, the method based on the Richards equation was selected for the simulation of processes. It was characterized using soil texture data obtained from the 'Land Use/Land Cover Area Frame Survey' (LUCAS) 2015 topsoil physical properties dataset (Ballabio et al., 2016). According to this dataset, five different soil textures are present in the area. These soils were further categorized based on soil carbon content data (LUCAS topsoil chemical properties dataset, (Ballabio et al., 2019)), resulting in a soil map with 18 classes. The hydraulic soil properties were defined using the van Genuchten method (van Genuchten, 1980), and parameter values were calculated using pedotransfer function equations from Wösten et al. (1999).

For the saturated zone, the MIKE SHE implemented 3D Finite Difference method was selected and it was considered as an 80 m deep single aquifer layer. The boundary condition was set as spatially distributed fixed heads along the boundary, with values representing the average groundwater levels along the boundary from 2009 to 2016. Saturated horizontal hydraulic conductivity values were sourced from the Netherlands REGIS II V2.2 hydrogeological model (Gunnink et al., 2013; Vernes et al., 2005). These values were extended to the Belgian part of the catchment through interpolation. Small streams and ditches having an average bed width less than approximately 1 m were not modelled in MIKE 11 but were incorporated into the model using the conceptual drainage component of MIKE SHE. Their levels were set equal to the average bed levels of these small drains with in each model grid. A summary of the datasets used to set-up the model is presented in Table 4.1 while the schematic representation of MIKE SHE model setup is shown in Figure 3.2.

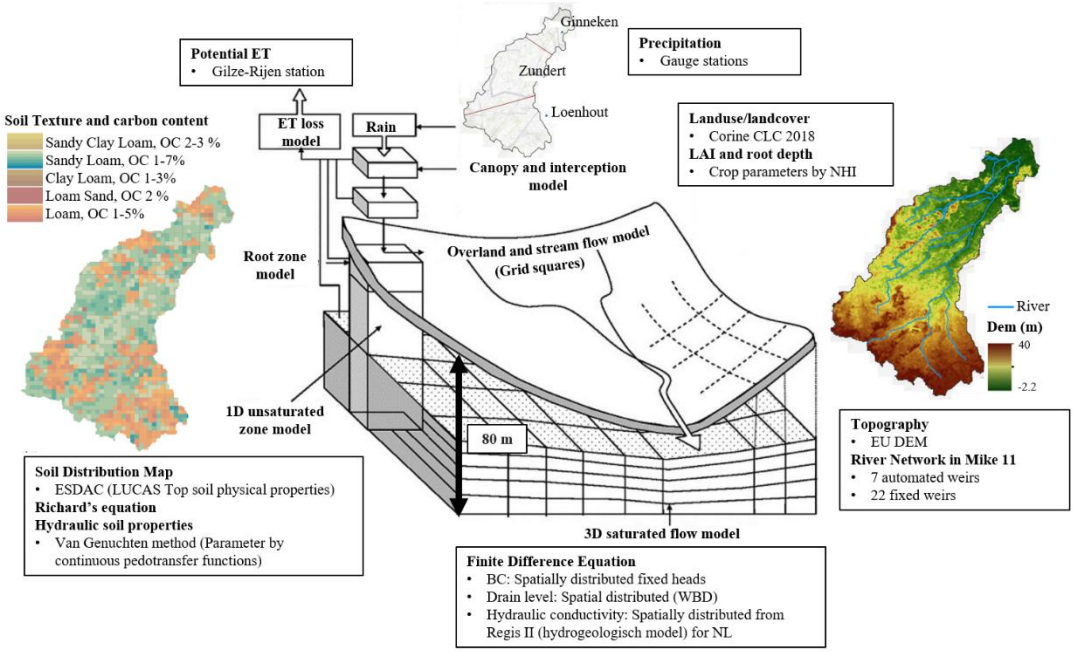

Figure 3.2. Schematic representation of MIKE SHE hydrological model for Aa of Weerijs

3.2.3 Calibration and validation

The model was set up for the period 15-09-2009 to 31-12-2019. The initial three-and-a-half months were considered as a model spinning up period. The traditional split sample approach was used for calibration and validation of the model. Years from 2010 to 2016 was considered for calibration while years 2017 to 2019 were used for validation. The period 2018-2019 was the driest, so it was kept in the validation period to assess the model performance in dry seasons. For model calibration, a manual, one-at-a-time approach was employed. Given the physically based nature of the model, most parameter values were obtained from independent source and existing literature. For the physically based distributed model like MIKE SHE, minimum number of parameters are suggested to be considered in calibration (Refsgaard, 1997). For instance, Al-Khudhairy et al. (1999) considered only three parameters in calibration. These were manning roughness coefficient for overland flow, hydraulic conductivity for saturated zone and the drainage time constant. In this study, the values of manning roughness coefficients and saturated hydraulic conductivity were taken from literature as mentioned in section 3.2.2. Only one parameter (drainage time constant) related to saturated zone was considered for calibration as it is more conceptual in nature. These initial values were obtained from literature which range between 1.50 exp^{-7} to 4.5 exp^{-7} 1/s corresponding to 77 days - 26 days (DHI, 2007; Brandyk et al., 2020; Refsgaard, 1997). The weighted mean of Nash-Sutcliffe Efficiency coefficient (MNSE) and Correlation coefficient (MR) were used as

target evaluation metrics with equal weights assigned to each site with its associated variable. The target variables included streamflow at 3 locations, groundwater levels (GWL) at 13 locations, and actual ET (AET) at 13 locations (Figure 3.1). During the validation (2017-2019), the same variables were considered, except for two groundwater locations (B49F0231 GW5 and B50A0234 GW4 Figure 3.1) due to data unavailability.

Table 3.1. Datasets used for model setup and performance evaluation

Data	**Temporal resolution**	**Spatial resolution**	**Source**
Rainfall	Daily	Point data	NL: Ginneken, Zundert (KNMI, n.d.); BE: Leonhout (VMM, n.d.)
Potential evapotranspiration	Daily	Point data	Gilze Rijen Weather station (KNMI, n.d.)
Vegetation parameters (LAI and root depth)	--	--	NHI (2008)
Actual evapotranspiration	Daily	100 m	Satellite-based evaporation data for the Netherlands SATDATA 3.0 (Meteobase, n.d.)
Observed groundwater levels	Daily, Bi-weekly	Point data	NL: WBD, UCSSD (n.d.) BE: DOV (n.d.)
Observed discharge	Daily	Point data	WBD
River geometric data	--	--	WBD
Topography	--	25 m	European Digital Elevation Model v1.1(CLMS, n.d.-b))
Land use land cover	--	100 m	Corine Land Cover 2018 (CLMS, n.d.-a)
Soil texture and typology	--	500 m	LUCAS 2015 topsoil physical properties dataset (Ballabio et al., 2016)
Soil carbon content (%)	--	500 m	LUCAS topsoil chemical properties dataset (Ballabio et al., 2019)

Acronyms used in the table: NL: Netherlands; BE: Belgium; LAI: Leaf area index; WBD: Water Board Brabantse Delta; DOV: Databank subsurface Flanders; LUCAS: Land Use/Land Cover Area Frame Survey

3.3 RESULTS AND DISCUSSION

3.3.1 Model Calibration and Validation

For the catchment average AET, the values of R and NSE for the calibration and validation periods were 0.91, 0.80, 0.926, and 0.822, respectively. Figure. 3.3 shows that the catchment average observed and simulated AET exhibit good agreement. The values of NSE and R at all locations for the calibration and validation period are provided in Table 3.2.

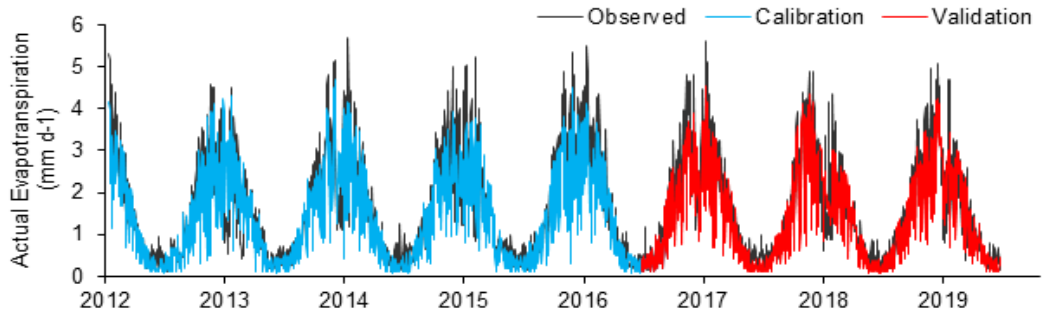

Figure 3.3.Observed and simulated catchment averaged actual evapotranspiration during the calibration and validation period

In terms of discharge at the catchment outlet, NSE and R values during calibration and validation were 0.88, 0.71, 0.87, and 0.71, respectively. While the model tended to underestimate the magnitude of high peaks, the plots in Figure. 3.4 demonstrate the reasonable capture of trends during both high and low flow periods, indicating the model's ability to reflect seasonal variations adequately.

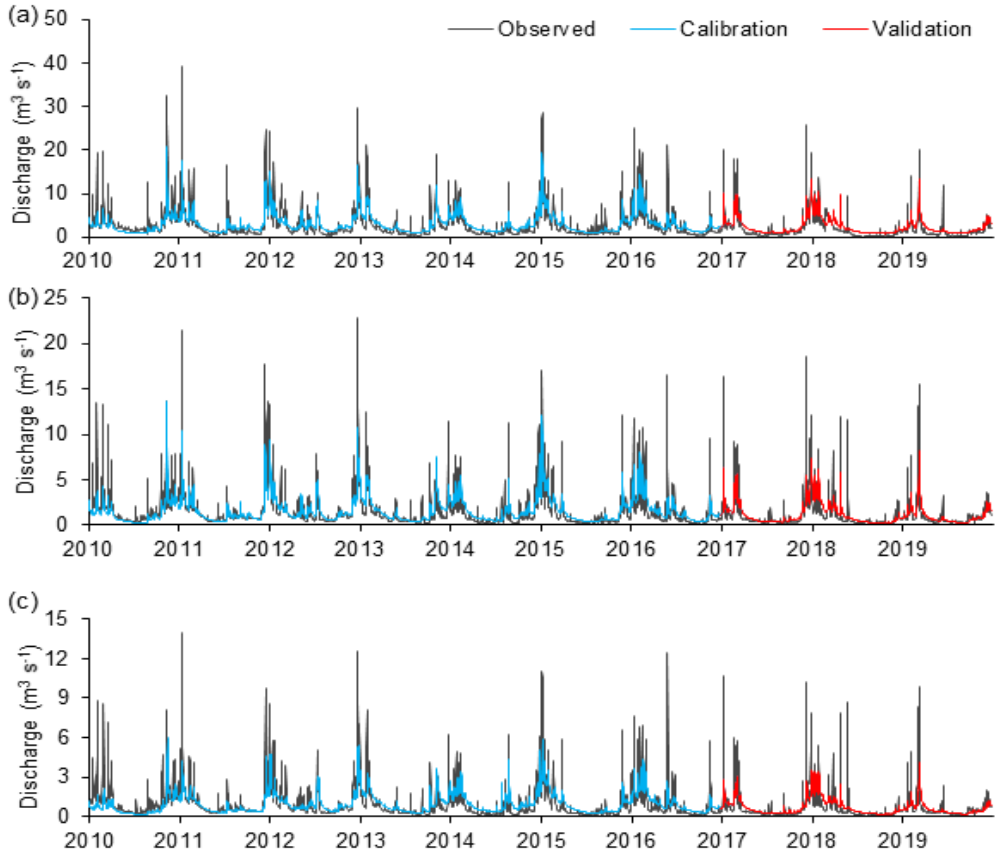

Figure 3.4. Observed and simulated stream flow during calibration and validation period (a) Q1: at the outlet, (b) Q2: in the middle, (c) Q3: at the Belgian border

The simulation of GWLs showed varying model efficacy across different locations. The plots of groundwater levels at four locations are presented in Figure 3.5. The model tended to slightly overestimate the GWLs in the upstream regions and around the catchment's outlet. Nevertheless, the model results demonstrated good agreement with observed data for GWLs, capturing seasonal variations and trends reasonably well (R= 0.77 for the average of all observed versus modelled outputs). At certain locations, for instance at GW7, the observed groundwater head showed the sharp decrease in levels in the summer months which the model fail to fully reproduce. This sharp decline is likely due to localised groundwater pumping near the groundwater well. The groundwater pumping was not included in the model due to unavailability of detail pumping data.

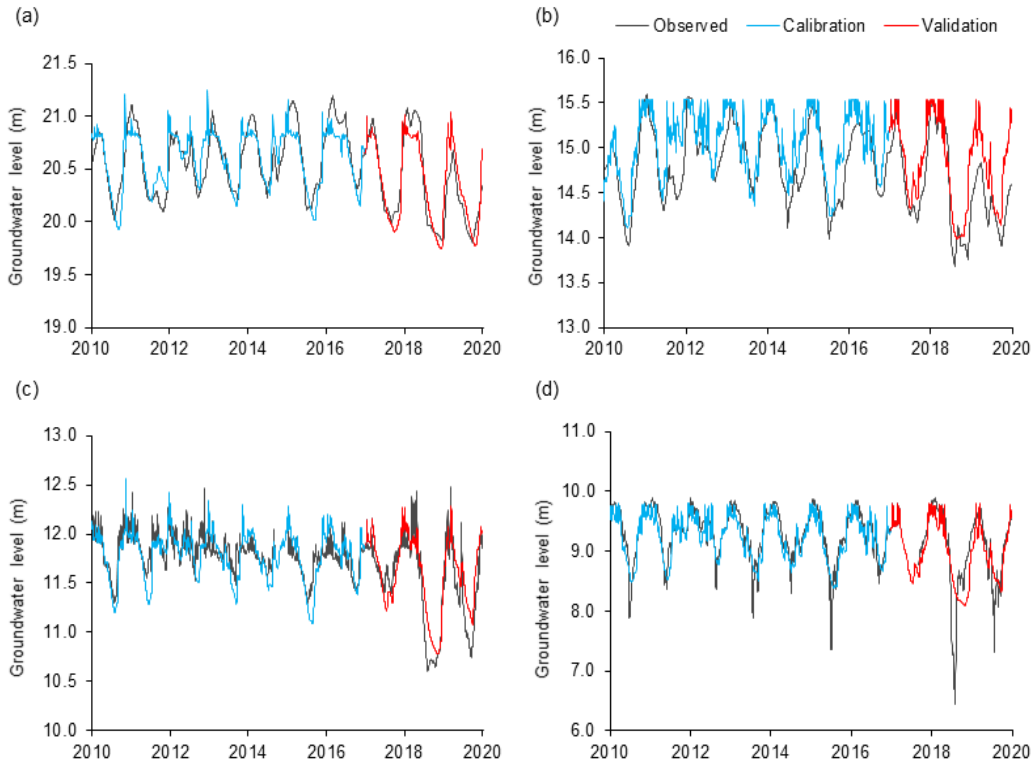

Figure 3.5. Observed and simulated Groundwater levels during the calibration and validation period at locations (a) GW13 (1-0334), (b) GW11 (1-0170), (c) GW9 (5219), (d) GW7 (B50C0079)

Table 3.2. Model performance evaluation during the calibration and validation period

Variable	Location	Calibration (2010-2016)			Validation (2010-2016)		
		R	NSE	KGE	R	NSE	KGE
Discharge	Q1 (Outlet)	0.88	0.71	0.60	0.87	0.71	0.61
	Q2 (Middle)	0.73	0.53	0.57	0.74	0.55	0.58
	Q3 (Border)	0.66	0.43	0.47	0.65	0.42	0.44
Groundwater level	GW9 (5219)	0.72	0.11	0.55	0.90	0.75	0.81
	GW3 (5332)	0.72	0.28	0.26	0.80	0.02	0.25
	GW1 (5170)	0.56	0.10	0.41	0.73	0.13	0.70
	GW2 (5165)	0.72	0.29	0.20	0.80	0.38	0.26
	GW8 (B50COO77)	0.89	0.51	0.76	0.83	0.39	0.70
	GW7 (B50C0079)	0.89	0.77	0.84	0.78	0.60	0.65
	GW6 (B50C0078)	0.85	0.58	0.47	0.87	0.39	0.38

	GW5 (B49F0231)	0.64	0.35	0.48	--	--	--
	GW4 (B50A0234)	0.66	0.14	0.16	--	--	--
	GW13 (1-(0344)	0.85	0.73	0.81	0.92	0.84	0.87
	GW10 (1-(0347)	0.89	0.16	0.54	0.84	0.15	0.76
	GW12 (1-342)	0.74	0.37	0.70	0.83	0.68	0.71
	GW11 (1-0170)	0.87	0.54	0.84	0.92	0.62	0.88
Actual Evapotranspiration	CP-1	0.88	0.74	0.75	0.84	0.70	0.78
	CP-2	0.86	0.73	0.82	0.85	0.72	0.85
	CP-3	0.91	0.74	0.77	0.71	0.33	0.67
	DU-1	0.87	0.57	0.62	0.86	0.55	0.63
	DU-2	0.89	0.74	0.84	0.89	0.74	0.85
	P-1	0.89	0.77	0.78	0.91	0.78	0.76
	P-2	0.86	0.72	0.83	0.72	0.44	0.71
	LPA	0.88	0.74	0.75	0.75	0.52	0.67
	NIA	0.87	0.74	0.82	0.78	0.59	0.74
	CF	0.66	0.20	0.60	0.58	0.03	0.53
	MF	0.87	0.54	0.64	0.72	0.04	0.50
	NG	0.82	0.55	0.75	0.72	0.25	0.63
	IM	0.82	0.42	0.43	0.65	0.15	0.31

R: Correlation coefficient; NSE: Nash-Sutcliffe Efficiency coefficient; KGE: Kling Gupta Efficiency coefficient; CP: Complex cultivation pattern; DU: Discontinuous urban fabric; NIA: Non-irrigated arable land; LPA: Land principally occupied by agriculture; CF: Conifer forest; NG: Natural grassland; IM: Inland marshes; MF: Mixed forest; P: Pastures.

3.3.2 Catchment water balance

The accumulated water balance of the catchment simulated by the model over the decade 2010 – 2019 is presented in the Figure 3.6. The main components are expressed in mm over the period of 10 years (round to nearest integer) on the conceptual cross-sectional view. The components are mentioned to reflect their position within the surface or subsurface layer of the hydrological component. The total precipitation over the catchment is 8251 mm. The simulated evapotranspiration (ET) is 5189 mm. It includes the ET from surface and sub-surface. Surface part of ET consists of evaporation from intercepted water by plants along with evaporation from ponded water. Transpiration and soil evaporation comprised the sub-surface part of ET. The results of simulated ET are in accordance with Huisman et al. (1998) where the ET for the Netherlands is reported as approximately 500 mm y^{-1} with values close 550 mm y^{-1} for the areas which are far from coast. The infiltrated water in the un-saturated zone is available for sub-surface evaporation process or for recharge to groundwater. In the zone where Aa of Weerijs is

located, the groundwater recharge is reported by Huisman et al. (1998) as 200-300 mm y^{-1} with large spatial variability. This value conforms with the results of MIKE SHE which has simulated the recharge of 288.8 mm y^{-1}. The water in saturated zone contributes significantly to streamflow while also lost to catchment boundaries as downstream groundwater outflow.

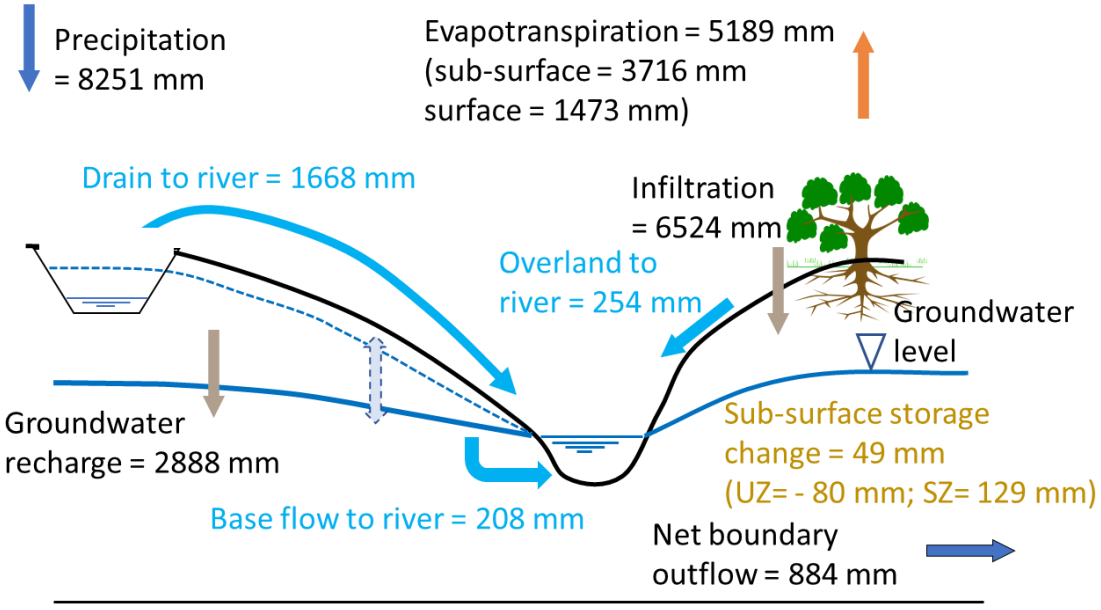

Figure 3.6. Conceptual representation of the key water balance components simulated by the model accumulated over the period 2010-2019

The obtained results from the model also agree with those of Dams et al. (2008), where the authors developed the model of Kleine Nete catchment in Belgium located in near vicinity to the Aa of weerijs. They reported the average annual precipitation, ET and groundwater recharge as 832 mm, 462 mm and 292 mm, respectively, which are very similar to the values that MIKE SHE model simulated for the Aa of Weerijs. Overall the results of water balance depict that because of the flat topography and relative permeable soils, the major amount of precipitation infiltrates in to sub-surface while a small fraction of about 254 mm is generated as direct run-off. The large portion of streamflow (1668 mm) comes from saturated zone via drainage network when the groundwater levels exceed the drainage levels. The remaining portion of streamflow (208 mm) comes from direct interaction of saturated zone with river as baseflow.

It is importance to mentioned that the reported water balance represents the spatial average of the catchment. The identified hydrological processes may vary spatially. For example, in the wet conditions there may be areas where the soil become fully saturated leading to temporary ponding of water on the surface (no unsaturated zone). From such locations, the water can evaporate or percolate again. Overall, the water balance provided

the better understanding of the catchment hydrology by highlighting contributions of individual component and exchanges between them.

3.4 CONCLUSIONS

Overall, the hydrological processes of the catchment are well captured by the MIKE SHE model. The perfromance of the model during calibration and validation was equally good. Notably, the period of 2018-2019 was the driest on the record but the model well reproduced the variables in this periods which indicates the realiablity of the model to be confidentilly used in drought related studies. Further, only limited parameters were considered in the calibration process but the model performed quite reasonably. This further increased the confidence in model for use in application such as evaluation of different earth observation datasets, climate change impact assessment and testing of NBS-based adaptive strategies. Not relying on extensive calibrated parameters ensures that any observed differences in outcomes can be more confidently attributed to scenarios or datasets rather than the compensation effects from finely tuned parameters.

4

EVALUATION OF PRECIPITATION PRODUCTS

Single performance metrics may be insufficient to identify the suitable gridded precipitation products for simulating hydrological variables. Conversely in a multi-metric approach, often all metrics from a specific set are collectively considered to compute an aggregated score. However, there can be multiple combinations possible depending on the total number of metrics leading to varying aggregated scores. In this study, a multi-metric, multiple combination evaluation approach is used to identify the most suitable precipitation product for reproducing discharge and groundwater levels with a specific hydrological model. The objective is to evaluate the influence of the choice of metrics on the identification of the most suitable precipitation products. To explore this, MIKE-SHE hydrological model for Aa of Weerijs catchment is forced with four different gridded precipitation products: ERA5-Land, IMERG-Final, MSWEP and EOBS. Five distinct scenarios are formulated to carry out the analysis using different timeseries based and hydrological signature-based metrics. The results revealed that no precipitation product consistently performed better than others across all metrics in precipitation estimation or reproducing hydrological variables. Testing of multiple metric combinations revealed that the identification of the most suitable product is sensitive to the choice of metrics. When the number of metrics considered for evaluation is small, then the likelihood of all the products to be identified as most suitable for precipitation estimation or reproducing hydrological variables is higher. The results strongly illustrate the significance of a multi-metric, multiple combination approach for the evaluation of gridded precipitation products in hydrological studies.

This chapter is based on the journal publication: Ali, M. H., Popescu, I., Hrachowitz, M., & Jonoski, A., 2025. Multi-metric multiple combination evaluation of precipitation products for hydrological simulations. Under review.

4.1 INTRODUCTION

In the era of advanced technology and remote-sensing, each passing year brings forth new datasets and hydrologists have greatly benefited from these advancements (Alfieri et al., 2022). The momentum seems to grow further as initiatives such as 'Early Warning for All' by the United Nations, 'Green Deal' by the European Union, 'Earth Intelligence for All' by Group on Earth Observations (GEO) and others, actively promote the generation and use of Earth observation (EO) products. One of the main drivers of the terrestrial hydrological cycle and an important input to hydrological models is precipitation. Gridded EO precipitation products provide advantages over local observations from gauging stations, such as lower costs, homogeneous coverage and easy data accessibility (Almagro et al., 2021; Dembele et al., 2020; Brocca et al., 2019). However, it is challenging to estimate precipitation using satellite data or models and it has many associated uncertainties (Gebrechorkos et al., 2024; Beck et al., 2017). The uncertainties in the precipitation products can cause up to 50 % error in variables simulated by hydrological models (Bárdossy et al., 2022), resulting in poor representation of hydrological responses. Therefore, it is important to evaluate their suitability before using them for hydrological applications.

In previous studies, the suitability of gridded EO precipitation products is evaluated mainly using two approaches (i) comparing estimated precipitation directly with observed data from gauging stations (Yang et al., 2024; Sun et al., 2018; Ayehu et al., 2018) and (ii) using precipitation products to force hydrological models and comparing the reproduced variables (e.g. streamflow) with observed data (Gebrechorkos et al., 2024; Ji et al., 2024; Lakew et al., 2020). In both approaches, researchers rely on error metrics to evaluate the goodness of fit between estimated and in-situ time series (Alexopoulos et al., 2023; Gebrechorkos et al., 2024; Dembele et al., 2020), which is standard practice for hydrologists (Jackson et al., 2019). The Nash-Sutcliffe efficiency (NSE) (Nash and Sutcliffe, 1970) and the Kling-Gupta efficiency (KGE) (Gupta et al., 2009) are frequently used metrics for the quantitative comparison between simulated timeseries and observed ones (Cinkus et al., 2023; Clark et al., 2021). However, each metric has its limitations. Such as NSE over-emphasises peak values due to use of squared sum of errors (SSE) which leads to an inflated importance of the absolute errors during high flows at the expense of low flows: as minimization target SSE leads to an imbalanced reduction of errors with more emphasizes on high values (Knoben et al., 2019; Onyutha, 2024). Conversely, the KGE is a decomposition of NSE into three components i.e. correlation, bias and the ratio of variances or coefficients of variation which to some extent complement the deficiencies of the NSE but still underestimate the variability of timeseries data (Liu, 2020). Both NSE and KGE can be strongly swayed by few outliers (Clark et al., 2021; Beven and Westerberg, 2011). To overcome the influence of high flows or peaks, various prior transformations on the observed and estimated timeseries

can be applied such as logarithmic transformation which allows a stronger emphasis on low flows (Lamontagne et al., 2020; Quesada-Montano et al., 2018). However, in the case of KGE, log transformation is not advised as it becomes unstable when the transformed series reaches near zero leading to possible misinterpretation of the results (Santos et al., 2018). In addition to these, many other error metrics are used by researchers; however, no single metric can comprehensively capture all aspects of a specific variable (Onyutha, 2024). Therefore, the use of a single metric for datasets evaluation is often insufficient (Cinkus et al., 2023). Acknowledging this, there is increasing understanding for the need of multi-metric approaches to evaluate EO precipitation products (Gebrechorkos et al., 2024; Le et al., 2020; Brocca et al., 2019). Additionally, the use of error metrics on timeseries alone cannot capture the specific features of streamflow regimes (e.g. magnitude and timing of high and low flows) and dominant catchment processes (e.g. base flow index, runoff ratio). These features of watersheds are instead described by hydrological signatures (Sawicz et al., 2011; Kiraz et al., 2023). Using hydrological signatures in combination with statistical error metrics can reflect more comprehensively the ability of precipitation products to reproduce flow (Almagro et al., 2021).

On the one hand, the multi-metric evaluation is suggested for comprehensive data product evaluation for hydrological applications (Jackson et al., 2019; Moges et al., 2022). On the other hand, it can lead to complex interpretations of the results due to conflicting outcomes of the individual metrics. Camici et al. (2020) considered only KGE to compare simulated and observed discharge with an argument that the limited number of performance metrics allows the communication of results in an effective way. Further, in studies where multiple metrics are used, the results are often presented individually for each metric rather than with thorough combined analyses (Gebrechorkos et al., 2024; Almagro et al., 2021; Yang et al., 2024). This can lead to opposing and unclear conclusions about the identification of the most suitable precipitation product for a given application. To overcome this, individual metrics can be aggregated into a single composite score (Akbas and Ozdemir, 2024; Kumar et al., 2024). However, the final score can vary based on the number of metrics aggregated, as multiple combinations are possible depending on the total number of metrics (number of combinations $= 2^n - 1$, where n is the total number of metrics).

Therefore, there is a need for an evaluation approach that not only considers multiple metrics but also systematically explores all possible combinations of those metrics to assess the robustness of precipitation product performance. This study presents a novel, comprehensive evaluation framework that exhaustively tests multiple combinations of selected metrics (approximately 33 million) to identify the most suitable gridded precipitation product for hydrological simulations. The core idea is that the most suitable product is not the one that performs best on a single or arbitrarily selected set of metrics, but rather the one that demonstrates consistent plausibility across the widest range of

metric combinations. To our knowledge, no previous study has implemented such a combinatorial, multi-metric evaluation to identify the most suitable gridded product for precipitation estimation and for reproducing hydrological variables with a model.

The objective is to evaluate the influence of metric selection on identifying the most suitable gridded precipitation products in comparison with in-situ precipitation gauge data and for reproducing hydrological variables (discharge and groundwater levels). In addition, the following specific research questions are addressed: Is the most suitable precipitation product identified by considering individual metrics the same as that identified by testing multiple combinations of metrics? Is the product identified as most suitable based on timeseries error metrics (such as KGE, NSE) the same as identified by hydrological signatures-based metrics to reproduce hydrological variables? Is the product identified as most suitable from comparison with station data is also the one that is the most suitable to reproduce hydrological variables? Is considering multiple metrics for the evaluation of precipitation product beneficial and can a minimum number of metrics needed for effective evaluation be determined?

To address these questions, four gridded precipitation products: fifth generation of European ReAnalysis (ERA5) Land, Integrated Multi-satellitE Retrievals for Global Precipitation Measurement (GPM IMERG Final), Multi-Source Weighted-Ensemble Precipitation (MSWEP) and the European gridded dataset of daily observations version 28 (EOBS) are analysed as a test case in this study. These products are used to force MIKE-SHE hydrological model for the study area. Overall, the research offers a comprehensive evaluation criterion for these EO data products through exhaustive metric combination analysis to identify the most suitable product for use with the MIKE-SHE hydrological model in the study area.

4.2 MATERIAL AND METHODS

The research was carried out focusing on Aa of Weerijs catchment. The MIKE-SHE hydrological model was developed for the area and utilized to carry out the research. The description of the study area, details of the input data and model setup are provided in the Chapter 3. Therefore, this information is not described here. The model is forced with the four selected gridded precipitation products (described in section 4.2.1). The scope of this study was not to evaluate the absolute performance of the hydrological model but to compare the relative performance of the considered precipitation products. The model was therefore not calibrated individually for each product but the same modelling structure with identical parameter values was used for all four products (as done by Gebrechorkos et al. (2024)). This ensured that each product was evaluated using the same model structure where the parameters did not compensate for the uncertainties of precipitation products.

4.2.1 Gridded precipitation products

There is a wide range of gridded precipitation products that have been utilized by the scientific community for distributed hydrological modelling (e.g. Chapter 2 section 2.3.1). The continuity of the product, its spatio-temporal resolution and coverage over the study area were the main criteria for selection of the products. In this study we have used the following gridded precipitation products that are available for the study area for at least daily time scale and a spatial resolution of 0.1 degree:

The fifth generation of European ReAnalysis (ERA5) Land is a reanalysis product by the European Centre for Medium-Range Weather Forecasts (ECMWF). It is available at 0.1° spatial resolution from 1950 to 2024 (Muñoz-Sabater et al., 2021). ERA5-Land is generated from the meteorological forcing data for ERA5 for land applications only and freely available from the Climate data store (CDS) by Copernicus (CDS, n.d).

Integrated Multi-satellitE Retrievals for Global Precipitation Measurement (GPM IMERG) is a product by NASA. IMERG has three versions: early, late and final which are defined by varying time delays in their availability (early: 4-hrs, late: 14-hrs and final: 3.5-months). In this study, IMERG Final version 7 is used. It is generated based on microwave-infrared retrievals from satellite data and calibrated using rain gauge data from global precipitation networks (Huffman et al., 2020). The product has a resolution of 0.1° and is available from 1998 to 2024. It is freely available from the Goddard Earth Sciences Data and Information Services Center by NASA Earthdata (GES-DISC, n.d).

Multi-Source Weighted-Ensemble Precipitation (MSWEP) is a global precipitation data product available at a resolution of 0.1°. It was developed by fusion of multiple data sources including satellite-based, reanalysis and gauge data (Beck et al., 2017; Beck et al., 2019). MSWEP has been used by researchers for many hydrological applications and reported among the most suitable products (Gebrechorkos et al., 2024; Dembele et al., 2020; Lakew et al., 2020). The MSWEP version 2.8 used in this study covers the period from 1979 to 2024 and is available to download from the GloH2O website on request (GloH2O, n.d).

The European gridded dataset of daily observations version 28 (EOBS v28.0) is a product with a resolution of 0.1° developed using data from 23600 meteorological stations across Europe. Initially, the dataset was developed for validation of European climate models and now also being used for monitoring climate across Europe. The daily values from stations are fitted using a deterministic model to capture the spatial trends then daily ensembles are generated using stochastic techniques (Cornes et al., 2018). We have used the daily ensemble mean data which is available to download from the European Climate Assessment and Dataset website (ECAD, n.d).

As ERA5-Land, IMERG-Final and MSWEP are available at sub-daily temporal resolution, they were aggregated to daily scale to match the resolution of EOBS and rain

station data. For brevity, hereafter we refer to 'ERA5-Land' as ERA5 and 'IMERG-Final' as IMERG.

4.2.2 In-situ data

The observed discharge at three locations along the main branch of river Aa of Weerijs was used for the calculation of metrics (Q1, Q2, and Q3 in Figure 3.1). The discharge data was provided by the Brabanste Delta water board (https://www.brabantsedelta.nl/, last access: 18 August 2024). The groundwater levels (GWL) at 13 locations were used for the calculation of related metrics (GW1 to GW13 in Figure 3.1). The groundwater data for the Netherlands area of the catchment was obtained from the Brabanste Delta water board and Data and Information of the Dutch Subsurface website (DINOloket, n.d.), while for the part of the catchment in Belgium, the data was available through Databank Ondergrond Vlaanderen (DOV, n.d.).

The daily precipitation data from three gauging stations was used for direct comparison with the gridded EO precipitation products. Two gauging stations, 'Ginneken' and 'Zunder' (R1 and R2 in Figure 3.1) are located in the Netherlands and data was obtained from the Royal Netherlands Meteorological Institute website (KNMI, n.d.) while for the third station 'Leonhout' (R3 in Figure 3.1) located in Belgium, the data was obtained from the Flemish Environment Agency website (VMM, n.d.).

4.2.3 Evaluation metrics

To explore the research questions, initially, the suitability of gridded products to estimate precipitation compared to station data is evaluated. Then, the model is individually forced with the four gridded precipitation products, and their suitability to reproduce discharge, groundwater levels and other hydrological signatures with the MIKE-SHE model are tested. For the evaluation of the difference between the reproduced and observed data, a wide range of metrics is considered and discussed below.

To identify the most plausible precipitation product for precipitation estimation, the difference between the precipitation estimates from the four gridded data products (ERA5, IMERG, MSWEP and EOBS) and in-situ data is quantified at the three precipitation gauging stations. The point to grid-cell data comparison approach is adopted as done by (Dembélé and Zwart, 2016; Ayehu et al., 2018). The alternative option was to upscale the point-based station data to the same grid scale as of precipitation products using interpolation techniques. However, there are many different interpolation techniques available that could be applied but each has its advantages and limitations (Hofstra et al., 2008). Therefore, to limit uncertainties and ambiguities involved in selecting an interpolation method, a simple point to grid-cell comparison method is selected for this study.

The selection of metrics was guided by the need to capture diverse aspects of precipitation product performance, both statistically and hydrologically. The evaluation metrics used to quantify the agreement between the precipitation data products and in-situ data at the gauging stations include timeseries metrics, precipitation extreme indices and categorical event detection metrics. Their details are described in Table 4.1. Among the six error indicators, two are the most frequently used indicators in hydrological studies i.e. NSE (M_{NSE}) and KGE (M_{KGE}). Further, Log NSE (M_{LNSE}) is also included to complement the low values in the series. In addition to normalized error indicators, the use of at least one absolute value error indicator has been recommended by (Ritter and Muñoz-Carpena, 2013). Therefore, the mean absolute error (M_{MAE}) is included as well. Apart from timeseries data, the signatures or precipitation extreme indices that have single value as output, are compared using the relative error (M_{ER}) (Euser et al., 2013). In addition to these statistical error metrics, the capability of precipitation data products to detect daily rainfall events is evaluated using categorical metrics: Probability of detection, False discovery rate, Equitable threat score and Frequency bias.

Table 4.1. Performance metrics for evaluation of precipitation product against station data

No.	Variable/ signature/ indices	Abbreviation	Performance metric	Description
1	Time series of rainfall	R	$M_{NSE,R}$; $M_{LNSE,R}$; $M_{KGE,R}$; $M_{MAE,R}$; $M_{CC,R}$	
2	Rain duration curve	RDC	$M_{NSE,RDC}$; $M_{LNSE,RDC}$; $M_{KGE,RDC}$; $M_{MAE,RDC}$	RDC represents a relationship between rainfall magnitudes and their exceedance probabilities. It gives insights into how often certain levels of rainfall occur.
3	Total rainfall on very wet days	R95pt0t	$M_{ER,R95pt0t}$	Sum of rainfall on days exceeding 95th percentile threshold (Casanueva et al., 2014)
4	Longest consecutive dry days	CDD	$M_{ER,CDD}$	Longest consecutive days when rainfall is less than 1 mm/day (Casanueva et al., 2014)

5	Longest consecutive wet days	CWD	$M_{ER,CWD}$	Longest consecutive days when rainfall is more than 1 mm/day (Casanueva et al., 2014)
6	Probability of detection	POD	M_{POD}	The ratio of the number of correctly detected events to the total number of actual events that occurred (Bouttier and Marchal, 2024)
7	False discovery rate	FDR	M_{FDR}	The proportion of false positives among all the positive detections (Bouttier and Marchal, 2024)
8	Equitable threat score	ETS	M_{ETS}	It measures how well a dataset captures the occurrence of rainfall compared to random chance (Bouttier and Marchal, 2024)
9	Frequency bias	FB	M_{FB}	Ratio of a captured event to actual events (Bouttier and Marchal, 2024)

In addition to the overall combined results, the metrics are also grouped into subcategories, comprising those related to timeseries, duration curves, categorical event detection metrics and precipitation extreme indices, to understand the performance of products well across different domains.

Next, the gridded precipitation products are used as model forcing and their adequacy to simulate discharge and groundwater level timeseries as well as various other hydrological signatures is quantified. For this, we included a range of hydrological signatures to quantify which precipitation data products have most plausibly reproduced multiple stream and groundwater signatures. These signatures are related to magnitude (e.g. high flow segment volume, mean discharge, median discharge, variance), distribution (duration curves), flow dynamics (base flow index, autocorrelation, runoff ratio) and responsiveness of the catchment (rising limb density, streamflow elasticity). The same six error indicators mentioned before (M_{NSE}, M_{LNSE}, M_{KGE}, M_{MAE}, M_{CC} and M_{ER}) are applied to observed and simulated timeseries of discharge and GWL along with other catchment signatures to quantify the differences. These metrics are listed in Table 4.2.

The selection was informed by the need to capture the diverse hydrological responses of the catchment, which is characterized by lowland hydrology, with moderate slopes, shallow groundwater tables, and a strong surface–subsurface interaction. For example, the inclusion of groundwater-sensitive indicators such as baseflow index and streamflow elasticity reflects the importance of groundwater contributions to streamflow in this region. Similarly, rising limb density and autocorrelation help assess the flashiness and memory effects of the system in response to precipitation inputs.

Table 4.2. Performance metrics for evaluation of simulated variables

No.	Variable/ signature	Abbreviation	Performance metrics	Description
1	Time series of stream flow	Q	$M_{NSE,Q}$; $M_{LNSE,Q}$; $M_{KGE,Q}$; $M_{MAE,Q}$; $M_{CC,Q}$	
2	Time series of groundwater levels	G	$M_{NSE,G}$; $M_{LNSE,G}$; $M_{KGE,G}$; $M_{MAE,G}$; $M_{CC,G}$	
3	Flow duration curve	FDC	$M_{NSE,FDC}$; $M_{LNSE,FDC}$; $M_{KGE,FDC}$; $M_{MAE,FDC}$	FDC represents a relationship between flow magnitudes and their exceedance probabilities. It gives insights into how often certain flows occur (Jothityangkoon et al., 2001)
4	Groundwater duration curve	GDC	$M_{NSE,GDC}$; $M_{LNSE,GDC}$; $M_{KGE,GDC}$; $M_{MAE,GDC}$	GDC represents a relationship between groundwater levels and their exceedance probabilities. It gives insights into how often certain levels occur (Hrachowitz et al., 2014)
5	FDC high flow segment volume	HFV	$M_{ER,HFV}$	It characterises the amount of flow from extreme events (exceedance probability < 2%) (Xia et al., 2024)

6	FDC mid flow segment slope	MFS	$M_{ER,MFS}$	It characterises the variability and behaviour of mid-range flows (exceedance probability between 20 – 70 %) (Xia et al., 2024)
7	Base flow index*	BFI	$M_{ER,BFI}$	Contribution of baseflow to streamflow (Sawicz et al., 2011; Zhang et al., 2020b)
8	Streamflow elasticity	SE	$M_{ER,SE}$	Sensitivity of streamflow to changes in precipitation (Sawicz et al., 2011)
9	Autocorrelation lag by 1 day	1-lag	$M_{ER,1\text{-}lag}$	The degree of similarity between time series and its shifted version. Thus, a reflection on the memory of the system (Hrachowitz et al., 2014; Euser et al., 2013)
10	Rising limb density (month^{-1})	RLD	$M_{ER,RLD}$	It depicts the 'flashiness' of the catchment's propensity (Sawicz et al., 2011)
11	Runoff ratio (monthly)	RR	$M_{NSE,RR}$; $M_{LNSE,RR}$; $M_{KGE,RR}$; $M_{MAE,RR}$	The portion of rainfall converted to streamflow by the catchment. It reflects the water use/storage in the catchment (Sawicz et al., 2011; Xu et al., 2021)
12	Mean discharge	MQ	$M_{ER,MQ}$	(Xia et al., 2024)
13	Mean log-transformed discharge	MLQ	$M_{ER,MLQ}$	

14	Median discharge	MDQ	$M_{ER,MDQ}$	(Xia et al., 2024)
15	Discharge variance	VQ	$M_{ER,VQ}$	
16	Variance of log-transformed discharge	VLQ	$M_{ER,VLQ}$	
17	Peak discharge	PQ	$M_{ER,PQ}$	(Xia et al., 2024)

*Base flow is simulated by the MIKE-SHE model and is compared with the gauge model's base flow for assessment of MER,BFI for each dataset.

The overall suitability of the four gridded precipitation products either based on their agreement with point observations (Table 4.1) or to reproduce the hydrological response of the study catchment (Table 4.2), was evaluated by combining the individual metrics into two different aggregate criteria. In the first criterion, the Euclidean distance (DE) from the perfect model (Hrachowitz et al., 2014) was calculated where each performance metric is assigned with an equal weight.

$$DE = \sqrt{\frac{\sum_{i=1}^{N}(P_i - Mi)^2}{N}} \qquad (4.1)$$

Where P_i are the perfect values of performance metrics, *Mi* are the actual values of performance metrics and *N* is the total number of metrics. Since each metric contributes equally to the DE, poor performance in a single metric (where *Mi* deviates significantly from *P*) will have a squared effect on the DE score. This means that a large difference in one metric can disproportionately increase the DE, even if the product performs very well in other metrics. This disproportionate effect could penalize a dataset based on a single metric, affecting the overall performance assessment.

To overcome this, an additional criterion based on the Plurality Rank Aggregation method (Roberts, 1991) is designed which involves assigning a percentage score to each dataset based on how frequently it ranks first (best) across various performance metrics. The scores are then summed up across all metrics. For example, if dataset A ranks first at two locations for discharge simulation in terms of NSE, while dataset B ranks first at one location, dataset A would receive a score of 67%, and dataset B would receive a score of 33% corresponding to metric $M_{NSE,Q}$. Then these scores would sum up to determine the best dataset across all metrics. This approach ensures that a dataset's poor performance in a single metric does not overly influence its overall ranking.

The percentage score (P*S*) for dataset *'j'* considering metric '*Mi*' is mathematical represented in Equation 4.2.

$$PS_j = \sum_{i=1}^{N} \left(\frac{T_{ij}}{L_i}\ x\ 100\right) \qquad (4.2)$$

Where T_{ij} is the total number of times dataset *'j'* ranks first for metric '*Mi*' across all locations, the L_i is the total number of locations for metric '*Mi*' and *N* is the total number of performance metrics.

4.2.4 Scenarios formulation

Five distinct scenarios are formulated to explore the research questions and mainly to assess how does the choice of evaluation metrics influence the identification of the most suitable gridded data product for precipitation estimation and for reproducing hydrological variables.

In the first scenario (SC-1), point to grid-cell comparison of data from precipitation products and three gauging stations is performed using performance metrics listed in Table 4.1. The aim is to identify the most plausible gridded product for precipitation estimation. In the second scenario (SC-2), the performance metrics applied to timeseries data of discharge and GWLs are considered. These are listed in rows 1 and 2 of Table 4.2. In the third scenario (SC-3), the focus is on metrics based on hydrological signatures which are listed in rows 3 to 17 of Table 4.2. This scenario explores which products reproduce hydrological responses in the catchment more plausibly and whether it is similar to the one identified as most suitable in scenario SC-2. The fourth scenario (SC-4) represents a more holistic approach that incorporates both timeseries and signature-based metrics corresponding to all metrics listed in Table 4.2. The aim is to determine how a comprehensive evaluation can alter the conclusions about which gridded product is overall the most suitable for hydrological simulation with the MIKE-SHE model in the study catchment. The results are also compared with scenario SC-1 to test whether the product identified as most suitable from comparison with station data is also the one that is the most suitable to reproduce hydrological variables.

Considering that researchers may select a different set of metrics, scenario SC-5 considers all the possible combinations of metrics listed in Table 4.1 and 4.2. This scenario acknowledges the subjectivity inherent in metric selection and demonstrates that different combinations can lead to different products being identified as the most suitable for a specific catchment. In this scenario, 65,535 possible combinations of metrics for precipitation estimation (from the set of 16 metrics), 33,55,4431 possible combinations for discharge (from the set of 25 metrics) and 511 possible combinations for GWLs (from the set of 9 metrics) were tested. The primary aim is to evaluate the influence of metric selection on identifying the most suitable precipitation products and to determine the products that are identified as suitable across majority of combinations. Further, outcomes

are used to examine whether considering multiple metrics for the evaluation of gridded precipitation products is beneficial and whether a minimum number of metrics needed for effective evaluation can be determined.

In all scenarios, the selected metrics are combined using two aggregation criteria for overall performance assessment i.e. DE (Equation 1) and PS (Equation 2).

4.3 RESULTS

4.3.1 Comparison of gridded precipitation products based hydrological simulations with gauge-based model

Hydrological variables were obtained as results of model runs with input precipitation from gauging stations, ERA5, IMERG, MSWEP and EOBS. The precipitation with the corresponding simulated discharge at the catchment's outlet on a daily scale for the period 2017-2019 is shown in Figure 4.1. The simulated discharge from the four gridded precipitation products (Q_{ERA5}, Q_{IMERG}, Q_{MSWEP} and Q_{EOBS}) is broadly consistent with the simulated discharge from the in-situ precipitation gauge data (Q_{Gauge}). In terms of KGE, the discharge is better reproduced by the IMERG at the outlet than the station data (0.68 vs 0.61). Whereas, in NSE, EOBS (0.69) performed better than IMERG (0.52) but not better than the gauge model (0.71). The performance of each product against the gauge data to simulate discharge is not consistent across different metrics (Figure 4.2a). For instance, EOBS is better in $M_{NSE,Q}$, $M_{LNSE,Q}$, $M_{MAE,Q}$, $M_{CC,Q}$, $M_{MAE,FDC}$ and $M_{KGE,RR}$ than the gauge model. The respective values are 0.57, 0.64, 0.70 $m^3 s^{-1}$, 0.77, 0.38 $m^3 s^{-1}$ and 0.77 against 0.56, 0.60, 0.73 $m^3 s^{-1}$, 0.76, 0.42 $m^3 s^{-1}$ and 0.51 for Q_{Gauge}, respectively. Whereas, IMERG performed better than the gauge model in eight metrics which is the highest among all products. These metrics are $M_{KGE,Q}$, $M_{NSE,FDC}$, $M_{KGE,FDC}$, $M_{ER,HFV}$, $M_{ER,1\text{-}lag}$, $M_{ER,VQ}$, $M_{ER,VLQ}$, $M_{ER,PQ}$ with respective values 0.68, 0.94, 0.75, 0.19, 0.28, 0.003, 0.22 and 0.08 against 0.59, 0.83, 0.63, 0.27, 0.36, 0.26 and 0.47 for Q_{Gauge}. In the case of ERA5 and MSWEP, although overall performance to reproduce discharge is comparatively poor among products but still for many metrics the values are better than the gauge model. For example, ERA5 has performed better in $M_{ER,MFS}$ (0.84 vs 0.95), $M_{ER,SE}$ (0.01 vs 0.06), $M_{ER,MQ}$ (0.01 vs 0.02), $M_{ER,MLQ}$ (0.09 vs 0.12) and MSWEP in $M_{LNSE,FDC}$ (0.89 vs 0.86), $M_{ER,RLD}$ (0.12 vs 0.20), $M_{NSE,RR}$ (0.73 vs 0.68), $M_{LNSE,RR}$ (0.75 vs 0.67), $M_{ER,MDQ}$ (0.18 vs 0.35). The results align with the findings of Almagro et al. (2021), who also observed that the precipitation product's performance in simulating discharge and signature is better than ground observed data at many locations in the Brazilian biomes including the Atlantic Forest, Cerrado, and Caatinga biomes.

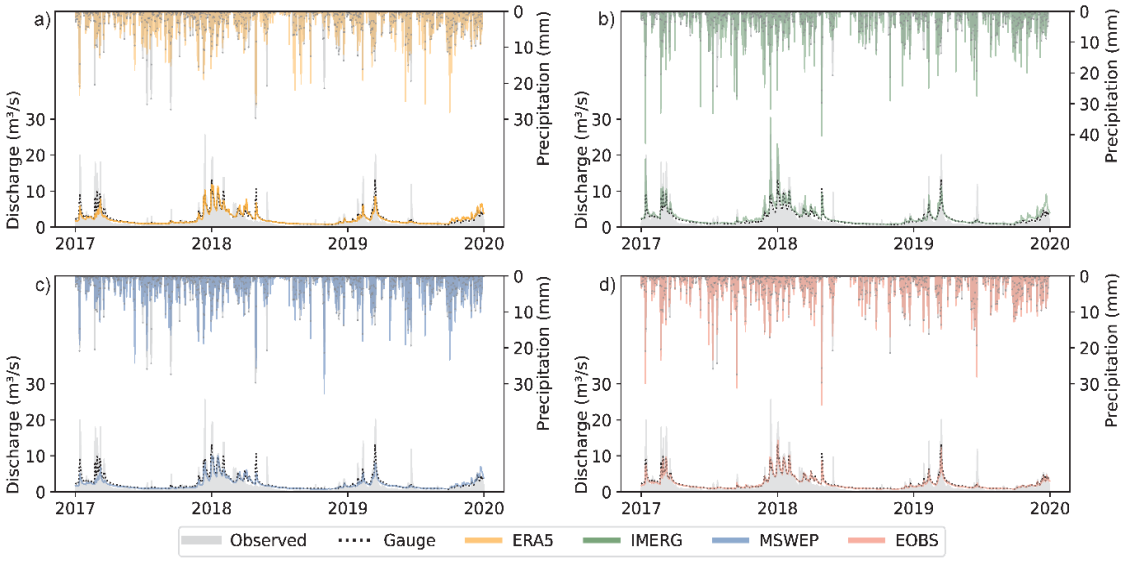

Figure 4.1. Observed and simulated discharge at the catchment outlet along with catchment average precipitation data from gauge station and the gridded precipitation products (a) ERA5, (b) IMERG, (c) MSWEP and (d) EOBS

In Figure 4.2, the values of metrics related to relative errors (M_{ER}) and MAE are inverted by subtracting them from 1 to ensure that higher values represent better performance. Greater variability is observed in discharge metrics' values across different precipitation

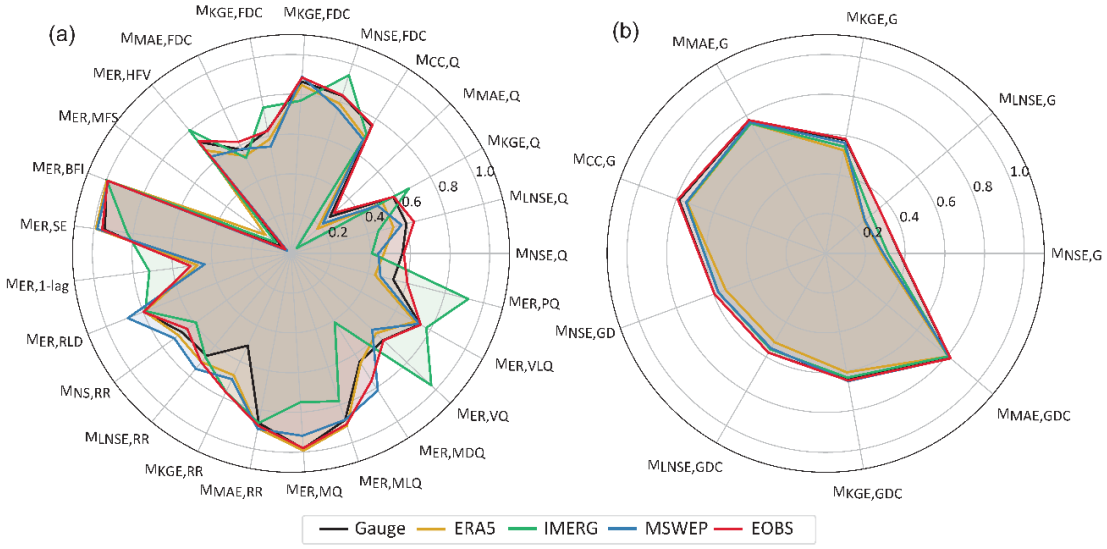

Figure 4.2. Average values of evaluation metrics for (a) discharge and (b) GWLs, across 3 discharge points and 13 groundwater points. Note: values of MAE are not normalized

products compared to the metrics' values for GWLs (Figure 4.2) which suggests that discharge is more sensitive to changes in precipitation than the GWLs. In eight out of nine metrics, EOBS performed equally well ($M_{LNSE,G}$, $M_{MAE,G}$, $M_{NSE,GDC}$, $M_{LNSE,GDC}$) or a bit better than the gauge model ($M_{NSE,G}$, $M_{KGE,G}$, $M_{CC,G}$, $M_{MAE,GDC}$) with a cumulative difference of only 0.002. MSWEP performed better than the gauge model only in $M_{KGE,GDC}$ (0.65 vs 0.64) and equally well in $M_{MAE,GDC}$ (0.180 vs 0.183). However, ERA5 and IMERG did not outperform the gauge model for groundwater simulation in any of the metrics.

The values of different metrics reflected the adequate ability of the model to capture the hydrological fluxes in the catchment. However, the main focus of the study is on the relative performance of precipitation products for hydrological simulations using a range of metrics, instead of assessing the model's own accuracy or effectiveness. Therefore, in the following sections, precipitation products are analysed in terms of their relative performance without comparing with the hydrological variables simulated with gauge-based model.

4.3.2 Scenario 1 comparison of gridded precipitation products with gauging station data

The spatial variability in the performance of gridded products across three precipitation stations (represented by diamonds) using the frequent applied metrics (KGE_R, NSE_R, $LNSE_R$ and MAE_R) are shown in Figure 4.3. Considering the timeseries (Figure 4.3a-d), EOBS has performed strongly in precipitation estimation across the majority of locations. The dominance is particularly visible in NSE_R (0.78 vs 0.443, 0.066, 0.463 for ERA5, IMERG and MSWEP, respectively), $LNSE_R$ (0.60 vs 0.57, 0.35, 0.59 for ERA5, IMERG and MSWEP, respectively) and MAE_R (0.9 mm d^{-1} vs 1.51 mm d^{-1}, 1.91 mm d^{-1}, 1.47 mm d^{-1} for ERA5, IMERG and MSWEP respectively) while in terms of KGE_R, MSWEP has outperformed EOBS at two locations (R1: 0.75 vs 0.72; R2: 0.77 vs 0.75) while at a third location (R3) EOBS has shown better results (0.78 vs 0.71). In contrast, ERA5 has shown limited performance with no dominance at any location while among all the products, IMERG has the poorest values for all the metrics. Comparing both ERA5 and IMERG with MSWEP, the difference in average KGE_R, NSE_R, $LNSE_R$ and MAE_R for ERA5 is only 0.5%, 4.4%, 3.6% and 2.5% while in the case of IMERG, the differences in metrics values are above 20%. For the metrics applied on the precipitation duration curve (Figure 3.4e-f), EOBS has the best value only at location R3 for KGE_{RDC} (0.86 vs 0.78, 0.85, 0.77 for ERA5, IMERG and MSWEP respectively) and NSE_{RDC} (0.97 vs 0.90, 0.96, 0.92 for ERA5, IMERG and MSWEP respectively). Whereas, ERA5 and MSWEP have better values than EOBS at locations R1 and R2 where ERA5 has shown dominance in terms KGE_{RDC} (R1: 0.95, R2: 0.98) and MAE_{RDC} (R1: 0.15 m d^{-1}, R2: 0.10 mm d^{-1})

while at the same locations, MSWEP is leading in terms of NSE_{RDC} (R1: 0.99, R2: 0.99) and $LNSE_{RDC}$ (R1: 0.97, R2: 0.99).

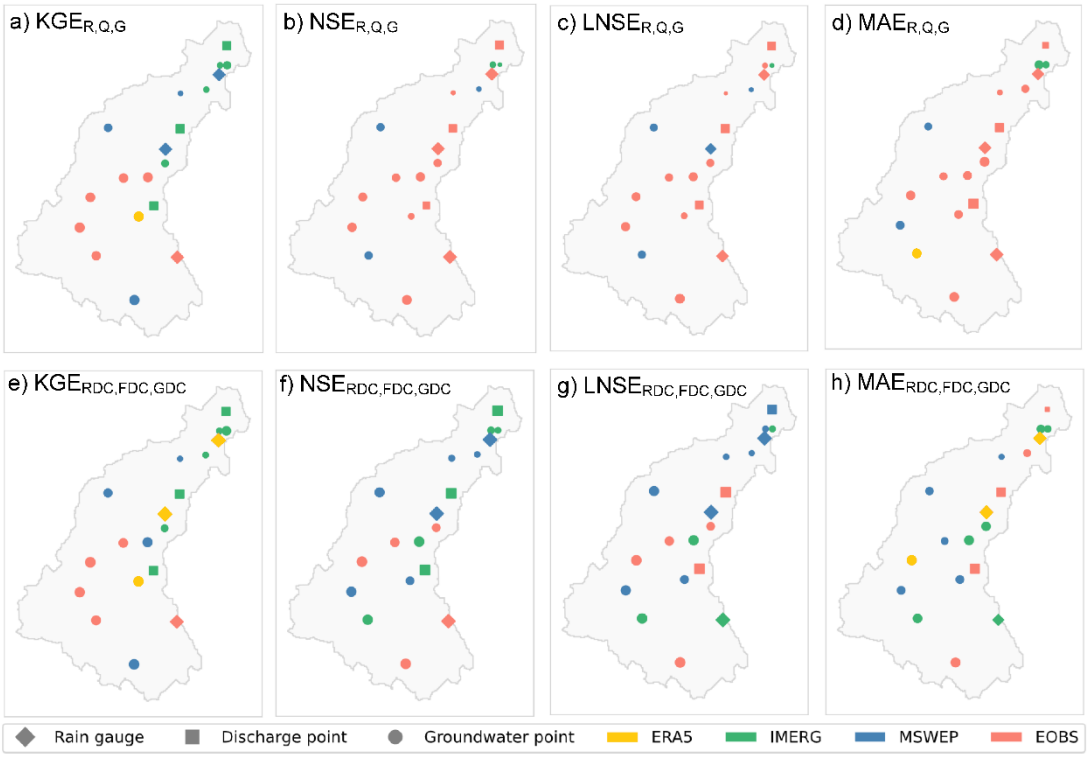

Figure 4.3. The best performing gridded product at each location on comparing with rain gauge data (diamonds, 3 locations), in simulating discharge (squares, 3 locations) and groundwater levels (circles, 13 locations) using metrics KGE, NSE, LNSE and MAE for timeseries (a-d) and duration curves (e-f). The colour of a marker represents the product with the best metric value at the specific location while the shape of a marker represents the variable. The size of a marker is proportional to the values of each metric. The MAE values (d and h) are normalized and inverted (subtracted from 1) to ensure that bigger markers represent better performance

Overall, the results of metrics applied to timeseries data (Figure 4.3a-b diamonds) clearly show the dominance of EOBS except for a few locations where MSWEP has better values. However, in terms of the rainfall duration curve (Figure 4.3e-f diamonds) each product has the best value at least at two locations affirming the strengths of these products with specific rainfall characteristics at particular locations. Considering the spatial distribution, it is complex to clearly identify any product as the most suitable one. Therefore, the

metrics are combined for the overall assessment using two criteria (DE and PS) explained in section 4.2.3 using Equations 4.1 and 4.2 and results are shown in Figure 4.4.

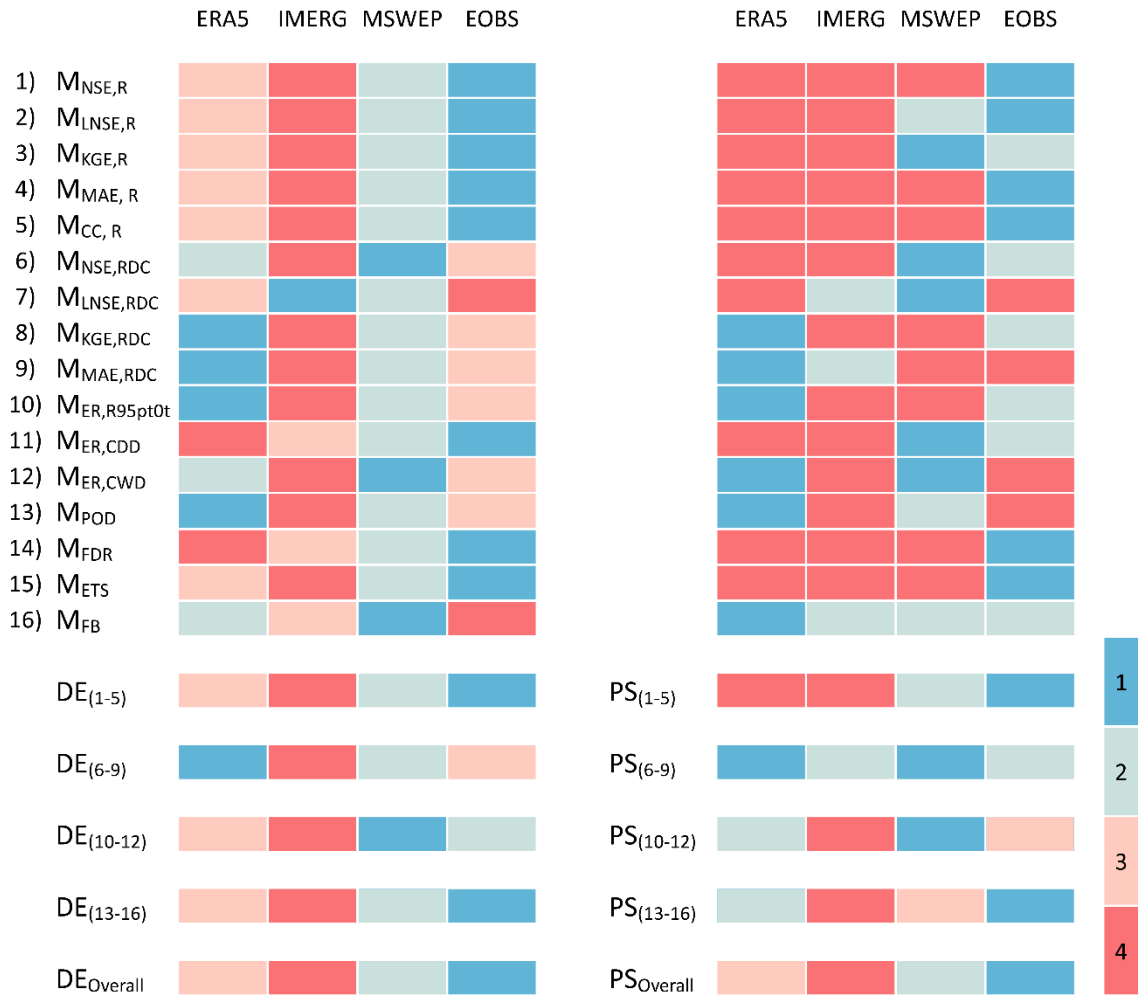

Figure 4.4. The performance of gridded precipitation products over the catchment for each metric (Table 4.1) represented individually and combined using criteria: (1) the Euclidean distance (DE) on the left side and (2) the Percentage score (PS) on the right side

EOBS has the best score across most of the timeseries metrics indicated by both criteria: $DE_{(1-5)}$ and $PS_{(1-5)}$ with scores of 0.467 and 400 respectively. The MSWEP has second best scores with $DE_{(1-5)} = 0.743$ and $PS_{(1-5)} = 100$. While for metrics applied to RDC, $DE_{(6-9)}$ supported ERA5 as the most suitable product with a score of 0.13 vs 0.32, 0.14, 0.24 for IMERG, MSWEP and EOBS respectively. Whereas, according to $PS_{6-9)}$ both MSWEP and ERA5 are equally suitable having equal scores (133). Therefore, in detecting the overall magnitude and frequency of rainfall, ERA5 and MSWEP are closest to the rain gauge station data. The aggregated score of precipitation extreme indices ($M_{ER,R95pt0t}$, $M_{ER,CDD}$ and $M_{ER,CWD}$) identified MSWEP as the most suitable product with $DE_{(10-12)}$ as

0.230 vs 0.37, 0.72, 0.36 for ERA5, IMERG and EOBS, respectively while as per $PS_{(10-12)}$ both MSWEP and ERA5 have same scores (107 vs 20, 67 for IMERG and EOBS, respectively). Considering the metric for the detection of events (M_{POD}), ERA5 has the top score (DE: 0.14, PS: 75). However, it showed the lowest performance in false discovery rate (M_{FDR}; DE: 0.21, PS: 0) which suggests that it detected rainfall events that did not actually occurred. Whereas, EOBS has the best scores in M_{FDR} (DE: 0.06, PS: 100) and M_{ETS} (DE: 0.40, PS: 100) that show its balance behaviour between detecting rainfall events without false alarms. Overall on combining the outcomes of detection metrics, EOBS stood out as the most suitable product as per both criteria with the value of DE as 0.23 vs 0.30, 0.37, 0.28 (PS: 220 vs 115, 20, 45) for ERA5, IMERG and MSWEP respectively.

Overall, the aggregated scores from both criteria considering all the metrics from Table 1, identified EOBS as the most suitable product to estimate precipitation in comparison with gauging station data. The DE (PS) score for EOBS is 0.35 (753) against 0.48 (355), 0.69 (107), 0.45 (385) for ERA5, IMERG and MSWEP, respectively. EOBS also has the best scores in most of the subcategories, especially in metrics for timeseries data. MSWEP also performed well with slightly lagging performance in a few metrics than EOBS and has second best overall scores. ERA5 has shown good performance in RDC metrics and extreme events magnitude but struggled in some event detection and timeseries related metrics. IMERG consistently underperformed across nearly all metrics except from $M_{LNSE,\ RDC}$ where it gained the best score. EOBS emerged as the most suitable product overall, especially for time series metrics, while MSWEP showed consistent secondary performance. ERA5 performed well for duration curve metrics and extreme events but had limitations in event detection. IMERG underperformed across most metrics. These results highlight the value of using multiple metrics for a comprehensive evaluation.

4.3.3 Scenario 2 comparison of gridded precipitation products to reproduce discharge and groundwater levels

The spatially distributed performance of precipitation products to simulate discharge and GWLs at different locations in the catchment evaluated in terms of M_{KGE}, M_{NSE}, M_{LNSE} and M_{MAE} are represented in Figure 4.3(a-d). For the discharge (represented by squares in Figure 4.3), EOBS has shown clear dominance in terms of M_{NSE}, M_{LNSE} and M_{MAE} at all three locations (Q1, Q2 and Q3) with average values of 0.57, 0.64 and 0.70 $m^3\ s^{-1}$ respectively. However, in terms of M_{KGE} (which is one of the most considered performance metrics in recent literature), IMERG has outperformed other products at all three locations (Q1: 0.68, Q2: 0.70, Q3: 0.66). Particularly when compared with EOBS, the percentage differences are 9.33 %, 10.55 % and 19.21 % at locations Q1, Q2 and Q3, respectively.

For GWLs (Figure 4.3a-d), EOBS performed slightly more plausibly than others, especially in the middle part of the catchment (GW6-11) where the average values of $M_{NSE,G}$ ($M_{LNSE,G}$) are 0.55 (0.54) against 0.47 (0.46), 0.43 (0.43) and 0.47 (0.47) for ERA5, IMERG and MSWEP, respectively. In terms of $M_{KGE,G}$, IMERG, MSWEP and EOBS have performed equally well by having the best score at four locations each with average values of 0.55, 0.56 and 0.58, respectively. ERA5 was the least frequent best performing product with best values only at GW10 for $M_{KGE,G}$ (0.81) and GW12 for $M_{MAE,G}$ (0.22 m).

The overall performance of gridded products to capture discharge and groundwater levels for the entire catchment aggregated using the DE and PS criteria are represented in Figure 4.5. The dominance of EOBS as the best performing product is clearly visible except for $M_{KGE,Q}$ where IMERG has performed better with values of DE: 0.32 and PS:100 against DE: 0.41 and PS:0 for EOBS. However, with respect to the final scores of DE and PS on aggregating all metrics, EOBS is identified as most suitable for simulating both discharge and GWLs (DE: 0.46 and PS: 723). The results are more ambiguous for the second best product. For discharge, according to DE, MSWEP has second best score (0.54 vs 0.59 for IMERG) whereas according to PS, IMERG has second best score (100 vs 0 for MSWEP). Contrary, in GWLs, IMERG is second best as per DE (0.51 against 0.52 for MSWEP) whereas MSWEP is second best as per PS (84.6 vs 76.9 for IMERG). However, the margin in DE (0.01) and PS (7.7) values for IMERG and MSWEP is not very high.

Considering discharge and GWL together, IMERG is in second place as per PS criteria (176.9 vs 84.6 for MSWEP) but it is in worst place as per DE criteria (0.55 vs 0.54, 0.53 for ERA5 and MSWEP, respectively). This may be due to its poor performance in M_{MAE} where its value is 23 % worse than MSWEP and its ‘square of difference from perfect values’ is approximately 52 % worse (see Equation 1). This significantly affected the overall ranking of IMERG according to the DE criteria.

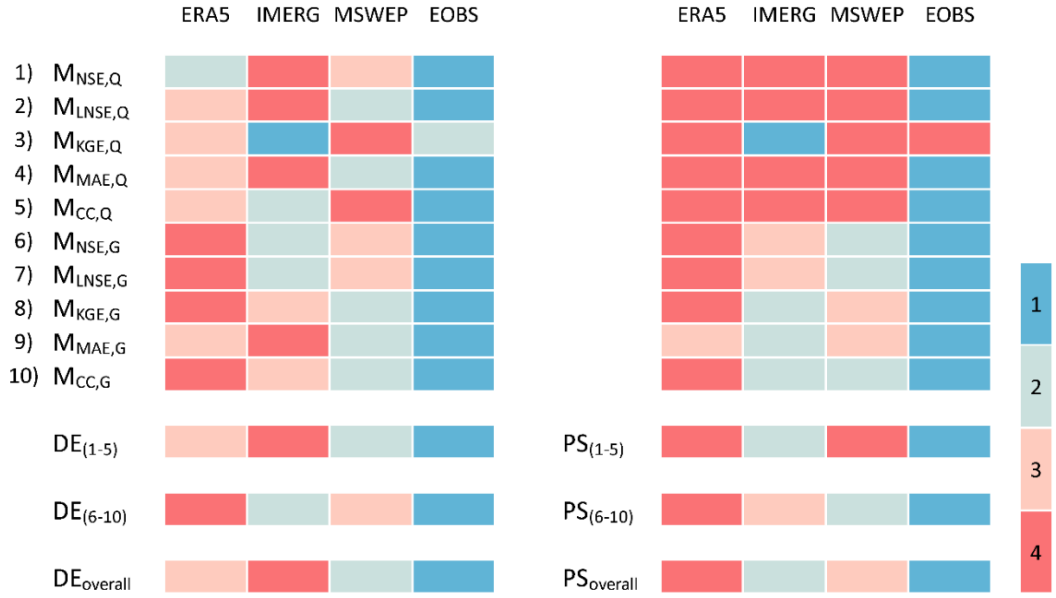

Figure 4.5. The performance of gridded precipitation products to reproduce discharge and groundwater levels evaluated using timeseries based metrics (Table 4.2, at 1 and 2) represented individually and combined using criteria: (1) DE on the left side and (2) PS on the right side. Performance is ranked on a scale from 1 to 4, with 1 representing the most suitable product while 4 representing the least one

Overall, IMERG despite having the best KGE values for discharge ($M_{KGE,Q}$, DE:0.10, PS:100), struggles with some other metrics such as $M_{LNSE,Q}$ (DE:0.29, PS:0) and $M_{MAE,Q}$ (DE:0.92, PS:0) indicating possible difficulties with log scaled flow (low flow conditions) and absolute error. On the other hand, EOBS demonstrated the best performance in simulating both discharge and GWLs and emerged as the best product overall for scenario SC-2. However, considering the spatially distributed results, its performance is not consistent at all the locations. MSWEP showed moderate consistent performance but did not attain the highest score in any single metric. ERA5 obtained the lowest score among the products reflecting comparatively large discrepancies from the observed data. In SC-2, EOBS was identified as the most suitable product overall for simulating both discharge and groundwater levels, despite some spatial inconsistencies. IMERG performed well in terms of KGE, particularly for discharge, but showed weaknesses in low-flow and absolute error metrics, affecting its overall ranking. MSWEP showed balanced but less dominant performance, while ERA5 consistently lagged behind.

4.3.4 Scenario 3 comparison of gridded precipitation products to reproduce signatures

In this scenario, the gridded precipitation products' suitability to reproduce flow and groundwater signatures has been analysed using 24 different metrics listed in Table 4.2 (3-17). The spatial distributed results of metrics applied to duration curves of discharge and GWLs are represented in Figure 4.3(e-h). For discharge (represented by squares), at all three locations, IMERG has the highest values for $M_{KGE,FDC}$ and $M_{NSE,FDC}$ with respective average values of 0.75 and 0.94 against ERA5 (0.58, 0.79), MSWEP (0.55, 0.76) and EOBS (0.63, 0.84), respectively. Whereas, in terms of $M_{LNSE,FDC}$ and $M_{MAE,FDC}$, IMERG is not among the top ranked at any of the discharge points. In $M_{LNSE,FDC}$, MSWEP has the highest values at Q1 (0.78) while EOBS has the highest at Q2 (0.96) and Q3 (0.93). While, for $M_{MAE,FDC}$, EOBS has the highest values across all three locations with an average of 0.38 $m^3 s^{-1}$ against 0.46 $m^3 s^{-1}$, 0.47 $m^3 s^{-1}$, 0.42 $m^3 s^{-1}$ for ERA5, IMERG and MSWEP, respectively.

IMERG attained the best scores in the metrics $M_{ER,HFV}$ (ERA5: 0.57, IMERG: 0.44, MSWEP: 0.61, EOBS: 0.52) and $M_{ER,\,PQ}$ (ERA5: 0.75, IMERG: 0.28, MSWEP: 0.73, EOBS: 0.63) that reflect the strength of the product to simulate high values comparatively better. Further, duration curves represent the distribution of magnitudes without considering time stamps and the results showed that IMERG excelled in simulating the high magnitudes (as evidenced by the metrics $M_{ER,HFV}$ and $M_{ER,\,PQ}$). This strength gave IMERG an advantage in terms $M_{NSE,FDC}$, as it is influenced by the high values and show enhanced efficiencies in such cases (as discussed in section 1). Conversely, in $M_{LNSE,FDC}$, the log transformation of data highlighted the low values and in such a situation MSWEP and EOBS performed better than IMERG.

Regarding the spatially distributed results of GWL duration curves (GDC; represented by circles in Figure 4.3e-f), the number of locations where EOBS is identified as most suitable for reproducing GDC has reduced compared to scenario SC-2. It lost the top rank at 1, 4, 5 and 6 number of locations in M_{KGE}, M_{NSE}, M_{LNSE} and M_{MAE} respectively. For instance, at location G5, the MSWEP ranked as first in $M_{NSE,GDC}$ where values are 0.47 (ERA5), 0.30 (IMERG), 0.62 (MSWEP) and 0.60 (EOBS). However, values are in close range for different products when averaged across all locations (G1-G13). For instance, the average values of $M_{NSE,GDC}$ for different products are 0.54 (ERA5), 0.57 (IMERG), 0.58 (MSWEP) and 0.60 (EOBS). Therefore, as per DE criteria (Figure 4.6, $DE_{(20\text{-}25)}$), EOBS remained the most suitable for reproducing groundwater signatures despite losing top rank at many locations (DE: 0.40, 0.37, 0.36, 0.35 for ERA5, IMERG, MSWEP and EOBS respectively). MSWEP is the second best as per DE criteria falling behind just by 0.01. However, it is the best performer as per PS criteria followed by IMERG, as in PS criteria the scoring is based on the percentage of times a product is ranked first (PS: 15, 123, 154, 108 for ERA5, IMERG, MSWEP and EOBS respectively).

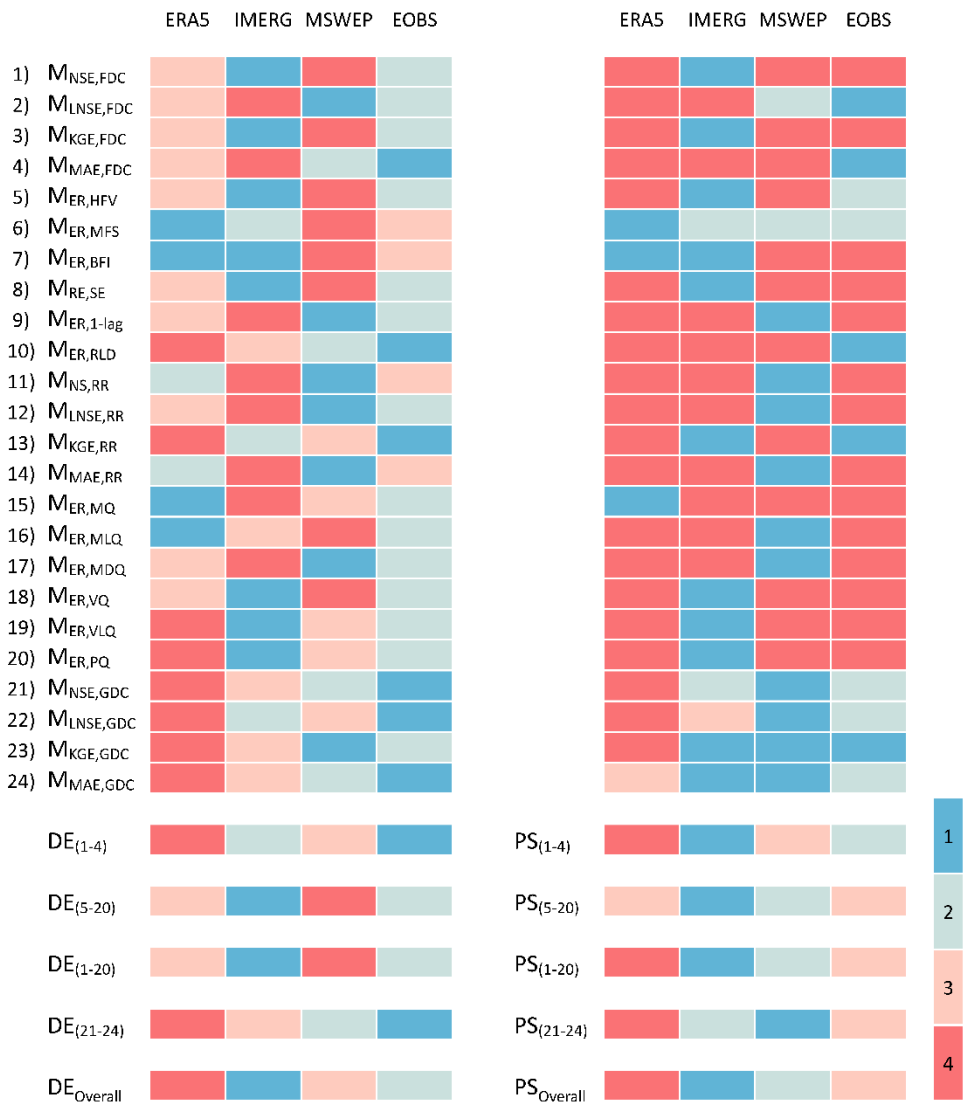

Figure 4.6. The performance of gridded precipitation products to reproduce discharge and groundwater signatures evaluated using signatures-based metrics (Table 4.2, row 3-17) represented individually and combined using criteria: (1) the Euclidean distance (DE) on the left side and (2) the Percentage score (PS) on the right side. Performance is ranked on a scale from 1 to 4, with 1 representing the most suitable product while 4 representing the least one

In discharge simulation, although, IMERG has higher average values of $M_{NSE,FDC}$ and $M_{KGE,FDC}$ than EOBS by 11.2 % and 15.9 % respectively, but the average values of $M_{LNSE,FDC}$ and $M_{MAE,FDC}$ are lower by 15.2 % and 18.9 %, respectively. Consequently, as per DE criteria ($DE_{(1-4)}$), IMERG is ranked second best after EOBS (DE: 0.34, 0.29, 0.33, 0.28 for ERA5, IMERG, MSWEP and EOBS, respectively) while it has higher score as

per PS criteria due to its better performance at more locations (PS: 0, 200, 33.3, 166.6 for ERA5, IMERG, MSWEP and EOBS, respectively).

In the metrics related to peak flows ($M_{ER,PQ}$), flow variance ($M_{ER,VQ}$ and $M_{ER,VLQ}$) and high segment flow ($M_{ER,HFV}$), IMERG attained high aggregated score than other products in capturing these flow signatures (DE:0.36 and PS:366.6). Whereas, in these metrics, EOBS ranked second (DE:0.56 and PS: 33). In addition to these, IMERG also performed best in metrics related to base flow index ($M_{ER,BFI}$, DE:0.05 and PS:100) and stream flow elasticity ($M_{ER,SE,}$ DE:0.53 and PS:100) indicating that most of the catchment characteristics are well captured by IMERG. However, in the metrics related to the runoff ratio ($M_{NSE,RR}$, $M_{LNSE,RR}$, $M_{MEA,RR}$ and $M_{KGE,RR}$), IMERG has comparatively the least aggregated DE score and MSWEP outranked other products with respective DE and PS scores of 0.24 and 300 against 0.29 and 100 for IMERG. In the metrics related to average flows ($M_{ER,MQ}$ and $M_{ER,MLQ}$) and mid-segment of FDC ($M_{ER,MFS}$), ERA5 attained the highest aggregated score which highlights its strength to simulate the average flows better than other products (DE: 0.56, 0.65, 0.65, 0.60 and PS: 166.6, 33.3, 133.3, 33.3 for ERA5, IMERG, MSWEP and EOBS, respectively).

Based on all metrics related to discharge (Figure 4.6, 1-20), IMERG is the most suitable in scenario SC-3 for reproducing flow signatures ($DE_{(1-20)}$:0.43 and $PS_{(1-20)}$:900). Whereas, for reproducing groundwater signatures, MSWEP attained highest score in PS criteria (154 vs 108 for EOBS), while EOBS ranked first as per DE criteria (0.35 vs 0.36 for MSWEP).

Given these results in scenario SC-3, each product has shown its strengths and weaknesses in terms of individual metrics. However, considering both discharge and groundwater signatures related metrics together, IMERG has the highest overall score in both DE and PS criteria and is identified as most suitable for reproducing the hydrological signature in the catchment (DE: 0.42 and PS: 1023). Whereas, EOBS is second best as per DE criteria (DE: 0.43 and PS: 541) and MSWEP is ranked second per PS criteria (DE: 0.46 and PS:820.5).

4.3.5 Scenario 4 comparison of precipitation gridded products to reproduce discharge, groundwater levels and hydrological signatures

In this scenario, all the metrics used in scenarios SC-2 and SC-3 are analysed together using both the DE and PS criteria. To evaluate the performance of gridded precipitation products in simulating the discharge and GWL along with relevant signatures, the DE and PS scores were also calculated separately for discharge and GWL by considering all the metrics that are related to these variables, as mentioned in Table 4.2. The results are represented in Figure 4.7. As per DE criteria, EOBS is the best precipitation product for simulating discharge (DE_Q: 0.45), GWL (DE_G: 0.42), and both together along with

signatures ($DE_{overall}$: 0.44). Whereas, IMERG is the second most suitable product with scores of 0.47, 0.45 and 0.46 for DE_Q, DE_G and $DE_{overall}$, respectively.

However, PS criteria generated different results when discharge or GWL were analysed separately. In the case of discharge, the top ranked product is IMERG (PS_Q: 1000) unlike in the DE criteria where EOBS (PS_Q: 833) holds the top spot. In GWL, EOBS remained top ranked in both criteria (PS_G: 430.8 and DE_G: 0.42). Whereas, the second best is different, which is MSWEP in the case of PS (PS_G: 238.5 and DE_G:0.46) and IMERG in the case of DE (PS_G: 200 and DE_G:0.45). However, the final ranks in overall results ($PS_{overall}$ and $DE_{overall}$) are the same in both criteria. The percentage difference in scores of DE and PS for ERA5, IMERG and MSWEP compared to EOBS are -10.8 %, -5.3 %, -9.6 % and -76.5 %, -5.1 %, -28.4 % respectively. The consistency in final rankings increases confidence in the suitability of best products for the simulation of hydrological processes, which is EOBS, with IMERG lagging only by approximately 5 % difference in both criteria.

Figure 4.7. The performance of precipitation gridded products to reproduce hydrological variables along with signature evaluated using all performance metrics (Table 2) combined using criteria: (1) DE on the left side and (2) PS on the right side. Performance is ranked on a scale from 1 to 4, with 1 representing the most suitable product while 4 representing the least one. DE_Q / PS_Q represents the results of metrics applied to discharge while DE_G / PS_G represents the results for GWL

Scenario SC-4 results show that EOBS as the most suitable precipitation product for reproducing discharge, groundwater levels, and related hydrological signatures, based on both DE and PS criteria. IMERG ranks second overall, with particularly strong performance for discharge under PS criteria. MSWEP shows moderate performance, especially for groundwater.

4.3.6 Scenario 5 comparison of gridded precipitation products considering all possible metrics combinations

In scenarios 1-4, the specific sets of metrics are considered to analyse that different sets of metrics can lead to varying conclusions about the most suitable gridded product for

estimation of precipitation compared to gauge data and for reproducing hydrological variables and signatures. There is a total of 50 metrics listed in Tables 4.1 and 4.2. Out of which 16 are related to rainfall, 25 to discharge and 9 to groundwater. The selection of metrics can be random from the total number of considered metrics leading to the possible number of combinations 65,535 for precipitation, 33,554,432 for discharge and 511 for groundwater. DE and PS values for each combination were calculated. The number of times each product ranked first in these combinations was summed and plotted against the number of metrics considered for making combinations from the set of total metrics (Figure 4.8).

The results of combinations indicated that when the number of considered metrics are less then more products have a chance to be ranked first. For instance, when a single metric is considered to identify the most suitable product for precipitation estimation then 31.3 %, 6.3 %, 12.5 %, 50 % of outcomes as per DE and 35.3 %, 0 %, 29.4 %, 35.3 % of outcomes as per PS supported ERA5, IMERG, MSWEP and EOBS, respectively. However, as the number of considered metrics is increasing, the likelihood of unsuitable products to be identified as most suitable is decreasing and outcomes are favouring fewer, more consistent performing products. For example, when any of the 7 out of 16 metrics are considered for evaluation of precipitation estimation then EOBS has a 74.8 % and 78.2 % likelihood to be identified as most suitable per DE and PS.

Similarly, in the case of discharge, when a single metric is considered then ERA5, IMERG, MSWEP and EOBS have 16 %, 36 %, 24 %, 24 % of results as per DE and 11.1 %, 37 %, 22.2 %, 29.6 % of results as per PS, respectively, that identified these products as most suitable for discharge simulation. Whereas, the number of metrics for which any single product has attained a 75% likelihood to be identified as most suitable is 16 as per DE (EOBS) and 19 as per PS (IMERG).

As per DE criteria for discharge (Figure 4.8c), if the considered metrics are more than 7, there is less than 1 % likelihood that ERA5 and MSWEP can be identified as best. While up to 23 metrics, there are 4.67 % of combinations where IMERG can be the top ranked product. As per PS criteria for discharge (Figure 4.8d), the results are 50 % converged towards IMERG when the number of metrics is 8 against 0.2 %, 19.3 % and 30.4 % likelihood for ERA5, MSWEP and EOBS respectively. The results highlighted the sensitivity of both the numbers and the choice of metrics for precipitation product evaluation. Testing multiple combinations reduces the likelihood of identifying the wrong product as the most suitable and the most persistent performing product can be identified.

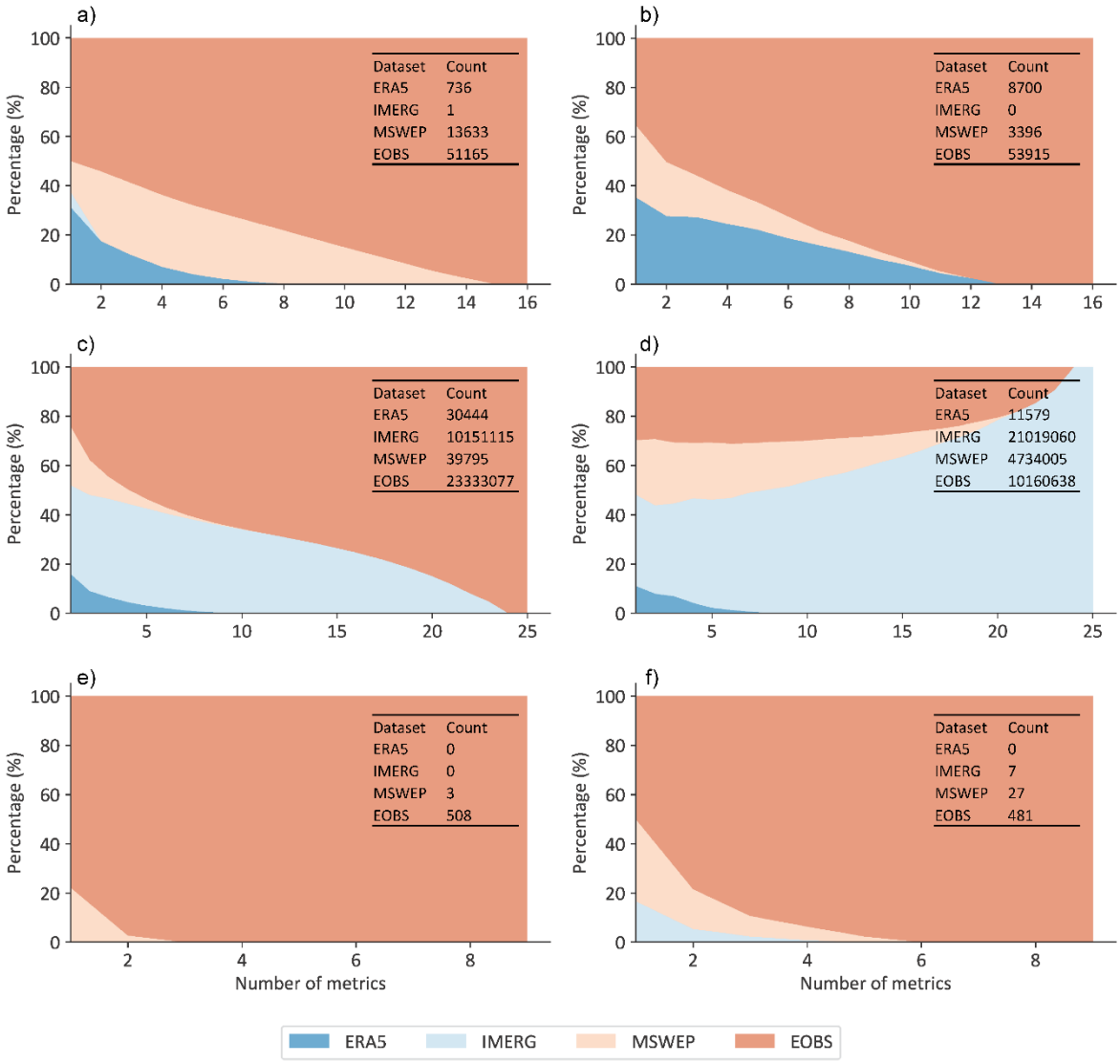

Figure 4.8. Stack area plots representing the percentage of time each gridded product identified as most suitable for precipitation estimation (a, b), discharge (c, d) and groundwater levels (e, f) corresponding to possible combinations considering a specific number of metrics from the set of metrics. The left panel (a,c and e) represents the result for DE criteria while the right panel (b,d and f) represents PS criteria

For GWLs, in both criteria, EOBS dominated by consistently ranking first for nearly all combinations. Especially in DE criteria (Figure 4.8e), out of 511 combinations, there are only three possible combinations where MSWEP could be at top. Under PS criteria (Figure 4.8f), IMERG and MSWEP have shown marginal existence by performing best in 7 and 27 combinations respectively but EOBS performance in GWLs metrics is plausible. However, there is a combination comprising of 5 metrics for which MSWEP is most suitable for GWL simulation. Similarly, in the case of discharge, the overall performance of ERA5 is very poor but still, there are 30,444 and 11,579 combinations of

metrics under DE and PS criteria, respectively, where it has been identified as the most suitable. This highlights the importance of metrics selection and the need for a detailed analysis considering all possible combinations which clearly illustrate the likelihood of all precipitation products to be identified as most suitable for hydrological applications.

Overall Scenario SC-5 demonstrates that the identification of the most suitable precipitation product is highly sensitive to the number and combination of metrics used particularly when then number of metrics are small. When fewer metrics are considered, the likelihood of misidentifying a less suitable product as the best increases. As more metrics are included, the outcomes converge towards consistently strong performers (EOBS for precipitation estimation and GWL simulation, and IMERG for discharge, particularly under PS criteria). This scenario highlights the critical importance of using multiple, diverse metrics to ensure robust and reliable evaluation of precipitation products in hydrological modelling.

4.4 Discussion

The main objective this study aims to address is to evaluate the influence of metric selection on identifying the most suitable gridded products for precipitation estimation from comparison with gauging station data and for reproducing hydrological variables (discharge and groundwater levels). The results of different scenarios and metrics combinations clearly reflect that the choice of evaluation metrics has a significant influence in determining the most suitable product. Depending on which metrics and which variables have been selected for evaluation, the results have varied a lot. For instance, individual metrics such as NSE applied to stream flow identified EOBS as most suitable for discharge simulation while KGE value for stream flow favoured IMERG (scenario SC-2). This contrast is due to the mathematical sensitivity of the metrics. NSE is highly sensitive to deviations between observed and simulated values because of its squared error formulation, which disproportionately penalizes errors in the timing and magnitude of peak flows. As a result, a few mismatches (especially during high-flow events) can significantly lower the NSE score, even when the overall hydrograph pattern is reasonably represented. The comparative low scores of IMERG than the EOBS in event detection metrics (Scenario SC-1) reflects its limitations in accurately capturing the timing and occurrence of rainfall events, which likely contributed to its lower score in NSE.

In contrast, KGE integrates three components (correlation, variability, and bias) into a single metric, providing a more balanced evaluation of the time series. This makes it more tolerant to timing errors compared to NSE and more reflective of overall hydrograph shape and consistency. Notably, the IMERG Final product is bias-corrected using monthly gauge data from Global Precipitation Climatology Center (Huffman et al., 2020),

which likely align its long-term mean and improve its performance in metrics that emphasize distribution and correlation, such as KGE. Further, hydrological signatures tend to evaluate specific aspects of the flow regime (e.g., peak flow volume, rising limb steepness, baseflow ratio) without being as sensitive to temporal alignment or individual outliers. This allows IMERG's strengths in capturing general hydrological aspects to be reflected more clearly in the signature-based analysis (scenario SC-3). Overall, EOBS performed well across a broader range of metrics and was identified as the most suitable for discharge and GWL simulation in scenario SC-2 and SC-4. Its consistently strong performance can be attributed to its gauge-based interpolation method, which aligns closely with observed station data. This illustrates the significance of interpreting metrics in the context of their mathematical sensitivities and the hydrological behaviours they emphasize.

Additionally, the results of scenario SC-5, where multiple combinations of metrics are tested, strongly support that the use of a single metric can lead to an unsuitable choice of gridded product either for precipitation estimation or hydrological simulations. The use of multiple metrics multiple combination provided a more robust and comprehensive assessment of the product's performance. Further, the use of different signatures in addition to timeseries based metrics, revealed the strengths and weaknesses of each product under varying hydrological conditions. This supports the findings of previous studies (Kiraz et al., 2023; Moges et al., 2022), which emphasize that relying solely on statistical performance measures may overlook important deficiencies in hydrological models and inputs. For instance, Kiraz et al. (2023) proposed a signature-based efficiency metric suitable for evaluating models in ungauged basins, showing that hydrological signatures can be regionalized and carry meaningful performance information beyond traditional metrics like NSE or KGE. Similarly, Moges et al. (2022) demonstrated that signature-based and process-based diagnostics can uncover functional mismatches in models that would otherwise appear satisfactory using only time series metrics. These studies reinforce our approach of using diverse time series metrics and hydrological signatures to perform a more comprehensive assessment of gridded precipitation product suitability.

Also, the results of scenario SC-5 reveal that the probability of consistently identifying the most suitable precipitation product increases with the number of metrics considered in the evaluation. This trend can be attributed to the fact that individual performance metrics capture distinct and often complementary aspects of model behaviour, such as central tendency (average conditions), variability, error magnitude, event detection capability, or responsiveness. Consequently, evaluations based on a limited or unbalanced set of metrics may reflect only partial product performance, leading to non-representative conclusions.

As the number of metrics increases, particularly when they are diverse and representative of multiple hydrological and statistical domains, the evaluation becomes more robust. This is because aggregating across multiple performance dimensions tends to mitigate the dominance of any single metric and minimizes the influence of outliers or artefacts. This approach improves the representativeness of the evaluation by combining time series statistical metrics with hydrological response characteristics, thereby increasing the stability of the product rankings.

The findings emphasize the importance of adopting multi-metric and multi-combination evaluation framework in hydrological modelling studies. Furthermore, the combinatorial analysis demonstrates that the selection of evaluation metrics significantly influences the outcome of product suitability assessments. This has important implications for future research, suggesting that the evaluation of precipitation products should move beyond conventional reliance on one or two widely used metrics (e.g., NSE or KGE), and instead adopt a more comprehensive, systematic approach. Incorporating a broader set of performance metrics can reduce the risk of overfitting product selection to a narrow evaluation scope and lead to more generalizable and defensible conclusions.

In this study, we attempted to determine the minimum number of metrics considering that the likelihood of identification of the most suitable product for precipitation estimation or hydrological simulations is at least more than 50 %. Few researchers have suggested the evaluation criteria should embrace at least one absolute error metric, one dimensionless metric for good of fit quantification and a graphical representation (Ritter and Muñoz-Carpena, 2013; Biondi et al., 2012) but any recommendation about the minimum number of metrics to be used for model evaluation was lacking. We agree that more metrics are better but due to the high computational burden and enhanced complexity related to result analyses, it will also become more challenging. Therefore, in scenario SC-5, it was explored by testing different numbers of metrics along with their possible combinations. In the case of precipitation estimation and discharge simulation, when the number of metrics considered is more than seven, the likelihood of the most unsuitable product to be ranked as best is less than 1 % and the likelihood of the most suitable product to be ranked at the top is more than 50 %. Whereas for the groundwater, the situation is quite different from the precipitation estimation and discharge, where the likelihood of the most suitable product to be identified as best is already about 90 % for GWL simulation by considering 3 metrics only. It is important to mention that the findings regarding the minimum number of metrics varied depending on the type of variable and the overall performance criteria (DE and PS). Moreover, the findings are based on the data from only one catchment whereas more generalizable outcomes could be achieved by extending the analysis to a larger number of watersheds (Kratzert et al., 2023).

The other question this research aimed to address was whether the product identified as most suitable based on comparison with station data is also the most suitable for reproducing hydrological variables? The results suggest that, although there is some alignment between the products' performance in precipitation estimation (as evaluated against gauge station data) and in hydrological simulations, this relationship is not consistent across all products and metrics. For instance, EOBS showed the best performance in precipitation estimation followed by MSWEP on the direct comparison with the gauge data (scenario SC-1). EOBS also performed well in simulating hydrological variables (scenarios SC-2 and SC-4). This indicated that the comparison with the gauging station data could be a good approximation for identifying the most suitable product for reproducing variables to some extent but could not be relied upon as the only criteria. This is because IMERG showed the worst performance in comparison with the gauge data but performed second best in reproducing hydrological variables (scenario SC-4) and best in reproducing signatures (scenario SC-3). Such discrepancy in outcomes suggests that the comparison of precipitation products with gauge data alone is not enough to judge the product's ability to simulate hydrological processes in the catchment. The findings align with Gebrechorkos et al. (2024), where the authors advocate the approach for precipitation products evaluation that considers the comparison of observed and simulated variables, as it can identify the product that can best capture the hydrological variability in the region. Similarly, Alexopoulos et al. (2023) did not compare the precipitation products with gauge data with an argument that gauges are only representative of the area that is covered by the measuring instrument (about 200 cm^2 for the well-known instrument). Whereas, the precipitation products might be outperforming gauge station data in capturing the spatial variability which is important in distributed hydrological simulations. Therefore, the multi-metric approach for comparison of simulated variables with the observed data is more comprehensive for the identification of the most suitable products for hydrological simulations instead of making a judgement based on comparison with the gauge data only.

Further, considering all metrics, no single precipitation product consistently performed well across all spatial locations in our study (Figure 4.3), which aligns with the findings of previous large scales studies (Gebrechorkos et al., 2024; Dembele et al., 2020; Beck et al., 2017). These studies report significant spatial variability in product performance, emphasizing that no single dataset performs best across all regions. For instance, Dembele et al. (2020) and Gebrechorkos et al. (2024) found that the top-performing product varied across climatic zones and basins, while Beck et al. (2017) highlighted that even globally well-performing datasets like MSWEP showed inconsistent accuracy across catchments. Although those studies covered much larger areas but similar pattern is observed in the lowland study area which reinforce the importance of product evaluation at comparative small scales as well.

Two independent criteria (DE and PS) for the multiple metric aggregation have be used to reach the final conclusions. Among these criteria, DE criteria have been employed by researchers in many studies to combine different metrics (Dembele et al., 2020; Hrachowitz et al., 2014; Hulsman et al., 2021). However, all metrics do not exhibit linear behaviour, for instance, the gain in NSE is gradual with the model improvement corresponding to a steep drop on large error (Jackson et al., 2019). If a product has performed very badly in specific metrics although it has performed very well in others, DE criteria can disproportionately penalize such product due to a squared difference from the best value (see Equation 1). Whereas, PS criteria is based on ranks ensures that the product is not unduly penalized by considering the number of times the product has been ranked first. While PS criteria is useful for identifying the products that perform well across multiple metrics and locations, it considers only rank and ignores the absolute values of the metrics. Therefore, consideration of dual criteria for overall performance evaluation has provided a more balanced perspective on the precipitation products evaluation and enhanced the confidence in the findings of the study.

While the findings of this study provide valuable insights into the impact of metric selection on precipitation product evaluation, it is important to acknowledge that the results are derived from a single catchment with lowland hydrological characteristics, mild slopes, and shallow groundwater tables. The performance of gridded precipitation products, and their ability to reproduce hydrological processes, can vary significantly across catchments with different climatic, topographic, and hydrological settings, such as arid regions, mountainous basins, or tropical catchments. As such, the generalizability of the identified best-performing products (e.g., EOBS or IMERG) may be limited beyond the context of this specific study area. However, the methodological framework developed in this study based on a multi-metric and multi-combination evaluation approach, is transferable and scalable. Future research may aim to replicate this across diverse hydro-climatic regions, allowing for broader conclusions on the performance of precipitation products as well as to make recommendations regarding the optimal number of metrics to be considered in the evaluation of EO precipitation products.

It is important to mention the limitations of the study. Firstly, the model was not calibrated separately for each precipitation product. The same approach has been adopted by Gebrechorkos et al. (2024) for the evaluation of precipitation products at the global scale. The parameter calibration for each product could lead to the compensation of biases in the input precipitation product (McMillan et al., 2016) which might impact the products evaluation, as the main evaluating tool which is the hydrological model, would vary for each dataset. On the other hand, there are studies (Dembele et al., 2020; Alexopoulos et al., 2023; Almagro et al., 2021) who did the calibration for each dataset. While we agree that the calibration could have improved the performance of each precipitation product but our focus was on relative performance evaluation. Further, in section 4.3.1, the results

showed that across different metrics gridded precipitation products have often performed better in simulating hydrological variables compared to gauge-based model, which supports that the base model contains the set of parameters that are not unduly biased towards any specific dataset and represents a neutral model. Secondly, the point to grid comparison of precipitation products with the rainfall gauge stations was carried. While this method is widely used in the literature (Bagiliko et al., 2025; Maranan et al., 2020; Ageet et al., 2022; Monsieurs et al., 2018; Ayehu et al., 2018; Dembélé and Zwart, 2016) and avoids additional uncertainty introduced by interpolation techniques, it does involve a scale mismatch between the spatial extent of a gridded pixel (~10 km²) and the point-based nature of gauge measurements (~200 cm²). This mismatch may introduce representation error, particularly in mountainous regions with high spatial variability in rainfall. However, in relatively flat lowland regions such as our study area, this effect is expected to be less pronounced. Future studies could explore the impact of alternative comparison methods, such as grid to grid evaluations by interpolating gauge data or using gauge corrected radar data, where appropriate.

4.5 Conclusions

This study evaluates the influence of the choice of performance metrics on the identification of the most suitable gridded product for precipitation estimation and reproducing hydrological variables. The research is done in Aa of Weerijs catchment using MIKE-SHE hydrological model over the period of 10-years (2010-2019) forced with four different precipitation products. The evaluation of gridded products is carried out for precipitation estimation compared to in-situ gauge data using 16 different performance metrics and for reproducing hydrological variables (discharge and GWLs) using 34 different metrics including hydrological signatures. The values of metrics are aggregated using two criteria (DE and PS) for the overall score. Further, all the possible combinations of metrics related to precipitation, discharge and groundwater are tested to explore the research objectives. The findings revealed that no precipitation product consistently performed better than others across all metrics in precipitation estimation or reproducing hydrological variables. For instance, EOBS performed best for reproducing discharge as per NSE value for stream flow while KGE for stream flow identified IMERG as the best product. It is not necessary that the precipitation product that is identified as most suitable for reproducing discharge and GWLs timeseries (EOBS) is also the most suitable for reproducing hydrological signatures (IMERG). Further, the comparison of precipitation products with gauging station data revealed that such evaluations may not consistently serve as a reliable procedure to determine the product's suitability for hydrological simulations. For instance, a relation was found in the case of EOBS where it has been identified as most suitable both for comparison with station data and also for simulating hydrological variables. However, IMERG poorly performed to estimate

precipitation relative to in-situ data from gauge stations but was identified as most suitable for simulating hydrological signatures. Therefore, we conclude that to identify the suitability of a product for hydrological processes, the reproduced hydrological variables are better to be evaluated with observed data.

Testing of multiple metric combinations demonstrated that when the number of metrics considered in evaluation criteria is small, then the likelihood of any product being identified as most suitable for precipitation estimation or reproducing hydrological variables is higher. In our case, when the number of metrics considered for evaluation is more than seven, then the likelihood of identification of the most suitable product for precipitation estimation and for discharge simulation is above 50 % and the likelihood of least suitable product to be chosen as best is less than 1 %. Whereas, for the GWLs, even with three metrics the likelihood of the most suitable product identification is above 90 %. These findings regarding the minimum number of metrics are specific to our study and may vary depending on catchment characteristics and the type of hydrological variables being studied. The multiple combination analysis highlighted the sensitivity of products' ranking to the choice of metrics. For instance, the overall aggregated scores determined that the performance of ERA5 was the worst among the four precipitation products for reproducing discharge but still there were about 30 thousand and 11 thousand possible combinations of metrics under DE and PS criteria, respectively, that ranked the product at the top. This describes that a selective set of metrics could lead to an unsuitable choice of precipitation product. Therefore, multi-metric, multiple combination analysis provides a comprehensive evaluation method for identifying the most suitable product for hydrological applications.

The findings of the study give a critical insight into the sensitivity associated with the choice of metrics and the significant influence of metric selection on identifying the most suitable precipitation products. Although the outcomes are limited to the study catchment but scientific community can benefit from the methodology proposed. The framework was developed and demonstrated in a well-instrumented catchment but it is adaptable to data-scarce regions as well where traditional ground-based observations are limited. In such contexts, alternative remotely sensed variables such as evapotranspiration or soil moisture can be used as evaluation variables, allowing the proposed multi-metric evaluation framework to still support the identification of the most suitable precipitation products based on broader hydrological behaviour. Further the application is not limited to precipitation products but can be applied to evaluate other EO products and to assess model performance in routine hydrological modelling practices.

5

CLIMATE AND LAND USE/LAND COVER CHANGE IMPACTS

The hydrological processes within the catchment are generally influenced by both climate change and land use/land cover (LULC) change. However, most of the studies are focused on their individual impact on the catchment's hydrology, while their combined effects have received little attention. This chapter presents study which employs the physically based fully distributed hydrological model, MIKE SHE, to analyse the separate and combined effect of climate and LULC change on the hydrology of a mesoscale catchment in the near future (2050s). An Artificial Neural Network - Cellular Automata (ANN-CA) based prediction model was trained to simulate the future LULC map. The future meteorological data under four climate change scenarios was obtained from the Royal Netherlands Meteorological Institute (KNMI). The model results showed that the combined effects of climate change with LULC changes did not significantly differ from the individual impact of climate change on the catchment scale. However, on the local scale, the changes in LULC can significantly influence the variations in groundwater table, soil moisture, and actual evapotranspiration ranging from approximately -6 to 15 %, -9 to 27 %, and -30 to 10 % respectively, depending on the specific change in LULC class and season. In summary, this chapter provides valuable insights into the complex interactions between LULC changes, climate change, and hydrology.

This chapter is based on the journal publication: Ali, M. H., Bertini, C., Popescu, I., & Jonoski, A., 2025. Comparative analysis of hydrological impacts from climate and land use/land cover changes in a lowland mesoscale catchment. International Journal of River Basin Management, 1–19. https://doi.org/10.1080/15715124.2025.2454692

5.1 INTRODUCTION

Climate change poses serious risks to water availability and food security, impeding progress towards Sustainable Development Goals. Its far-reaching adverse effects influence both natural ecosystems and human communities, revealing disparities across different systems, regions, and sectors (Lee et al., 2024). The IPCC Sixth Assessment Report (AR6, 2023) stated with a high degree of confidence that the rate of rise in global surface temperature since 1970 has surpassed that of any other 50-year period in the past 2000 years. This continuous temperature rise underscores the increasingly apparent climate-driven changes (Blöschl et al., 2019).

Climatic variations, particularly changes in precipitation and temperature, can profoundly affect both the hydrological state and the spatiotemporal distribution of water resources (Sorribas et al., 2016; Sunde et al., 2017). To counter these, water management strategies need to prioritize climate change, emphasizing the implementation of basin-scale hydrological management techniques (IWMI, 2019). However, selecting appropriate adaptation strategies necessitates a thorough understanding of the potential impact of global climate change on the local environment (Adib et al., 2020). Therefore, one of the initial steps in assessing the impact of climate change on hydrological systems involves comprehending how future climate signals will influence key catchment hydrological variables.

Alongside climate change, land use/land cover (LULC) change is also one of the important drivers of hydrological variations (Rigby et al., 2022; Kundu et al., 2017; Trang et al., 2017). Changes in LULC can influence hydrological processes, such as evapotranspiration (ET), interception, infiltration, and surface runoff. These effects occur through direct alterations to the landscape's morphology and physiology, as well as indirect modifications to the soil and atmospheric boundary layers (Zhang et al., 2018).

Research examining the impact of human-induced changes in landscape patterns and climate change has gathered significant attention. However, the majority of this research has primarily focused on either the effects of climate change or changes in land use, rather than considering both factors combined (Nazeer et al., 2022; Gurara et al., 2021; Kay et al., 2021; Adib et al., 2020). In addition to that, when these factors are examined together, the emphasis of the study is often centered on evaluating variations in surface hydrological variables alone (Ma et al., 2023; Lyu et al., 2023; Zhang et al., 2023; Sinha et al., 2020; Iqbal et al., 2022) or only on groundwater dynamics (Hanifehlou et al., 2022; Ghimire et al., 2021).

Furthermore, the existing literature presents a certain level of variation regarding the individual influence of climate change and LULC change on hydrology. While some studies assert that LULC change had a more significant impact on hydrological variables in their study areas (Zhang et al., 2023; Zhou et al., 2019), others highlighted the

prominent influence of climate change (Huq and Abdul-Aziz, 2021; Ye et al., 2023; Iqbal et al., 2022) (Fu et al., 2019). Consequently, a dedicated combined analysis for a specific catchment becomes imperative (Wedajo et al., 2022). Further, the positive or negative change in the climatic variables due to climate change is quite uncertain as the Global Climate Models (GCM)/Regional Climate Models (RCM) differ for each study site, along with climate and land use characteristics (Blöschl et al., 2019; Song et al., 2021). Hence, conducting a study for the area of interest with a focus on local changes is seen as crucial for a comprehensive assessment of catchment surface and subsurface hydrological changes, which is necessary for the development of effective water management practices.

In recent years, nearly all regions of Europe have experienced significant impacts from droughts affecting critical systems such as agriculture, water supply, energy, river transport, and ecosystems. These impacts are projected to intensify further attributed to climate change (Rossi et al., 2023). In the summer of 2018, the Netherlands experienced below average precipitation during May, June, July, September, and October. The Southern and Eastern regions of the country were more affected by this dry period, leading to significant impacts on crop yield and grasslands due to a reduction in water availability (Philip et al., 2020). The situation was similar in the Aa of Weerijs catchment, which is situated in the south of the Netherlands and shared with Belgium. The main land use in the area is agriculture, which highly depends on water resources. It is important to analyse the future local hydrological trends in the catchment to prepare for long term effective management practices in the area. Therefore, focusing on this catchment, this chapter aims to analyse both the individual and combined impacts of future projected changes in LULC and meteorological variables on surface and subsurface hydrology. Additionally, it seeks to address a knowledge gap about how crucial is it to consider future LULC changes alongside changes in meteorological variables under climate change when assessing the future hydrological state of a mesoscale (346 km^2) catchment. To conduct the analysis, a fully distributed hydrological model using MIKE SHE modelling tool was setup with historical data. The simulation results were then compared by running the model with: future meteorological data from KNMI'23 climate scenarios alone, with only the ANN-CA predicted future LULC map, and with both combined.

Following this introduction, the chapter provides the details of the research materials and methods utilized. Subsequently, the results obtained from the research are presented, along with a comprehensive discussion of the findings. Finally, the chapter concludes with a summary of the key findings and their implications.

5.2 MATERIALS AND METHODS

The research was carried out for the Aa of Weerijs catchment. The MIKE-SHE hydrological model was developed for the area and utilized to carry out the research. The

description of the study area, details of the input data and model setup are provided in the Chapter 3. Therefore, this information is not described here.

5.2.1 Future land use / land cover projection

LULC plays an important role in hydrology as changes in it can disturb water and energy balances consequently affecting processes such as transpiration, interception, evaporation, and infiltration. The impact of future LULC can be assessed in two ways. The first option involves considering a hypothetical scenario where one LULC type undergoes a complete transformation into another type (Zhang et al., 2020a). This approach is, however, subjective and lacks specificity. Alternatively, the impact can be evaluated by simulating future LULC using prediction models based on past changes and other influencing variables (Getachew et al., 2021). These prediction models generally use techniques such as Cellular Automata (CA), the Markov Chain Model (Marhaento et al., 2018), and Artificial Neural Networks (ANN). CA is a commonly used method that predicts the evolution in LULC based on the initial state, neighbouring cells, and transition rules. Complicated transition rules are often defined by coupling neural networks with CA (Liu et al., 2017). Machine learning algorithms can facilitate the learning of change factors based on historical data from two periods to simulate the change rules for future maps.

In this study, ANN-CA was used to simulate the potential future LULC map because of its consistently satisfactory performance over the literature (Roy and Rahman, 2023; Kafy et al., 2020). For this task, we utilized QGIS 2.18 and the MOLUSCE plugin. Given the availability of CLC maps for the earliest (1990) and most recent (2018) years, the subsequent predicted map was generated for the year 2046 considering it as a representation of the average LULC condition of the catchment in the 2050s. The process involved two phases. In the first phase, CLC maps for 2006 and 2012 were treated as dependent variables, while raster maps of Euclidean distance from rivers, roads, and digital elevation served as independent variables. The dependent variables were used by the tool to calculate pixel-by-pixel change map while Pearson correlations are calculated between independent variables. The Multilayer Perceptron (MLP) ANN was then trained to predict transition potential. Afterward, CA was employed to simulate the LULC map for 2018, which was validated against the CLC map for that year. The finest results were achieved with parameter values of learning rate = 0.10, hidden layers = 1 with 10 neurons, momentum = 0.050, and iterations = 1000. The kappa coefficients ($k_{overall}$, k_{histo}, and k_{loc}) and percentage of correctness were used to quantify the agreement between the reference and simulated LULC map.

In the second phase, using the above mentioned finalized parameters of the model, the map for 2046 was simulated using the CLC maps from 1990 and 2018, along with the aforementioned independent variables. It is worth mentioning here that the future map was simulated under a business-as-usual scenario, without incorporating any landscape

planning policies or restrictions on specific LULC classes. The study's objective was not to generate various future landscapes but to find out the hydrological significance of incorporating future LULC maps in climate change studies. Therefore, the business-as-usual scenario was chosen to generate the future LULC map assuming it as a representative of a worst-case scenario.

5.2.2 Future meteorological projections

To run the hydrological model for future climate change analysis, rainfall, and potential evapotranspiration (PET) data are required. For this study, the future climate data is obtained from KNMI (Koninklijk Nederlands Meteorologisch Instituut), the meteorological institute of the Netherlands. The dataset is known as KNMI'23 climate scenarios, as it was made publicly available in October 2023. These scenarios are based on the Coupled Model Intercomparison Project (CMIP6) model runs and translate the Intergovernmental Panel on Climate Change (IPCC) 2021 global climate projections for the Netherlands. The KNMI's Global Circulation Model (GCM) EC-Earth3 model, which is also part of Coupled Model Intercomparison Project (CMIP6) models, was re-tuned to reduce the bias and resampled based on CMIP6 target values. The results were then dynamically downscaled with the regional atmospheric climate model RACMO, also owned by KNMI. In the end, the outputs of RACMO were bias-corrected based on observed data (1991-2020) using the Quantile Delta Mapping method (Cannon et al., 2015). More details can be found in the scientific report by KNMI (van Dorland et al., 2023).

KNMI'23 scenarios consist of six paths that describe the possible future climate in the Netherlands around the years 2050, 2100, and 2150. In this study, we are focused only on the near future (2050). For that time frame, the climate scenarios data is available from 2036 to 2065, with the 30-year time horizon representing the averaging condition of 2050. The scenarios are based on the three levels of CO_2 emissions, according to the Shared Socioeconomic Pathways (SSP): high 'H' (SSP5-8.5), moderate 'M' (SSP2-4.5), and low 'L' (SSP1-2.6). Each emission scenario is further combined with wetting scenario 'N' ('Wet' is 'Nat' in Dutch) and drying scenario 'D' ('Dry' is 'Droog' in Dutch) based on the circulation of precipitation. The wetting scenario represents a wetting trend in winter and moderate drying in summer, while the drying scenario provides drier conditions in summer and moderate wetting in winter. Consequently, the six resulting scenarios are HN, HD, MN, MD, LN, and LD.

In this study, scenarios MN and MD were not considered due to our focus on extreme climate change scenarios. Our analysis concentrated on the high CO_2 emissions scenarios (HN, HD) and low CO_2 emissions scenarios (LN, LD). Moreover, as scenarios MN and MD lie between the high and low envelopes, their elimination did not affect the high and low values of the results. The data at the daily time step is available at a resolution of 0.5°

by 0.65˚ and covers only the Dutch part of the catchment. To overcome this issue, the model grids belonging to the Belgian part of the catchment were filled with data from the closest neighbouring grid cells. The time series were extracted from the gridded data at the locations where the three rain stations (Ginneken, Zundert, and Leonhout) are situated (Figure 3.1) and presented interpolated over the model domain using Thiessen polygons to keep the methodological consistency with the base model.

Moreover, the future projected rainfall and PET for the time horizon 2050 (2036-2065) were compared with observed data from the base period (2011-2020) to calculate the projected relative change in rainfall and PET. To analyse extreme events, the statistical metric 'R95pTOT' was calculated for each season using catchment average rainfall data for the base period and future scenarios. R95pTOT quantifies the contribution of very wet days to the total rainfall, with the threshold for very wet days set at the 95th quantile of daily rainfall data for the base period. It is also defined as the sum of rain in wet days, i.e. days with rainfall above the 95th percentile. Further, the rainfall duration curves were plotted to compare the low, middle, and high-intensity rainfall events for the base period and four climate projection scenarios. The 95th and 30th percentile lines were marked as thresholds for comparison of high and low intensity rainfall events (Jian et al., 2022).

5.2.3 Simulation scenario design

To assess the impacts of climate change and LULC change on the hydrology of the Aa of Weerijs catchment and to elucidate the significance of incorporating future LULC considerations in climate change studies, three simulation scenarios were developed. The first scenario exclusively considered future LULC changes, obtained with the developed ANN-CA model. The second scenario solely accounted for changes in future meteorological variables and employed the developed MIKE SHE model forced with the KNMI'23 climate projections. The third scenario, instead, considered both future LULC and climate change. Further details are provided in Table 5.1.

To analyse the results under these scenarios, the relative changes in seasonal catchment averages for AET, discharge at the catchment outlet, recharge to groundwater (recharge), and base plus drain flow to the river (subsurface flow) were computed using Equation 5.1.

$$\Delta = \frac{X_{scenario} - X_{base}}{X_{base}} \times 100 \qquad (5.1)$$

where Δ represents relative change, X_{base} is the variable value simulated during the base period and $X_{scenario}$ is the variable simulated under the respective scenario. A positive value of Δ indicates an increase while a negative value indicates a decrease. For the GWT, as the levels are referenced to the surface, the terms in the numerator of Equation 5.1 were inverted to maintain consistency in sign conventions.

The results were further examined at the local level, considering seasonal spatially distributed values for AET, soil moisture (SM) in the top 10 cm layer, and GWT using Equation 5.1 at each grid cell, and results are presented as maps.

Table 5.1. Description of designed simulation scenarios

Abbreviation	Meteorological data	LULC map
SC1	Observed data for base period (2010-2019)	2046
SC2	Climate scenarios LD, LN, HD, and HN for 2050-time horizon (2036-2065)	2018
SC3	Climate scenarios LD, LN, HD, and HN for 2050-time horizon (2036-2065)	2046

5.3 RESULTS AND DISCUSSION

5.3.1 Future land use / land cover simulation

CLC maps of the years 1990 and 2018, along with other driver variables such as Euclidean distance from rivers, roads, and DEM, were used to simulate the future LULC map of the year 2046 using the developed ANN-CA model. Before simulating the future LULC map, the LULC prediction model was validated using the CLC 2018 map. The agreement between the reference and simulated map was assessed using the kappa coefficients ($k_{overall}$, k_{histo}, k_{loc}) and the percentage of correctness. Their values were 0.94, 0.97, 0.95, and 95.7 % respectively, lying in the high agreement range (Roy and Rahman, 2023; Viera and Garrett, 2005). The map of 2046 was then simulated using the validated model (Figure A1 in Appendix).

According to the CLC map, the area was categorized into 17 different land use classes, which were aggregated into 5 major classes following Feranec et al. (2016) for understanding the major shifts in the LULC (Table 5.2). According to the results, the built-up area has shown a consistent increase over the examined period. Starting at 39 km² (11.3 %) in 1992, it expanded to 47 km² (13.6 %) in 2018 and is projected to further grow to 52.8 km² (15.3 %) by 2046. This pattern reflects further urbanization and infrastructure development in the area. Agricultural lands experienced a minor decrease from 263.3 km² (76.1%) in 1992 to 251.8 km² (72.8 %) in 2018. The map of 2046 suggested a continued decline to 244.5 km² (70.7 %) but still agriculture remained the dominant LULC in the region. Considering the changes within the agricultural class of landcover, 1.75 km² of area has been projected to shift from ‘Complex cultivation patterns’ (CCP) to ‘Land principally occupied by agriculture’ (LPA). The category of ‘Forest and

semi-natural' (FSN) areas demonstrated minor positive growth, increasing from 38.3 km² (11.1 %) in 2018 to 39.8 km² (11.5 %) in 2046. Wetlands remained relatively stable over the years. Starting at 6.8 km² (2 %) in 1992, they decreased slightly to 6.5 km² (1.9 %) in 2018, but the projected map maintained this stability at 6.5 km² (1.9 %) in 2046. Similarly, for the water bodies, the simulated covered area remained 2.3 km² (0.7 %).

In general, there has not been any unrealistic LULC change in the region which is predicted by the ANN-CA model. The simulated map for the year 2046 indicated an expansion of built-up areas, particularly around existing urban zones, encroaching into agricultural areas. It is important to note that the simulated future map for the year 2046 was generated under a business-as-usual scenario, without the integration of specific landscape planning policies or restrictions on LULC classes. The choice of a business-as-usual scenario serves as a representation of a worst-case scenario, emphasizing the potential impacts of unchecked urban expansion and changes in agricultural land use. By doing so, the study aims to highlight the hydrological consequences associated with the absence of proactive planning measures or land management policies in the face of future climate and LULC changes. This approach provides valuable insights into the potential challenges and risks that may arise under such conditions, contributing to a more comprehensive understanding of the complex interactions between land use, climate, and hydrology.

Table 5.2. Areas under historical (1990, 2018) and future simulated (2046) LULC maps

Corine land use / land cover class	**Aggregated class**	**Historical**				**Simulated**	
		1990		2018		2046	
		km²	%	km²	%	km²	%
Discontinuous urban fabric Industrial or commercial units Road and rail networks and associated land Green urban areas Sport and leisure facilities	Built-up area	39	11.3	47	13.6	52.8	15.3
Non-irrigated arable land Pastures Complex cultivation patterns Land principally occupied by agriculture, with	Agricultural	263.3	76.1	251.8	72.8	244.5	70.7

significant areas of natural vegetation							
Broad-leaved forest Coniferous forest Mixed forest Natural grasslands Moors and heathland Transitional woodland-shrub	Forest and semi-natural	34.8	10.1	38.3	11.1	39.8	11.5
Inland marshes	Wetlands	6.8	2	6.5	1.9	6.5	1.9
Water bodies	Water bodies	2	0.6	2.3	0.7	2.3	0.7

5.3.2 Future meteorological projections

The 10 years from 2010 to 2019 were considered as a baseline period to calculate the relative change (Equation 5.1) as a percentage difference for rainfall and PET, for the assessment of projected meteorological changes in the 2050 horizon. The outcomes of the comparison across all scenarios are presented in a range based on the highest and lowest values achieved overall. The findings indicated that in all months the percentage change in PET is positive under each scenario, indicating an increase in future conditions. In contrast, rainfall exhibited a more random pattern (Figure 5.1). During winter months (DJF: December, January, February), minor variations in rainfall are observed in January and December. However, In February, the percentage increase ranged from 17.3% to 24%, making it the wettest month in the winter season. In March and April, there is a notable increase in rainfall percentages (ranging from 3.9 to 14.7 % and 6.9 to 11.3 %, respectively) compared to December and January. Conversely, the rise in PET during these months is less pronounced, ranging from 1.6 to 5.3 % and 3.3 to 6.7 %, respectively. The combined effects contribute to making March and April relatively wetter. Conversely, in December and January, the relative percentage differences in rainfall are lower (-1.2 to 6.6 % and -5.2 to 2.6 %, respectively), while PET shows more substantial increases (ranging from 8 to 10.1 % and 14 to 15.8 %, respectively), leading to relatively low wet conditions. This shift indicates a temporal change in the rainfall pattern, transitioning from the winter months (December and January) to the spring months (March and April), resulting in increased rainfall during the latter period.

The months of May, July, and August show an increase in PET accompanied by a decrease in rainfall. In June, rainfall is projected to decrease by -1.6 % under the HD scenario, while it is expected to increase upto 7.9 % in other scenarios with a maximum value under HN scenarios, respectively. However, PET in June is projected to increase under all scenarios by 4.1 to 8.5 %, not balancing the increase in rainfall, likely making the overall conditions drier. August emerges as the driest month, characterized by a rise in PET and a decline in rainfall in the ranges of 12.6 to 17.3 % and 7.9 to 18.3 %, respectively. Moving to autumn (SON: September, October, and November), there is an overall major increase in rainfall compared to other seasons (13 to 15.5 %), but PET also shows an upward trend (Figure 5.1). Winter also shows an increase in rainfall (2 to 9.1 %) but is accompanied by a simultaneous rise in PET (8.8 to 10.1 %), consequently balancing out the increase in rainfall.

For the rainfall, the results align with the broader consensus that Europe is expected to experience wetter conditions in winter and drier conditions during summers, especially in the Northern part of Europe (e.g., (Sassi et al., 2019)). However, with the temperature rise, PET will also be increasing. The future scenarios indicate that the percentage increase in PET (6.7 to 10.1 %) is more pronounced compared to the rise in rainfall (1.4 to 6.1 %) on an annual scale. This suggests that the catchment may face increased stress in terms of water availability. Moreover, focusing specifically on the summer months (JJA: June, July, August), the findings suggest a tendency for decreased rainfall (3.4 to 11.3 %) coupled with a substantial increase in PET (7.5 to 12.4 %). This combination

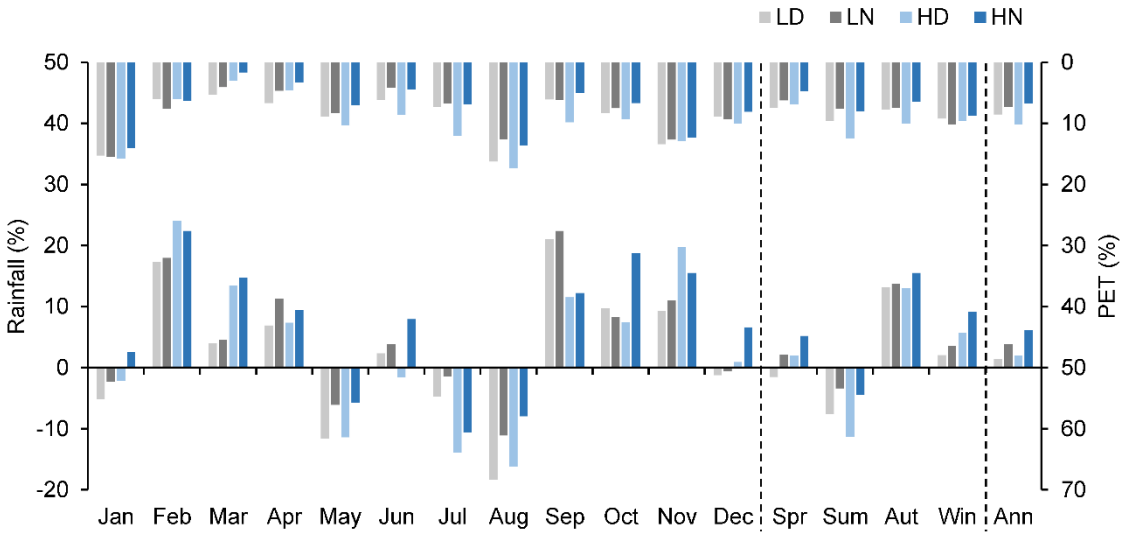

Figure 5.1.Relative change in rainfall and PET calculated in percentage under the KNMI'23 climate projection scenarios for the time horizon 2050 with reference to the base period. Dashed lines separate the plots that indicate the averages across seasons and annual data (spr: spring, sum: summer, aut: autumn, win: winter, ann: annual)

further emphasizes the potential for water stress during the critical summer months. The observed increasing trends of PET in the Netherlands are consistent with the findings of Philip et al. (2020), wherein the importance of PET in characterizing the summer droughts in the Netherlands is highlighted and attributed to changes in atmospheric circulation.

The observed trends regarding the increase ET and decreased precipitation during summer under future climate broadly align with findings from other regions in the Netherlands such as Dommel catchment (van Vliet et al., 2012), Keersop catchment (Visser et al., 2012) and Veluwe region (Van Huijgevoort et al., 2020). To analyse extreme events, the statistical metric 'R95pTOT' was calculated for each season under both the base and future scenarios (Table A1 in Appendix A). During the base period, summer exhibited the highest total rainfall from very wet days, aligning with the findings of Whitford et al. (2023). These higher values indicate that the majority of summer rainfall occurs in short periods with high intensity. Conversely, R95pTOT values were lowest in spring. In future climate scenarios, R95pTOT values are notably low, suggesting a decrease in the intensity of extreme events and a shift towards more events with a lower intensity of rainfall.

This observation was further analysed by plotting duration curves for both the base and future scenarios using daily rainfall and their corresponding exceedance probability (Figure 5.2). While there is minimal difference between the duration curves of the four future scenarios, a comparison between the base period and future scenarios indicates a decrease in high rainfall events under all scenarios, accompanied by a significant increase in low rainfall events. Days with rainfall greater than approximately 2.2 mm are decreasing, while days with lower rainfall are increasing. This result, however, is potentially influenced by the different nature of the in-situ data used for the base period, i.e. point-based, and of the climate projections, i.e. grid-based. Indeed, rain gauges, strategically positioned on the ground, are designed to measure precipitation at specific locations which enable them to capture localized events like heavy downpours. In contrast, future scenarios are the climate model outputs that operate on a broader spatial scale where each grid cell represents an averaged value for climate variables, providing a more generalized view over larger regions but also less capabilities in representing extremes.

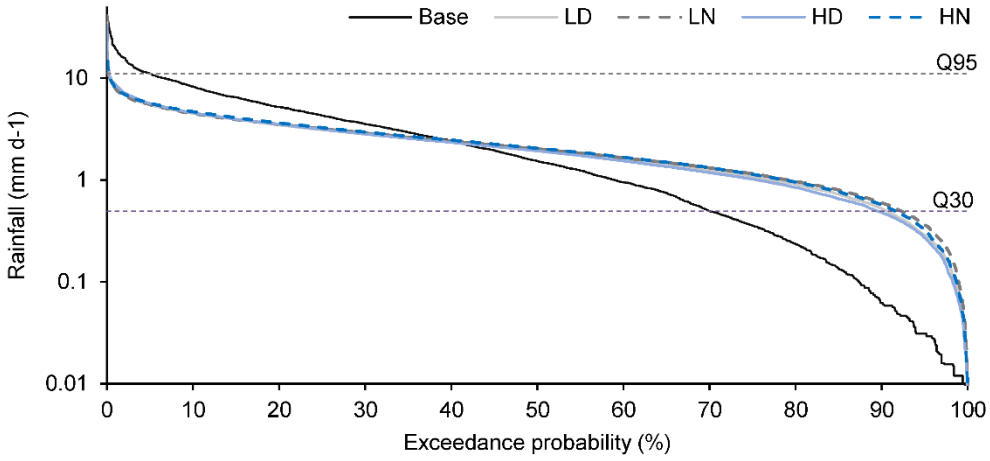

Figure 5.2. Rainfall duration curve for the base period (2010-2019) and KNMI'23 climate scenarios (2050). Q30 and Q95 are 30th and 95th quantiles, respectively

5.3.3 Model Calibration and Validation

For the catchment average AET, the values of R and NSE for the calibration and validation periods were 0.91, 0.80, 0.926, and 0.822, respectively. In terms of discharge at the catchment outlet, NSE and R values during calibration and validation were 0.88, 0.71, 0.87, and 0.71, respectively. Results demonstrate the reasonable capture of trends during both high and low flow periods, indicating the model's ability to reflect seasonal variations adequately. The simulation of GWLs showed varying model efficacy across different locations. The model tended to slightly overestimate the GWLs in the upstream regions and around the catchment's outlet. Nevertheless, the model results demonstrated good agreement with observed data for GWLs, capturing seasonal variations and trends reasonably well (R= 0.77 for the average of all observed versus modelled outputs). The results are presented in detail in Chapter 3.

5.3.4 Impact on catchment hydrology under designed scenarios

Scenario SC1, under future LULC changes

In scenario SC1, the model was simulated for the base period 2010 to 2019 using a future LULC map (2046) to assess the individual effects of LULC changes on the catchment's hydrology. The impacts have been assessed on various simulated variables, including discharge at the catchment outlet, AET, subsurface flow, and recharge at the catchment scale. In addition, the impacts on AET, GWT, and SM (top 10 cm) were evaluated at the local scale as well.

Under the future LULC change, the effects on hydrology at the catchment level are minimal. The mean monthly discharge is almost the same as the base model with a minor increase (Figure 5.3). The maximum observed increase occurs during autumn, with only a 0.7 % rise, while the minimum increase is during the spring months, equal to 0.2 % (Table 5.3). This may be attributed to the projected increase in built-up areas in the future, where the expansion of the built-up area (1.7 %) dominates the forest and semi-natural (FSN) area expansion (0.4 %). This LULC change reduced actual evapotranspiration (AET), leading to more water being retained in the soil and subsequently contributed to increased subsurface flow to river by 0.3 to 1.1 %, with the maximum rise observed in autumn.

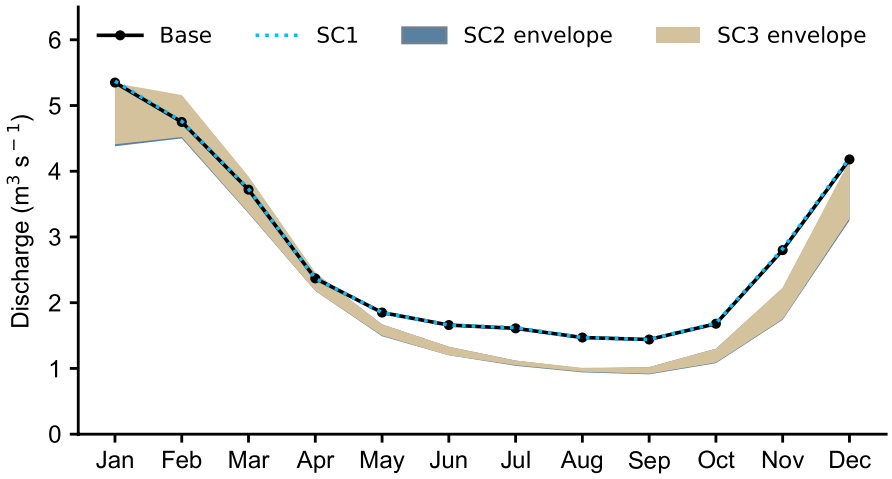

Figure 5.3. Mean monthly discharge at the catchment outlet under the base, SC1, SC2, and SC3 scenarios. For SC2 and SC3, the envelope represents the range between the highest and lowest values under LD, LN, HD, and HN climate scenarios

The AET is reduced on the catchment scale by -0.2 %, -0.3 %, and -0.3 % in the spring, summer, and autumn respectively, which may be due to a decrease in transpiration from areas that have been converted to built-up areas. On the local scale (Figure 5.4), considering only the areas where LULC change is projected to occur, the changes in AET range from -30 to 22 %. Specifically, areas converted to built-up from agriculture and those transitioning from CCP to LPA exhibited a wide range of percentage changes during the spring and summer. In the summer, AET decreased by up to -20 % for most of the areas that transitioned to built-up and LPA, while it increased by up to 5 % for the areas that transitioned to FSN (Figure 5.5). During the winter season, AET for LPA started to increase, reached its maximum in the spring, and decreased in the summer and autumn. This pattern is likely attributed to the sowing and harvesting season for crops in that area. In spring, crops are in full growth, resulting in the maximum AET. In autumn, all

transitioned areas experienced a decrease in AET ranging from 0 to -20 %, while the transitioned area to FSN class showed minimal change. In winter, all transitioned cells experience an increase in AET, with a maximum of 8 % in places that have been transitioned to built-up areas.

Considering catchment average values, the recharge to groundwater was increased during the summer, autumn, and winter (1.7 %, 0.7 %, and 0.1 %), while experiencing a slight reduction in the spring (0.4 %). However, on a local scale, the change in GWT fluctuated between -10 to 10 %. The changes were mostly positive in autumn and winter. During the spring and summer, most of the transitioned areas exhibited positive change except for a few areas belonging to the built-up area and LPA classes, where the change was negative. Overall, the change in GWT is minimal compared to the variations in AET and SM.

In spring, SM values varied from -8 to 10 %, with most transitioned areas exhibiting negative changes. During the summer, SM in areas that transitioned to LPA and FSN remained minimal while most of the built-up area exhibited changes, ranging from -5 to 18 %. In autumn, apart from areas that transitioned to FSN, where SM decreased by up to -2 %, other areas exhibited positive changes of up to 7 %. During the winter months, SM remained almost unchanged, although AET and GWT exhibited positive changes. This could be due to the presence of already high-water content in the soil layer during winter, keeping SM relatively unaffected.

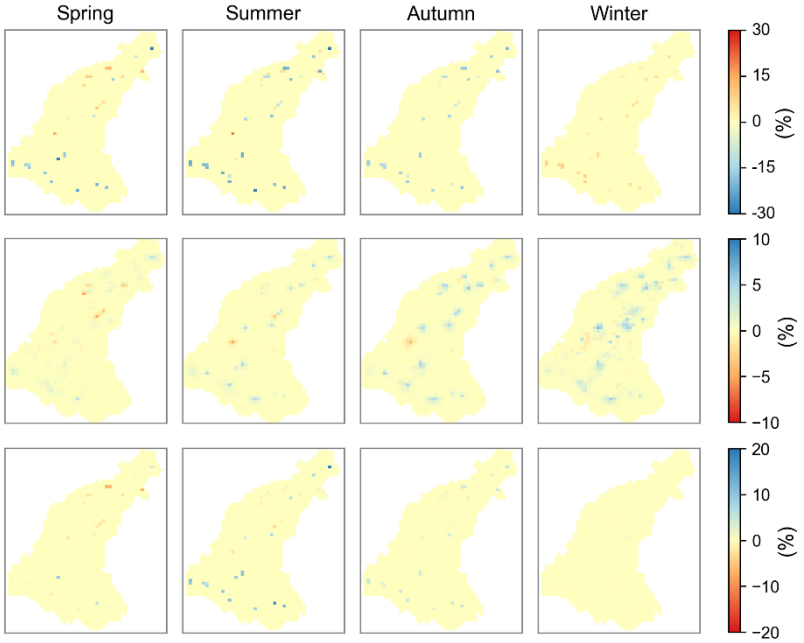

Figure 5.4. Relative change in simulated AET (upper), GWT (middle), and SM (lower) under base period and SC1 scenarios, calculated as a percentage on the seasonal basis

The percentage differences in AET, SM, and GWT under future LULC (2046), relative to the base period, were plotted against each other to analyse their relationships and sensitivities in different seasons and during transitions of the area from one LULC class to another. GWT changes exhibit minimal sensitivity to variations in SM and AET in spring and summer where wide changes in SM and AET correspond to minor GWT variations. In autumn, the relations between changes in SM and AET become relatively more sensitive to GWT changes, with an increase in SM by up to 7 % and a decrease in AET by up to -20 % resulting in a change of GWT by a maximum of 10 %. However, during winter months, even with no change in SM and an increase in AET ranging from 0 to 8 %, the GWT across transitioned areas increased up to a maximum of 8 %. This increase may be attributed to the slower subsurface hydrological flows compared to the topsoil and surface processes (Yang et al., 2020; Leong and Yokoo, 2022). Another

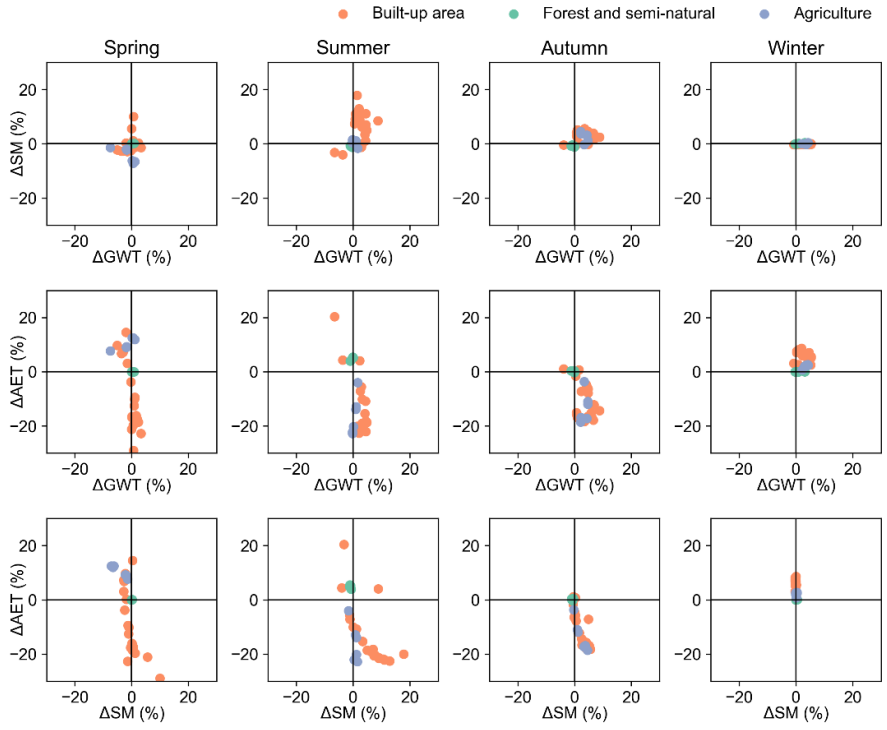

Figure 5.5. The relationship between the relative change in AET, SM, and GWT on a seasonal basis under the base period and scenario SC1, focusing only on pixels where the LULC is projected to change in the year 2046. Orange represents map pixels transitioning from agriculture to 'Built-up area', green represents pixels transitioning from agriculture to 'Forest and semi-natural (FSN) class', while blue represents pixels projected to change from a 'Complex cultivation pattern (CCP)' to 'Lands principally occupied by agriculture (LPA)'

contributing factor could be the higher saturation of the soil during the winter, where excess rainfall directly contributes to groundwater storage (Van Huijgevoort et al., 2020).

The relationship between AET and SM is comparatively more responsive. The maximum positive change in SM (up to 18 %) is observed in the summer, corresponding to a change in AET (up to -22 %) for areas that transitioned from agriculture to built-up areas. For areas transitioning into forest and semi-natural areas or LPA, the change remains minimal. In autumn, the decrease in AET (up to 20 %) causes an increase of up to 7 % in SM. Whereas, in winter, even with an increase in AET (up to 10 %), SM remains mostly unchanged.

The relationship between the variables is non-linear and varies depending on the seasons and the transitioned class of LULC. Changes in areas transitioning to FSN remained minimal. Areas transitioning into LPA experienced an increase in AET during spring, causing a decrease in SM. During summer, AET decreased in these cells, leading to an increase in SM, and the same process continued in autumn. In winter, they reached higher saturation levels, and SM remained unaffected despite an increase in AET. Whereas, for areas transitioning to the built-up areas from agriculture, the trend remained random during spring and summer, but they followed a similar trend as LPA during autumn and winter.

Scenario SC2, under future climate change

In scenario SC2, the model was simulated using climate projections data for the horizon 2050 (2036-2065), together with the LULC map of the base period, to assess the individual impact of climate change on the catchment's hydrology. The model results revealed that the discharge at the catchment outlet is projected to decrease in January and from April to December under all climate scenarios considered. The lowest average discharges are projected to be observed in September. However, an exception to this trend is noted in February and March, where an increase in discharge relative to the base model is projected only under the HN scenario (Figure 5.3). It may be attributed to the increased value of PET under all scenarios.

On a seasonal scale, the discharge is projected to decrease by 27.3 to 32.2 % and 23.8 to 37 % in summer and autumn, respectively. In contrast, it ranges between -11.4 to 1.1 % and -14.4 to 2 % in spring and winter, respectively (Table 5.3). This reduction in discharge is likely attributed to a change in catchment average AET which is projected to increase under all climate scenarios by 11.9 to 13.5 %, 15.7 to 16.5 %, 11.2 to 13 %, and 13.8 to 15.2 % in spring, summer, autumn, and winter, respectively. The values across different areas exhibit variation, with certain regions projecting an increase in AET up to 30 %, particularly during summer and autumn under LN and HN scenarios (Figure 5.6). Notably, these areas are characterized by LULC class built-up area and LPA. Conversely, during

winter, the change in AET from built-up areas and LPA is less pronounced, with dominance shifting towards LULC classes FSN and CCP.

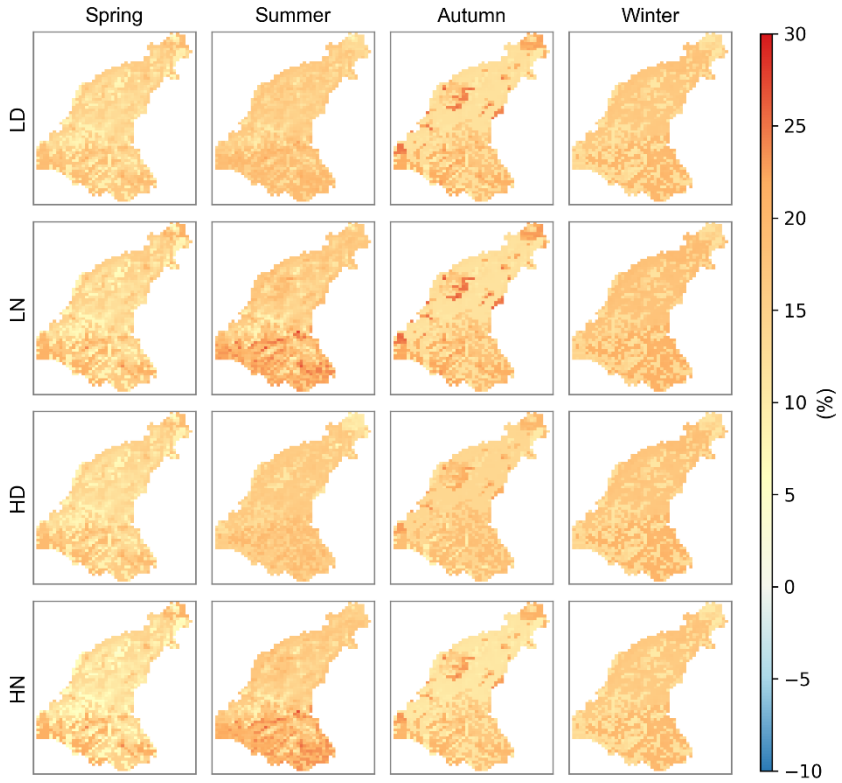

Figure 5.6. Relative change in simulated AET under the base period and SC2 scenario calculated as a percentage on seasonal basis

The maximum change in SM is projected during summer under climate change scenarios LD and HD, where certain areas belonging to classes FSN and CCP show a reduction of up to -38 % and -40 % (Figure 5.7). Meanwhile, under LN and HN scenarios, SM across the region ranges from -35 to 5 %. Positive changes are observed only in a small region, possibly attributed to a comparatively lesser increase in AET over those regions. In autumn, SM exhibited both positive and negative changes in the catchment. Under scenarios LD and HD, most areas show negative changes, while the trend reversed under scenarios LN and HN. During winter and spring, the catchment generally experiences positive changes under all scenarios, except for a small section towards the north side of the catchment where changes are negative. Although the trend across different LULC classes appears random, no direct correlation with specific LULC classes influencing an increase or decrease in SM has been identified. However, the negative change (up to -40 %) exhibited during summer outweighs the positive change (up to 10 %) observed during winter. Similarly, the catchment's average recharge to groundwater is projected to

decrease by -107.6 to -139.5 % during summer, whereas in spring (-11 to -31.8 %) and autumn (-8.4 to -28.3 %), the change in relative to base period is comparatively less (Table 4). During winter, an increase is projected by 2.4 % and 7.8 % under HD and HN

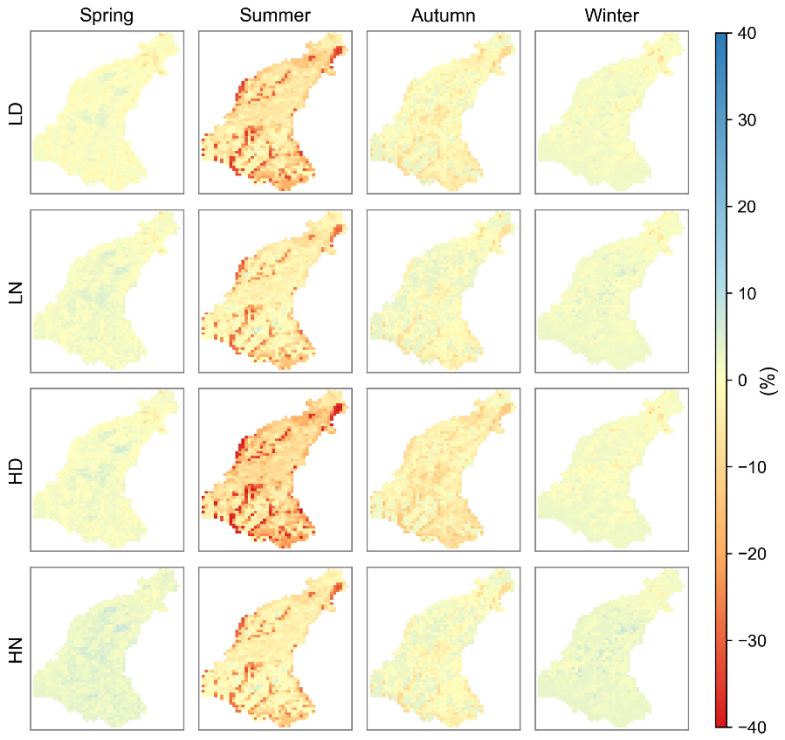

Figure 5.7. Relative change in simulated SM under the base period and SC2 scenario, calculated as a percentage on the seasonal basis

scenarios, while LD and LN scenarios anticipated a reduction of -3 % and -0.4 %, respectively. These findings highlight the season-specific and scenario-dependent nature of changes in SM. The spatial distribution of percentage change in GWT is shown in Figure 5.8.

On the local scale, during the summer months, negative changes in GWT are observed across all areas under all scenarios. The maximum negative change, reaching -50 %, is projected under LD and HD scenarios, while it is -30 % under LN and HN scenarios in certain areas having LULC class as agricultural. Moving to autumn, some areas exhibit a GWT increase of 25 %, but the major portion of the catchment is likely to have negative changes. Notably, in the central area of the catchment, GWT is projected to decrease by a maximum of -60 % and -75 % under LD and HD scenarios, respectively. Even during winter, changes in the catchment are not spatially uniform, with positive changes observed in the central portion and negative changes in the southern and northern areas of the catchment. A similar trend is observed in spring, though the magnitude of change is comparatively less than in winter.

It is worth noting that across all scenarios and seasons, negative changes in GWT are consistently observed in the area near the outlet of the catchment (north part). The general groundwater flow in the catchment is from southeast to northwest. Due to a lower water table in the middle and upper portions of the catchment, groundwater flow towards the outlet might be comparatively less, impacting the area near the outlet across all seasons.

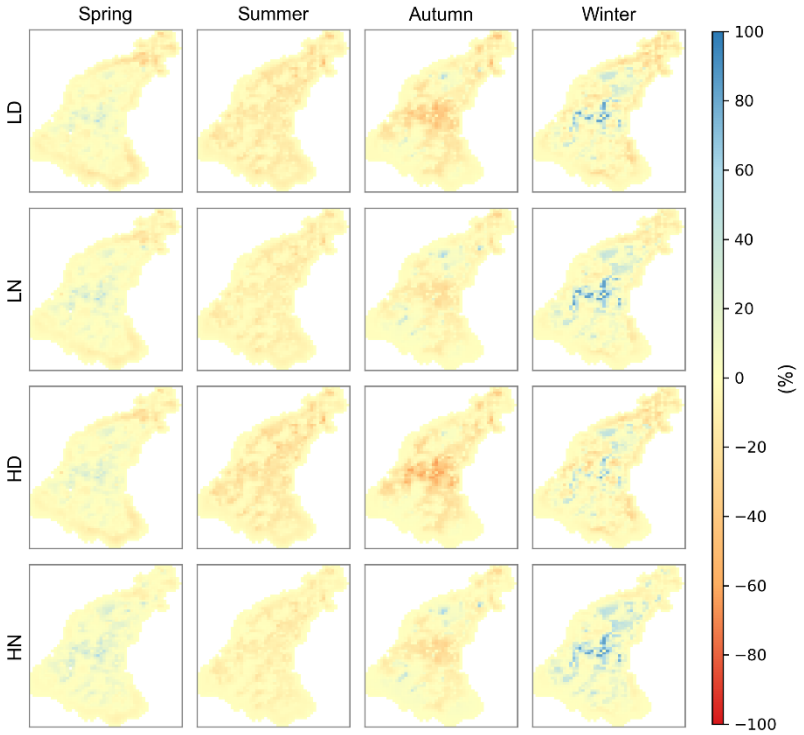

Figure 5.8. Relative change in simulated GWT under the base period and SC2 scenario, calculated as a percentage on the seasonal basis

As discussed in Section 5.3.2, despite an increase in autumn rainfall, the discharge at the catchment outlet, subsurface flows, recharge, and GWT at most locations exhibited a negative change. Even the SM for the topsoil layer did not show a spatially consistent positive change across the catchment. This phenomenon may be attributed to additional summer stress generated in the catchment due to low rainfall and higher AET. The additional rainfall, compared to the base period, occurring in autumn is consumed to overcome the prevailing summer drawdowns in GWT and soil water content. On the other hand, in spring, the projected increase in rainfall is comparatively less than in autumn, but the discharge at the outlet, along with other variables, exhibited a more positive change than in autumn. This may be because in winter, the GWT and water content in the soil are relatively high, and even a comparatively smaller increase in rainfall contributes more prominently to different hydrological components. This aligns with the findings of

Assouline et al. (2024), Alam et al. (2024) and Ran et al. (2022), who highlighted the influence of antecedent conditions on flow generation.

Scenario SC3, under future climate and LULC change

In scenario SC3, the model was simulated with climate projections referred to the horizon 2050 (2036-2065), together with the generated future LULC to assess the combined effects on the catchment's hydrology. Notably, the discharge at the catchment outlet across different months under scenario SC3 closely resembles that of scenario SC2, where only climate change was considered (Figure 5.3). The maximum increase in discharge, compared to scenario SC2, is projected to be 0.5 % in winter and 0.3 % in summer. This modest change may be attributed to the projected expansion of built-up areas in the future, where the development of the built-up area (1.7 %) dominates over FSN area expansion (0.4 %). A similar trend was observed in scenario SC1, though the comparative increase in discharge in scenario SC3 is less than that observed in SC1. Likewise, the subsurface flow to the river is projected to increase under the combined effect of climate change and future LULC changes, but the increase in the catchment average is minimal (Table 5.3).

The situation with AET mirrors the discharge trends. When considering catchment average values, AET is projected to decrease by 0.3 to 0.4 % compared to the individual effect of climate change in the summers, with no projected change in winter. However, to assess changes at the local scale, the spatially distributed relative change in AET compared to the base period was calculated (Figure 5.9), and found that AET under scenario SC3 is almost identical to scenario SC2, except for a few locations where the relative change in AET has altered. To identify the exact locations where the change has happened under scenario SC3, the differences in percentage changes under scenarios SC2 and SC3 relative to the base model were computed and are represented in Figure A2 (Appendix A). In spring, summer, and autumn, significant changes in AET are observed over areas that are projected to undergo LULC transition. For example, in summer, compared to scenario SC2, AET is projected to be less by up to 30 % in areas transitioning from agriculture to built-up, while it will be more by up to 5 % in areas transitioning to FSN from agriculture. In spring and autumn, the differences are comparatively less, and there is no change in winter.

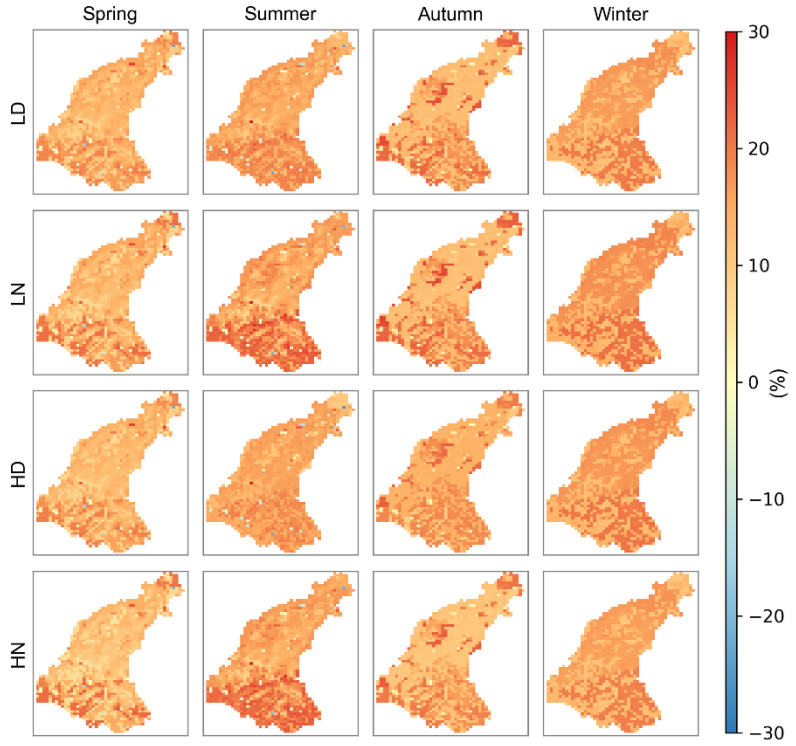

Figure 5.9. Relative change in simulated AET under the base period and SC3 scenario, calculated as a percentage on the seasonal basis

The spatial distribution of SM under scenario SC3 is represented in Figure 5.10. Similar to AET, the relative change in SM compared to the base period under the combined effect of climate change and future LULC is within the same range as that of the individual effect of climate change, with only a few areas exhibiting notable differences as presented in Figure A3 (Appendix A). A noteworthy observation is the increased number of areas showing positive changes in summers under the combined effect of climate change and future LULC. These new areas with positive changes in summer are predominantly those that are projected to undergo a transition from agriculture to built-up areas in the future LULC map. The maximum projected change in these areas is reaching up to a maximum of 30 %. Conversely, in areas transitioning to FSN, the change is reduced, up to a maximum of -4 %. During the winter, there is no change in simulated SM under scenarios SC2 and SC3.

Considering the catchment average values, recharge to groundwater is projected to decrease under scenario SC3, aligning with the trend observed in scenario SC2. However, under scenario SC3, the recharge values differ by a maximum of 0.6 % and 0.7 % in summer and winter, respectively, under the HD scenario of climate change. In other seasons and climate scenarios, the differences are even less (Table 5.3). Similar to AET

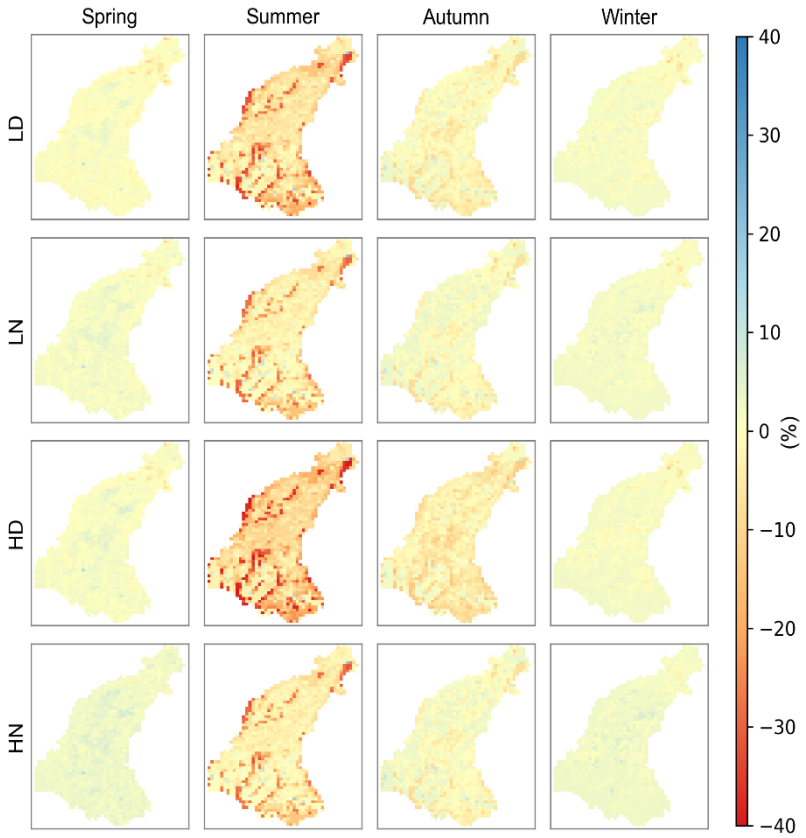

Figure 5.10. Relative change in simulated SM under the base period and SC3 scenario, calculated as a percentage on the seasonal basis

and SM, the variations in GWT at the local scale in transitioning areas are more pronounced than changes in catchment averages. The spatial distribution of GWT and the differences in percentage changes under scenarios SC2 and SC3 relative to the base model are illustrated in Figure 5.11 and Figure A4 Appendix A, respectively. The seasonal and spatial trends under scenario SC3 are consistent with those of SC2, but in a few of the areas, the values of percentage change have shifted within the range of -5 to 15 %. For instance, during winter, in areas transitioning to the built-up, the GWT is projected to further rise by 15 % compared to the relative change projected under scenario SC2. These changes are particularly noticeable in autumn and winter compared to spring and summer.

It is crucial to note that the changes in GWT are not limited to the areas that are projected to undergo future LULC transitions, but changes in neighboring areas are also observed. In contrast to GWT, the influence on neighboring areas has not been observed for SM. This distinction may be attributed to the modelling constraints in MIKE SHE, where the exchange of flow in the unsaturated zone is primarily permitted in the vertical direction, limiting the simulation of soil moisture exchanges in the horizontal direction.

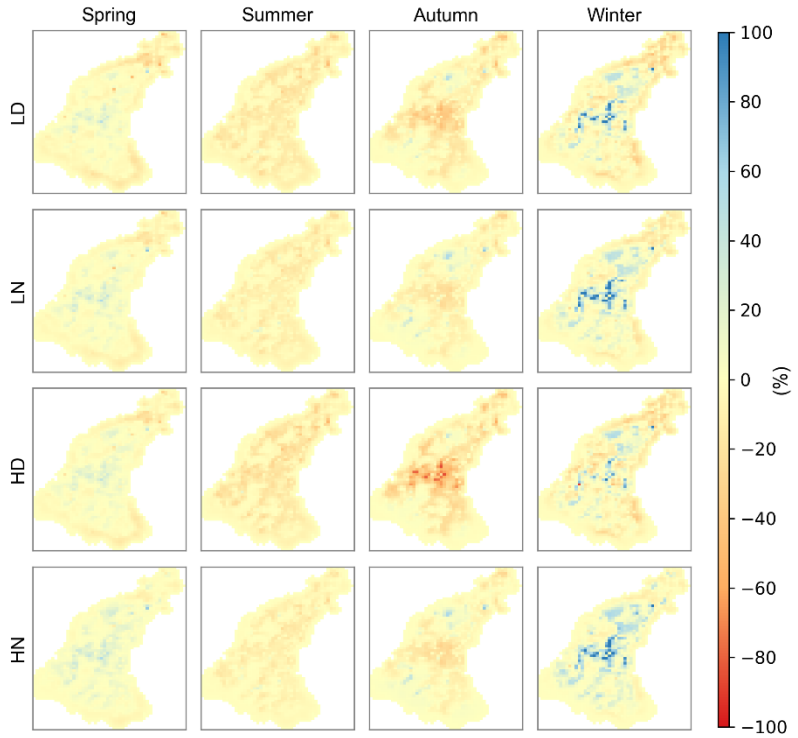

Figure 5.11. Relative change in simulated GWT under the base period and SC3 scenario, calculated as a percentage on the seasonal basis

The overall findings suggest that hydrological components are more influenced by climate change alone (SC2) than by the LULC change scenario (SC1). Furthermore, on the catchment scale, the combined effect of climate and LULC changes (SC3) does not significantly differ from the individual effect of climate change (SC2). These results align with studies conducted by Getachew et al. (2021) and Yan et al. (2019), both of which identified hydrological components as more sensitive to climate change on both seasonal and annual scales. In the combined effect of LULC and climate change (SC3), the impact of climate change appears to be somewhat dampened by the effects of LULC change. Similar findings have been reported by Tirupathi and Shashidhar (2020), although in this study, the offsetting influence of LULC change is very minimal, accounting for less than 1 % on the catchment scale.

However, in contrast to this, the impact of LULC changes is more pronounced at the local scale, particularly in areas projected to transition from one LULC class to another. The incorporation of LULC changes, alongside climate change, can significantly influence the relative changes in GWT, SM, and AET on the local scale, with variations referred to scenario SC2 ranging from approximately -6 to 15 %, -9 to 27 %, and -30 to 10 %, respectively, depending upon the specific change in LULC class and season.

Table 5.3. Relative change in water balance component calculated as percentage change with reference to the base period for design scenarios SC1, SC2, and SC3.

	Scenario SC1					Scenario SC2				Scenario SC3			
	Spr	Sum	Aut	Win		Spr	Sum	Aut	Win	Spr	Sum	Aut	Win
Δ AET (%)	-0.2	-0.3	-0.3	0.1	LD	13.5	15.7	12.3	14.2	13.4	15.4	12.2	14.2
					LN	13.3	16.5	12.4	15.2	13.2	16.2	12.3	15.2
					HD	13	15.7	13	14.6	12.8	15.3	12.7	14.6
					HN	11.9	16.6	11.2	13.8	11.8	16.3	11	13.8
Δ Base + drain flow to river (%)	0.3	0.7	1.1	0.5	LD	-11.7	-44.4	-42.2	-12.6	-11.4	-43.9	-41.6	-12
					LN	-7	-40.1	-32.2	-4.8	-6.7	-39.6	-31.6	-4.3
					HD	-4	-44.5	-47.4	-11.3	-3.5	-43.9	-46.7	-10.6
					HN	3.7	-36.6	-29.8	5.2	4	-36.1	-29.2	5.8
Δ Recharge (%)	-0.4	1.7	0.7	0.1	LD	-31.8	-121.1	-21.9	-3	-32	-120	-21.2	-2.7
					LN	-25.4	-107.6	-12.7	-0.4	-25.6	-106.7	-11.9	-0.1
					HD	-20.5	-139.5	-28.3	2.4	-20.6	-138.4	-27.4	2.7
					HN	-11	-116.1	-8.4	7.8	-11.1	-115.2	-7.7	8.1
Δ Discharge													
0.2					LD	-11.4	-32.2	-33.3	-14.4	-11.1	-31.9	-32.9	-13.9
					LN	-7.7	-29.5	-25.7	-7.2	-7.5	-29.2	-25.3	-6.8
0.3													
0.7													
0.3													

HD	-4.9	-32.3	-37	-13	-4.6	-32	-36.6	-12.4	
HN	1.1	-27.3	-23.8	2	1.4	-27	-23.4	2.4	

This nuanced spatial distribution of changes in hydrological variables underscores the role of LULC changes in conjunction with climate impacts, highlighting specific areas undergoing transitions as significant contributors to the observed variations in hydrological dynamics. Understanding these localized effects is crucial for effective water resource management and climate change adaptation strategies within the catchment. These findings underscore the importance of considering both climate change and future LULC changes in assessing the hydrological response of the catchment particularly if the focus is on local scales.

5.4 CONCLUSIONS

This research assesses the response of surface (AET, discharge) and subsurface (recharge, GWT, SM, and lateral flow) hydrological components to the separate and combined future changes in climate and LULC at a catchment and local scales for the Aa of Weerijs catchment. To conduct the research, a physically based fully distributed hydrological model was set up for the study area, using MIKE SHE and MIKE 11 modelling tools. The ANN-CA technique was employed to simulate future LULC changes using the MOLUSCE plugin of QGIS. Validation of the LULC prediction model demonstrated satisfactory accuracy, with kappa coefficients ranging from 0.94 to 0.97 and a percentage correctness of 95.7 %. The analysis of historical (2018) and simulated LULC for the year 2046 identified a 1.7 % expansion in built-up and a 0.4 % increase in FSN class.

For meteorological projections under climate change, the data was acquired from KNMI'23 climate scenarios for the 2050 horizon (2036-2065). The time series of catchment average rainfall and PET were compared with data from the historical (base) period and the results suggested an overall increase in PET across all scenarios, with varying patterns of rainfall changes. The increase in PET is more pronounced than the changes in rainfall. The summer showed a tendency for decreased rainfall coupled with a substantial increase in PET, highlighting potential water stress during critical periods.

The simulated results only with future LULC changes revealed that the impacts on catchment hydrology are minimal. The expansion of built-up areas contributes to a modest increase in discharge and subsurface flow, while changes in AET, GWT, and SM show localized variations. Under the individual impacts of climate change, the changes in hydrological variables are comparatively more pronounced. Considering both future LULC and climate change demonstrated that while hydrological variables were more

sensitive to climate change alone, the combined effects did not significantly differ from the individual impact of climate change on the catchment scale. However, at the local scale, especially in areas undergoing LULC transitions, the combined effects exhibited significant variations in hydrological variables.

To address the specific research question raised, we concluded that for the lowland catchment with a size of 346 km^2 and projected increase in built-up area by 1.7 % and FSN by 0.4 %, the impact of including future LULC data in addition to climate change projections, is not significant at the catchment scale, as it accounts for very minimal changes in hydrological variables (>1 %). However, at the local scales, it can significantly influence the relative changes in GWT, SM, and AET with variations ranging from approximately -6 to 15 %, -9 to 27 %, and -30 to 10 % respectively, depending on the specific change in LULC class and season. The spatial distribution of changes in AET, SM, and GWT emphasizes the importance of considering localized impacts for effective water resource management. The study underscores the importance of considering both climate and land use dynamics for a comprehensive understanding of hydrological changes in the face of future challenges.

While this study has provided valuable insights, there are certain limitations that warrant consideration. Firstly, the future LULC scenario adopted here is based on a business-as-usual approach. A more nuanced understanding could be achieved by formulating different scenarios for future LULC, incorporating constraints on LULC class expansion, and considering local landscape policies, municipal priorities, or broader European-level policies. Such considerations could enhance the refinement of future LULC projections. Secondly, the study focused only on rainfall, PET, and LULC under future changes. Global warming may trigger additional factors, such as groundwater abstraction or direct water abstraction from rivers, which could impact discharge and GWT. Additionally, changes in groundwater boundary conditions, not accounted for in this study's future scenarios, could further influence hydrological dynamics. Therefore, future research activities could address these limitations by incorporating these additional factors. The effect of these factors might not be significant alone but studying the coupled effects of various drivers would provide a more comprehensive understanding of future hydrological dynamics. Such insights could offer more detailed information to policymakers, aiding in the development of informed and robust strategies for sustainable water resource management.

6

NATURE BASE SOLUTIONS FOR CLIMATE ADAPTATION

Nature based solutions (NBSs) are a potential alternative to the traditional grey infrastructure for climate adaptation. However, their effectiveness in mitigating drought impacts is underexplored. This chapter presents the methodology for designing and assessing the potential of NBS-based adaptive strategies for drought mitigation with focus on surface as well as sub-surface hydrological components using an integrated distributed hydrological model. The methodology is demonstrated for Aa of Weerijs catchment using the MIKE SHE modelling system. The NBSs assessed include ditch blocking, tree planting, wetland restoration, infiltration ponds, heathland restoration and brook bed barriers. Based on the model results, individual measures were spatially mapped to develop two adaptation strategies, each differing in spatial extent. The Key Performance Indicators (KPIs) were designed to be relatable to key stakeholders, such as the number of days with a ban on water extraction from surface and groundwater. The performance of the strategies was evaluated using the designed KPIs under future climate scenarios. The results showed that strategy with a larger spatial extent has more positive impacts on the KPIs. The adaptation strategies enhanced the groundwater recharge and reduced the number of ban days for groundwater extraction with almost eliminating the ban days in the downstream part of the catchment.

This chapter is an edited version of the journal publication: Jonoski, A., Ali, M. H., Bertini, C., Popescu, I., van Andel, S.J., & Lansu, A., 2025. Model-based design of drought-related climate adaptation strategies using nature-based solutions: case study of the Aa of Weerijs catchment in the Netherlands. Nature-Based Solutions, 100264. https://doi.org/10.1016/j.nbsj.2025.100264

6.1 INTRODUCTION

The indications of escalating climate change are prominent and can no longer be ignored in any region or sector of the world (Forster et al., 2024). The IPCC Sixth Assessment Report (AR6, 2023) stated with a high degree of confidence that the rate of rise in global surface temperature since 1970 has surpassed that of any other 50-year period in the past 2000 years. Due to these changes, the hydrological cycle is accelerating leading to more frequent and stronger weather extremes including floods and droughts both at regional and global scales (Wang et al., 2021; Chiang et al., 2021). In a warming climate, frequent periods with less than average precipitation are anticipated. During such periods, the decrease in runoffs may be comparatively more than the corresponding decrease in precipitation (Massari et al., 2022) driven by higher evaporation rate and drier soil resulting from higher temperatures. In general, water management systems around the world are designed based on the assumption that the statistical properties of the flow remain constant over time, also known as stationarity (Villarini and Wasko, 2021). However, due to human influence and climate change, the assumption about the stationarity has become questionable (Milly et al., 2008). As a result, water management creates a prodigious impediment for decision makers. Often, grey measures such as dams and reservoirs are built to alleviate flood and drought hazards due to their rapid and visible effects but these measures need large investment, frequent maintenance and are categorized as inflexible approaches (Brink et al., 2016; Wu et al., 2023; Schneider et al., 2017). In addition to adverse effects on the downstream ecosystem, such measures are generally designed for certain life periods, are not environmentally friendly and lack the capability to adapt to changing climate.

The formulation of adaptive strategies for droughts is primarily focused on retaining the water in the catchment either by increasing storage or by slowing surface or sub surface flow. Some of these actions are considered important for flood management as well but are imperative for droughts (POM, 2014). Many countries are nowadays focused on envisaging adaptation and mitigation strategies based on green infrastructure and ecosystem-based adaptive measures to reduce their exposure to hydro-meteorological hazards (Shah et al., 2023; Davies et al., 2021). Such kind of measures offer greener and eco-friendly alternatives to traditional engineering solutions for hydro-meteorological risk reduction (Ruangpan et al., 2020) in cost effective ways (Ruangpan et al., 2024). The International Union for Conservation of Nature (IUCN) defines Nature Base Solution (NBS) as “actions to protect, sustainably manage, and restore natural and modified ecosystems that address societal challenges effectively and adaptively, simultaneously providing human well-being and biodiversity benefits” (IUCN, n.d.).

NBSs are the potential, greener and eco-friendly alternative to the grey infrastructure for climate adaptation (Yimer et al., 2024; Debele et al., 2019; Ruangpan et al., 2020) with their multiple co-benefits such as better water quality, improved soil health, biodiversity

enhancement, natural area for recreation and better land use management and planning (Nesshöver et al., 2017; Penning et al., 2023). However, in research, much attention has been given to testing the potential of NBSs for flood management while their potential for drought management is barely touched. For instance, a recent literature review by Yimer et al. (2024) found that only 6 % of European case studies and 14 % of global case studies were focused on NBSs for drought adaptation. Apart from this, the research on the potential of NBSs in urban areas is more developed compared to their implementation in rural areas at the catchment scale for drought management (Yimer et al., 2024; Johnson et al., 2022). Further, the impacts of a single type of NBS may be known but it is challenging to design strategies where different NBS types are required to be spatially mapped due to the multiple objectives NBSs need to achieve (Guido et al., 2023).

In order to assess the usefulness of nature based adaptive measures on local and basin scale and their long-term efficacy to mitigate or reduce climate change induced risks, detailed hydrological and/or hydrodynamic models are required. However, the lack of proper modelling approaches to test the impact of NBSs (Kumar et al., 2021) is another hindrance to understanding their potential for drought adaptation. Particularly, in flat landscapes, the aim is to enhance sub-surface storage in the wet period so it can be used in the dry periods. To carry out such analysis, integrated surface-subsurface hydrological modelling is required (Yimer et al., 2024) which can simultaneously provide results in terms of observable variables such as river discharge and groundwater levels, together with water balance variations associated with the interactions between surface and sub-surface. In past research, where the integrated models have been used, the focus was on the surface water and groundwater recharge, without discussing the actual groundwater levels (Fennell et al., 2023; Holden et al., 2022). The deficiency of appropriate quantitative tools and comprehensive simulated results adds to the lack of evidence regarding the successful implementation of NBSs. The tools to engage stakeholders with diverse interests and attitudes (e.g. Farmers, local and regional authorities) in the design of NBS-based adaptation strategies are still very limited (Bogatinoska et al., 2022). Further, for the quantification of the impact of such strategies, scientific research argues for the use of more generic KPIs where comparisons across studies and catchments could be made conveniently (Penning et al., 2023). Whereas, stakeholders (water managers and private land owners) may require specific KPIs that are relatable to observable variables and address actual water management actions.

In this research we aim to assess the potential of the NBSs for mitigating hydrological drought impact considering both surface (discharge) and subsurface (groundwater levels) variables. More specifically, a methodology to design the NBS-based adaptation strategies using integrated hydrological model is presented. To carry out the research, Aa of Weerijs catchment served as the study area. The integrated hydrological model was developed for the area using MIKE SHE modelling system and used for assessing NBSs

of drought mitigating under current and future meteorological conditions under climate change.

The following sections present a methodology, followed by results and discusion. In the end main findings are summerized in conclusions.

6.2 METHODS

The research was carried out using MIKE SHE hydrological model for the Aa of Weerijs catchment. The description of the study area and model setup are presented in the Chapter 3. For assessing the performance of NBSs under future climate change, the KNMI'23 dataset was used. The dataset along with hydrological condition in the catchment under future climate condition are explained in Chapter 5. For brevity, these aspects are not repeated in this chapter.

6.2.1 Methodological framework

The main methodological steps followed to design the adaptation strategies are presented in Figure 6.1. A fully distributed and integrated surface water groundwater model was

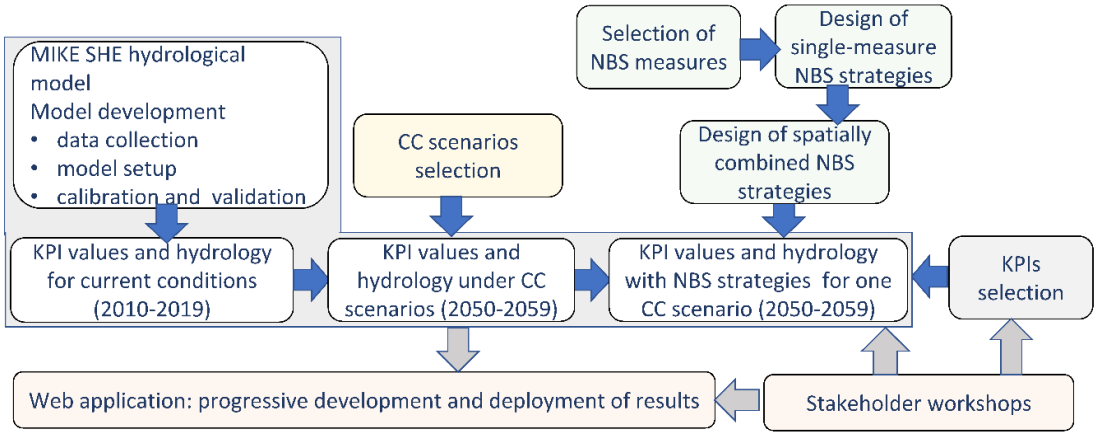

Figure 6.1. Methodological steps for the design and evaluation of the NBS-based adaptation strategies

developed for the catchment using MIKE SHE modelling system that simultaneously captures the surface and subsurface hydrological dynamics of the catchment. This model acted as the main tool for designing of the adaptation strategies. A set of KPIs related to the observable hydrological variable were selected in consultation with the main stakeholders (Water Board Brabantse Delta and Province of Noord Brabant) and used for the performance evaluation of the NBS strategies under the current and future climatic conditions. Out of the four climate change scenarios from the KNMI'23 dataset, only the

one which is categorised by high CO_2 emissions and a drying climate (HD scenario) was selected for the performance analysis of the strategies as this scenario is expected to result in the most prolonged drought period. The design of strategies included the testing of single measures, finding appropriate ways to model them and adjusting them spatially to formulate combined strategies. The formulation of NBS strategies and the selection of KPIs to assess their performance were conducted in consultation with the local stakeholders through devoted meetings. A web application was developed to facilitate knowledge sharing, communication of methodologies and results, and to support informed decision-making and stakeholder engagement in NBS-based design of strategies. The web application is publicly available and can be accessed via the link https://eiffel.un-ihe.org/EIFFEL-prod.

6.2.2 Key performance indicators

The characterization of hydrological droughts using indices/indicators is well established (Sahani et al., 2019). However, there is no universal consensus on the use of any particular indicator (Van Loon, 2015) as the selection of indicator is dependent on the intended use of water and it can be very diverse. Further, the selection of appropriate KPI is also challenging when it is also required to assess the impact of adaptation strategies including NBS-based strategies. The successful implementation of such strategies is dependent upon the recognition of their benefits by the stakeholders, which can be better demonstrated by KPIs that align well with their immediate concerns and water use needs.

Aa of Weerijs catchment has recently experienced summer droughts, particularly in 2018 and then again in 2022. In these periods, the bans on the water extractions on the surface water (withdrawal of water from the rivers) were imposed by the key stakeholders of the area, the Province of Noord Brabant (PNB- the regional government body charged with spatial planning) and the Water Board Brabantse Delta (WBD – the regional government body charged with managing water). Based on the water availability in the channels, water extraction bans are imposed for irrigation of specific crops or complete bans on water abstraction for irrigation. The lower the surface water discharge in the rivers, the greater the limitations in the water abstractions. A similar concept is adopted here to define the two new KPIs in consultation with WBD to ascertain the present condition and to evaluate the performance of the designed strategies. The KPIs link the actions taken by WBD to manage water shortages to the percentiles of the long-term observations of streamflow and groundwater levels (GWLs). The streamflow and GWLs are monitored at several locations across the catchment by the WBD and can be used to restrict water extraction if the water levels are below certain percentile-based pre-defined thresholds. The developed KPIs are Surface Water Availability (SWA) and Groundwater Availability (GWA). They represent the number of days when the surface water/ groundwater is sufficiently available, limited available and not available. These are calculated at each

monitoring location. For defining the categories (no-, limited- or sufficient- availability) threshold used is as follows: if the discharge (GWL) is below the 10th percentile then there is a total extraction ban and the status is 'not available'. If discharge (GWL) is between the 10th and 40th percentile then a partial ban is introduced and water is said to have 'limited availability'; if discharge (GWL) is above the 40th percentile, no ban is introduced and water has 'sufficient availability' for any usage. Further instead of considering the thresholds for the whole time series, these can be defined seasonally. In this research, the thresholds defined for summer months (June, July, August) are considered as the objective was to observe the impact of NBS strategies on the drought conditions and it is the most affected period of the year by drought events for the study area. The thresholds are presented in Table 6.1. The model simulated discharge and GWLs were considered for determining thresholds, ensuring that the KPIs are calculated using the same procedure under both current and future conditions with or without NBS. Since the observed data under future conditions and with NBS strategies is unavailable. Thus, using the simulated variables for KPI calculation ensured consistency in methodology across all cases. Further, the use of modelled results provides flexibility in computing KPIs at any location across the catchment, whereas observed data is available only at limited locations. The values of the KPIs are calculated for the summer seasons under three scenarios: current conditions (2010-2019), climate change conditions (2050-2059), and climate change with NBS adaptation strategies (2050-2059). Further, the number of days falling within each category of threshold is aggregated over the entire period.

Table 6.1. Summary of the thresholds, (water) availability class and bans on water extraction used to compute the Surface Water Availability (SWA) and Groundwater Availability (GWA)

Discharge/Groundwater level	Availability class	Ban on water extraction
$\boldsymbol{x < 10^{th}\ percentile}$	No availability	Total ban
$\boldsymbol{10^{th} \leq x \leq 40^{th}\ percentile}$	Limited availability	Partial ban
$\boldsymbol{x > 40^{th}\ percentile}$	Sufficient availability	No ban

6.2.3 NBS types and modelling

In the Netherlands, Climate change impacts are presented to stakeholders through various mediums, one of which is the climate impact atlas (Klimaateffectatlas, n.d.). Steered by

information available on such portals, Provincial authorities, water boards and municipalities conduct their local climate impact analyses and develop adaptation strategy plans. In the Province of North Brabant, such plan specially addressing the floods and drought are developed by PNB and WBD. The PNB also has a platform (PNB, n.d.) which provide information on both planned and implemented adaptation measures and many of which prominently feature NBS. The current strategy of the authorities (2022-2027) for the water and land management is 'nature-based solutions where possible, technical solutions where necessary' (WBD, n.d.).

The recent European research project named Co-adapt (Co-Adapt, n.d.), contributed to the first GIS based assessment of types and spatial distribution of potential NBSs in whole province, which included the Dutch part of the Aa of Weerijs catchment. A set of NBS types was proposed using information regarding the water system, average GWLs, landscape topography, land use and land cover, together with data on NBSs from existing projects and plans. For each NBS type, an 'opportunity map' was created, covering all possible areas where that NBS type can potentially be implemented. These maps have been provided by the Province for this research, and served as the basis for the design of the NBS-based adaptation strategy. An example of the opportunity maps is presented in Figure 6.2.

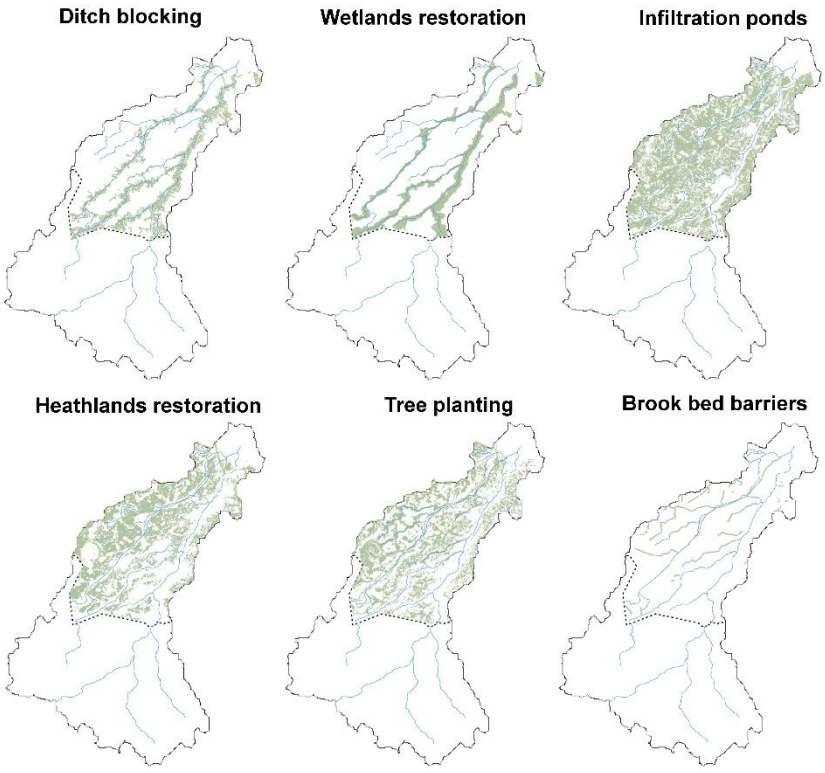

Figure 6.2. Opportunity maps for potential implementation of different types of NBSs within the Dutch part of the Aa of Weerijs catchment

The design of our adaptation strategies started by modelling single-type NBSs (*single-measure strategy*) within the developed hydrological model, using the opportunity maps as inputs. Six different types of NBS -Ditch Blocking, Tree Planting, Wetlands Restoration, Heathlands Restoration, Infiltration Ponds, Brook Bed Barriers- were pre-selected based on their potential beneficial effects for drought adaptation shown in literature (Fennell et al., 2023; Raymond et al., 2017; Holden et al., 2022) and on the *Co-adapt* project outcomes. Ditch Blocking consists in blocking the flow from small channels to larger streams, causing the water to slow down and allowing it to infiltrate in the sub-surface. From a modelling perspective, ditches in our MIKE SHE model are modelled through conceptual sub-surface drainage in the saturated zone. Ditch Blocking is hence reproduced in the model by reducing the parameter "drain time constant" by two-thirds with respect to initial values (range 1.50 exp^{-7} - 4.5 exp^{-7} 1/s - corresponding to 77 days - 26 days) in the cells where the block is applied. The initial values (without NBS) have been obtained after calibration, using ranges reported in literature (DHI, 2007; Refsgaard, 1997; Brandyk et al., 2020). Brook Bed Barriers is a NBS where the natural barriers such as wooden logs or stones are used to form small bumps on the small water streams that increase flow resistance, reducing downstream flow velocity, and enhancing water retention in upstream sections (Szarek-Gwiazda et al., 2023; Quinn et al., 2013). These inline features are modelled in the MIKE 11 river network by weirs as represented by other authors as well who used similar approaches with other software tools (Guido et al., 2023; Thomas and Nisbet, 2012; Metcalfe et al., 2017). Wetland Restoration aims to store water and increasing its retention in the application area. In our hydrological model, this NBS is introduced by changing the existing vegetation type to a new one, characterised by Leaf Area Index (LAI) of 2.5 and Root Depth (RD) of 450 mm. These average values of vegetation parameters are taken from NHI (2008) and Breuer et al. (2003). Additionally, the Strickler roughness coefficient value is set to 15 $m^{1/3}$ s^{-1} in areas where wetlands are restored (Janssen, 2023; Chow, 1959). The overland flow detention storage is set at 0.15 m to represent the typical shallow ponding and temporary water retention characteristic of wetlands (Mitsch and Gosselink, 2015; Tousignant et al., 1999). Wetlands store more organic matter compared to crop areas, which would alter the soil hydraulic properties in the area where wetlands are restored. The changes in the soil properties are incorporated in the model by recalculating the soil hydraulic properties based on the potential changes in the soil organic content as studied by (Guo and Gifford, 2002; Beillouin et al., 2023) and using equations of continuous pedotransfer functions from Wösten et al. (1999). Infiltration Ponds are areas with highly permeable material that allows water to infiltrate into the sub-surface. As such, they are introduced in our MIKE SHE model by providing the top 30 cm layer of soil as sandy soil to facilitate infiltration (Hsieh and Davis, 2005; Woods Ballard et al., 2015) and corresponding soil hydraulic parameters are calculated using equations of continuous pedotransfer functions from by Wösten et al. (1999). Strickler roughness coefficient is set as 40 $m^{1/3}$ s^{-1} (Engman, 1986) and the overland

detention storage is set at 0.15 m to represent the temporary surface ponding as suggested in Woods Ballard et al. (2015). Heathlands Restoration aims at reducing transpiration and interception from plants with large canopy cover. For this reason, they are represented in our hydrological model reducing the LAI and RD parameters, according to the values suggested by NHI (2008) for heathlands. Further, Strickler roughness coefficient is set at 20 $m^{1/3}$ s^{-1} in these areas (Papaioannou et al., 2018), same as in the base model for heathlands. Tree planting can play a dual role in hydrology. Trees function as 'pumps' through enhanced ET (Chen et al., 2023) and as 'sponges' by improving soil infiltration (Peña-Arancibia et al., 2019). The overall hydrological effects of tree planting within a specific catchment are therefore dependent upon the complex interplay between these two fundamental processes. They are modelled by modifying LAI, RD, Strickler coefficient and soil hydraulic properties to capture the influence of roots in the infiltration process. The values of LAI and RD are kept same as used in base model for the forest areas and these values were taken from NHI (2008). Strickler roughness coefficient is set at 10 $m^{1/3}$ s^{-1} (Papaioannou et al., 2018; Freeman et al., 1998). Similar to wetlands, trees also increase organic content in the soil leading to enhanced water holding capacity. This process is incorporated in the modelling by calculating the soil hydraulic parameters using equations of continuous pedotransfer functions from Wösten et al. (1999), considering the potential percentage changes in soil organic content values based on (Beillouin et al., 2023).

Each of the NBSs described was modelled independently within MIKE SHE in current conditions (2010-2019). Both KPIs, i.e. GWA and SWA, were computed for each of the single-measures, and the NBS types that did not provide improvement in terms of surface and groundwater availability were excluded from further analysis, which resulted in the exclusion of Tree Planting and Brook Bed barriers from the next step of analysis.

Table 6.2. NBS types considered in the Aa of Weerijs catchment and approaches taken for their modelling in the MIKE SHE hydrological model

NBS type	**Main drought-related function**	**Modelling approach**
Ditch blocking	Slowing down drain flow and allowing more infiltration upstream	Conceptual drain time constant reduced by 2/3 of the initial values (DHI, 2007; Refsgaard, 1997; Brandyk et al., 2020)
Wetlands restoration	Water storage and retention	Modified vegetation parameters: LAI = 2.5, RD = 450 mm (NHI, 2008; Breuer et al., 2003); Flow detention storage introduced (0.15m) (Mitsch and

		Gosselink, 2015; Tousignant et al., 1999); Modified Strickler roughness coefficient = 15 $m^{1/3}/s$ (Janssen, 2023; Chow, 1959); Modified soil hydraulic properties (Wösten et al., 1999; Guo and Gifford, 2002; Beillouin et al., 2023)
Infiltration ponds	Increase of infiltration into the sub-surface	Sandy soil in the top 30 cm (Hsieh and Davis, 2005; Woods Ballard et al., 2015); Flow detention storage introduced (0.15m) (Woods Ballard et al., 2015); Modified Strickler roughness coefficient = 40 $m^{1/3}/s$ (Engman, 1986) and soil hydraulic properties (Wösten et al., 1999)
Heathlands restoration	Reduce interception and transpiration from currently forested areas	Reduced LAI and RD according to (NHI, 2008); Modified Strickler roughness coefficient (Papaioannou et al., 2018)
Tree planting	Increased infiltration and soil water retention; enhanced flow resistance	Modified LAI and RD values (NHI, 2008); Modified Strickler roughness coefficient (Papaioannou et al., 2018; Freeman et al., 1998); Modified soil hydraulic properties in trees' root zone (Beillouin et al., 2023; Wösten et al., 1999)
Brook bed barriers	Slowing down upstream river flow and allowing more infiltration	Using weirs in Mike 11 river model to represent barriers (Guido et al., 2023; Thomas and Nisbet, 2012; Metcalfe et al., 2017)

6.2.4 NBS-based adaptation strategies

The single NBS measures were used as the foundation to design the spatially combined adaptation strategies. The opportunity maps of single NBS measures cover quite a large area and implementing them at every potential location may not be feasible. Therefore, the design of the combined adaptation strategies was restricted to the spatial domain

which are already identified for the nature by the Province. As an outcome, two strategies were developed (S1 and S2), which differ in their spatial extents. In S1, the spatial extent was limited to the area proposed under the "Nature Management Plan" (NMP) which was developed in the 1990s. While the S2 covers larger spatial extent, for which along with NMP a recently defined "Green Blue Mantel" (GBM) area was included. The GBM has been designated as a buffer zone surrounding the nature network of province which can be used to support climate proofing as well as nature and landscape enhancement. These steps ensured that the proposed NBS adaptation strategies are embedded in the existing water and land management plans regarding climate adaptation and nature enhancement. These two areas (NMP and GMB) are shown in Figure 6.3.

The potential locations of individual measures, as shown in the opportunity maps, are determined based on the geospatial analyses. Therefore, there are chances that locations may overlap where different type of single measures could potentially be implemented. Further, as the hydrological processes are complex, different measures at a particular location may have different effects on different hydrological components. Consequently, single measures were combined into strategies based on their performance with respect to groundwater conditions improvement as the main criterion. The groundwater conditions were prioritized, as for the drought adaption the aim was to store more water in the sub-surface storage. Increasing groundwater storage eventually supports greater water retention in the catchment and contributes to base flow.

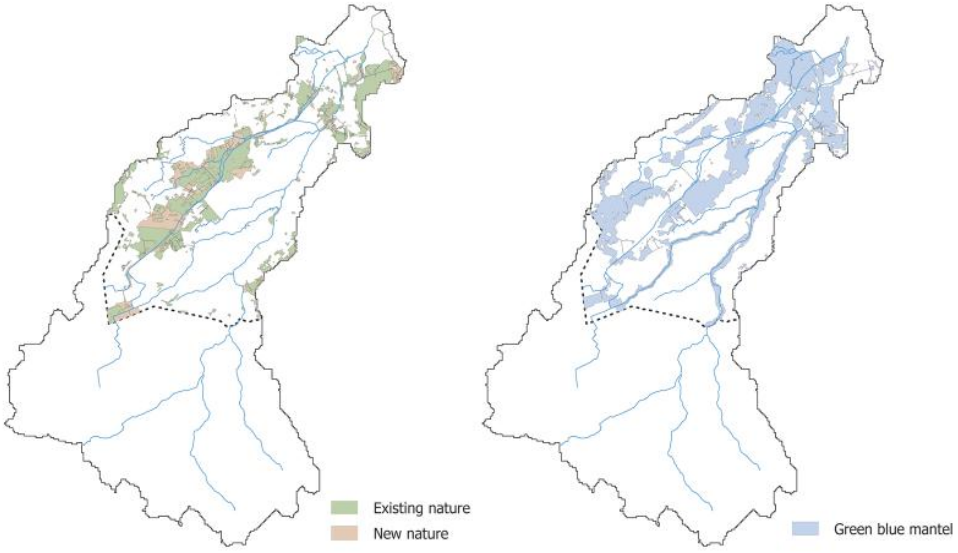

Figure 6.3. Spatial domains used for designing strategies S1 and S2

The locations where the single measures had negative impact on the GWLs were excluded. Only the locations where the results were positive where included in the formulation of strategies. The final locations selected for each measure were determined based on evaluating where the particular measure demonstrated the greatest positive impact. For

instance, if there was a spatial overlap or conflict at a location then the measure with higher positive impact was provided. It is important to note that Ditch blocking consistently showed positive effects on all the locations where it was provided. So, it was provided in combination with other measures at some locations.

For the performance assessment of the strategies (S1 and S2), the climate scenario HD was selected as it represents the most severe drought conditions. This scenario may not be most likely but to best reveal the potential of strategies it was selected for simulations. The outcomes were analysed in term of KPIs. Further, the water balances of the catchment were computed to provide supporting information on the hydrological changes introduced by the strategies.

6.3 RESULTS AND DISCUSSION

6.3.1 Single measures and water balance results

The flow duration curves for the streamflow at the catchment outlet, based on the single measures and considering only the values from the summer months (June, July, August) are shown in Figure 6.4. The infiltration ponds and heathlands restoration have reduced the high flows and increased the low flows. The trend is more prominent for the infiltration ponds compared to heathlands restoration. The wetlands restoration reduced the high flows while remaining neutral when the flow is less than about 2 $m^3 s^{-1}$. Similarly, for the ditch blocking the low flow remained unaffected while the flows above 8 $m^3 s^{-1}$ increased marginally. Tree planting has a negative effect on high as well as low flows whereas brook bed barriers remained neutral.

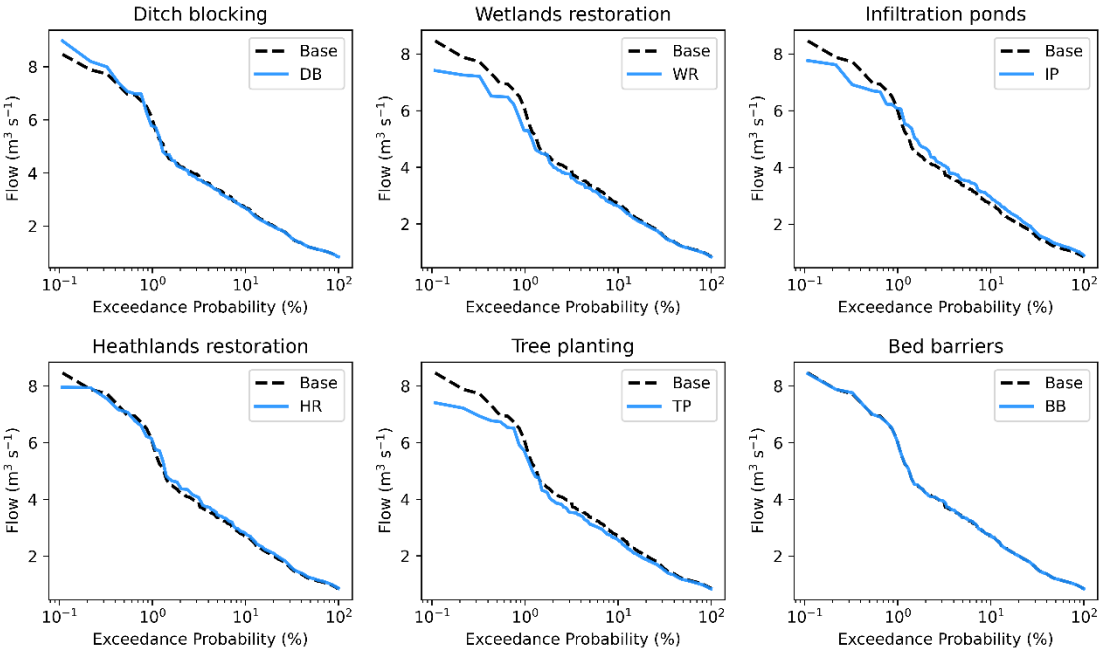

Figure 6.4. Flow duration curve for summer months at catchment's outlet

The average change in the groundwater level during the summer months for each single measure compared to base conditions is shown in Figure 6.5. The spatial maps show the areas with increase (blue) and decrease (red) in GWLs across the catchment. The ditch blocking, infiltration ponds and heathlands restoration have positive effects on the GWLs at all the locations where they were implemented. In particular, the most substantial change is demonstrated by infiltration ponds where the change at a few locations reaches up to 0.45 m. Heathlands restoration also contributed to the moderate increase in the north-east and central areas of the catchment. Ditch blocking produced the increase typically in the range of 0.1 to 0.3 m. Wetlands restoration presented mixed effects where some areas exhibited an increase of up to 0.1 m – 0.4 m and some regions showed declines. This may be due to the dual influence of increased ET and storage change, where the local conditions decide the net effect on the GWLs. The brook bed barriers showed a negligible impact on the GWLs mostly within the range of 0.01 m. Tree planting is the only measure with a widespread decrease in GWL, reaching up to -0.2 to -0.3 m at some locations. This is consistent with the increased ET as observed in the water balance (Table 6.3) which depicted that trees are causing significant water loss due to increased vegetation uptake.

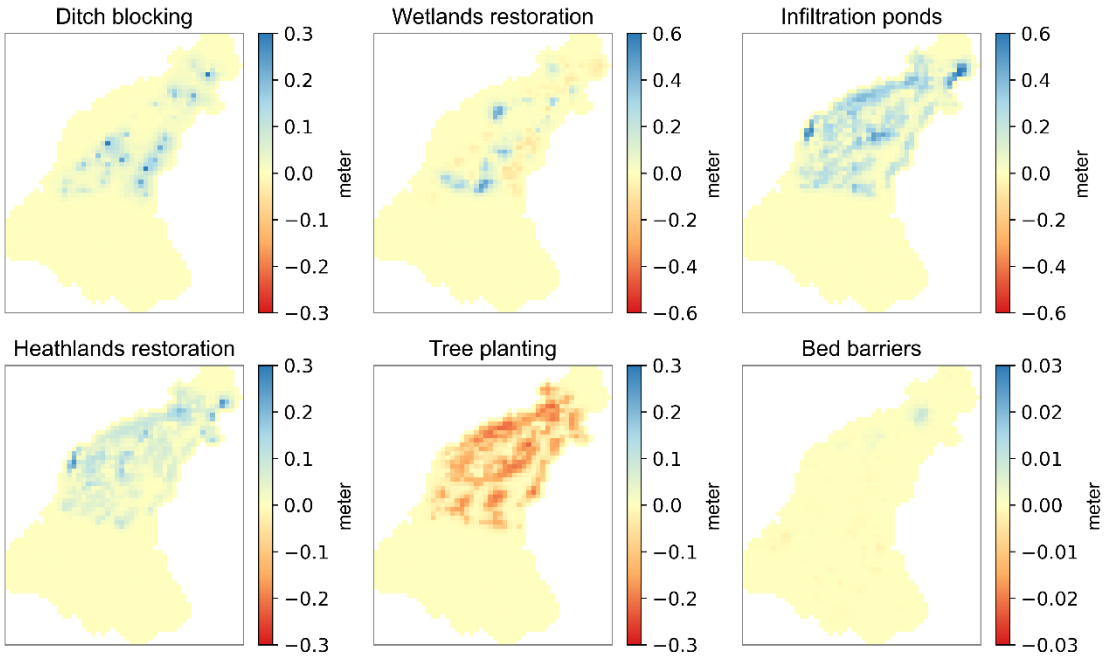

Figure 6.5. Average change in groundwater levels in summer months due to singles measure compared to base conditions

The summarized main water balance components of the base model and single measure under the current condition (2010-2019) for the whole catchment are presented in Table 6.3. The values are accumulated over the entire period and rounded off to integer values. It is important to mention that the evaporation from the surface consists of evaporation from canopy interception, ponded water on the surface and open water. While the sub-surface component of ET consists of soil evaporation and transpiration. The infiltered water to un-saturated zone is available for sub-surface ET and groundwater recharge. For the ditch blocking increase in the GWLs was observed (Figure 6.5) whereas in water balance a slight decrease in the recharge was observed (from 2888 mm to 2830 mm). Ditch blocking is a measure that disrupts drainage network by slowing the lateral subsurface flow and retaining water that is already in the subsurface rather than enhancing vertical recharge. The sub-surface storage change remained almost the same (49 mm vs 50 mm) while the base flow increased from 208 mm to 215 mm. Overall, ditch blocking resulted in a rise of GWLs due to enhanced water retention via reduced lateral drainage rather than increased vertical input. The catchment average rise in GWL during the summer at locations with positive response to ditch blocking is 4.9 cm which is in accordance with the findings of Stachowicz et al. (2025), who observed a rise of about 6 cm due to ditch blocking in the catchments in Norway. Infiltration ponds demonstrated the highest increase in recharge among the tested measures (3135). This led to an increase in base flow and sub-surface storage. On average, at the location with positive impacts of infiltration ponds, the GWLs rose by 14.6 cm. Similarly, heathlands enhanced the average

GWL by 5.4 cm by slightly reduced ET (5115 mm) and increased recharge (2953 mm). Consequently, the river runoff also increased. Wetlands restoration led to an increase in surface ET but also a slight increase in recharge. This suggests the improved water residence time has been facilitated by wetlands. At locations where wetlands showed a positive impact on GWL, the average summer rise was about 9 cm, whereas areas showing a negative response showed a mean decline of about 4 cm.

Tree planting enhanced ET (5189 mm to 5346 mm) from both surface and sub-surface. Consequently, this led to reduced groundwater recharge and river runoff. Similar conclusions have been reported by van Meerveld and Seibert (2025) in their recent review article that in general tree plantation will increase ET, and reduce recharge and streamflow specifically in low flow periods. However, this should not be considered as an excuse to clear-cut the forests as they provide many other benefits such as carbon sequestration, biodiversity enhancement, cool, etc. Brook bed barrier showed negligible changes in the water balance suggesting minimal hydrological change at the catchment scale.

Table 6.3. Accumulate water balances for the base model along with single measures for the period 2010-2019

Water balance component	**Values for each Case (all values are expressed in mm)**						
	Base	**DB**	**WR**	**IP**	**HR**	**TP**	**BB**
Precipitation	8251	8251	8251	8251	8251	8251	8251
Total Evapotranspiration	5189	5194	5267	4955	5115	5346	5189
- From sub-surface	3716	3715	3672	3779	3663	3808	3715
- From surface	1473	1479	1595	1176	1452	1537	1474
Infiltration	6524	6467	6482	6840	6540	6487	6523
Groundwater recharge	2888	2830	2890	3135	2953	2699	2888
River runoff	2130	2119	2058	2285	2184	2010	2130
- From drain flow	1668	1597	1670	1830	1712	1579	1668
- From base flow	208	215	212	220	211	202	208
- From overland flow	254	307	176	235	261	229	254
Sub-surface storage change	49	50	46	65	53	37	49
- From unsaturated zone	-80	-80	-81	-76	-79	-82	-80
- From saturated zone	129	130	127	141	132	119	129
Boundary outflow	884	889	882	946	899	859	884

Tree planting demonstrated a consistently negative impact on GWL while brook bed barriers remained neutral with no significant changes in the water balance components. Therefore, these two measures were excluded from the formulation of combined strategies and are not discussed further in the following sections.

6.3.2 NBS adaptation strategies and their KPIs and water balance results

The single measures (ditch blocking, infiltration ponds, heathlands restorations and wetlands restorations) were combined following the procedure described in the methodology to formulate two strategies S1 and S2. These two strategies are presented in Figure 6.6.

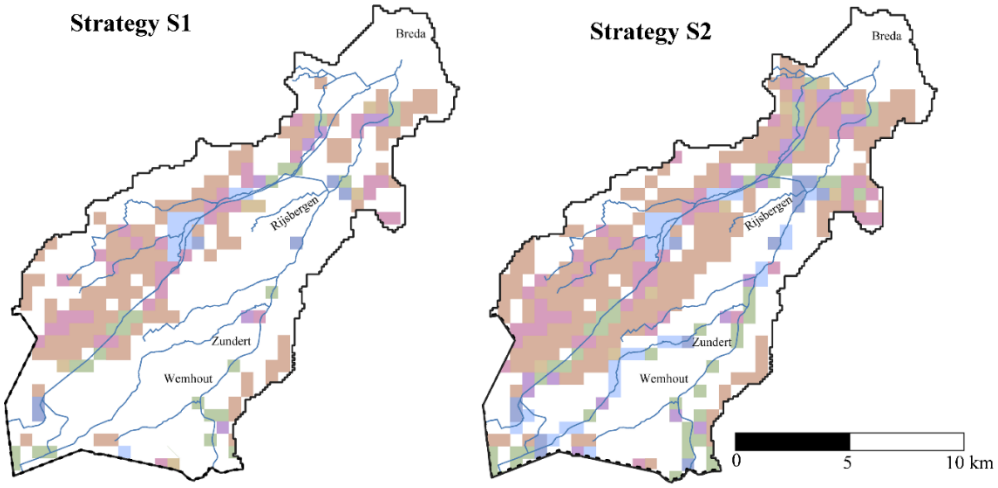

NBS Measure	Strategy S1		Strategy S2	
	Km²	% of catchment size	Km²	% of catchment size
Ditch Blocking (DB)	6.25	1.8	12.5	3.6
Heathland restoration	9.75	2.8	14.0	4.0
Heathland restoration and DB	1.75	0.5	4.48	1.3
Infiltration ponds	30.0	8.7	47.2	13.6
Infiltration ponds and DB	1.50	0.4	2.05	0.6
Wetland restoration	2.75	0.8	7.28	2.1
Wetland restoration and DB	1.50	0.4	3.20	0.9

Figure 6.6. Spatial design of S1 (left panel) and S2 (right panel) NBS adaptation strategies

Clearly visible in Figure 6.6, S1 has small spatial extent compared to S2, which covers larger area. Following the land use map of the area along with two nature management plan (NMP and GBM, Figure 6.3), there seems to be more opportunities to implement NBS towards the west side of the catchment. Western side is already covered with more natural area as compared to the eastern side which is more dedicated to agricultural activities. This spatial pattern may be because of the reason that the main branch (Aa of Weerijs) is toward the east side of the catchment, historically favoring agricultural development. Additionally, the two strategies also cover more spatial area towards the west side of the catchment because of overlap with NMP and GBM. Therefore, these strategies mainly propose the expansion of current natural area with NBSs on that side of catchment. On the eastern side, strategies S2 offers more opportunities but only in close

vicinity to the Aa of Weerijs river. This spatial distribution of the NBSs in the S1 and S2 has direct implications for the outcomes under climate scenario HD (referred to HD-CC from now on) in term of obtained KPI. Figure 6.7 showed the results for KPI SWA under HD-CC and HD-CC with S1 and S2. The situation under HD-CC is becoming worse where the number of days with no availability and limited availability has increased. The trend is similar at all three locations. All these locations are towards the eastern side of catchment along the main Aa of Weerijs river. With the implementation of strategies S1 and S2, SWA has improved, but the magnitude of improvement is greater for S2 than for S1, particularly at most downstream location (Q1). As the NBS implementation is more focused on the eastern side, so the effect on SWA is significant only after the tributaries from the eastern side join the main Aa of Weerijs river upstream location Q1.

The variation in the value of KPI due to spatial distribution of NBS in S1 and S2 are even more prominent in terms of GWA results as they are more dispersed across the catchment. The results of GWA are shown in Figure 6.8. Even the results of HD-CC scenario alone show the more severe impact on the well locations which are towards the east side of the catchment (e.g. GW-2,3,6) as compared to west (e.g. GW-4,5), due to extensive

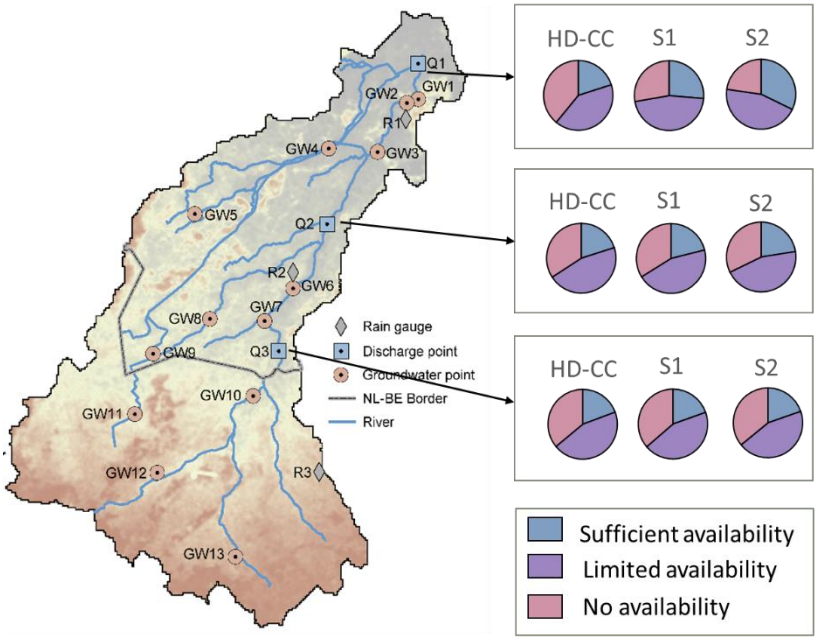

Figure 6.7. Surface Water Availability (SWA) results for climate change scenario HD (HD-CC) and nature-based solutions adaptation strategies S1 and S2

agriculture toward east and more already existing natural area towards the west. The most significant improvements with the strategies S1 and S2 are observed on the locations which in the downstream part of the catchment (GW-1,2,3, and 4), where with S2 the days with 'no availability' are almost fully eliminated. Similar is the situation at GW5,

which is more upstream but located on the western side where it is surrounded by more NBSs. At the locations which are further upstream such as GW6,7 and 8, S1 hardly enhanced SWA due to limited implementation of NBS at these locations. Whereas under S2 improvements are more noticeable due to more spatial coverage of NBS around these locations. At the points which are in Belgium hardly any improvement is noticeable.

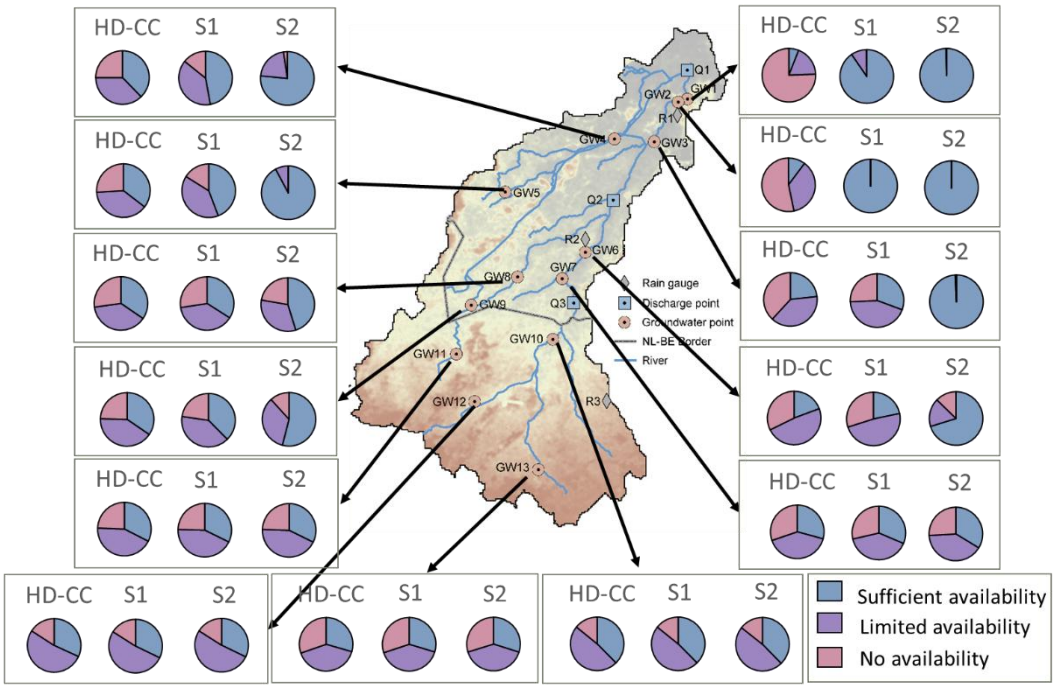

Figure 6.8. Groundwater Availability (GWA) results for climate change scenario HD (HD-CC) and nature-based solutions adaptation strategies S1 and S2.

Overall, the results demonstrated that in addition to the improvements at the local locations where NBS are implemented, the positive impacts are accumulated from upstream to downstream for both surface and groundwater. These findings are in accordance with other literature that investigated the impacts of spatially distributed NBS strategies (Fennell et al., 2023).

The hydrological conditions under the climate change scenario HD along with the implemented strategies S1 and S2 are further analyzed by computing the water balances of hydrological components for the period 2050-2059 and are presented in Table 6.4. Under the HD-CC, the most significant change compared to the current condition (Table 6.3) is in terms of ET which increased by about 14 %. The precipitation is also reduced but only by about 2 %. So, the main component is the increased ET which induced the prominent negative impacts on GWA and SWA under climate change. Under S1 and S2, the increase in ET was reduced and consequently, infiltration and recharge were increased.

Table 6.4. Accumulated water balances for the HD scenario, S1 and S2 strategies (2050-2059)

Water balance component	Values for each Case (all values are expressed in mm		
	HC-CC	**S1**	**S2**
Precipitation	8060	8060	8060
Total Evapotranspiration	5939	5816	5752
- From Sub-surface	3051	3201	3290
- From Surface	2887	2617	2462
Infiltration	5062	5336	5493
Groundwater recharge	2089	2211	2277
River runoff	1379	1462	1496
- From drain flow	1094	1171	1201
- From base flow	174	182	191
- From overland flow	111	109	104
Sub-surface storage change	44	56	63
- From unsaturated zone	-78	-75	-74
- From saturated zone	122	131	137
Boundary outflow	699	727	749

The results are further analyzed to understand how these strategies behave under different seasons. The average seasonal variations of the key hydrological components over the 10-year simulation period (2050-2059) under HD-CC, S1 and S2 are represented in Figure 6.9. The results show the already mentioned effect from the strategies S1 and S2 but these are more prominent during spring and summer. For instance, the average ET under HD-CC during summer is 261 mm/season but is reduced to 251 mm/season under S2 and consequently infiltration is increased from 82 mm/season to 98 mm/season under S2. The negative value of recharge under CC-HD shows that groundwater is losing water due to evapotranspiration. However, this negative recharge is reduced under S1 and S2. Overall, the results depict that the goal to increase sub-surface storage is achieved but a considerable positive impact came from the implementation of NBS on larger area.

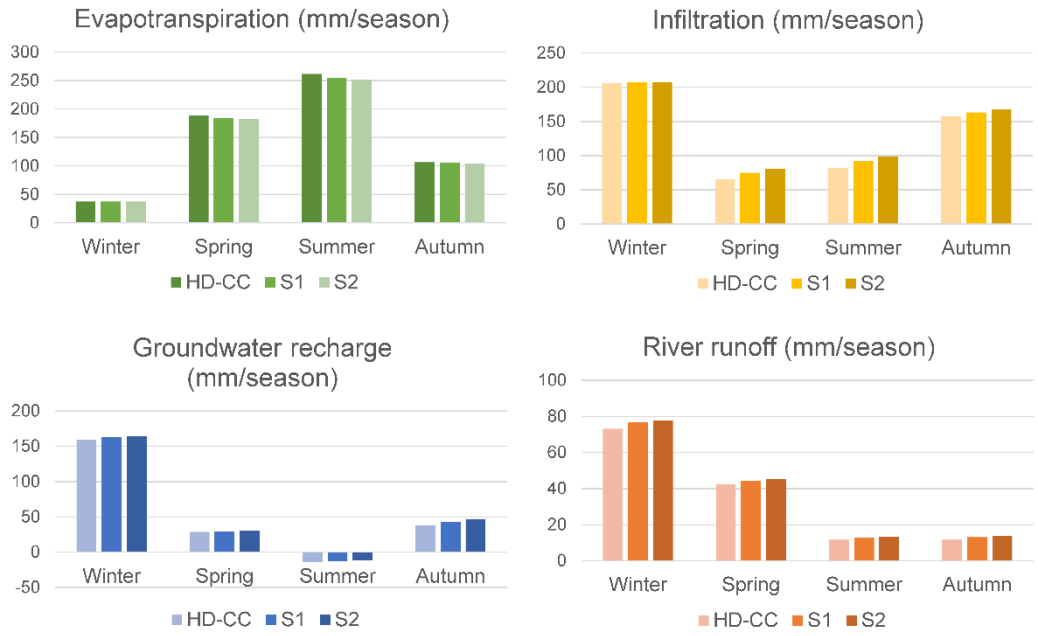

Figure 6.9. Seasonal variation of key water balance components, represented as average seasonal values over the 10-year simulation period, under HD climate change scenario (HD-CC), and adaptation strategies S1 and S2

The decrease in ET due to NBS strategies is primarily because they enable more water to infiltrate into the sub-surface consequently leaving less water on the surface to evaporate. It is also evident from the water balance (Table 6.4) that actual ET from sub-surface increased under two NBS strategies while surface related Actual ET reduced. This is attributed to multiple combined effects from different types of NBS present in the strategies such as change of vegetation parameters due to wetlands and heathlands, enhancement of infiltration with infiltration ponds, and slowing of lateral flow with ditch blocking. The combined effects led to an increase in SWA and GWA. In literature, similar effects have been reported that examined the role of NBS in mitigating drought impacts (Fennell et al., 2023; Holden et al., 2022; Welderufael et al., 2013). However, the catchment characteristics or implemented NBS might be different, but the results conclude that NBSs based adaptation strategies have a potential to perform across different scales and climates as long as they are designed to increase retention and infiltrations. With our research using an integrated model, we provided further such evidence that support the NBS strategies.

Our results showed that the proposed NBS strategies in Aa of Weerijs catchment led to higher river discharges in the winter seasons. This is generally undesirable due to the potential of flood nuisance, but in Aa of Weerijs it is not a primary concern as the

catchment is well protected from flooding. Future research may focus on designing strategies that consider high flows as well. It is important to mention that the results are specific to the study area. The results may vary for other catchments depending upon the meteorological conditions and characteristics of the catchment such as landscape, land use, soil properties, etc. It should be expected that allocating larger areas to NBS would yield more benefits as we observed in the case of S1 and S2. The most significant general contribution lies in the development of a methodology that provides clear and interconnected steps for selecting, designing and evaluating NBS strategies for drought using the integrated hydrological model that simulates surface and sub-surface processes simultaneously. Further, in the methodological step, the key aspect is the identification of the KPIs that need to be finalized in association with the stakeholders. This ensures that the KPIs are aligned with stakeholder priorities and are meaningful for both assessment and decision-making. The actual single measures may vary for different catchments depending on the objectives to achieve and the opportunities a particular landscape offers. Our procedural steps for model-based testing of NBS measures and designing the subsequent spatially distributed strategies would still be applicable.

6.4 CONCLUSIONS

This research proposed the methodology for design and catchment-scale evaluation of NBS-based adaptation strategies to mitigate hydrological drought, using indicators that are close to stakeholders' needs and practices. The methodology used an integrated hydrological model based on MIKE SHE software as the main tool to analyse surface and groundwater behaviour in catchment under: (1) current climate conditions, (2) single NBSs, (3) projected near future climate change, and (4) combined NBS-based adaptation strategies. In addition to the use of groundwater level difference, flow duration curves, and water balance are computed to assess the current conditions and the effect of single NBS measures. Further, the effect of climate change and NBS measures (single or combined strategies) on surface and sub-surface condition of the catchment are assessed using two newly introduced KPI (SWA and GWA). These indicators were developed in consultation with stakeholders and express the surface and groundwater availability status connecting the traditional threshold with the actions on withdrawal.

Six different individual NBS measures were assessed using the integrated hydrological model with the aim of retaining water in the catchment for longer and enhancing groundwater recharge. Among these, the most positive impacts were observed for infiltration ponds and heathlands restoration where they increased recharge and consequently contributed to enhanced baseflow. Ditch blocking did not notably improve the recharge but effectively reduced the lateral drainage flow from the sub-surface, consequently increasing groundwater levels. Wetlands restoration demonstrated both positive as well as negative effects. Tree plantation led to enhanced ET and induced

negative impacts on the groundwater and streamflow. Brook bed barriers showed negligible response to surface and sub-surface components. The four single measures (infiltration ponds, heathland restoration, ditch blocking, and wetlands restoration) with the positive response on the groundwater were combined spatially to develop two strategies S1 and S2. Both strategies reduced ET and enhanced the infiltration and recharge, consequently increasing the runoff, achieving the main aim of their application. Strategies S2 (with a larger spatial extent) provided a comparatively more positive effect on surface and groundwater by completely eliminating 'no availability' days at monitoring locations near the downstream part of the catchment. Further, in both strategies, the positive impacts of NBS are accumulated from upstream to downstream.

This assessment was mainly focused on drought adaptation but can be extended to flood adaptation strategies by following the proposed methodology, once the flood-related KPIs are identified in consultation with local stakeholders. Further, we believe that the proposed methodology is not limited to Aa of Weerijs but is readily transferable to other case studies.

7

SYNTHESIS AND OUTCOME

7.1 INTRODUCTION

The previous chapters address the research objective regarding the potential of EO datasets for hydrological modeling, the evaluation of precipitation products suitability for producing surface and subsurface hydrological variables, and the potential of NBS-based adaptation strategies to mitigate drought impacts. This chapter reflects on the findings of the previous chapters in the light of the research objectives presented in Chapter 1. Further, the limitations of the work are discussed and finally in the end the outlook on the topic is provided, identifying further prospects for future research efforts.

7.2 SYNTHESIS

The first objective that the study aims to address is to analyse *the potential of EO data products for distributed hydrological modelling* which is a topic of considerable importance due to challenges posed by data scarcity. Through an extensive PRISMA based systematic literature review (Chapter 2), the analysis provided a thorough examination of multiple dataset types (precipitation, LULC, soil properties, leaf area index (LAI), snow cover, evapotranspiration, soil moisture and temperature) across the catchment scales. The EO data products are helpful for hydrological modelling at regional to global scales, offering broad spatial and temporal coverage. However, the performance and reliability of these datasets are highly variable depending on geographic region, catchment size and hydrological variable of interest. The main synthesis on the EO datasets is that they can fill data gaps in the poorly monitored regions and improve the spatial coverage, but their use remains heavily dependent on careful evaluation. The review (Chapter 2) highlighted that no single EO dataset consistently performs best across different environments or hydrological variables, suggesting that the performance of specific datasets is conditional and context-specific rather than universally identical.

Chapter 2 also highlights the variation in EO dataset usage across micro-, meso- and macro-scale catchments and the relationship between dataset utility and catchment size is established. At the smaller catchment scales (micro- and meso-scale), the utilization and potential of EO datasets remained largely unexplored in practice. The in-situ data is preferred at these scales due to concerns about the coarse spatial resolution of the EO datasets. While the EO products may have the potential to support distributed hydrological modelling at small scales, further performance evaluation studies are needed to unveil this potential fully. The trend might evolve as the fine resolution datasets become more widely available. In the end, the catchment scale- and dataset type-wise knowledge gaps have been identified.

Although the literature search was comprehensive, it is important to mention that it covered the articles published between 2016 and 2021 and relied on two databases. The

relevant studies published outside this time window or on other platforms may have been overlooked. Further, most of the studies were from China and USA, which might have introduced regional bias. Moreover, the review could have been further strengthened by incorporating a systematic synthesis of the comparative accuracy of EO datasets in hydrological simulations. However, this was challenging to incorporate due to the lack of use of standardized evaluation criteria or metrics in the reviewed articles.

While the review categorizes knowledge gaps across dataset types for different catchment scales, one of the common gaps identified is the lack of common evaluation criteria used for selecting the most suitable datasets for the specific hydrological purpose. This gap is consistent across catchment scales and persists irrespective of data type. Although many reviewed articles provided comparative statements about the dataset performance, they did not provide any systematic approach to identify the most suitable dataset for hydrological modelling. Therefore, in the second objective, we *evaluated the influence of the choice of performance metrics on the identification of the most suitable data product for hydrological simulations and developed a comprehensive methodology to identify suitable products.*

In Chapter 4, we presented the development and application of multi-metric, multi combination evaluation framework to identify suitable EO products for simulating hydrological variables. The study directly reflects on the identified gap regarding the lack of a comprehensive method to select a suitable dataset. The methodology was applied to a lowland transboundary catchment using the MIKE SHE model and four precipitation products (EOBS, MSWEP, IMERG Final and ERA5 Land) were rigorously evaluated by testing approximately 33 million combinations of selected metrics. The core concept is that the most suitable product is not the one that performs best on a single or arbitrarily selected set of metrics, but rather the one that demonstrates consistent plausibility across the widest range of metric combinations.

The results of different scenarios and metrics combinations clearly reflect that the choice of evaluation metrics has a significant influence on determining the most suitable product. Depending on which metrics and which variables have been selected for evaluation, the results have varied a lot. Testing of multiple combinations of metrics strongly supported that the use of a single metric can lead to an unsuitable choice of gridded product, either for precipitation estimation or hydrological simulations. The use of multi-metrics multiple combinations approach provided a more robust and comprehensive assessment of the product's performance. The identification of the most suitable precipitation product is highly sensitive to the number and combination of metrics used, particularly when the number of metrics is small. When fewer metrics were considered (chapter 3), the likelihood of misidentifying a less suitable product as the best increases. As more metrics were included, the outcomes converged towards consistently strong performers. Overall, the study highlighted and cautioned that the arbitrary metric selection based on a few

unbalanced metric sets can lead to false identification of the most suitable product. Further, the inclusion of hydrological signatures in the evaluation process enhanced the diagnostic power that traditional statistical error metrics alone could not provide. Moreover, the aggregation of multiple performance combinations using both Euclidean Distance and Plurality Score based criteria enabled a more comprehensive and transparent comparison across datasets, serving as a template for future evaluations. The study also reflected that no single precipitation product consistently performed better than others across all metrics in precipitation estimation or reproducing hydrological variables. At a few locations, the precipitation product's performance in simulating discharge and signature is even better than ground observed data, but it was not consistent across all observation locations. This outcome directly reinforces the findings of Chapter 2 that EO dataset performance is context-specific and therefore, relying on limited or singular evaluation metrics can lead to misleading conclusions.

The findings of the study reflect a critical insight into the sensitivity associated with the choice of metrics and the significant influence of metric selection on identifying the most suitable precipitation products. Although the outcomes are limited to the study catchment, but scientific community can benefit from the methodology proposed. The framework was developed and demonstrated in a well-instrumented catchment, but it is adaptable to data-scarce regions as well, where traditional ground-based observations are limited. In such contexts, alternative remotely sensed variables such as evapotranspiration or soil moisture can be used as evaluation variables, allowing the proposed multi-metric evaluation framework to still support the identification of the most suitable precipitation products based on broader hydrological behaviour. Further, the application is not limited to precipitation products but can be applied to evaluate other EO products and to assess model performance in routine hydrological modelling practices.

Following the evaluation of the EO datasets and the development of a comprehensive framework for their selection in Chapter 4, the third objective (Chapter 5) extended the application of the hydrological modelling to *analyse the individual and combined impacts of future projected changes in LULC and meteorological variables on surface and subsurface hydrology*. The MIKE SHE model used in this study was hybrid in terms of input data as it integrated EO datasets, specifically DEM, land use and soil texture, with meteorological data from local stations. In chapter 4, precipitation products demonstrated their potential to be used as input datasets. However, the use of local station data for this study was a deliberate choice to ensure comparability and credibility of the results, particularly in the communication with local stakeholders. This reflects that the balance between EO and in-situ data usage can ensure an operational modelling environment where stakeholders' trust and data reliability are harmonized. Scientifically, this objective reflects on a critical gap by analysing the combined hydrological impact of both LULC and meteorological changes, which are often considered in isolation in climate impact

studies. The use of recently released KNMI'23 climate projections further strengthened the study's relevance and timeliness, as it offers up-to-date meteorological projection data for scenario analysis. The other major strength that the study offered was the prediction of the future LULC map using ANN-CA. The integration of KNMI'23 scenarios with the future LULC map allowed to capture both the catchment scale averages and local scale sensitivities of hydrological variables towards meteorological inputs and land use change.

For the simulation of future land use, on one side, the choice of a business-as-usual scenario serves as a representation of a worst-case trajectory, emphasizing the potential hydrological impacts of unchecked urban expansion and changes in agricultural land use without interventions of land management or policy-driven planning. On the other hand, it reflects the simplistic scenario that does not account for socioeconomic, political, or environmental factors that could change future land use dynamics or trends assumed under the business-as-usual scenario. Therefore, this scenario is useful for stress-testing of hydrological systems and should be interpreted as a boundary case rather than a definitive forecast.

The model results revealed that under future climate change, the catchment will experience more water stress. This is primarily due to an increase in evapotranspiration due to a temperature rise. The main reflection of the objective is that, on the catchment scale, impacts of climate change on the hydrological variables are comparatively more pronounced than the LULC change. The hydrological impact due to future LULC accounts for very minimal changes in hydrological variables (>1 %) at the catchment scale. However, at the local scales, particularly in zones transitioning from agriculture to built-up or semi-natural areas, LULC change significantly influenced the relative changes in groundwater level, soil moisture and actual evapotranspiration. Under the combined effects, LULC changes appeared to slightly buffer the effects of climate change. Overall, the climate change remained the principal driver of hydrological impacts, while LULC changes can influence the spatial distribution of impacts in the transformed areas.

After the climate change impact analyses (Chapter 5), the final objective was *to evaluate the potential of NBSs for mitigating drought impacts* and *to formulate adaptation strategies to achieve maximum water conservation in subsurface.* Chapter 6 expanded the scope of this thesis from dataset evaluation and future scenario analysis to the design and evaluation of NBS-based adaptive strategies. MIKE SHE model was used to simulate the effects of six individual NBS types and a framework was developed to spatially combine the most effective single NBS into composite adaptive strategies. The systematic selection of final NBS types and their spatial allocation within the strategies (S1 and S2), considering both the regional land use plans and hydrological impact, is the strength of the method that enhances its acceptability, scalability and adaptability. Further, the study's strength is reinforced by the incorporation of KPIs that are stakeholders' relevant and bridge the gap between model output and decision-making needs. The KPIs were

designed in consultation with regional stakeholders, specifically professionals from the Water Board and the Province. It is important to recognise that the implementation of NBS may involve a diverse group of stakeholders with different priorities and KPIs may need to be adapted accordingly.

The single NBS measures tested in this study were categorized in the prior project as suitable for sub-surface water conditions based on GIS based assessment that considered the physical characteristics of the catchment and average groundwater levels. However, the model results depicted that the hydrological effects were not uniformly positive at all the locations. While some measures led to noticeable improvement in the groundwater levels, others (Tree planting and brook bed barriers) remain neutral or even negative. Also, for the same measure, the results have varied across the catchment. This highly reflects the importance of validating GIS based opportunity mapping with hydrological modelling, as spatial suitability alone does not guarantee hydrological effectiveness.

Out of six different individual NBS measures that were assessed for their potential to retain water within the catchment for longer and enhance groundwater recharge, the most positive impacts were observed for infiltration ponds and heathland restoration. Ditching blocking did not notably improve the recharge but effectively reduced the lateral drainage flow from the sub-surface which consequently increased groundwater levels. Wetlands restoration demonstrated both positive as well as negative effects. In contrast, tree plantation led to enhanced evapotranspiration and induced negative impacts on the groundwater and streamflow. Brook bed barriers showed a negligible response to surface and sub-surface components.

Based on the findings, four measures (infiltration ponds, heathland restoration, ditch blocking, and wetlands restoration) were combined spatially to develop two strategies (S1 and S2). The selection and spatial allocation were driven by performance with respect to groundwater level improvement, as the primary focus of the study was to enhance sub-surface storage. It is important to note that different spatial maps might have emerged if the criteria prioritized different objectives. Both strategies succeeded in reducing ET and enhancing infiltration and recharge, consequently increasing the runoff, and improving water availability during summer. Strategies S2, with a larger spatial extent, delivered comparatively more substantial hydrological benefits, including the complete elimination of ‘no availability’ days at the downstream monitoring locations. The results also reflected that the positive impacts due to NBS are accumulated from upstream to downstream. However, the quantum of the positive impact is closely related to the area allocated to each measure, which may conflict with other land use priorities. Moreover, the KPIs considered are solely focused on water availability in the catchment and do not account for potential co-benefits of NBS, nor do they include any economic cost-benefit analysis.

In summary, the research begins with identifying the potential and limitation of EO datasets, then progresses towards the development of comprehensive multiple metrics-based evaluation framework for identifying the most suitable datasets, followed by the impact assessment of combined climate and LULC change and in the end, culminates in the design of NBS-based drought adaptation strategies. Each objective is linked to the preceding one, providing a transparent methodological framework that is transferable and adaptable across different hydrological contexts. The finding underscores that no single dataset, evaluation metrics, or NBS-based intervention is universally optimal. Their effectiveness is, rather, context dependent and is most meaningfully assessed when spatial variability and stakeholders' perspectives are taken into consideration.

7.3 OUTLOOK

This thesis proposes the methodological frameworks for two aims: First, to identify suitable EO datasets for hydrological modeling and second, to evaluate the potential of NBSs for mitigating drought impacts and designing adaptive strategies through integrated hydrological modelling. In the previous section, we reflected on the strengths and limitations of these approaches. Despite the challenges, the research meaningfully advances the knowledge and the findings demonstrate clear potential for the implementation and adaptation of these methods across various locations and settings. Therefore, to further advance the evaluation criteria of EO datasets towards establishing a standardized methodology and to further investigate the potential of NBS-based adaptive strategies to mitigate climate impact, future opportunities are discussed below.

Regarding the potential of EO datasets for distributed hydrological modelling, the literature review conducted identified gaps categorized based on the dataset type and spatial scale (Table 2.1). The identified gap highlights the need for future research to explore and evaluate the effectiveness of different EO datasets in hydrological modelling at various scales, with a particular focus on micro- and meso-scale catchments. This could lead to the identification of more appropriate datasets for hydrological modelling and will enhance the credibility of these datasets for usage in operations as well. Although in the review, all the commonly used datasets for hydrological modelling are covered. But future review could benefit from a more focused in-depth analysis. For instance, by focusing on a single dataset type or increasing the temporal scope of covered literature. This will lead to a more in-depth assessment of dataset specific advancements and knowledge gaps. In addition to the use of EO dataset for model setup, these have wide potential to be used in model calibration, validation and data assimilation. The review only cursory touch on these applications of EO datasets. Future studies could therefore focus on in depth review of EO datasets for particular modelling functions.

Regarding the identification of suitable products for hydrological simulation, a comprehensive, multi-metric, multiple combination evaluation approach has been developed to identify the most suitable precipitation product for reproducing discharge and groundwater levels with a specific hydrological model. The methodology was applied to precipitation products, but it can be implemented to identify other suitable EO datasets. The future study could explore the broader applicability of methodology to other EO datasets. Further, the multi-metric, multiple combination criteria offer potential beyond dataset selection. It could be used as an objective function for calibration and validation of the model. Its applicability and robustness need to be tested across diverse modelling goals. Further, the combinatorial analysis demonstrates that the selection of evaluation metrics significantly influences the outcome of product suitability assessments. Although a wide range of metrics was used but still the selection of metrics remains subjective. The future research could test the methodology with a different set of metrics and compare whether the findings remain consistent or change.

Importantly, the methodology was implemented in a single, small scale catchment, whereas more generalizable outcomes could be achieved by extending the analysis to a broader set of watersheds. The methodological framework developed in this study, based on a multi-metric and multi-combination evaluation approach, is transferable and scalable. Future research may aim to replicate this across diverse hydro-climatic regions, allowing for broader conclusions on the performance of precipitation products as well as to make recommendations regarding the optimal number of metrics to be considered in the evaluation of EO precipitation products and beyond. Overall, methodology represents an important step toward standardizing EO dataset assessment, but not the definitive one. Rather, it invites further research to expand, adapt, and refine the approach for wider hydrological practice.

Regarding the combined assessment of climate and LULC change, the future map was simulated under a business-as-usual scenario. A more nuanced understanding could be achieved by formulating different scenarios for future LULC, incorporating constraints on LULC class expansion, and considering local landscape policies, municipal priorities, stakeholder perspectives, or broader European-level policies. Such considerations could enhance the refinement of future LULC projections. Further, the study considered only rainfall, PET, and LULC under future changes. Global warming may trigger additional factors, such as groundwater abstraction or direct water abstraction from rivers, which could impact discharge and GWT. Additionally, changes in groundwater boundary conditions, not accounted for in this study's future scenarios, could further influence hydrological dynamics. The change in hydrological variables, such as soil moisture and temperature, along with changes in land use, can also affect the soil hydraulic properties. The impact of land use changes on soil properties and their subsequent effects on hydrological processes is under explored area of research. Therefore, future research

activities could explore these additional factors. The effect of these factors might not be significant alone, but studying the coupled effects of various drivers would provide a more comprehensive understanding of future hydrological dynamics.

Regarding the NBS strategies for climate adaptation, the research particularly focused on water conservation for drought adaptation. Future research may focus on designing strategies that consider both high and low flows. The existing methodology can be extended to flood adaptation strategies by identifying the flood-related KPIs in consultation with local stakeholders. Further, in the methodological steps, the key aspect is the identification of the KPIs in consultation with the stakeholders. This ensures that the KPIs are aligned with stakeholder priorities and are meaningful for both assessment and decision-making. However, in this research, consultation was limited to the representatives from the Water Board and the Province. A broader and diverse group of stakeholders may be consulted to design the KPIs. It will ensure the broader social acceptability of the designed strategies in the community. The NBSs are assessed on their performance for enhancing surface water and groundwater availability. Their co-benefits, such as carbon sequestration, water purification, biodiversity enhancement, etc, along with cost benefit analyses, can be focused on in future research.

The NBSs were modelled in a small-scale catchment using an integrated hydrological model. To expand its utility, different methods can be explored to upscale the results, for instance, by training a machine learning model on hydrological model outputs and GIS based opportunity maps to identify other locations where the NBS interventions may yield positive impacts, depending on the defined KPIs. Moreover, NBS strategies in this research were designed on a basin scale, the implementation of which falls out of the scope and capacity of individual landowners or farmers. Future research could explore field scale NBS interventions that the landowner can feasibly implement in their field.

To conclude, these future directions will broaden the scope and scale of EO datasets applicability, promote the development of standardized evaluation criteria, advance the NBS-based adaptation strategies design, and strengthen stakeholder engagement in hydrological modelling and sustainable water resource management.

REFERENCES

Abhishek and Kinouchi, T.: Synergetic application of GRACE gravity data, global hydrological model, and in-situ observations to quantify water storage dynamics over Peninsular India during 2002–2017, Journal of Hydrology, 596, 126069, https://doi.org/10.1016/j.jhydrol.2021.126069, 2021.

Abiodun, O. O., Guan, H., Post, V. E. A., and Batelaan, O.: Comparison of MODIS and SWAT evapotranspiration over a complex terrain at different spatial scales, Hydrology and Earth System Sciences, 22, 2775-2794, 10.5194/hess-22-2775-2018, 2018.

Adib, M. N. M., Rowshon, M. K., Mojid, M. A., and Habibu, I.: Projected streamflow in the Kurau River Basin of Western Malaysia under future climate scenarios, Scientific Reports, 10, 8336, 10.1038/s41598-020-65114-w, 2020.

Ageet, S., Fink, A. H., Maranan, M., Diem, J. E., Hartter, J., Ssali, A. L., and Ayabagabo, P.: Validation of satellite rainfall estimates over equatorial East Africa, Journal of Hydrometeorology, 23, 129-151, 2022.

Akbas, A. and Ozdemir, H.: Comparing Satellite, Reanalysis, Fused and Gridded (In Situ) Precipitation Products Over Türkiye, International Journal of Climatology, 2024.

Al-Areeq, A. M., Al-Zahrani, M. A., and Sharif, H. O.: The performance of physically based and conceptual hydrologic models: A case study for makkah watershed, saudi arabia, Water (Switzerland), 13, 10.3390/w13081098, 2021.

Al-Khudhairy, D., Thompson, J., Gavin, H., and Hamm, N.: Hydrological modelling of a drained grazing marsh under agricultural land use and the simulation of restoration management scenarios, Hydrological Sciences Journal, 44, 943-971, 1999.

Alam, S., Kaenel, M. v., Su, L., and Lettenmaier, D. P.: The role of antecedent winter soil moisture carryover on spring runoff predictability in snow-influenced Western US catchments, Journal of Hydrometeorology, 25, 1561-1575, 2024.

Alataway, A. and El Alfy, M.: Rainwater harvesting and artificial groundwater recharge in arid areas: Case study in Wadi Al-Alb, Saudi Arabia, Journal of Water Resources Planning and Management, 145, 10.1061/(ASCE)WR.1943-5452.0001009, 2019.

Alexopoulos, M. J., Müller-Thomy, H., Nistahl, P., Šraj, M., and Bezak, N.: Validation of precipitation reanalysis products for rainfall-runoff modelling in Slovenia, Hydrology and Earth System Sciences, 27, 2559-2578, 10.5194/hess-27-2559-2023, 2023.

Alfieri, L., Avanzi, F., Delogu, F., Gabellani, S., Bruno, G., Campo, L., Libertino, A., Massari, C., Tarpanelli, A., Rains, D., Miralles, D. G., Quast, R., Vreugdenhil, M., Wu, H., and Brocca, L.: High-resolution satellite products improve hydrological modeling in northern Italy, Hydrology and Earth System Sciences, 26, 3921-3939, 10.5194/hess-26-3921-2022, 2022.

Ali, M. H., Popescu, I., Jonoski, A., and Solomatine, D. P.: Remote sensed and/or global datasets for distributed hydrological modelling: A review, Remote Sensing, 15, 1642, 2023.

Allen, R. G., Pereira, L. S., Howell, T. A., and Jensen, M. E.: Evapotranspiration information reporting: I. Factors governing measurement accuracy, Agricultural Water Management, 98, 899-920, 2011.

Almagro, A., Oliveira, P. T. S., and Brocca, L.: Assessment of bottom-up satellite rainfall products on estimating river discharge and hydrologic signatures in Brazilian catchments, Journal of Hydrology, 603, 126897, 2021.

Amjad, M., Yilmaz, M. T., Yucel, I., and Yilmaz, K. K.: Performance evaluation of satellite-and model-based precipitation products over varying climate and complex topography, Journal of Hydrology, 584, 124707, 2020.

Appel, F., Koch, F., Rösel, A., Klug, P., Henkel, P., Lamm, M., Mauser, W., and Bach, H.: Advances in snow hydrology using a combined approach of GNSS in situ stations, hydrological modelling and earth observation—A case study in Canada, Geosciences, 9, 10.3390/geosciences9010044, 2019.

AR6: IPCC, 2023: Climate Change 2023: Synthesis Report, Summary for Policymakers. Contribution of Working Groups I, II and III to the Sixth Assessment Report of the Intergovernmental Panel on Climate Change. IPCC, Geneva, Switzerland, 2023.

Arthur, E., Anyemedu, F. O. K., Gyamfi, C., Asantewaa - Tannor, P., Adjei, K. A., Anornu, G. K., and Odai, S. N.: Potential for small hydropower development in the Lower Pra River Basin, Ghana, Journal of Hydrology: Regional Studies, 32, 10.1016/j.ejrh.2020.100757, 2020.

Assouline, S., Sela, S., Dorman, M., and Svoray, T.: Runoff generation in a semiarid environment: The role of rainstorm intra-event temporal variability and antecedent soil moisture, Advances in Water Resources, 188, 104715, https://doi.org/10.1016/j.advwatres.2024.104715, 2024.

Ayala, A., Farías-Barahona, D., Huss, M., Pellicciotti, F., McPhee, J., and Farinotti, D.: Glacier runoff variations since 1955 in the Maipo River basin, in the semiarid Andes of central Chile, Cryosphere, 14, 2005-2027, 10.5194/tc-14-2005-2020, 2020.

Ayehu, G. T., Tadesse, T., Gessesse, B., and Dinku, T.: Validation of new satellite rainfall products over the Upper Blue Nile Basin, Ethiopia, Atmospheric Measurement Techniques, 11, 1921-1936, 2018.

Bagiliko, J., Stern, D., Ndanguza, D., and Torgbor, F. F.: Validation of satellite and reanalysis rainfall products against rain gauge observations in Ghana and Zambia, Theoretical and Applied Climatology, 156, 1-20, 2025.

Bakke, S. J., Ionita, M., and Tallaksen, L. M.: The 2018 northern European hydrological drought and its drivers in a historical perspective, Hydrology and Earth System Sciences, 24, 5621-5653, 10.5194/hess-24-5621-2020, 2020.

Ballabio, C., Panagos, P., and Monatanarella, L.: Mapping topsoil physical properties at European scale using the LUCAS database, Geoderma, 261, 110-123, 10.1016/j.geoderma.2015.07.006, 2016.

Ballabio, C., Lugato, E., Fernández-Ugalde, O., Orgiazzi, A., Jones, A., Borrelli, P., Montanarella, L., and Panagos, P.: Mapping LUCAS topsoil chemical properties at

European scale using Gaussian process regression, Geoderma, 355, 113912, 10.1016/j.geoderma.2019.113912, 2019.

Bárdossy, A., Kilsby, C., Birkinshaw, S., Wang, N., and Anwar, F.: Is precipitation responsible for the most hydrological model uncertainty?, Frontiers in Water, 4, 836554, 2022.

Barnett, T. P., Adam, J. C., and Lettenmaier, D. P.: Potential impacts of a warming climate on water availability in snow-dominated regions, Nature, 438, 303-309, 2005.

Baroni, G., Schalge, B., Rakovec, O., Kumar, R., Schüler, L., Samaniego, L., Simmer, C., and Attinger, S.: A comprehensive distributed hydrological modeling intercomparison to support process representation and data collection strategies, Water Resources Research, 55, 990-1010, 2019.

Beck, H. E., Pan, M., Lin, P., Seibert, J., van Dijk, A. I. J. M., and Wood, E. F.: Global Fully Distributed Parameter Regionalization Based on Observed Streamflow From 4,229 Headwater Catchments, Journal of Geophysical Research: Atmospheres, 125, 10.1029/2019JD031485, 2020.

Beck, H. E., Pan, M., Roy, T., Weedon, G. P., Pappenberger, F., Van Dijk, A. I., Huffman, G. J., Adler, R. F., and Wood, E. F.: Daily evaluation of 26 precipitation datasets using Stage-IV gauge-radar data for the CONUS, Hydrology and Earth System Sciences, 23, 207-224, 2019.

Beck, H. E., Vergopolan, N., Pan, M., Levizzani, V., Van Dijk, A. I., Weedon, G. P., Brocca, L., Pappenberger, F., Huffman, G. J., and Wood, E. F.: Global-scale evaluation of 22 precipitation datasets using gauge observations and hydrological modeling, Hydrology and Earth System Sciences, 21, 6201-6217, 2017.

Becker, R., Koppa, A., Schulz, S., Usman, M., aus der Beek, T., and Schüth, C.: Spatially distributed model calibration of a highly managed hydrological system using remote sensing-derived ET data, Journal of Hydrology, 577, 10.1016/j.jhydrol.2019.123944, 2019.

Beers, M., Coenen, D., Herman, K., and Karin, M.: Watersysteemanalyse Aa of Weerijs Report, https://www.brabantsedelta.nl/watersysteemanalyses-kaderrichtlijn-water-krw, 2018.

Beillouin, D., Corbeels, M., Demenois, J., Berre, D., Boyer, A., Fallot, A., Feder, F., and Cardinael, R.: A global meta-analysis of soil organic carbon in the Anthropocene, Nature Communications, 14, 3700, 2023.

Bense, V., Read, T., and Verhoef, A.: Using distributed temperature sensing to monitor field scale dynamics of ground surface temperature and related substrate heat flux, Agricultural and Forest Meteorology, 220, 207-215, 2016.

Beven, K. and Westerberg, I.: On red herrings and real herrings: disinformation and information in hydrological inference, Hydrological Processes, 25, 1676-1680, https://doi.org/10.1002/hyp.7963, 2011.

Bhatta, B.: Analysis of urban growth and sprawl from remote sensing data, Springer Science & Business Media2010.

Biondi, D., Freni, G., Iacobellis, V., Mascaro, G., and Montanari, A.: Validation of hydrological models: Conceptual basis, methodological approaches and a proposal for a code of practice, Physics and Chemistry of the Earth, Parts a/b/c, 42, 70-76, 2012.

Blöschl, G., Hall, J., Viglione, A., Perdigão, R. A., Parajka, J., Merz, B., Lun, D., Arheimer, B., Aronica, G. T., and Bilibashi, A.: Changing climate both increases and decreases European river floods, Nature, 573, 108-111, 2019.

Bogatinoska, B., Lansu, A., Hugé, J., and Dekker, S. C.: Participatory design of nature-based solutions: usability of tools for water professionals, Sustainability, 14, 5562, 2022.

Boussinesq, J.: Recherches théoriques sur l'écoulement des nappes d'eau infiltrées dans le sol et sur le débit des sources, Journal de mathématiques pures et appliquées, 10, 5-78, 1904.

Bouttier, F. and Marchal, H.: Probabilistic short-range forecasts of high-precipitation events: optimal decision thresholds and predictability limits, Natural Hazards and Earth System Sciences, 24, 2793-2816, 10.5194/nhess-24-2793-2024, 2024.

Brandyk, A., Kaca, E., Oleszczuk, R., Urbański, J., and Jadczyszyn, J.: Conceptual model of drainage-sub irrigation system functioning-first results from a case study of a lowland valley area in Central Poland, Sustainability, 13, 107, 2020.

Breuer, L., Eckhardt, K., and Frede, H.-G.: Plant parameter values for models in temperate climates, Ecological Modelling, 169, 237-293, 2003.

Brink, E., Aalders, T., Ádám, D., Feller, R., Henselek, Y., Hoffmann, A., Ibe, K., Matthey-Doret, A., Meyer, M., and Negrut, N. L.: Cascades of green: A review of ecosystem-based adaptation in urban areas, Global environmental change, 36, 111-123, 2016.

Brocca, L., Filippucci, P., Hahn, S., Ciabatta, L., Massari, C., Camici, S., Schüller, L., Bojkov, B., and Wagner, W.: SM2RAIN–ASCAT (2007–2018): Global daily satellite rainfall data from ASCAT soil moisture observations, Earth System Science Data, 11, 1583-1601, 2019.

Brocca, L., Ciabatta, L., Massari, C., Moramarco, T., Hahn, S., Hasenauer, S., Kidd, R., Dorigo, W., Wagner, W., and Levizzani, V.: Soil as a natural rain gauge: Estimating global rainfall from satellite soil moisture data, Journal of Geophysical Research: Atmospheres, 119, 5128-5141, 2014.

Brocca, L., Hasenauer, S., Lacava, T., Melone, F., Moramarco, T., Wagner, W., Dorigo, W., Matgen, P., Martínez-Fernández, J., and Llorens, P.: Soil moisture estimation through ASCAT and AMSR-E sensors: An intercomparison and validation study across Europe, Remote Sensing of Environment, 115, 3390-3408, 2011.

Brown, R. D. and Mote, P. W.: The response of Northern Hemisphere snow cover to a changing climate, Journal of Climate, 22, 2124-2145, 2009.

Bugan, R., García, C. L., Jovanovic, N., Teich, I., Fink, M., and Dzikiti, S.: Estimating evapotranspiration in a semi-arid catchment: A comparison of hydrological modelling and remote-sensing approaches, Water South Africa, 46, 158-170, 10.17159/wsa/2020.v46.i2.8231, 2020.

Busari, I. O., Demirel, M. C., and Newton, A.: Effect of using multi-year land use land cover and monthly lai inputs on the calibration of a distributed hydrologic model, Water (Switzerland), 13, 10.3390/w13111538, 2021.

Camici, S., Massari, C., Ciabatta, L., Marchesini, I., and Brocca, L.: Which rainfall score is more informative about the performance in river discharge simulation? A comprehensive assessment on 1318 basins over Europe, Hydrology and Earth System Sciences, 24, 4869-4885, 10.5194/hess-24-4869-2020, 2020.

Cannon, A. J., Sobie, S. R., and Murdock, T. Q.: Bias correction of GCM precipitation by quantile mapping: how well do methods preserve changes in quantiles and extremes?, Journal of Climate, 28, 6938-6959, doi.org/10.1175/JCLI-D-14-00754.1, 2015.

Casanueva, A., Rodríguez-Puebla, C., Frías, M. D., and González-Reviriego, N.: Variability of extreme precipitation over Europe and its relationships with teleconnection patterns, Hydrology and Earth System Sciences, 18, 709-725, 10.5194/hess-18-709-2014, 2014.

CLIMATE DATA STORE (CDS) BY COPERNICUS: EUROPEAN REANALYSIS (ERA5) LAND: https://cds.climate.copernicus.eu/datasets/reanalysis-era5-land?tab=overview, last access: 17 August.

Cenci, L., Laiolo, P., Gabellani, S., Campo, L., Silvestro, F., Delogu, F., Boni, G., and Rudari, R.: Assimilation of H-SAF Soil Moisture Products for Flash Flood Early Warning Systems. Case Study: Mediterranean Catchments, IEEE Journal of Selected Topics in Applied Earth Observations and Remote Sensing, 9, 5634-5646, 10.1109/JSTARS.2016.2598475, 2016.

Chen, G., Meng, T., Wu, W., Si, B., Li, M., Liu, B., Wu, S., Feng, H., and Siddique, K. H.: Evaluating potential groundwater recharge in the unsteady state for deep-rooted afforestation in deep loess deposits, Science of the Total Environment, 858, 159837, 2023.

Chen, J., St-Denis, B. G., Brissette, F. P., and Lucas-Picher, P.: Using natural variability as a baseline to evaluate the performance of bias correction methods in hydrological climate change impact studies, Journal of Hydrometeorology, 17, 2155-2174, 2016a.

Chen, L. and Wang, L.: Recent advance in earth observation big data for hydrology, Big Earth Data, 2, 86-107, 2018.

Chen, Y., Li, J., and Xu, H.: Improving flood forecasting capability of physically based distributed hydrological models by parameter optimization, Hydrology and Earth System Sciences, 20, 375-392, 10.5194/hess-20-375-2016, 2016b.

Chiang, F., Mazdiyasni, O., and AghaKouchak, A.: Evidence of anthropogenic impacts on global drought frequency, duration, and intensity, Nature communications, 12, 2754, 2021.

Chirachawala, C., Shrestha, S., Babel, M. S., Virdis, S. G., and Wichakul, S.: Evaluation of global land use/land cover products for hydrologic simulation in the Upper Yom River Basin, Thailand, Science of the total environment, 708, 135148, 2020.

Chow, V. T.: Open-channel hydraulics: New York, US Army Corps of Engineers, Hydrologic Engineering, 1959.

Cinkus, G., Mazzilli, N., Jourde, H., Wunsch, A., Liesch, T., Ravbar, N., Chen, Z., and Goldscheider, N.: When best is the enemy of good – critical evaluation of performance criteria in hydrological models, Hydrology and Earth System Sciences, 27, 2397-2411, 10.5194/hess-27-2397-2023, 2023.

Clark, M. P., Bierkens, M. F., Samaniego, L., Woods, R. A., Uijlenhoet, R., Bennett, K. E., Pauwels, V., Cai, X., Wood, A. W., and Peters-Lidard, C. D.: The evolution of process-based hydrologic models: historical challenges and the collective quest for physical realism, Hydrology and Earth System Sciences, 21, 3427-3440, 2017.

Clark, M. P., Vogel, R. M., Lamontagne, J. R., Mizukami, N., Knoben, W. J., Tang, G., Gharari, S., Freer, J. E., Whitfield, P. H., and Shook, K. R.: The abuse of popular performance metrics in hydrologic modeling, Water Resources Research, 57, e2020WR029001, 2021.

COPERNICUS LAND MONITORING SERVICE CORINE LAND COVER 2018: https://land.copernicus.eu/pan-european/corine-land-cover/clc2018, last access: 27 November.

COPERNICUS LAND MONITORING SERVICE CORINE EU-DIGITAL ELEVATION MODEL: https://land.copernicus.eu/imagery-in-situ/eu-dem/eu-dem-v1-1-and-derived-products/eu-dem-v1.1?tab=download., last access: 27 November.

CO-ADAPT- CLIMATE ADAPTATION THROUGH CO-CREATION: https://co-adapt-water.eu/ last access: 29 November.

Corbari, C., Jovanovic, D. S., Nardella, L., Sobrino, J., and Mancini, M.: Evapotranspiration estimates at high spatial and temporal resolutions from an energy–water balance model and satellite data in the capitanata irrigation consortium, Remote Sensing, 12, 1-24, 10.3390/rs12244083, 2020.

Corbari, C., Huber, C., Yesou, H., Huang, Y., Su, Z., and Mancini, M.: Multi-satellite data of land surface temperature, lakes area, and water level for hydrological model calibration and validation in the Yangtze river Basin, Water (Switzerland), 11, 10.3390/w11122621, 2019.

Cornelissen, T., Diekkrüger, B., and Bogena, H. R.: Using high-resolution data to test parameter sensitivity of the distributed hydrological model HydroGeoSphere, Water (Switzerland), 8, 10.3390/w8050202, 2016.

Cornes, R. C., van der Schrier, G., van den Besselaar, E. J., and Jones, P. D.: An ensemble version of the E-OBS temperature and precipitation data sets, Journal of Geophysical Research: Atmospheres, 123, 9391-9409, 2018.

Craglia, M., Hradec, J., Nativi, S., and Santoro, M.: Exploring the depths of the global earth observation system of systems, Big Earth Data, 1, 21-46, 2017.

Cui, X., Guo, X., Wang, Y., Wang, X., Zhu, W., Shi, J., Lin, C., and Gao, X.: Application of remote sensing to water environmental processes under a changing climate, Journal of Hydrology, 574, 892-902, 2019.

Dahri, Z. H., Ludwig, F., Moors, E., Ahmad, S., Ahmad, B., Ahmad, S., Riaz, M., and Kabat, P.: Climate change and hydrological regime of the high-altitude Indus basin under

extreme climate scenarios, Science of the Total Environment, 768, 10.1016/j.scitotenv.2020.144467, 2021.

Dai, Y., Shangguan, W., Wei, N., Xin, Q., Yuan, H., Zhang, S., Liu, S., Lu, X., Wang, D., and Yan, F.: A review of the global soil property maps for Earth system models, Soil, 5, 137-158, 2019.

Dams, J., Woldeamlak, S., and Batelaan, O.: Predicting land-use change and its impact on the groundwater system of the Kleine Nete catchment, Belgium, Hydrology and Earth System Sciences, 12, 1369-1385, 2008.

Dash, S. and Kumar, M.: Spatio-temporal variation in the water cycle: Case studies of different geographical locations, in: Water Sustainability and Hydrological Extremes, Elsevier, 27-43, 2025.

Davies, C., Chen, W. Y., Sanesi, G., and Lafortezza, R.: The European Union roadmap for implementing nature-based solutions: A review, Environmental Science and Policy, 121, 49-67, 2021.

de Klein, J. J. and Koelmans, A. A.: Quantifying seasonal export and retention of nutrients in West European lowland rivers at catchment scale, Hydrological Processes, 25, 2102-2111, 2011.

Debele, S. E., Kumar, P., Sahani, J., Marti-Cardona, B., Mickovski, S. B., Leo, L. S., Porcù, F., Bertini, F., Montesi, D., and Vojinovic, Z.: Nature-based solutions for hydro-meteorological hazards: Revised concepts, classification schemes and databases, Environmental Research, 179, 108799, 2019.

Dembele, M., Schaefli, B., and Van De Giesen, N.: Suitability of 17 gridded rainfall and temperature datasets for large-scale hydrological modelling in West Africa, Hydrology and Earth System Sciences, 24, 5379-5406, 10.5194/hess-24-5379-2020, 2020.

Dembélé, M. and Zwart, S. J.: Evaluation and comparison of satellite-based rainfall products in Burkina Faso, West Africa, International Journal of Remote Sensing, 37, 3995-4014, 2016.

Dembélé, M., Ceperley, N., Zwart, S. J., Salvadore, E., Mariethoz, G., and Schaefli, B.: Potential of satellite and reanalysis evaporation datasets for hydrological modelling under various model calibration strategies, Advances in Water Resources, 143, 10.1016/j.advwatres.2020.103667, 2020.

DHI: MIKE-SHE Volume 1: User Guide, 2007.

DATA AND INFORMATION OF THE DUTCH SUBSURFACE: https://www.dinoloket.nl/ondergrondgegevens, last access: 27 November.

Dong, C.: Remote sensing, hydrological modeling and in situ observations in snow cover research: A review, Journal of Hydrology, 561, 573-583, 2018.

DATABANK ONDERGROND VLAANDEREN: https://www.dov.vlaanderen.be/portaal/?module=freatischgrondwaterverkenner, last access: 27 November.

EUROPEAN CLIMATE ASSESSMENT AND DATASET (ECAD): E-OBS GRIDDED DATASET: https://www.ecad.eu/download/ensembles/download.php, last access: 17 August.

Ehret, U., Zehe, E., Wulfmeyer, V., Warrach-Sagi, K., and Liebert, J.: HESS Opinions" Should we apply bias correction to global and regional climate model data?", Hydrology and Earth System Sciences, 16, 3391-3404, 2012.

Engman, E. T.: Roughness coefficients for routing surface runoff, Journal of Irrigation and Drainage Engineering, 112, 39-53, 1986.

Euser, T., Winsemius, H. C., Hrachowitz, M., Fenicia, F., Uhlenbrook, S., and Savenije, H. H. G.: A framework to assess the realism of model structures using hydrological signatures, Hydrology and Earth System Sciences, 17, 1893-1912, 10.5194/hess-17-1893-2013, 2013.

Evenson, G. R., Jones, C. N., McLaughlin, D. L., Golden, H. E., Lane, C. R., Ben, D., Alexander, L. C., Lang, M. W., McCarty, G. W., and Sharifi, A.: A watershed-scale model for depressional wetland-rich landscapes, Journal of Hydrology X, 1, 10.1016/j.hydroa.2018.10.002, 2018.

Fang, H., Baret, F., Plummer, S., and Schaepman-Strub, G.: An overview of global leaf area index (LAI): Methods, products, validation, and applications, Reviews of Geophysics, 57, 739-799, 2019.

Fennell, J., Soulsby, C., Wilkinson, M. E., Daalmans, R., and Geris, J.: Time variable effectiveness and cost-benefits of different nature-based solution types and design for drought and flood management, Nature-Based Solutions, 3, 100050, 2023.

Feranec, J., Hazeu, G., Kosztra, B., and Arnold, S.: CORINE land cover nomenclature, European Landscape Dynamics: CORINE Land Cover Data; Feranec, J., Soukup, T., Hazeu, G., Jaffrain, G., Eds, 17-25, 2016.

Fernandes, L. C., Paiva, C. M., and Rotunno Filho, O. C.: Evaluation of six empirical evapotranspiration equations-case study: Campos dos Goytacazes/RJ, Revista Brasileira de Meteorologia, 27, 272-280, 2012.

Forster, P. M., Smith, C., Walsh, T., Lamb, W. F., Lamboll, R., Hall, B., Hauser, M., Ribes, A., Rosen, D., Gillett, N. P., Palmer, M. D., Rogelj, J., von Schuckmann, K., Trewin, B., Allen, M., Andrew, R., Betts, R. A., Borger, A., Boyer, T., Broersma, J. A., Buontempo, C., Burgess, S., Cagnazzo, C., Cheng, L., Friedlingstein, P., Gettelman, A., Gütschow, J., Ishii, M., Jenkins, S., Lan, X., Morice, C., Mühle, J., Kadow, C., Kennedy, J., Killick, R. E., Krummel, P. B., Minx, J. C., Myhre, G., Naik, V., Peters, G. P., Pirani, A., Pongratz, J., Schleussner, C. F., Seneviratne, S. I., Szopa, S., Thorne, P., Kovilakam, M. V. M., Majamäki, E., Jalkanen, J. P., van Marle, M., Hoesly, R. M., Rohde, R., Schumacher, D., van der Werf, G., Vose, R., Zickfeld, K., Zhang, X., Masson-Delmotte, V., and Zhai, P.: Indicators of Global Climate Change 2023: annual update of key indicators of the state of the climate system and human influence, Earth System Science Data, 16, 2625-2658, 10.5194/essd-16-2625-2024, 2024.

Freeman, G. E., Copeland, R. R., Rahmeyer, W., and Derrick, D. L.: Field determination of Manning's n value for shrubs and woody vegetation, in: Engineering Approaches to Ecosystem Restoration, 48-53, 1998.

Fu, Q., Shi, R., Li, T., Sun, Y., Liu, D., Cui, S., and Hou, R.: Effects of land-use change and climate variability on streamflow in the Woken River basin in Northeast China, River research and applications, 35, 121-132, 10.1002/rra.3397, 2019.

Gampe, D., LudwigA, R., Qahman, K., and Afifi, S.: Applying the Triangle Method for the parameterization of irrigated areas as input for spatially distributed hydrological modeling - Assessing future drought risk in the Gaza Strip (Palestine), Science of the Total Environment, 543, 877-888, 10.1016/j.scitotenv.2015.07.098, 2016.

Gebrechorkos, S. H., Leyland, J., Dadson, S. J., Cohen, S., Slater, L., Wortmann, M., Ashworth, P. J., Bennett, G. L., Boothroyd, R., Cloke, H., Delorme, P., Griffith, H., Hardy, R., Hawker, L., McLelland, S., Neal, J., Nicholas, A., Tatem, A. J., Vahidi, E., Liu, Y., Sheffield, J., Parsons, D. R., and Darby, S. E.: Global-scale evaluation of precipitation datasets for hydrological modelling, Hydrology and Earth System Sciences, 28, 3099-3118, 10.5194/hess-28-3099-2024, 2024.

GODDARD EARTH SCIENCES DATA AND INFORMATION SERVICES CENTER (GES DISC) BY NASA EARTHDATA: GPM IMERG FINAL PRECIPITATION L3 1 DAY 0.1 DEGREE X 0.1 DEGREE V07: https://disc.gsfc.nasa.gov/datasets/GPM_3IMERGDF_07/summary, last access: 17 August.

Getachew, B., Manjunatha, B., and Bhat, H. G.: Modeling projected impacts of climate and land use/land cover changes on hydrological responses in the Lake Tana Basin, upper Blue Nile River Basin, Ethiopia, Journal of Hydrology, 595, 125974, 10.1016/j.jhydrol.2021.125974, 2021.

Ghimire, U., Shrestha, S., Neupane, S., Mohanasundaram, S., and Lorphensri, O.: Climate and land-use change impacts on spatiotemporal variations in groundwater recharge: A case study of the Bangkok Area, Thailand, Science of the Total Environment, 792, 148370, 10.1016/j.scitotenv.2021.148370, 2021.

Gleason, K. E. and Nolin, A. W.: Charred forests accelerate snow albedo decay: parameterizing the post-fire radiative forcing on snow for three years following fire, Hydrological Processes, 30, 3855-3870, 10.1002/hyp.10897, 2016.

Glenn, E. P., Huete, A. R., Nagler, P. L., Hirschboeck, K. K., and Brown, P.: Integrating remote sensing and ground methods to estimate evapotranspiration, Critical Reviews in Plant Sciences, 26, 139-168, 2007.

GLOBAL HYDROLOGICAL INFORMATION SYSTEM (GLOH2O): MULTI-SOURCE WEIGHTED-ENSEMBLE PRECIPITATION (MSWEP): https://www.gloh2o.org/mswep, last access: 17 August.

Guido, B. I., Popescu, I., Samadi, V., and Bhattacharya, B.: An integrated modeling approach to evaluate the impacts of nature-based solutions of flood mitigation across a small watershed in the southeast United States, Natural Hazards and Earth System Sciences, 23, 2663-2681, 10.5194/nhess-23-2663-2023, 2023.

Guillevic, P. C., Privette, J. L., Coudert, B., Palecki, M. A., Demarty, J., Ottlé, C., and Augustine, J. A.: Land Surface Temperature product validation using NOAA's surface climate observation networks—Scaling methodology for the Visible Infrared Imager Radiometer Suite (VIIRS), Remote Sensing of Environment, 124, 282-298, 2012.

Gunnink, J., Maljers, D., Van Gessel, S., Menkovic, A., and Hummelman, H.: Digital Geological Model (DGM): a 3D raster model of the subsurface of the Netherlands, Netherlands Journal of Geosciences, 92, 33-46, 10.1017/S0016774600000263, 2013.

Guo, L. B. and Gifford, R. M.: Soil carbon stocks and land use change: a meta analysis, Global change biology, 8, 345-360, 2002.

Gupta, H. V., Kling, H., Yilmaz, K. K., and Martinez, G. F.: Decomposition of the mean squared error and NSE performance criteria: Implications for improving hydrological modelling, Journal of hydrology, 377, 80-91, 2009.

Gurara, M. A., Jilo, N. B., and Tolche, A. D.: Modelling climate change impact on the streamflow in the Upper Wabe Bridge watershed in Wabe Shebele River Basin, Ethiopia, International Journal of River Basin Management, 21, 181-193, 10.1080/15715124.2021.1935978, 2021.

Ha, L. T., Bastiaanssen, W. G. M., van Griensven, A., van Dijk, A. I. J. M., and Senay, G. B.: Calibration of spatially distributed hydrological processes and model parameters in SWAT using remote sensing data and an auto-calibration procedure: A case study in a Vietnamese river basin, Water (Switzerland), 10, 10.3390/w10020212, 2018.

Hanifehlou, A., Hosseini, S. A., Javadi, S., and Sharafati, A.: Sustainable exploitation of groundwater resources considering the effects of climate change and land use to provide adaptation solutions (case study of the Hashtgerd plain), Acta Geophysica, 70, 1829-1846, 10.1007/s11600-022-00843-2, 2022.

Hansen, J., Ruedy, R., Sato, M., and Lo, K.: Global surface temperature change, Reviews of Geophysics, 48, 2010.

Hanzer, F., Helfricht, K., Marke, T., and Strasser, U.: Multilevel spatiotemporal validation of snow/ice mass balance and runoff modeling in glacierized catchments, Cryosphere, 10, 1859-1881, 10.5194/tc-10-1859-2016, 2016.

Hartanto, I. M., van der Kwast, J., Alexandridis, T. K., Almeida, W., Song, Y., van Andel, S. J., and Solomatine, D. P.: Data assimilation of satellite-based actual evapotranspiration in a distributed hydrological model of a controlled water system, International Journal of Applied Earth Observation and Geoinformation, 57, 123-135, 10.1016/j.jag.2016.12.015, 2017.

Hedrick, A. R., Marks, D., Marshall, H. P., McNamara, J., Havens, S., Trujillo, E., Sandusky, M., Robertson, M., Johnson, M., Bormann, K. J., and Painter, T. H.: From drought to flood: A water balance analysis of the Tuolumne River basin during extreme conditions (2015–2017), Hydrological Processes, 34, 2560-2574, 10.1002/hyp.13749, 2020.

Her, Y. and Heatwole, C.: Two-dimensional continuous simulation of spatiotemporally varied hydrological processes using the time-area method, Hydrological Processes, 30, 751-770, 10.1002/hyp.10644, 2016.

Herman, M. R., Nejadhashemi, A. P., Abouali, M., Hernandez-Suarez, J. S., Daneshvar, F., Zhang, Z., Anderson, M. C., Sadeghi, A. M., Hain, C. R., and Sharifi, A.: Evaluating the role of evapotranspiration remote sensing data in improving hydrological modeling predictability, Journal of Hydrology, 556, 39-49, 10.1016/j.jhydrol.2017.11.009, 2018.

Heße, F., Zink, M., Kumar, R., Samaniego, L., and Attinger, S.: Spatially distributed characterization of soil-moisture dynamics using travel-time distributions, Hydrology and Earth System Sciences, 21, 549-570, 10.5194/hess-21-549-2017, 2017.

Hofstra, N., Haylock, M., New, M., Jones, P., and Frei, C.: Comparison of six methods for the interpolation of daily, European climate data, Journal of Geophysical Research: Atmospheres, 113, 2008.

Holden, P. B., Rebelo, A. J., Wolski, P., Odoulami, R. C., Lawal, K. A., Kimutai, J., Nkemelang, T., and New, M. G.: Nature-based solutions in mountain catchments reduce impact of anthropogenic climate change on drought streamflow, Commun Earth Environ, 3, 51, 2022.

Höllering, S., Wienhöfer, J., Ihringer, J., Samaniego, L., and Zehe, E.: Regional analysis of parameter sensitivity for simulation of streamflow and hydrological fingerprints, Hydrology and Earth System Sciences, 22, 203-220, 10.5194/hess-22-203-2018, 2018.

Hostache, R., Rains, D., Mallick, K., Chini, M., Pelich, R., Lievens, H., Fenicia, F., Corato, G., Verhoest, N. E. C., and Matgen, P.: Assimilation of Soil Moisture and Ocean Salinity (SMOS) brightness temperature into a large-scale distributed conceptual hydrological model to improve soil moisture predictions: the Murray-Darling basin in Australia as a test case, HYDROLOGY AND EARTH SYSTEM SCIENCES, 24, 4793-4812, 10.5194/hess-24-4793-2020, 2020.

Hrachowitz, M., Fovet, O., Ruiz, L., Euser, T., Gharari, S., Nijzink, R., Freer, J., Savenije, H., and Gascuel-Odoux, C.: Process consistency in models: The importance of system signatures, expert knowledge, and process complexity, Water resources research, 50, 7445-7469, 2014.

Hsieh, C.-h. and Davis, A. P.: Evaluation and optimization of bioretention media for treatment of urban storm water runoff, Journal of Environmental Engineering, 131, 1521-1531, 2005.

Huang, S., Eisner, S., Haddeland, I., and Mengistu, Z. T.: Evaluation of two new-generation global soil databases for macro-scale hydrological modelling in Norway, Journal of Hydrology, 610, 127895, 2022.

Huang, S., Eisner, S., Magnusson, J. O., Lussana, C., Yang, X., and Beldring, S.: Improvements of the spatially distributed hydrological modelling using the HBV model at 1 km resolution for Norway, Journal of Hydrology, 577, 10.1016/j.jhydrol.2019.03.051, 2019.

Huffman, G. J., Bolvin, D. T., Braithwaite, D., Hsu, K.-L., Joyce, R. J., Kidd, C., Nelkin, E. J., Sorooshian, S., Stocker, E. F., and Tan, J.: Integrated multi-satellite retrievals for the global precipitation measurement (GPM) mission (IMERG), Satellite precipitation measurement: Volume 1, 343-353, 2020.

Huisman, P., Cramer, W., van Ee, G., Hooghart, J. C., Salz, H., and Zuidema, F. C.: Water in the Netherlands, Netherlands Hydrological Society, 1998.

Hulsman, P., Hrachowitz, M., and Savenije, H. H.: Improving the representation of long-term storage variations with conceptual hydrological models in data-scarce regions, Water Resources Research, 57, e2020WR028837, https://doi.org/10.1029/2020WR028837, 2021.

Huq, E. and Abdul-Aziz, O. I.: Climate and land cover change impacts on stormwater runoff in large-scale coastal-urban environments, Science of the Total Environment, 778, 146017, 10.1016/j.scitotenv.2021.146017, 2021.

Ichiba, A., Gires, A., Tchiguirinskaia, I., Schertzer, D., Bompard, P., and Veldhuis, M. C. T.: Scale effect challenges in urban hydrology highlighted with a distributed hydrological model, Hydrology and Earth System Sciences, 22, 331-350, 10.5194/hess-22-331-2018, 2018.

Imhoff, R. O., van Verseveld, W. J., van Osnabrugge, B., and Weerts, A. H.: Scaling Point-Scale (Pedo)transfer Functions to Seamless Large-Domain Parameter Estimates for High-Resolution Distributed Hydrologic Modeling: An Example for the Rhine River, Water Resources Research, 56, 10.1029/2019WR026807, 2020.

Iqbal, M., Wen, J., Masood, M., Masood, M. U., and Adnan, M.: Impacts of Climate and Land-Use Changes on Hydrological Processes of the Source Region of Yellow River, China, Sustainability, 14, 10.3390/su142214908, 2022.

NATURE-BASED SOLUTIONS, INTERNATIONAL UNION FOR CONSERVATION OF NATURE: https://www.iucn.org/our-work/nature-based-solutions, last access: 13 December 2024.

IWMI: Innovative Water Solutions for Sustainable Development; IWMI Strategy 2019–2023, Colombo, Sri Lanka, 36, 2019.

Jackson, E. K., Roberts, W., Nelsen, B., Williams, G. P., Nelson, E. J., and Ames, D. P.: Introductory overview: Error metrics for hydrologic modelling–A review of common practices and an open source library to facilitate use and adoption, Environmental Modelling and Software, 119, 32-48, 2019.

Janssen, C.: Manning'sn values for various land covers to use for dam breach analyses by NRCS in Kansas, 2023.

Jehanzaib, M., Sattar, M. N., Lee, J.-H., and Kim, T.-W.: Investigating effect of climate change on drought propagation from meteorological to hydrological drought using multi-model ensemble projections, Stochastic Environmental Research and Risk Assessment, 34, 7-21, 2020.

Ji, P., Yuan, X., Jiao, Y., and Zhang, M.: On the reliability of 12 high-resolution precipitation products for process-based hydrological modeling in China, Journal of Hydrology, 628, 130598, 2024.

Jian, S., Yin, C., Wang, Y., Yu, X., and Li, Y.: The possible incoming runoff under extreme rainfall event in the Fenhe river basin, Frontiers in Environmental Science, 10, 812351, 2022.

Jiang, D. and Wang, K.: The role of satellite-based remote sensing in improving simulated streamflow: A review, Water, 11, 1615, 2019.

Jiang, L., Wu, H., Tao, J., Kimball, J. S., Alfieri, L., and Chen, X.: Satellite-based evapotranspiration in hydrological model calibration, Remote Sensing, 12, 10.3390/rs12030428, 2020.

Jin, X. and Jin, Y.: Calibration of a distributed hydrological model in a data-scarce basin based on GLEAM datasets, Water (Switzerland), 12, 10.3390/w12030897, 2020.

Johnson, B. A., Kumar, P., Okano, N., Dasgupta, R., and Shivakoti, B. R.: Nature-based solutions for climate change adaptation: A systematic review of systematic reviews, Nature-Based Solutions, 2, 100042, 2022.

Jonckheere, I., Fleck, S., Nackaerts, K., Muys, B., Coppin, P., Weiss, M., and Baret, F.: Review of methods for in situ leaf area index determination: Part I. Theories, sensors and hemispherical photography, Agricultural and forest meteorology, 121, 19-35, 2004.

Jothityangkoon, C., Sivapalan, M., and Farmer, D.: Process controls of water balance variability in a large semi-arid catchment: downward approach to hydrological model development, Journal of hydrology, 254, 174-198, 2001.

Kafy, A.-A., Rahman, M. S., Hasan, M. M., and Islam, M.: Modelling future land use land cover changes and their impacts on land surface temperatures in Rajshahi, Bangladesh, Remote Sensing Applications: Society and Environment, 18, 100314, 2020.

Kappas, M. W. and Propastin, P. A.: Review of available products of leaf area index and their suitability over the formerly Soviet Central Asia, Journal of Sensors, 2012, 2012.

Karimi, P. and Bastiaanssen, W. G.: Spatial evapotranspiration, rainfall and land use data in water accounting–Part 1: Review of the accuracy of the remote sensing data, Hydrology and Earth System Sciences, 19, 507-532, 2015.

Kay, A., Griffin, A., Rudd, A., Chapman, R., Bell, V., and Arnell, N.: Climate change effects on indicators of high and low river flow across Great Britain, Advances in Water Resources, 151, 103909, 10.1016/j.advwatres.2021.103909, 2021.

Keesstra, S., Nunes, J., Novara, A., Finger, D., Avelar, D., Kalantari, Z., and Cerdà, A.: The superior effect of nature based solutions in land management for enhancing ecosystem services, Science of the Total Environment, 610, 997-1009, 2018.

Khairul, I. M., Mastrantonas, N., Rasmy, M., Koike, T., and Takeuchi, K.: Inter-Comparison of Gauge-Corrected Global Satellite Rainfall Estimates and Their Applicability for Effective Water Resource Management in a Transboundary River Basin: The Case of the Meghna River Basin, Remote Sensing, 10, 10.3390/rs10060828, 2018.

Khan, S., Khan, F., and Guan, Y.: Assessment of gridded precipitation products in the hydrological modeling of a flood-prone mesoscale basin, Hydrology Research, 53, 85-106, 2022.

Khan, U., Ajami, H., Tuteja, N. K., Sharma, A., and Kim, S.: Catchment scale simulations of soil moisture dynamics using an equivalent cross-section based hydrological modelling approach, Journal of Hydrology, 564, 944-966, 10.1016/j.jhydrol.2018.07.066, 2018.

Kiraz, M., Coxon, G., and Wagener, T.: A Signature-Based Hydrologic Efficiency Metric for Model Calibration and Evaluation in Gauged and Ungauged Catchments, Water Resources Research, 59, e2023WR035321, https://doi.org/10.1029/2023WR035321, 2023.

HOME - KLIMAATEFFECTATLAS NETHERLANDS: https://www.klimaateffectatlas.nl/en/ last access: 22 November.

KONINKLIJK NEDERLANDS METEOROLOGISCH INSTITUUT (ROYAL NETHERLANDS METEOROLOGICAL INSTITUTE): https://www.knmi.nl/nederland-nu/klimatologie, last access: 27 November.

Knoben, W. J. M., Freer, J. E., and Woods, R. A.: Technical note: Inherent benchmark or not? Comparing Nash–Sutcliffe and Kling–Gupta efficiency scores, Hydrology and Earth System Sciences, 23, 4323-4331, 10.5194/hess-23-4323-2019, 2019.

Konapala, G., Mishra, A. K., Wada, Y., and Mann, M. E.: Climate change will affect global water availability through compounding changes in seasonal precipitation and evaporation, Nature communications, 11, 1-10, 2020.

Koppa, A., Gebremichael, M., Zambon, R. C., Yeh, W. W. G., and Hopson, T. M.: Seasonal Hydropower Planning for Data-Scarce Regions Using Multimodel Ensemble Forecasts, Remote Sensing Data, and Stochastic Programming, Water Resources Research, 55, 8583-8607, 10.1029/2019WR025228, 2019.

Kratzert, F., Nearing, G., Addor, N., Erickson, T., Gauch, M., Gilon, O., Gudmundsson, L., Hassidim, A., Klotz, D., and Nevo, S.: Caravan-A global community dataset for large-sample hydrology, Scientific Data, 10, 61, 2023.

Kumar, P., Debele, S. E., Sahani, J., Rawat, N., Marti-Cardona, B., Alfieri, S. M., Basu, B., Basu, A. S., Bowyer, P., and Charizopoulos, N.: Nature-based solutions efficiency evaluation against natural hazards: Modelling methods, advantages and limitations, Science of the Total Environment, 784, 147058, 2021.

Kumar, R., Singh, S., Kumar, R., Singh, A., Bhardwaj, A., Sam, L., Randhawa, S. S., and Gupta, A.: Development of a glacio-hydrological model for discharge and mass balance reconstruction, Water Resources Management, 30, 3475-3492, 2016.

Kumar, S. V., Dirmeyer, P. A., Peters-Lidard, C. D., Bindlish, R., and Bolten, J.: Information theoretic evaluation of satellite soil moisture retrievals, Remote sensing of environment, 204, 392-400, 2018.

Kumar, V., Borgemeister, C., Tischbein, B., and Kumar, N.: Evaluation and inter-comparison of twenty-three gridded rainfall products representing a typical urban monsoon climate in India, Theoretical and Applied Climatology, 1-25, https://doi.org/10.1007/s00704-024-05191-3, 2024.

Kundu, S., Khare, D., and Mondal, A.: Individual and combined impacts of future climate and land use changes on the water balance, Ecological Engineering, 105, 42-57, 10.1016/j.ecoleng.2017.04.061, 2017.

Kunnath-Poovakka, A., Ryu, D., Renzullo, L. J., and George, B.: The efficacy of calibrating hydrologic model using remotely sensed evapotranspiration and soil moisture for streamflow prediction, Journal of Hydrology, 535, 509-524, 10.1016/j.jhydrol.2016.02.018, 2016.

Lai, C., Zhong, R., Wang, Z., Wu, X., Chen, X., Wang, P., and Lian, Y.: Monitoring hydrological drought using long-term satellite-based precipitation data, Science of the total environment, 649, 1198-1208, 2019.

Laiolo, P., Gabellani, S., Campo, L., Silvestro, F., Delogu, F., Rudari, R., Pulvirenti, L., Boni, G., Fascetti, F., Pierdicca, N., Crapolicchio, R., Hasenauer, S., and Puca, S.: Impact

of different satellite soil moisture products on the predictions of a continuous distributed hydrological model, International Journal of Applied Earth Observation and Geoinformation, 48, 131-145, 10.1016/j.jag.2015.06.002, 2016.

Lakew, H. B., Moges, S. A., and Asfaw, D. H.: Hydrological performance evaluation of multiple satellite precipitation products in the upper Blue Nile basin, Ethiopia, Journal of Hydrology: Regional Studies, 27, 10.1016/j.ejrh.2020.100664, 2020.

Lamontagne, J. R., Barber, C. A., and Vogel, R. M.: Improved estimators of model performance efficiency for skewed hydrologic data, Water Resources Research, 56, e2020WR027101, 2020.

Lazin, R., Shen, X., Koukoula, M., and Anagnostou, E.: Evaluation of the Hyper-Resolution Model-Derived Water Cycle Components Over the Upper Blue Nile Basin, Journal of Hydrology, 590, 10.1016/j.jhydrol.2020.125231, 2020.

Le, M.-H., Lakshmi, V., Bolten, J., and Du Bui, D.: Adequacy of satellite-derived precipitation estimate for hydrological modeling in Vietnam basins, Journal of Hydrology, 586, 124820, https://doi.org/10.1016/j.jhydrol.2020.124820, 2020.

Lee, H., Calvin, K., Dasgupta, D., Krinner, G., Mukherji, A., Thorne, P., Trisos, C., Romero, J., Aldunce, P., and Ruane, A. C.: Climate change 2023 synthesis report summary for policymakers, 2024.

Leong, C. and Yokoo, Y.: A multiple hydrograph separation technique for identifying hydrological model structures and an interpretation of dominant process controls on flow duration curves, Hydrological Processes, 36, e14569, 2022.

Li, H., Li, X., Yang, D., Wang, J., Gao, B., Pan, X., Zhang, Y., and Hao, X.: Tracing Snowmelt Paths in an Integrated Hydrological Model for Understanding Seasonal Snowmelt Contribution at Basin Scale, Journal of Geophysical Research: Atmospheres, 124, 8874-8895, 10.1029/2019JD030760, 2019.

Liao, C. and Zhuang, Q.: Quantifying the Role of Snowmelt in Stream Discharge in an Alaskan Watershed: An Analysis Using a Spatially Distributed Surface Hydrology Model, Journal of Geophysical Research: Earth Surface, 122, 2183-2195, 10.1002/2017JF004214, 2017.

Lilly, A., Boorman, D., and Hollis, J.: The development of a hydrological classification of UK soils and the inherent scale changes, in: Soil and Water Quality at Different Scales, Springer, 299-302, 1998.

Liu, D.: A rational performance criterion for hydrological model, Journal of Hydrology, 590, 125488, 2020.

Liu, J., Duan, Z., Jiang, J., and Zhu, A.-X.: Evaluation of three satellite precipitation products TRMM 3B42, CMORPH, and PERSIANN over a subtropical watershed in China, Advances in Meteorology, 2015, 151239, 2015.

Liu, S., Xu, Z., Zhu, Z., Jia, Z., and Zhu, M.: Measurements of evapotranspiration from eddy-covariance systems and large aperture scintillometers in the Hai River Basin, China, Journal of Hydrology, 487, 24-38, 2013.

Liu, X., Liang, X., Li, X., Xu, X., Ou, J., Chen, Y., Li, S., Wang, S., and Pei, F.: A future land use simulation model (FLUS) for simulating multiple land use scenarios by coupling human and natural effects, Landscape and Urban Planning, 168, 94-116, 10.1016/j.landurbplan.2017.09.019, 2017.

Liu, Y. Y., Dorigo, W. A., Parinussa, R., de Jeu, R. A., Wagner, W., McCabe, M. F., Evans, J., and Van Dijk, A.: Trend-preserving blending of passive and active microwave soil moisture retrievals, Remote Sensing of Environment, 123, 280-297, 2012.

Loliyana, V. D. and Patel, P. L.: A physics based distributed integrated hydrological model in prediction of water balance of a semi-arid catchment in India, Environmental modelling and software, 127, 104677, 10.1016/j.envsoft.2020.104677, 2020.

Luo, M., Meng, F., Liu, T., Duan, Y., Frankl, A., Kurban, A., and de Maeyer, P.: Multi-model ensemble approaches to assessment of effects of local climate change on water resources of the Hotan River basin in Xinjiang, China, Water (Switzerland), 9, 10.3390/w9080584, 2017.

Lyu, Y., Chen, H., Cheng, Z., He, Y., and Zheng, X.: Identifying the Impacts of Land Use Landscape Pattern and Climate Changes on Streamflow From Past to Future, Journal of Environmental Management, 345, 118910, 10.1016/j.jenvman.2023.118910, 2023.

Ma, H., Zhong, L., Fu, Y., Cheng, M., Wang, X., Cheng, M., and Chang, Y.: A study on hydrological responses of the Fuhe River Basin to combined effects of land use and climate change, Journal of Hydrology: Regional Studies, 48, 101476, 10.1016/j.ejrh.2023.101476, 2023.

Ma, L., He, C., Bian, H., and Sheng, L.: MIKE SHE modeling of ecohydrological processes: Merits, applications, and challenges, Ecological Engineering, 96, 137-149, 10.1016/j.ecoleng.2016.01.008, 2016.

Macalalad, R. V., Xu, S. C., Badilla, R. A., Paat, S. F., Tajones, B. C., Chen, Y. B., and Bagtasa, G.: Flash flood modeling in the data-poor basin: A case study in Matina River Basin, TROPICAL CYCLONE RESEARCH AND REVIEW, 10, 87-95, 10.1016/j.tcrr.2021.06.003, 2021.

MacAlister, C. and Subramanyam, N.: Climate change and adaptive water management: innovative solutions from the global South, 2018.

Mao, R. J., Wang, L., Zhou, J., Li, X. P., Qi, J., and Zhang, X. T.: Evaluation of Various Precipitation Products Using Ground-Based Discharge Observation at the Nujiang River Basin, China, Water, 11, 10.3390/w11112308, 2019.

Maranan, M., Fink, A. H., Knippertz, P., Amekudzi, L. K., Atiah, W. A., and Stengel, M.: A process-based validation of GPM IMERG and its sources using a mesoscale rain gauge network in the West African forest zone, Journal of Hydrometeorology, 21, 729-749, 2020.

Marhaento, H., Booij, M. J., and Hoekstra, A. Y.: Hydrological response to future land-use change and climate change in a tropical catchment, Hydrological sciences journal, 63, 1368-1385, 10.1080/02626667.2018.1511054, 2018.

Massari, C., Avanzi, F., Bruno, G., Gabellani, S., Penna, D., and Camici, S.: Evaporation enhancement drives the European water-budget deficit during multi-year droughts,

Hydrology and Earth System Sciences, 26, 1527-1543, 10.5194/hess-26-1527-2022, 2022.

Maza, M., Srivastava, A., Bisht, D. S., Raghuwanshi, N. S., Bandyopadhyay, A., Chatterjee, C., and Bhadra, A.: Simulating hydrological response of a monsoon dominated reservoir catchment and command with heterogeneous cropping pattern using VIC model, Journal of Earth System Science, 129, 10.1007/s12040-020-01468-z, 2020.

McCabe, M. F., Rodell, M., Alsdorf, D. E., Miralles, D. G., Uijlenhoet, R., Wagner, W., Lucieer, A., Houborg, R., Verhoest, N. E., and Franz, T. E.: The future of Earth observation in hydrology, Hydrology and earth system sciences, 21, 3879-3914, 2017.

McMillan, H., Booker, D., and Cattoën, C.: Validation of a national hydrological model, Journal of Hydrology, 541, 800-815, 2016.

Metcalfe, P., Beven, K., Hankin, B., and Lamb, R.: A modelling framework for evaluation of the hydrological impacts of nature-based approaches to flood risk management, with application to in-channel interventions across a 29-km2 scale catchment in the United Kingdom, Hydrological processes, 31, 1734-1748, 2017.

THE ONLINE ARCHIVE OF HISTORICAL PRECIPITATION AND EVAPORATION IN THE NETHERLANDS: https://www.meteobase.nl/?tb=rasterdata&dp=rasterdata&dp_sub=introductie, last access: 27 November.

Milly, P. C., Betancourt, J., Falkenmark, M., Hirsch, R. M., Kundzewicz, Z. W., Lettenmaier, D. P., and Stouffer, R. J.: Stationarity is dead: Whither water management?, Science, 319, 573-574, 2008.

Mimeau, L., Esteves, M., Zin, I., Jacobi, H. W., Brun, F., Wagnon, P., Koirala, D., and Arnaud, Y.: Quantification of different flow components in a high-altitude glacierized catchment (Dudh Koshi, Himalaya): some cryospheric-related issues, Hydrology and Earth System Sciences, 23, 3969-3996, 10.5194/hess-23-3969-2019, 2019.

Mitsch, W. J. and Gosselink, J. G.: Wetlands, John wiley & sons2015.

Moges, E., Ruddell, B. L., Zhang, L., Driscoll, J. M., Norton, P., Perez, F., and Larsen, L. G.: HydroBench: Jupyter supported reproducible hydrological model benchmarking and diagnostic tool, Frontiers in Earth Science, 10, 884766, https://doi.org/10.3389/feart.2022.884766, 2022.

Mohammadi, A., Karimzadeh, S., Jalal, S. J., Kamran, K. V., Shahabi, H., Homayouni, S., and Al-Ansari, N.: A Multi-Sensor Comparative Analysis on the Suitability of Generated DEM from Sentinel-1 SAR Interferometry Using Statistical and Hydrological Models, Sensors, 20, 7214, 2020.

Monsieurs, E., Kirschbaum, D. B., Tan, J., Maki Mateso, J.-C., Jacobs, L., Plisnier, P.-D., Thiery, W., Umutoni, A., Musoni, D., and Bibentyo, T. M.: Evaluating TMPA rainfall over the sparsely gauged East African Rift, Journal of Hydrometeorology, 19, 1507-1528, 2018.

Moore, I. D., Gessler, P. E., Nielsen, G., and Peterson, G.: Soil attribute prediction using terrain analysis, Soil science society of america journal, 57, 443-452, 1993.

Müller-Schmied, H., Cáceres, D., Eisner, S., Flörke, M., Herbert, C., Niemann, C., Peiris, T. A., Popat, E., Portmann, F. T., and Reinecke, R.: The global water resources and use model WaterGAP v2. 2d: Model description and evaluation, Geoscientific Model Development, 14, 1037-1079, 2021.

Muñoz-Sabater, J., Dutra, E., Agustí-Panareda, A., Albergel, C., Arduini, G., Balsamo, G., Boussetta, S., Choulga, M., Harrigan, S., and Hersbach, H.: ERA5-Land: A state-of-the-art global reanalysis dataset for land applications, Earth system science data, 13, 4349-4383, 2021.

Munzimi, Y. A., Hansen, M. C., and Asante, K. O.: Estimating daily streamflow in the Congo Basin using satellite-derived data and a semi-distributed hydrological model, Hydrological Sciences Journal, 64, 1472-1487, 10.1080/02626667.2019.1647342, 2019.

Nachabe, M., Shah, N., Ross, M., and Vomacka, J.: Evapotranspiration of two vegetation covers in a shallow water table environment, Soil Science Society of America Journal, 69, 492-499, 2005.

Nash, J. E. and Sutcliffe, J. V.: River flow forecasting through conceptual models part I—A discussion of principles, Journal of hydrology, 10, 282-290, 1970.

Nazeer, A., Maskey, S., Skaugen, T., and McClain, M. E.: Changes in the hydro-climatic regime of the Hunza Basin in the Upper Indus under CMIP6 climate change projections, Scientific Reports, 12, 21442, 10.1038/s41598-022-25673-6, 2022.

Nesru, M., Shetty, A., and Nagaraj, M. K.: Multi-variable calibration of hydrological model in the upper Omo-Gibe basin, Ethiopia, Acta Geophysica, 68, 537-551, 10.1007/s11600-020-00417-0, 2020.

Nesshöver, C., Assmuth, T., Irvine, K. N., Rusch, G. M., Waylen, K. A., Delbaere, B., Haase, D., Jones-Walters, L., Keune, H., and Kovacs, E.: The science, policy and practice of nature-based solutions: An interdisciplinary perspective, Science of the total environment, 579, 1215-1227, 2017.

NHI: Nederlands Hydrological Instrumentation Model reporting: Sub-report Crop characteristics, Nederlands Hydrologisch Instrumentarium, Netherlands, 2008.

Ocio, D., Beskeen, T., and Smart, K.: Fully distributed hydrological modelling for catchment-wide hydrological data verification, Hydrology Research, 50, 1520-1534, 2019.

Onyutha, C.: Pros and cons of various efficiency criteria for hydrological model performance evaluation, Proceedings of International Association of Hydrological Sciences, 385, 181-187, https://doi.org/10.5194/piahs-385-181-2024, 2024.

Page, M. J., McKenzie, J. E., Bossuyt, P. M., Boutron, I., Hoffmann, T. C., Mulrow, C. D., Shamseer, L., Tetzlaff, J. M., Akl, E. A., and Brennan, S. E.: The PRISMA 2020 statement: an updated guideline for reporting systematic reviews, International journal of surgery, 88, 105906, 2021.

Pakoksung, K. and Takagi, M.: Effect of satellite based rainfall products on river basin responses of runoff simulation on flood event, Modeling Earth Systems and Environment, 2, 10.1007/s40808-016-0200-0, 2016.

Pakoksung, K. and Takagi, M.: Effect of DEM sources on distributed hydrological model to results of runoff and inundation area, Modeling Earth Systems and Environment, 7, 1891-1905, 10.1007/s40808-020-00914-7, 2021.

Pan, S. L., Liu, L., Bai, Z. X., and Xu, Y. P.: Integration of Remote Sensing Evapotranspiration into Multi-Objective Calibration of Distributed Hydrology-Soil-Vegetation Model (DHSVM) in a Humid Region of China, Water, 10, 10.3390/w10121841, 2018.

Papaioannou, G., Efstratiadis, A., Vasiliades, L., Loukas, A., Papalexiou, S. M., Koukouvinos, A., Tsoukalas, I., and Kossieris, P.: An operational method for flood directive implementation in ungauged urban areas, Hydrology, 5, 24, 2018.

Paz, I., Willinger, B., Gires, A., de Souza, B. A., Monier, L., Cardinal, H., Tisserand, B., Tchiguirinskaia, I., and Schertzer, D.: Small-scale rainfall variability impacts analyzed by fully-distributed model using C-band and X-band radar data, Water (Switzerland), 11, 10.3390/w11061273, 2019.

Peña-Arancibia, J. L., Bruijnzeel, L. A., Mulligan, M., and Van Dijk, A. I.: Forests as 'sponges' and 'pumps': Assessing the impact of deforestation on dry-season flows across the tropics, Journal of Hydrology, 574, 946-963, 2019.

Penning, E., Burgos, R. P., Mens, M., Dahm, R., and de Bruijn, K.: Nature-based solutions for floods AND droughts AND biodiversity: Do we have sufficient proof of their functioning?, Cambridge Prisms: Water, 1, e11, 2023.

Philip, S. Y., Kew, S. F., Van Der Wiel, K., Wanders, N., and Van Oldenborgh, G. J.: Regional differentiation in climate change induced drought trends in the Netherlands, Environmental Research Letters, 15, 094081, 10.1088/1748-9326/ab97ca, 2020.

CLIMATE ADAPTATION PORTAL PROVINCE OF NORTH BRABANT: https://www.klimaatadaptatiebrabant.nl/, last access: 22 November.

POM, W.: EU policy document on natural water retention measures, Technical Report-2014-082. Prepared by the drafting team of the Water …, 2014.

Popescu, I.: Floods in a Changing Climate: Inundation Modelling (Di Baldassarre, G.), Cambridge University Press2013.

Qi, W., Zhang, C., Fu, G., Sweetapple, C., and Zhou, H.: Evaluation of global fine-resolution precipitation products and their uncertainty quantification in ensemble discharge simulations, Hydrology and Earth System Sciences, 20, 903-920, 10.5194/hess-20-903-2016, 2016.

Quesada-Montano, B., Westerberg, I. K., Fuentes-Andino, D., Hidalgo, H. G., and Halldin, S.: Can climate variability information constrain a hydrological model for an ungauged Costa Rican catchment?, Hydrological Processes, 32, 830-846, 2018.

Quinn, P., O'Donnell, G., Nicholson, A., Wilkinson, M., Owen, G., Jonczyk, J., Barber, N., Hardwick, M., and Davies, G.: Potential use of runoff attenuation features in small rural catchments for flood mitigation, Newcastle University (ed) Newcastle upon Tyne, Newcastle, 2013.

Rajib, A., Evenson, G. R., Golden, H. E., and Lane, C. R.: Hydrologic model predictability improves with spatially explicit calibration using remotely sensed evapotranspiration and biophysical parameters, Journal of Hydrology, 567, 668-683, 10.1016/j.jhydrol.2018.10.024, 2018.

Rajib, M. A., Merwade, V., and Yu, Z.: Multi-objective calibration of a hydrologic model using spatially distributed remotely sensed/in-situ soil moisture, Journal of Hydrology, 536, 192-207, 10.1016/j.jhydrol.2016.02.037, 2016.

Ran, Q., Wang, J., Chen, X., Liu, L., Li, J., and Ye, S.: The relative importance of antecedent soil moisture and precipitation in flood generation in the middle and lower Yangtze River basin, Hydrology and Earth System Sciences, 26, 4919-4931, 10.5194/hess-26-4919-2022, 2022.

Rasheed, N. J., Al-Khafaji, M. S., Alwan, I. A., Al-Suwaiyan, M. S., Doost, Z. H., and Yaseen, Z. M.: Survey on the resolution and accuracy of input data validity for SWAT-based hydrological models, Heliyon, 10, e38348, https://doi.org/10.1016/j.heliyon.2024.e38348, 2024.

Raymond, C., Breil, M., Nita, M., Kabisch, N., de Bel, M., Enzi, V., Frantzeskaki, N., Geneletti, G., Lovinger, L., and Cardinaletti, M.: An impact evaluation framework to support planning and evaluation of nature-based solutions projects. Report prepared by the EKLIPSE Expert Working Group on Nature-Based Solutions to Promote Climate Resilience in Urban Areas, Centre for Ecology and Hydrology2017.

Raz-Yaseef, N., Yakir, D., Schiller, G., and Cohen, S.: Dynamics of evapotranspiration partitioning in a semi-arid forest as affected by temporal rainfall patterns, Agricultural and Forest Meteorology, 157, 77-85, 2012.

Refsgaard, C. J., Storm, B., and Clausen, T.: Système Hydrologique Europeén (SHE): review and perspectives after 30 years development in distributed physically-based hydrological modelling, Hydrology Research, 41, 355-377, 10.2166/nh.2010.009, 2010.

Refsgaard, J. C.: Parameterisation, calibration and validation of distributed hydrological models, Journal of hydrology, 198, 69-97, 1997.

Ren, Y. and Liu, S.: A simple regional snow hydrological process-based snow depth model and its application in the Upper Yangtze River Basin, Hydrology Research, 50, 672-690, 10.2166/nh.2019.079, 2019.

Richards, L. A.: CAPILLARY CONDUCTION OF LIQUIDS THROUGH POROUS MEDIUMS, Physics, 1, 318-333, 10.1063/1.1745010, 1931.

Rigby, A. M., Butcher, P. W., Ritsos, P. D., and Patil, S. D.: LUCST: A novel toolkit for Land Use Land Cover change assessment in SWAT+ to support flood management decisions, Environmental Modelling and Software, 156, 105469, 10.1016/j.envsoft.2022.105469, 2022.

Ritter, A. and Muñoz-Carpena, R.: Performance evaluation of hydrological models: Statistical significance for reducing subjectivity in goodness-of-fit assessments, Journal of Hydrology, 480, 33-45, 2013.

Roberts, F. S.: Characterizations of the plurality function, Mathematical Social Sciences, 21, 101-127, 1991.

Rossi, L., Wens, M., de Moel, H., Cotti, D., Sabino Siemons, A.-S., Toreti, A., Maetens, W., Masante, D., Van Loon, A., and Hagenlocher, M.: European Drought Risk Atlas, 2023.

Roy, B. and Rahman, M. Z.: Spatio-temporal analysis and cellular automata-based simulations of biophysical indicators under the scenario of climate change and urbanization using artificial neural network, Remote Sensing Applications: Society and Environment, 31, 100992, 10.1016/j.rsase.2023.100992, 2023.

Ruangpan, L., Vojinovic, Z., Di Sabatino, S., Leo, L. S., Capobianco, V., Oen, A. M., McClain, M. E., and Lopez-Gunn, E.: Nature-based solutions for hydro-meteorological risk reduction: a state-of-the-art review of the research area, Natural Hazards and Earth System Sciences, 20, 243-270, 2020.

Ruangpan, L., Vojinovic, Z., Plavšić, J., Curran, A., Rosic, N., Pudar, R., Savic, D., and Brdjanovic, D.: Economic assessment of nature-based solutions to reduce flood risk and enhance co-benefits, Journal of Environmental Management, 352, 119985, 2024.

Sahani, J., Kumar, P., Debele, S., Spyrou, C., Loupis, M., Aragão, L., Porcù, F., Shah, M. A. R., and Di Sabatino, S.: Hydro-meteorological risk assessment methods and management by nature-based solutions, Science of the Total Environment, 696, 133936, 2019.

Sahoo, S., Khatun, M., Pradhan, S., and Das, P.: Evaluation of a physically based model to assess the eco-hydrological components on the basin hydrology, Sustainable Water Resources Management, 7, 10.1007/s40899-021-00536-6, 2021.

Santos, L., Thirel, G., and Perrin, C.: Technical note: Pitfalls in using log-transformed flows within the KGE criterion, Hydrology and Earth System Sciences, 22, 4583-4591, 10.5194/hess-22-4583-2018, 2018.

Sassi, M., Nicotina, L., Pall, P., Stone, D., Hilberts, A., Wehner, M., and Jewson, S.: Impact of climate change on European winter and summer flood losses, Advances in Water Resources, 129, 165-177, 10.1016/j.advwatres.2019.05.014, 2019.

Sawicz, K., Wagener, T., Sivapalan, M., Troch, P. A., and Carrillo, G.: Catchment classification: empirical analysis of hydrologic similarity based on catchment function in the eastern USA, Hydrology and Earth System Sciences, 15, 2895-2911, 10.5194/hess-15-2895-2011, 2011.

Schneider, C., Flörke, M., De Stefano, L., and Petersen-Perlman, J. D.: Hydrological threats to riparian wetlands of international importance–a global quantitative and qualitative analysis, Hydrology and Earth System Sciences, 21, 2799-2815, 2017.

Seiler, C. and Moene, A. F.: Estimating actual evapotranspiration from satellite and meteorological data in Central Bolivia, Earth Interactions, 15, 1-24, 2011.

Sen-Gupta, A. and Tarboton, D. G.: A tool for downscaling weather data from large-grid reanalysis products to finer spatial scales for distributed hydrological applications, Environmental Modelling and Software, 84, 50-69, 10.1016/j.envsoft.2016.06.014, 2016.

Seneviratne, S. I., Corti, T., Davin, E. L., Hirschi, M., Jaeger, E. B., Lehner, I., Orlowsky, B., and Teuling, A. J.: Investigating soil moisture–climate interactions in a changing climate: A review, Earth-Science Reviews, 99, 125-161, 2010.

Shah, D., Pandya, M., Trivedi, H., and Jani, A.: Estimating minimum and maximum air temperature using MODIS data over Indo-Gangetic Plain, Journal of earth system science, 122, 1593-1605, 2013.

Shah, M. A. R., Xu, J., Carisi, F., De Paola, F., Di Sabatino, S., Domeneghetti, A., Gerundo, C., Gonzalez-Ollauri, A., Nadim, F., and Petruccelli, N.: Quantifying the effects of nature-based solutions in reducing risks from hydrometeorological hazards: Examples from Europe, International journal of disaster risk reduction, 93, 103771, 2023.

Sharif, H. O., Al-Zahrani, M., and El Hassan, A.: Physically, fully-distributed hydrologic simulations driven by GPM satellite rainfall over an urbanizing arid catchment in Saudi Arabia, Water (Switzerland), 9, 10.3390/w9030163, 2017.

Sheffield, J., Wood, E. F., Pan, M., Beck, H., Coccia, G., Serrat-Capdevila, A., and Verbist, K.: Satellite remote sensing for water resources management: Potential for supporting sustainable development in data-poor regions, Water Resources Research, 54, 9724-9758, 2018.

Singh, L. and Saravanan, S.: Evaluation of various spatial rainfall datasets for streamflow simulation using SWAT model of Wunna basin, India, International Journal of River Basin Management, 20, 389-398, 10.1080/15715124.2020.1776305, 2020.

Singh, S., Bhardwaj, A., Singh, A., Sam, L., Shekhar, M., Martín-Torres, F. J., and Zorzano, M.-P.: Quantifying the congruence between air and land surface temperatures for various climatic and elevation zones of Western Himalaya, Remote Sensing, 11, 2889, 2019.

Sinha, R. K., Eldho, T. I., and Subimal, G.: Assessing the impacts of land use/land cover and climate change on surface runoff of a humid tropical river basin in Western Ghats, India, International Journal of River Basin Management, 21, 141-152, 10.1080/15715124.2020.1809434, 2020.

Siqueira, V. A., Paiva, R. C. D., Fleischmann, A. S., Fan, F. M., Ruhoff, A. L., Pontes, P. R. M., Paris, A., Calmant, S., and Collischonn, W.: Toward continental hydrologic-hydrodynamic modeling in South America, Hydrology and Earth System Sciences, 22, 4815-4842, 10.5194/hess-22-4815-2018, 2018.

Song, Y. H., Chung, E. S., and Shahid, S.: Spatiotemporal differences and uncertainties in projections of precipitation and temperature in South Korea from CMIP6 and CMIP5 general circulation model s, International Journal of Climatology, 41, 5899-5919, 2021.

Sonnenborg, T. O., Christiansen, J. R., Pang, B., Bruge, A., Stisen, S., and Gundersen, P.: Analyzing the hydrological impact of afforestation and tree species in two catchments with contrasting soil properties using the spatially distributed model MIKE SHE SWET, Agricultural and Forest Meteorology, 239, 118-133, 10.1016/j.agrformet.2017.03.001, 2017.

Sorribas, M. V., Paiva, R. C., Melack, J. M., Bravo, J. M., Jones, C., Carvalho, L., Beighley, E., Forsberg, B., and Costa, M. H.: Projections of climate change effects on discharge and inundation in the Amazon basin, Climatic change, 136, 555-570, 10.1007/s10584-016-1640-2, 2016.

Soulis, K. X., Psomiadis, E., Londra, P., and Skuras, D.: A new model-based approach for the evaluation of the net contribution of the european union rural development program to the reduction of water abstractions in agriculture, Sustainability (Switzerland), 12, 10.3390/su12177137, 2020.

Stachowicz, M., Lyngstad, A., Osuch, P., and Grygoruk, M.: Hydrological Response to Rewetting of Drained Peatlands—A Case Study of Three Raised Bogs in Norway, Land, 14, 142, 2025.

Stoll, M. J. and Brazel, A. J.: Surface-air temperature relationships in the urban environment of Phoenix, Arizona, Physical Geography, 13, 160-179, 1992.

Strohmeier, S., López López, P., Haddad, M., Nangia, V., Karrou, M., Montanaro, G., Boudhar, A., Linés, C., Veldkamp, T., and Sterk, G.: Surface Runoff and Drought Assessment Using Global Water Resources Datasets - from Oum Er Rbia Basin to the Moroccan Country Scale, Water Resources Management, 34, 2117-2133, 10.1007/s11269-019-02251-6, 2020.

Sun, W., Ma, J., Yang, G., and Li, W.: Statistical and hydrological evaluations of multi-satellite precipitation products over Fujiang River Basin in humid southeast China, Remote Sensing, 10, 10.3390/rs10121898, 2018.

Sunde, M. G., He, H. S., Hubbart, J. A., and Urban, M. A.: Integrating downscaled CMIP5 data with a physically based hydrologic model to estimate potential climate change impacts on streamflow processes in a mixed-use watershed, Hydrological Processes, 31, 1790-1803, 10.1002/hyp.11150, 2017.

Szarek-Gwiazda, E., Ciszewski, D., and Kownacki, A.: The effects of channelization with low in-stream barriers on macroinvertebrate communities of mountain rivers, Water, 15, 1059, 2023.

Tesemma, Z., Wei, Y., Peel, M., and Western, A.: The effect of year-to-year variability of leaf area index on Variable Infiltration Capacity model performance and simulation of runoff, Advances in Water Resources, 83, 310-322, 2015.

Teweldebrhan, A. T., Burkhart, J. F., and Schuler, T. V.: Parameter uncertainty analysis for an operational hydrological model using residual-based and limits of acceptability approaches, Hydrology and Earth System Sciences, 22, 5021-5039, 10.5194/he-22-5021-2018, 2018.

Thiemig, V., Rojas, R., Zambrano-Bigiarini, M., and De Roo, A.: Hydrological evaluation of satellite-based rainfall estimates over the Volta and Baro-Akobo Basin, Journal of Hydrology, 499, 324-338, 2013.

Thomas, H. and Nisbet, T.: Modelling the hydraulic impact of reintroducing large woody debris into watercourses, Journal of Flood Risk Management, 5, 164-174, 2012.

Thompson, J. R., Sørenson, H. R., Gavin, H., and Refsgaard, A.: Application of the coupled MIKE SHE/MIKE 11 modelling system to a lowland wet grassland in southeast England, Journal of Hydrology, 293, 151-179, https://doi.org/10.1016/j.jhydrol.2004.01.017, 2004.

Tirupathi, C. and Shashidhar, T.: Investigating the impact of climate and land-use land cover changes on hydrological predictions over the Krishna river basin under present and

future scenarios, Science of the Total Environment, 721, 137736, 10.1016/j.scitotenv.2020.137736, 2020.

Tomasella, J., Hodnett, M. G., Cuartas, L. A., Nobre, A. D., Waterloo, M. J., and Oliveira, S. M.: The water balance of an Amazonian micro-catchment: The effect of interannual variability of rainfall on hydrological behaviour, Hydrological Processes: An International Journal, 22, 2133-2147, 2008.

Tousignant, E., Fankhauser, O., and Hurd, S.: Guidance manual for the design, construction and operations of constructed wetlands for rural applications in Ontario, 1999.

Trang, N. T. T., Shrestha, S., Shrestha, M., Datta, A., and Kawasaki, A.: Evaluating the impacts of climate and land-use change on the hydrology and nutrient yield in a transboundary river basin: A case study in the 3S River Basin (Sekong, Sesan, and Srepok), Science of the Total Environment, 576, 586-598, 10.1016/j.scitotenv.2016.10.138, 2017.

UNION OF CONCERNED SCIENTISTS SATELLITE DATABASE: https://www.ucsusa.org/resources/satellite-database, last access: 13 February.

UNECE: Good Practices and Lessons Learned in Data-sharing in Transboundary Basins, United Nations Publications2024.

van den Eertwegh, G., Bartholomeus, R., de Louw, P., Witte, F., van Dam, J., van Deijl, D., Hoefsloot, P., Clevers, S., Hendriks, D., van Huijgevoort, M., Hunink, J., Mulder, N., Pouwels, J., and de Wit, J.: Drought in sandy areas of South, Central and East Netherlands: Report phase 1: development of a uniform method for analysis of drought and interim findings, KnowH2O2019.

Van Der Velde, R., Colliander, A., Pezij, M., Benninga, H. J. F., Bindlish, R., Chan, S. K., Jackson, T. J., Hendriks, D. M. D., Augustijn, D. C. M., and Su, Z.: Validation of SMAP L2 passive-only soil moisture products using upscaled in situ measurements collected in Twente, the Netherlands, Hydrology and Earth System Sciences, 25, 473-495, 10.5194/hess-25-473-2021, 2021.

van Dorland, R., Beersma, J., Bessembinder, J., and Bloemendaal, N.: KNMI National Climate Scenarios 2023 for the Netherlands, Scientific Report, Royal Netherlands Meteorological Institute, De Bilt2023.

van Genuchten, M. T.: A Closed-form Equation for Predicting the Hydraulic Conductivity of Unsaturated Soils, Soil Science Society of America Journal, 44, 892-898, https://doi.org/10.2136/sssaj1980.03615995004400050002x, 1980.

Van Huijgevoort, M. H., Voortman, B. R., Rijpkema, S., Nijhuis, K. H., and Witte, J.-P. M.: Influence of climate and land use change on the groundwater system of the Veluwe, The Netherlands: A historical and future perspective, Water, 12, 2866, 2020.

Van Loon, A. F.: Hydrological drought explained, Wiley Interdisciplinary Reviews: Water, 2, 359-392, 2015.

van Meerveld, I. and Seibert, J.: Reforestation effects on low flows: Review of public perceptions and scientific evidence, Wiley Interdisciplinary Reviews: Water, 12, e1760, 2025.

van Oostende, M., Hieronymi, M., Krasemann, H., Baschek, B., and Röttgers, R.: Correction of inter-mission inconsistencies in merged ocean colour satellite data, Frontiers in Remote Sensing, 3, 10.3389/frsen.2022.882418, 2022.

van Vliet, M. T. H., Blenkinsop, S., Burton, A., Harpham, C., Broers, H. P., and Fowler, H. J.: A multi-model ensemble of downscaled spatial climate change scenarios for the Dommel catchment, Western Europe, Climatic Change, 111, 249-277, 10.1007/s10584-011-0131-8, 2012.

Vázquez, R., Feyen, L., Feyen, J., and Refsgaard, J.: Effect of grid size on effective parameters and model performance of the MIKE-SHE code, Hydrological processes, 16, 355-372, 2002.

Vernes, R., Van Doorn, T. H., Bierkens, M., Van Gessel, S., and De Heer, E.: Van gidslaag naar hydrogeologische eenheid: toelichting op de totstandkoming van de dataset REGIS II, 2005.

Vertessy, R. A., Watson, F. G., and Sharon, K.: Factors determining relations between stand age and catchment water balance in mountain ash forests, Forest Ecology and Management, 143, 13-26, 2001.

Viera, A. J. and Garrett, J. M.: Understanding interobserver agreement: the kappa statistic, Family Medicine, 37, 360-363, 2005.

Villarini, G. and Wasko, C.: Humans, climate and streamflow, Nature Climate Change, 11, 725-726, 2021.

Visser, A., Kroes, J., van Vliet, M. T., Blenkinsop, S., Fowler, H. J., and Broers, H. P.: Climate change impacts on the leaching of a heavy metal contamination in a small lowland catchment, Journal of contaminant hydrology, 127, 47-64, 2012.

VLAAMSE MILIEUMAATSCHAPPIJ (FLEMISH ENVIRONMENT AGENCY) PORTAL: VLAANDEREN \ WATERINFO: https://www.waterinfo.be/Themas#item=rainfall/more%20information/gauged%20rainfall, last access: 27 November.

Wanders, N., Karssenberg, D., Bierkens, M., Parinussa, R., de Jeu, R., van Dam, J., and de Jong, S.: Observation uncertainty of satellite soil moisture products determined with physically-based modeling, Remote Sensing of Environment, 127, 341-356, 2012.

Wang, H. and Chen, Y.: Identifying key hydrological processes in highly urbanized watersheds for flood forecasting with a distributed hydrological model, Water (Switzerland), 11, 10.3390/w11081641, 2019.

Wang, J., Zhuo, L., Han, D., Liu, Y., and Rico-Ramirez, M. A.: Hydrological model adaptability to rainfall inputs of varied quality, Water Resources Research, 59, e2022WR032484, 2023.

Wang, S., Zhang, L., She, D., Wang, G., and Zhang, Q.: Future projections of flooding characteristics in the Lancang-Mekong River Basin under climate change, Journal of Hydrology, 602, 126778, 2021.

WATERSCHAP BRABANTSE DELTA, WATERBEHEERPROGRAMMA WATERSCHAP BRABANTSE DELTA 2022-2027: KLIMAATBESTENDIG EN VEERKRACHTIG

WATERLANDSCHAP, 2022.: https://lokaleregelgeving.overheid.nl/CVDR666825/1#, last access: 22 November.

Wedajo, G. K., Muleta, M. K., and Awoke, B. G.: Impacts of combined and separate land cover and climate changes on hydrologic responses of Dhidhessa River basin, Ethiopia, International Journal of River Basin Management, 22, 57-70, 10.1080/15715124.2022.2101464, 2022.

Welderufael, W., Woyessa, Y., and Edossa, D.: Impact of rainwater harvesting on water resources of the modder river basin, central region of South Africa, Agricultural water management, 116, 218-227, 2013.

Western, A. W., Grayson, R. B., and Green, T. R.: The Tarrawarra project: high resolution spatial measurement, modelling and analysis of soil moisture and hydrological response, Hydrological processes, 13, 633-652, 1999.

Whitford, A. C., Blenkinsop, S., Pritchard, D., and Fowler, H. J.: A gauge-based sub-daily extreme rainfall climatology for western Europe, Weather and Climate Extremes, 41, 100585, 10.1016/j.wace.2023.100585, 2023.

Witter, V. J. and Raats, T.: Hydrological criteria for durable water systems, IAHS PUBLICATION, 231-238, 2001.

Woods Ballard, B., Wilson, S., Udale-Clarke, H., Illman, S., Scott, T., Ashley, R., and Kellagher, R.: The SuDS Manual; CIRIA: London, UK, 2015, Google Scholar, 2015.

Worqlul, A. W., Ayana, E. K., Yen, H., Jeong, J., MacAlister, C., Taylor, R., Gerik, T. J., and Steenhuis, T. S.: Evaluating hydrologic responses to soil characteristics using SWAT model in a paired-watersheds in the Upper Blue Nile Basin, Catena, 163, 332-341, 2018.

Wösten, J., Lilly, A., Nemes, A., and Le Bas, C.: Development and use of a database of hydraulic properties of European soils, Geoderma, 90, 169-185, 1999.

Wu, J., Nunes, J. P., Baartman, J. E. M., and Faúndez Urbina, C. A.: Testing the impacts of wildfire on hydrological and sediment response using the OpenLISEM model. Part 1: Calibration and evaluation for a burned Mediterranean forest catchment, Catena, 207, 10.1016/j.catena.2021.105658, 2021.

Wu, Y., Sun, J., Hu, B., Xu, Y. J., Rousseau, A. N., and Zhang, G.: Can the combining of wetlands with reservoir operation reduce the risk of future floods and droughts?, Hydrology and Earth System Sciences, 27, 2725-2745, 10.5194/hess-27-2725-2023, 2023.

Xia, W., Akhtar, T., Lu, W., and Shoemaker, C. A.: Enhanced watershed model evaluation incorporating hydrologic signatures and consistency within efficient surrogate multi-objective optimization, Environmental Modelling and Software, 175, 105983, 2024.

Xu, X., Li, J., and Tolson, B. A.: Progress in integrating remote sensing data and hydrologic modeling, Progress in Physical Geography, 38, 464-498, 2014.

Xu, Z., Cheng, L., Liu, P., Makarieva, O., and Chen, M.: Detecting and quantifying the impact of long-term terrestrial water storage changes on the runoff ratio in the head regions of the two largest rivers in China, Journal of Hydrology, 601, 126668, 2021.

Yan, R., Cai, Y., Li, C., Wang, X., and Liu, Q.: Hydrological responses to climate and land use changes in a watershed of the Loess Plateau, China, Sustainability, 11, 1443, 10.3390/su11051443, 2019.

Yang, L., Shi, Z., Liu, R., and Xing, M.: Evaluating the performance of global precipitation products for precipitation and extreme precipitation in arid and semiarid China, International Journal of Applied Earth Observation and Geoinformation, 130, 103888, 2024.

Yang, N., Zhang, J., Liu, J., Liu, G., Liao, A., and Wang, G.: Analysis of Event-based Hydrological Processes at the Hydrohill Catchment Using Hydrochemical and Isotopic Methods, Proceedings of International Association of Hydrological Sciences, 383, 99-110, 10.5194/piahs-383-99-2020, 2020.

Yang, Y., Xiao, P., Feng, X., and Li, H.: Accuracy assessment of seven global land cover datasets over China, Journal of Photogrammetry and Remote Sensing, 125, 156-173, 2017.

Ye, C., Dang, T. D., Xu, X., Stewart, C. J., Arias, M. E., Zhang, Y., and Zhang, Q.: Coupled effects of future rainfall and land use on urban stormwater drainage system in Tampa, Florida (USA), Ecological Indicators, 153, 110402, 10.1016/j.ecolind.2023.110402, 2023.

Yimer, E. A., De Trift, L., Lobkowicz, I., Villani, L., Nossent, J., and van Griensven, A.: The underexposed nature-based solutions: A critical state-of-art review on drought mitigation, Journal of Environmental Management, 352, 119903, 2024.

Zhang, B., Kang, S., Li, F., and Zhang, L.: Comparison of three evapotranspiration models to Bowen ratio-energy balance method for a vineyard in an arid desert region of northwest China, Agricultural and forest meteorology, 148, 1629-1640, 2008.

Zhang, H., Wang, B., Li Liu, D., Zhang, M., Leslie, L. M., and Yu, Q.: Using an improved SWAT model to simulate hydrological responses to land use change: A case study of a catchment in tropical Australia, Journal of Hydrology, 585, 124822, 10.1016/j.jhydrol.2020.124822, 2020a.

Zhang, J., Zhang, Y., Song, J., Cheng, L., Paul, P. K., Gan, R., Shi, X., Luo, Z., and Zhao, P.: Large-scale baseflow index prediction using hydrological modelling, linear and multilevel regression approaches, Journal of Hydrology, 585, 124780, 2020b.

Zhang, L., Ren, D., Nan, Z., Wang, W., Zhao, Y., Zhao, Y., Ma, Q., and Wu, X.: Interpolated or satellite-based precipitation? Implications for hydrological modeling in a meso-scale mountainous watershed on the Qinghai-Tibet Plateau, Journal of Hydrology, 583, 124629, https://doi.org/10.1016/j.jhydrol.2020.124629, 2020c.

Zhang, Y., He, Y., and Song, J.: Effects of climate change and land use on runoff in the Huangfuchuan Basin, China, Journal of Hydrology, 626, 130195, 10.1016/j.jhydrol.2023.130195, 2023.

Zhang, Y., Li, W., Sun, G., Miao, G., Noormets, A., Emanuel, R., and King, J. S.: Understanding coastal wetland hydrology with a new regional-scale, process-based hydrological model, Hydrological Processes, 32, 3158-3173, 10.1002/hyp.13247, 2018.

Zhou, Q., Leng, G., Su, J., and Ren, Y.: Comparison of urbanization and climate change impacts on urban flood volumes: Importance of urban planning and drainage adaptation, Science of the Total Environment, 658, 24-33, 10.1016/j.scitotenv.2018.12.184, 2019.

APPENDIX A

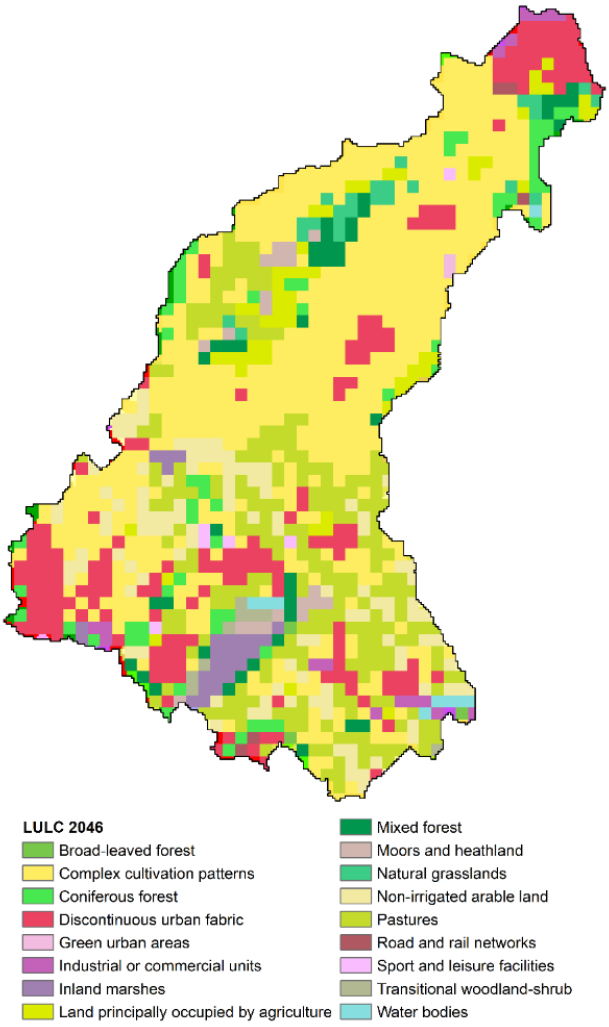

Figure A1. The simulated LULC map of 2046

Table A1. The values of 'R95pTot' for the catchment average rainfall for the base period and future climate scenarios

Seasons	**Base period**	**Climate scenarios**			
		LD	LN	HD	HN
Spring	287.7	11.9	0	40.2	12.1
Summer	472.3	37.3	40.5	104.7	67.7
Autumn	361.8	92.7	39.9	57.2	29.4
Winter	378.1	0	0	12	0

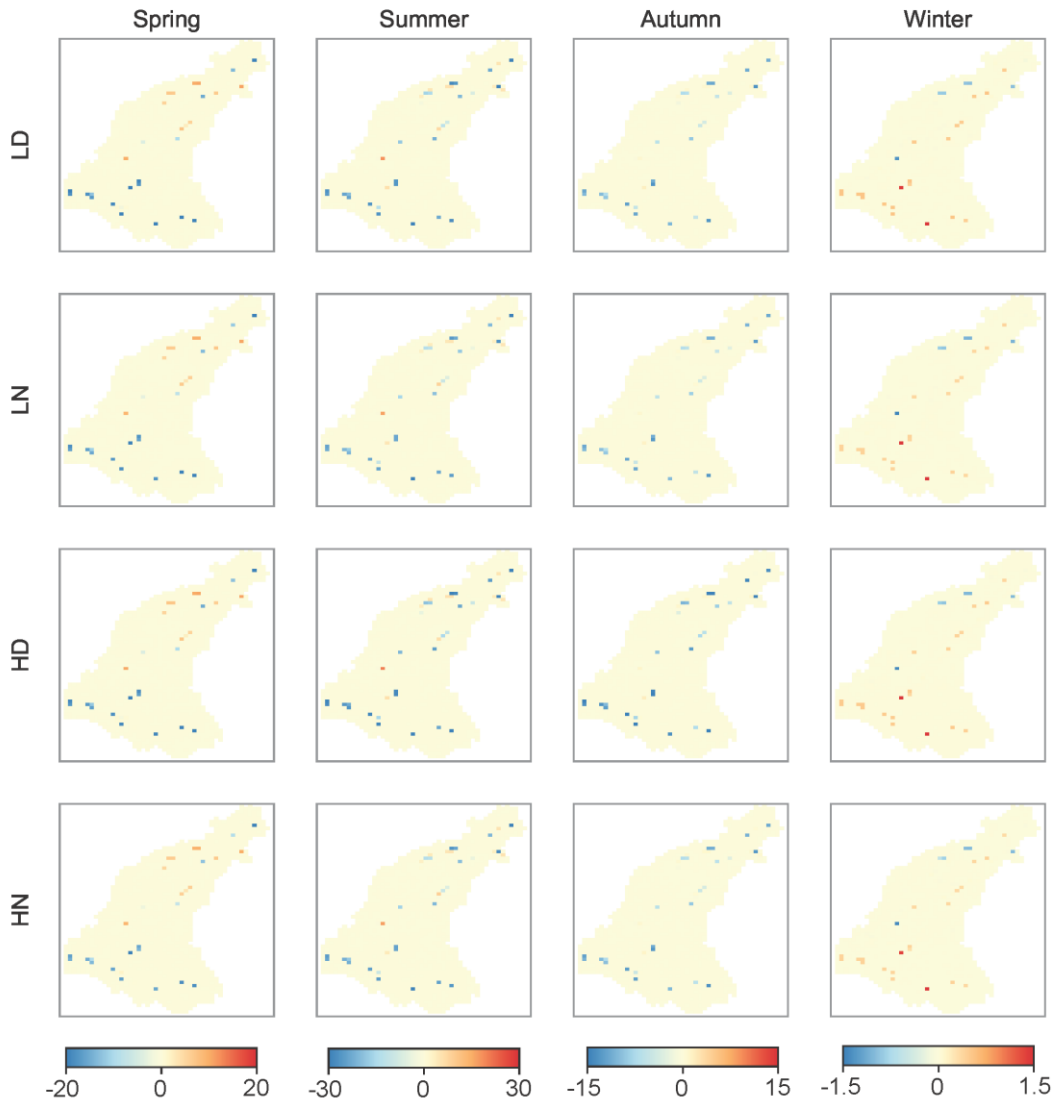

Figure A2. The difference in the relative change (%) of simulated AET between SC3 and SC2 scenarios on a seasonal basis

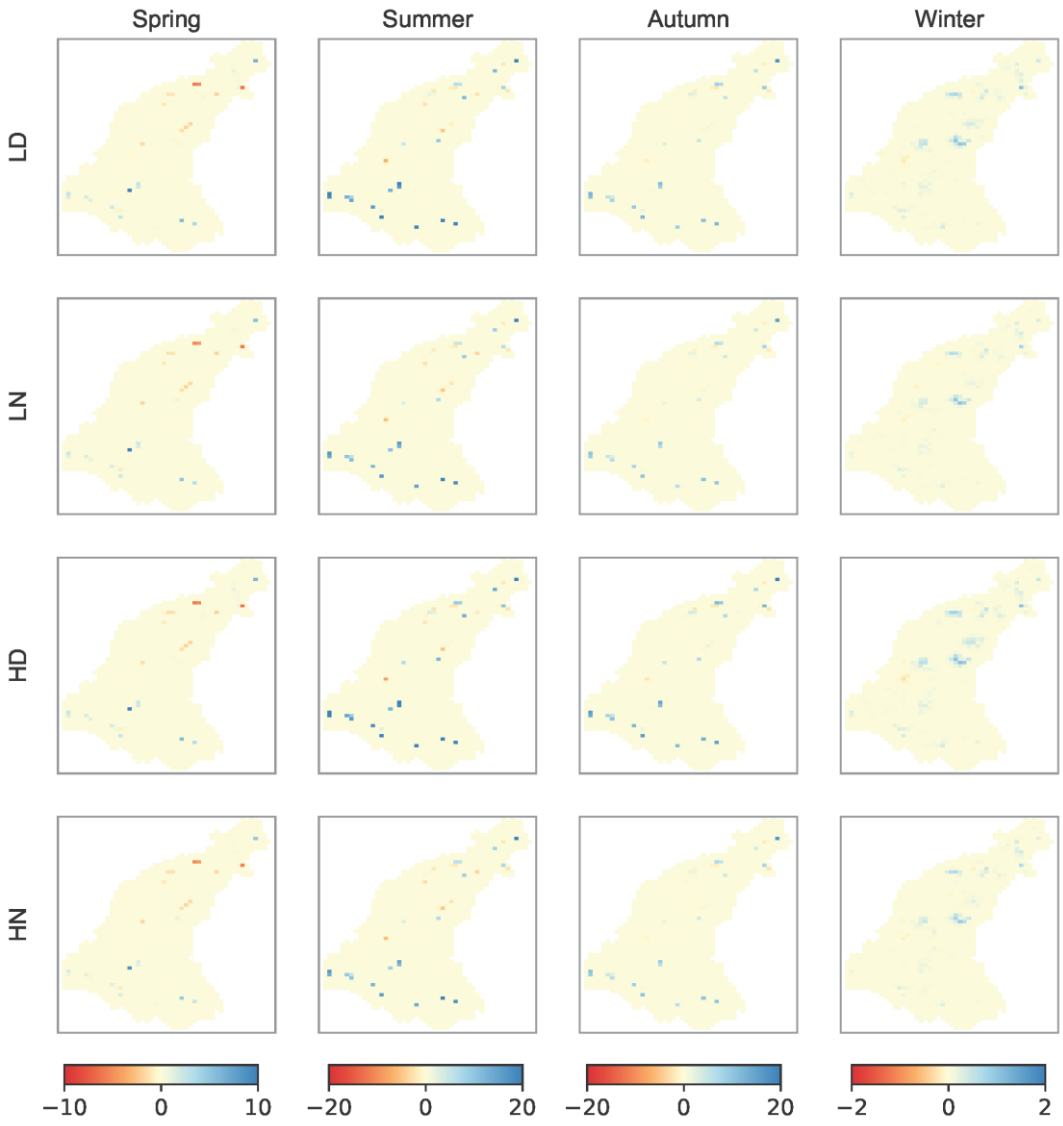

Figure A3. The difference in the relative change (%) of simulated SM between SC3 and SC2 scenarios on a seasonal basis

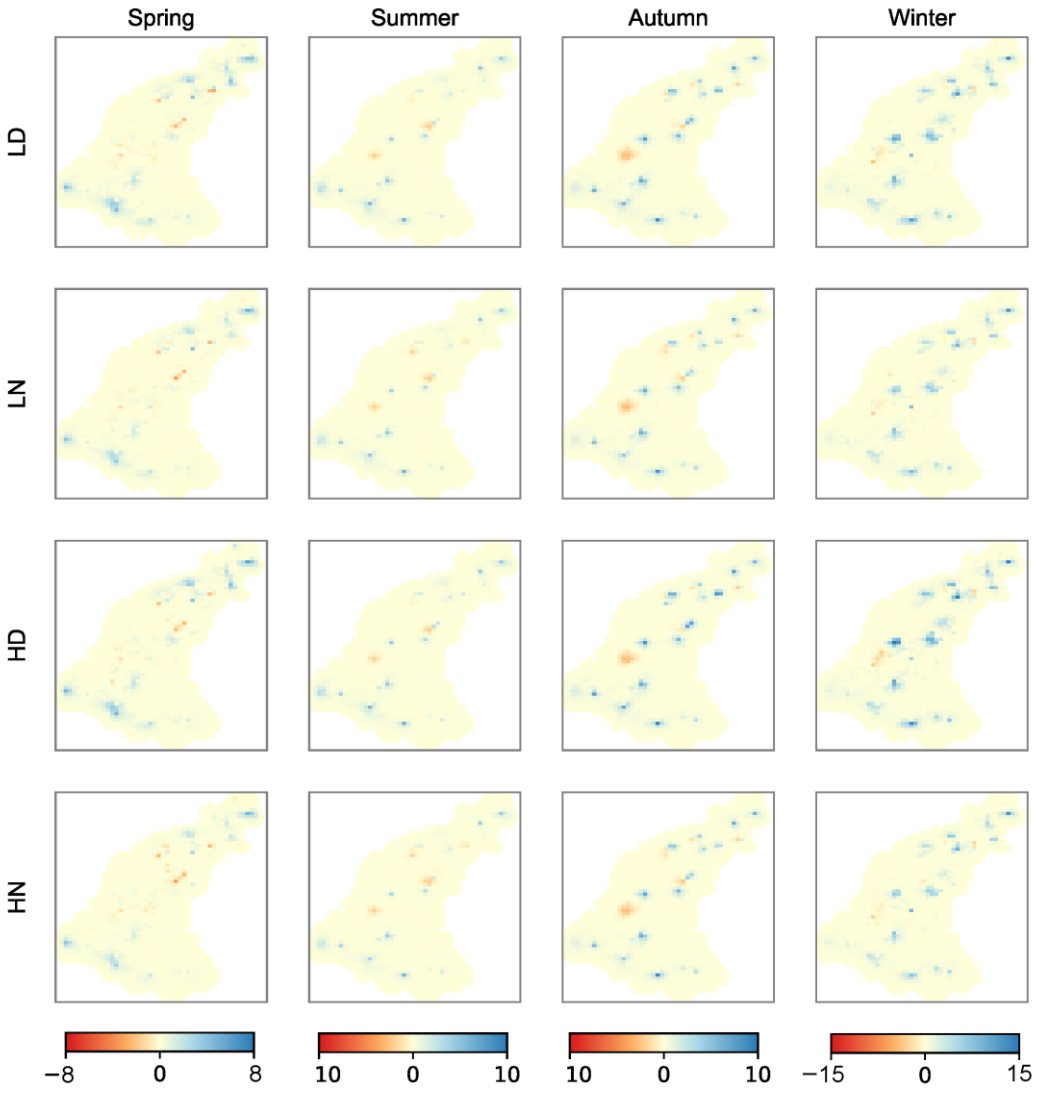

Figure A4. The difference in the relative change (%) of simulated GWT between SC3 and SC2 scenarios on a seasonal basis

LIST OF ACRONYMS

2D	Two Dimensional
ECMWF	European Centre for Medium-Range Weather Forecasts
EOBS	European observation dataset
ERA5	European Centre for Medium-Range Weather Forecasts Reanalysis V5
IMERG	Integrated Multi-satellitE Retrievals for GPM (Global Precipitation Measurement)
IPCC	Intergovernmental Panel on Climate Change
KGE	Kling Gupta Efficiency Coefficient
KPI	Key Performance Indicators
KNMI	Royal Netherlands Meteorological Institute
LULC	Land Use Land Cover
MIKE SHE	MIKE System Hydrologique European
MSWEP	Multi-Source Weighted-Ensemble Precipitation
NASA	National Aeronautics and Space Administration
NSE	Nash-Sutcliffe Efficiency Coefficient

LIST OF TABLES

LIST OF FIGURES

ABOUT THE AUTHOR

Muhammad Haris Ali did his B.Sc. in Civil Engineer from University of Engineer and Technology, Lahore, Pakistan. After bachelors, he joined the Punjab Irrigation Department, Pakistan where he gained hands-on experience in both field operations and modelling of water system for manging floods and drought conditions. In 2016, he came to IHE Delft Netherlands on scholarship to purse his M.Sc. Degree in Water Science and Engineering – Specialisation in Hydroinformatics. He graduated with distinction (Cum Laude) in 2018. In August 2021, Haris began his Ph.D. in the Hydroinformatic group at IHE Delft. The PhD research was funded by European Union project Eiffel. His contributions led to the project's successful and timely completion.

In addition to his academic endeavours, Haris has handful experience in practical water management, catchment modelling and consulting on climate change adaptation strategies.

JOURNALS PUBLICATIONS

Ali, M.H., Popescu, I., Jonoski, A., & Solomatine, D.P., 2023. Remote Sensed and/or Global Datasets for Distributed Hydrological Modelling: A Review. Remote Sensing, 15, 1642. https://doi.org/10.3390/rs15061642

Bogatinoska, B., Lansu, A., Hugé, J., **Ali, M. H.**, Dekker, S. C., & Stoorvogel, J.,2024. Analysing landscape multi-functionality by integrated modelling. Environmental Modelling & Software, 106116. https://doi.org/10.1016/j.envsoft.2024.106116

Ali, M. H., Bertini, C., Popescu, I., & Jonoski, A., 2025. Comparative analysis of hydrological impacts from climate and land use/land cover changes in a lowland mesoscale catchment. International Journal of River Basin Management, 1–19. https://doi.org/10.1080/15715124.2025.2454692

Jonoski, A., **Ali, M. H.**, Bertini, C., Popescu, I., van Andel, S.J., & Lansu, A., 2025. Model-based design of drought-related climate adaptation strategies using nature-based solutions: case study of the Aa of Weerijs catchment in the Netherlands. Nature-Based Solutions, 100264. https://doi.org/10.1016/j.nbsj.2025.100264

Ali, M. H., Popescu, I., Hrachowitz, M., & Jonoski, A., 2025. Multi-metric multiple combination evaluation of precipitation products for hydrological simulations. Under review.

CONFERENCE PROCEEDINGS

Ali, M. H., Popescu, I., Jonoski, A., and Solomatine, D., 2022. Review of scientific literature on the use of globally available remote sensed data products for distributed hydrological modelling., EGU General Assembly 2022, Vienna, Austria, 23–27 May, EGU22-10200, https://doi.org/10.5194/egusphere-egu22-10200.

Ali, M. H., Popescu, I., Jonoski, A., & Solomatine, D., 2023. Climate impact on surface-subsurface hydrology considering meteorological and land use projections., EGU General Assembly 2023, Vienna, Austria, 23–28 Apr, EGU23-2627, https://doi.org/10.5194/egusphere-egu23-2627.

Ali, M. H., Popescu, I., Jonoski, A., & Solomatine, D.: Potential of infiltration ponds as Managed Aquifer Recharge method to address water stress in lowland meso-scale catchment, 4th IAHR Young Professionals congress 2023, online, 22-24 Nov, ISBN: 978-90-833476-5-3, P 172-173, https://www.iahr.org/library/infor?pid=29801.

Ali, M. H., Hrachowitz, M., Popescu, I., & Jonoski, A., 2024 Signatures-based appraisal of global rainfall datasets to capture hydrological trends in a meso-scale catchment, EGU General Assembly 2024, Vienna, Austria, 14–19 Apr, EGU24-8064, https://doi.org/10.5194/egusphere-egu24-8064.

Ali, M. H., Bertini, C., Popescu, I., Jonoski, A., & Jan, S., 2024. Future Hydrological Dynamics Under Climate Change in The Aa of Weerijs Catchment. In 15th International Conference on Hydroinformatics (p. 206). https://doi.org/10.3850/iahr-hic2483430201-206.

Ali, M. H., Popescu, I., & Jonoski, A., 2024. The Potential of Nature-Based Solutions for Drought Adaptation: Modelling and Application in the Aa of Weerijs Catchment, Netherlands. Boussinesq Lecture 2024, Amsterdam, Netherlands.

Netherlands Research School for the
Socio-Economic and Natural Sciences of the Environment

D I P L O M A

for specialised PhD training

The Netherlands research school for the
Socio-Economic and Natural Sciences of the Environment
(SENSE) declares that

Muhammad Haris Ali

born on 10 December 1990 in Okara, Pakistan

has successfully fulfilled all requirements of the
educational PhD programme of SENSE.

Delft, 4 February 2026

SENSE coordinator PhD education

Dr Ir Peter Vermeulen

The SENSE Director

Dr Jampel Dell'Angelo

The SENSE Research School declares that **Muhammad Haris Ali** has successfully fulfilled all requirements of the educational PhD programme of SENSE with a work load of 52.9 EC, including the following activities:

SENSE PhD Courses

- Environmental research in context (2021)
- Research in context activity: 'Organising the PhD-symposium at IHE Delft: Water in context of Triple planetary crises' (2023)

Selection of Other PhD and Advanced MSc Courses

- PhD Start up, TU Delft (2022)
- Engineering Ethics, TU Delft (2022)
- QGIS for Hydrological Applications, IHE Delft (2022)
- Creative Tools for Scientific Writing, TU Delft (2022)
- Coaching Individual Students and Project Group, TU Delft (2022)
- Writing Successful Project Proposals, IHE Delft (2022)
- Data Visualisation – A practical approach, TU Delft (2023)
- Scientific Writing and Skills Development, IHE Delft (2023)
- Catchment Science, University of Birmingham (2023)
- Software Carpentry Workshops, TU Delft (2023)
- Data Visualisation as a tool for Scientific Research (using R), TU Delft (2023)
- Career Development – Personality Matters, TU Delft (2024)
- Designing Scientific Posters, TU Delft (2024)
- Deep Learning, Vrije Universiteit Amsterdam (2024)

Management and Didactic Skills Training

- Member IHE PhD Board 2021-2023
- Supervising five MSc students with thesis (2022-2024)
- Teaching the MSc course 'Integrated Coastal Area and River Basin Management' (2022)
- Teaching Assistant in the MSc/ PhD level courses 'Operational water management (2022 & 2023) & 'River Flood Analysis Modelling' (2023) & 'Using Open Data, QGIS and HEC-RAS for Hydraulic Modelling' (2023)

Selection of Oral Presentations

- *Climate impact on surface-subsurface hydrology considering meteorological and land use projections.* EGU, 24-28 April 2023, Vienna, Austria
- *Signatures-based appraisal of global rainfall datasets to capture hydrological trends in a meso-scale catchment.* EGU, 14 – 19 April 2024, Vienna, Austria
- *Potential of infiltration ponds as Managed Aquifer Recharge method to address water stress in lowland meso-scale catchment.* 4th IAHR Young Professionals congress 2023, online, 22-24 November 2023, Online
- *The potential of nature-based solutions for drought adaptation: modelling and application in the Aa of Weerijs catchment, Netherlands.* Boussinesq lecture, 10 October 2024, Amsterdam, the Netherlands

IHE DELFT
Institute for Water Education
under the auspices of UNESCO

TU Delft Delft University of Technology

Nature Based Solutions (NBSs) offer adaptable, eco-friendly alternatives to grey infrastructure for long-term climate change resilience. However, in research to date, their potential for drought mitigation remains underexplored. Hydrological models that are capable of simulating integrated surface and subsurface hydrological processes can be potentially used to assess the effectiveness of different NSBs for drought mitigation. Yet, the accuracy of models to efficiently simulate the hydrological processes significantly depends on the quality and availability of input data. Earth Observation (EO) datasets offer a wide range of hydrological data with comprehensive spatial and temporal coverage, yet their quality remains uncertain and requires evaluation across different scales and regions.

This research focuses on designing nature-based climate adaptation strategies through EO-informed hydrological modelling. A comprehensive framework was developed to evaluate the suitability of EO products for simulating hydrological variables using multi-metric, multiple combination approach. Additionally, the methodology was proposed to design and catchment-scale evaluation of nature-based adaptation strategies by integrating individual NBSs to mitigate drought impacts. The methodologies were applied to the Aa of Weerijs catchment in the Netherlands. The results enhance both EO products evaluation for hydrological simulations and the design of nature-based adaptation strategies for drought mitigation under changing climatic conditions.

This book is printed on paper from sustainably managed forests and controlled sources

9 789073 445772